

YOU BUILD ME UP, YOU BREAK ME DOWN

Molecular mechanisms of
blood-retinal barrier development
and disruption

Anne-Eva van der Wijk

Ter nagedachtenis aan Joanna (1986-2016)

Kun je het je voorstellen? Dertig worden in deze absurde, onbegrijpelijke wereld!

Ze fronste haar wenkbrauwen. - HARUKI MURAKAMI, uit 1q84

ISBN: 978-94-6182-917-7

The studies described in this thesis were carried out at the departments of Ophthalmology and Medical Biology of the Academic Medical Center (AMC), University of Amsterdam, Amsterdam, The Netherlands.

Printing of this thesis was financially supported by Landelijke Stichting voor Blinden en Slechtzienden (LSBS).

Cover (front) - Mask of the retinal vasculature of a 5 days old mouse. The vasculature was stained with isolectin B4, (back) - bovine retinal endothelial cells stained for β -actin.

Lay-out and cover design: Anne-Eva van der Wijk

Printing: Off Page, Amsterdam

Copyright © 2018 by A.E. van der Wijk.

All rights reserved. No part of this publication may be reproduced, stored or transmitted in any way without prior permission from the author.

YOU BUILD ME UP, YOU BREAK ME DOWN

Molecular mechanisms of
blood-retinal barrier development and disruption

ACADEMISCH PROEFSCHRIFT

ter verkrijging van de graad van doctor
aan de Universiteit van Amsterdam
op gezag van de Rector Magnificus
prof. dr. ir. K.I.J. Maex

ten overstaan van een door het College voor Promoties ingestelde commissie,
in het openbaar te verdedigen in de Agnietenkapel
op vrijdag 9 november 2018, te 12.00 uur

door
Anne-Eva van der Wijk
geboren te Groningen

PROMOTIECOMMISSIE

Promotores:	Prof.dr. R.O. Schlingemann	AMC-UvA
	Prof.dr. C.J.F. van Noorden	AMC-UvA
Co-promotor:	Dr. I. Klaassen	AMC-UvA
Overige leden:	Prof.dr. E.T. van Bavel	AMC-UvA
	Prof.dr. C.J.M. de Vries	AMC-UvA
	Prof.dr. C.J.F. Boon	AMC-UvA
	Dr. J.D. van Buul	Sanquin
	Prof.dr. M.C. Harmsen	Rijksuniversiteit Groningen
	Prof.dr. H.E. de Vries	Vrije Universiteit Amsterdam

Faculteit der Geneeskunde

TABLE OF CONTENTS

1	Introduction and scope of the thesis	7
 Part I. Development of the blood-retinal barrier and the role of PLVAP in blood-retinal barrier development and disruption		
2	Spatial and temporal recruitment of the neurovascular unit during development of the mouse blood-retinal barrier	17
3	Formation of the retinal vasculature and blood-retinal barrier during early development and the role of plasmalemma vesicle-associated protein (PLVAP)	35
4	Plasmalemma vesicle-associated protein (PLVAP) has a key role in blood-retinal barrier loss	69
 Part II. The role of inflammation and therapeutic interventions in blood-retinal barrier disruption		
5	Is leukostasis a crucial step or epiphenomenon in the pathogenesis of diabetic retinopathy?	91
6	TNF α -induced disruption of the blood-retinal barrier <i>in vitro</i> is regulated by cyclic AMP levels	111
7	Glucocorticoids exert differential effects on the endothelium in an <i>in vitro</i> model of the blood-retinal barrier	131
8	General discussion and summary	151
&	Addendum	
	Nederlandse samenvatting en conclusies	156
	List of publications	162
	Curriculum vitae	163
	Portfolio	164
	Dankwoord	166



1

INTRODUCTION AND SCOPE OF THE THESIS

INTRODUCTION

Diabetes mellitus is a global epidemic, and it is predicted that the prevalence of diabetic patients increases from 382 million in 2013 to an estimated 592 million by 2035¹. Diabetic patients suffer from many complications, including macrovascular pathology such as ischemic heart disease and stroke, and microvascular pathology such as neuropathy, nephropathy, and diabetic retinopathy (DR). Over one-third of diabetic persons has some form of DR, and approximately 5-10% develop vision-threatening complications such as proliferative DR and macular edema².

The earliest clinical changes in the diabetic retina occur in the microvasculature and, as such, DR has traditionally been considered to be a vascular disease. Pathological clinical hallmarks of DR include intraretinal hemorrhages, pericyte loss, microaneurysms, lipid exudates, thickening of the lamina basalis, capillary nonperfusion, macular edema and, in the case of proliferative DR, retinal neovascularization and vitreous hemorrhage³. Proliferative DR prevails in patients with type 1 diabetes, but diabetic macular edema (DME) is the primary cause of vision loss in patients with type 2 diabetes. Given the high prevalence of type 2 diabetes, DME is the leading cause of vision loss in the working-age population⁴.

The blood-retinal barrier (BRB)

The retina is part of the central nervous system and is metabolically highly active due to the presence of the photoreceptors – in fact, it has a higher oxygen consumption per unit tissue weight than any other human tissue⁵. To ensure sufficient blood supply to provide oxygen and nutrients to the retina in combination with its functions in vision, it has two distinct vascular beds, *i.e.*, behind the retina the choriocapillaris to feed the retinal pigment epithelium and photoreceptors in the outer retina, and the inner retinal vasculature, emerging from the central retinal artery⁶. The choriocapillaris is a single layer of densely arranged capillaries and consists of fenestrated (leaky) endothelium, facilitating rapid supply of nutrients to the outer retina. In contrast, the retinal circulation that supplies the inner retina is formed by 3 interconnected vascular plexi that have a continuous barrier-type endothelium. This barrier-type endothelium of the retina is analogous to the endothelium that forms the blood-brain barrier. It has no fenestrations and is characterized by a high number of tight and adherens junctions that limit paracellular transport between the endothelial cells, and a paucity of intracellular pinocytotic vesicles to keep transcytosis across the endothelium to a minimum⁷. Together with perivascular cell types like pericytes and glial cells, the endothelial cells of the retina form the neurovascular unit and provide the inner blood-retinal barrier (BRB). This BRB ensures maintenance of homeostasis of the neural retina and protects the retina against potentially harmful substances that are present in the circulation. Although disruption of the BRB is an essential step in the development of retinal disease such as DME, its mechanisms are poorly understood. It is known that focal and diffuse BRB disruption, associated with retinal ischemia caused by capillary non-perfusion⁸, leads to vascular leakage and the development of DME. To date, there are

1

2

3

4

5

6

7

8

&

2 mechanistic explanations at the molecular level for BRB disruption, namely increased paracellular leakage, caused by impaired functioning of tight junctions, or increased transcellular leakage, caused by increased vesicle-mediated transcytosis. Extravasation of plasma proteins such as albumin is crucial in the development of DME⁹, whereas proteins of this size are unlikely to cross the endothelium via paracellular transport⁷. Therefore, increased transcytosis may well be the most important mechanism of the development of DME.

Transcytosis and the role of plasmalemma vesicle-associated protein (PLVAP)

Plasmalemma vesicle-associated protein (PLVAP, also known as PV-1 or FELS) is associated with endothelial transcellular transport. It is an endothelial cell-specific protein that is absent in mature barrier endothelium of the BRB, the blood-brain barrier and the testis^{10, 11}. In pathological conditions, such as DR¹² and glioblastoma¹³⁻¹⁵, PLVAP is upregulated and is associated with loss of barrier function. PLVAP is a structural component of fenestral and stomatal diaphragms of fenestrae, caveolae and trans-endothelial channels¹⁶. In non-barrier endothelium, it is constitutively expressed in capillaries, venules and small- and medium-sized veins¹⁷ and prevents excessive protein leakage into tissues^{18, 19}, a function that is apparently not needed in a properly functioning blood-brain barrier or BRB. Vascular endothelial growth factor (VEGF) is a major inducer of BRB breakdown^{20, 21} and also a driver of PLVAP expression^{20, 22}. However, the exact function of PLVAP in vascular permeability and angiogenesis, specifically in the context of barrier-forming endothelium, is still unclear.

Inflammation as a cause of BRB disruption?

Hypoxia-induced VEGF is one of the main drivers of BRB disruption, but a percentage of patients does not respond sufficiently to anti-VEGF therapies²³. It has been suggested that, in addition to VEGF, proinflammatory cytokines such as tumor necrosis factor (TNF α) and interleukins (IL1 β , IL6, IL8) are also involved in BRB disruption^{24, 25}, because elevated levels of these cytokines have been detected in the vitreous of patients with DR²⁶⁻²⁹. Moreover, VEGF, TNF α and IL1 β affect BRB function in *in vitro* models of the BRB³⁰⁻³² and in (diabetic) animal models^{30, 33, 34} by reducing expression of tight and adherens junctions. In diabetic animal models, leukostasis in BRB capillaries has been associated with the development of sequelae characteristic of preclinical DR^{25, 35}. Add the successful use of glucocorticoid therapy in the treatment of DME into this equation, and the foundation for the assumption that human DR and DME are caused by low-grade chronic inflammation is laid.

On the other hand, small clinical trials of anti-TNF α antibodies or soluble TNF α receptors in patients with ocular diseases such as DME have had limited success to date^{24, 36-39}. Moreover, leukostasis as a causative factor in the development of human DR remains speculative, since *in vivo* assessment of leukostasis in the human retina is not yet possible. Lastly, whereas the anti-inflammatory effects of glucocorticoids are well-known and suggested to be responsible for resolving DME, the beneficial effects on retinal swelling are fast (sometimes within 24 h). This timeframe advocates for direct effects on

the endothelium, rather than for counteracting inflammatory events in the retina, which usually involves transcriptional and translational regulation. Taken together, the relevance and contribution of inflammation as an inducer of BRB disruption and subsequent DME remains controversial.

SCOPE OF THE THESIS

The aim of this thesis is to:

- describe the formation of the BRB during early development at cellular and molecular levels, because understanding of physiological BRB formation may give us insights in the mechanisms of pathological BRB disruption,
- elucidate the role of PLVAP in BRB formation and disruption, and
- critically evaluate the contribution and possible mechanisms of inflammatory conditions in the development of DME and DR.

In part I of the thesis, a detailed overview of the formation of the BRB and the role of PLVAP in barrier endothelium is given. The retinal vasculature develops postnatally in mice, and thus neonatal mice are an excellent animal model to study BRB development. In **chapter 2**, the temporal and spatial recruitment of the neurovascular unit in the neonatal mouse retina is described, using retinal wholemounts of mice from postnatal day (P) 3 to P25. We apply fluorescence immunohistochemistry to stain the retinal vasculature, pericytes and astrocytes and assess expression of different markers of polarized astrocytic end-feet and pericytes. In **chapter 3**, BRB formation in neonatal mouse retinas is studied at the molecular level, with a specific focus on PLVAP and proteins involved in paracellular transport, transcellular transport and VEGF signaling. Transgenic heterozygous *Plvap* mice have been used as an animal model to determine the role of PLVAP in formation of the BRB and retinal vasculature. **Chapter 4** describes the role of PLVAP in VEGF-induced and hypoxia-induced retinal permeability by knocking down PLVAP expression in an *in vitro* BRB model and in the mouse oxygen-induced retinopathy model.

In part II of this thesis, the contribution of inflammation to BRB disruption is studied. **Chapter 5** is a critical review of the current literature on the involvement of leukostasis in the development of human DR. In **chapter 6**, the role of TNF α in the induction of endothelial permeability and its mechanism is investigated in an *in vitro* BRB model. In **chapter 7**, the effects of glucocorticoids that are used in the clinic and mechanisms of action of glucocorticoid-induced barrier enhancement are studied in an *in vitro* BRB model.

1

2

3

4

5

6

7

8

&

REFERENCES

- Guariguata L, Whiting DR, Hambleton I, Beagley J, Linnenkamp U, Shaw JE. Global estimates of diabetes prevalence for 2013 and projections for 2035. *Diabetes Res Clin Pract* 2014;103:137-149.
- Yau JW, Rogers SL, Kawasaki R, et al. Global prevalence and major risk factors of diabetic retinopathy. *Diabetes Care* 2012;35:556-564.
- Garner A. Histopathology of diabetic retinopathy in man. *Eye* 1993;7:250-253.
- Ding J, Wong TY. Current epidemiology of diabetic retinopathy and diabetic macular edema. *Curr Diab Rep* 2012;12:346-354.
- Arden GB, Sidman RL, Arap W, Schlingemann RO. Spare the rod and spoil the eye. *Br J Ophthalmol* 2005;89:764-769.
- Hildebrand GD, Fielder AR. Anatomy and physiology of the retina. In: Reynolds J, Olitsky S (eds), *Pediatric Retina*. Berlin Heidelberg: Springer-Verlag; 2011:39-65.
- Abbott NJ, Patabendige AA, Dolman DE, Yusof SR, Begley DJ. Structure and function of the blood-brain barrier. *Neurobiol Dis* 2010;37:13-25.
- Mathews MK, Merges C, McLeod DS, Luttj GA. Vascular endothelial growth factor and vascular permeability changes in human diabetic retinopathy. *Invest Ophthalmol Vis Sci* 1997;38:2729-2741.
- Cunha-Vaz JG, Travassos A. Breakdown of the blood-retinal barriers and cystoid macular edema. *Surv Ophthalmol* 1984;28 Suppl:485-492.
- Schlingemann RO, Hofman P, Anderson L, Troost D, van der Gaag R. Vascular expression of endothelial antigen PAL-E indicates absence of blood-ocular barriers in the normal eye. *Ophthalmic Res* 1997;29:130-138.
- Stan RV, Ghitescu L, Jacobson BS, Palade GE. Isolation, cloning, and localization of rat PV-1, a novel endothelial caveolar protein. *J Cell Biol* 1999;145:1189-1198.
- Schlingemann RO, Hofman P, Vrensen GF, Blaauwgeers HG. Increased expression of endothelial antigen PAL-E in human diabetic retinopathy correlates with microvascular leakage. *Diabetologia* 1999;42:596-602.
- Leenstra S, Troost D, Das PK, Claessen N, Becker AE, Bosch DA. Endothelial cell marker PAL-E reactivity in brain tumor, developing brain, and brain disease. *Cancer* 1993;72:3061-3067.
- Schlingemann RO, Bots GTAM, Van Duinen SG, Ruiter DJ. Differential expression of endothelium-specific antigen PAL-E in vasculature of brain tumors and preexistent brain capillaries. *Annals of the New York Academy of Sciences* 1988;529:111-114.
- Carson-Walter EB, Hampton J, Shue E, et al. Plasmalemmal vesicle associated protein-1 is a novel marker implicated in brain tumor angiogenesis. *Clin Cancer Res* 2005;11:7643-7650.
- Stan RV. Multiple PV1 dimers reside in the same stomatal or fenestral diaphragm. *Am J Physiol Heart Circ Physiol* 2004;286:H1347-1353.
- Schlingemann RO, Dingjan GM, Emeis JJ, Blok J, Warnaar SO, Ruiter DJ. Monoclonal-antibody PAL-E specific for endothelium. *Lab Invest* 1985;52:71-76.
- Herrnberger L, Seitz R, Kuespert S, Bosl MR, Fuchshofer R, Tamm ER. Lack of endothelial diaphragms in fenestrae and caveolae of mutant Plvap-deficient mice. *Histochem Cell Biol* 2012;138:709-724.
- Stan RV, Tse D, Deharvengt SJ, et al. The diaphragms of fenestrated endothelia: gatekeepers of vascular permeability and blood composition. *Dev Cell* 2012;23:1203-1218.
- Hofman P, Blaauwgeers HG, Tolentino MJ, et al. VEGF-A induced hyperpermeability of blood-retinal barrier endothelium in vivo is predominantly associated with pinocytotic vesicular transport and not with formation of fenestrations. *Curr Eye Res* 2000;21:637-645.
- Hofman P, Blaauwgeers HG, Vrensen GF, Schlingemann RO. Role of VEGF-A in endothelial phenotypic shift in human diabetic retinopathy and VEGF-A-induced retinopathy in monkeys. *Ophthalmic Res* 2001;33:156-162.
- Strickland LA, Jubb AM, Hongo JA, et al. Plasmalemmal vesicle-associated protein (PLVAP) is expressed by tumour endothelium and is upregulated by vascular endothelial growth factor-A (VEGF). *J Pathol* 2005;206:466-475.
- Ford JA, Lois N, Royle P, Clar C, Shyangdan D, Waugh N. Current treatments in diabetic macular oedema: systematic review and meta-analysis. *BMJ Open* 2013;3.
- Arias L, Caminal JM, Badia MB, Rubio MJ, Catala J, Pujol O. Intravitreal infliximab in patients with macular degeneration who are nonresponders to anti-vascular endothelial growth factor therapy. *Retina* 2010;30:1601-1608.
- Joussen AM, Poulaki V, Mitsiades N, et al. Nonsteroidal anti-inflammatory drugs prevent early diabetic retinopathy via TNF-alpha suppression. *FASEB J* 2002;16:438-440.
- Cicik E, Tekin H, Akar S, et al. Interleukin-8, nitric oxide and glutathione status in proliferative vitreoretinopathy and proliferative diabetic retinopathy. *Ophthalmic Res* 2003;35:251-255.
- Funatsu H, Noma H, Mimura T, Eguchi S. Vitreous inflammatory factors and macular oedema. *Br J Ophthalmol* 2012;96:302-304.
- Koskela UE, Kuusisto SM, Nissinen AE, Savolainen MJ, Liinamaa MJ. High vitreous concentration of IL-6 and IL-8, but not of adhesion molecules in relation to plasma concentrations in proliferative diabetic retinopathy. *Ophthalmic Res* 2013;49:108-114.

29. Zhou J, Wang S, Xia X. Role of intravitreal inflammatory cytokines and angiogenic factors in proliferative diabetic retinopathy. *Curr Eye Res* 2012;37:416-420.
30. Avelaira CA, Lin CM, Abcouwer SF, Ambrosio AF, Antonetti DA. TNF-alpha signals through PKCzeta/NF-kappaB to alter the tight junction complex and increase retinal endothelial cell permeability. *Diabetes* 2010;59:2872-2882.
31. Forster C, Burek M, Romero IA, Weksler B, Couraud PO, Drenckbahni D. Differential effects of hydrocortisone and TNF alpha on tight junction proteins in an in vitro model of the human blood-brain barrier. *J Physiol-London* 2008;586:1937-1949.
32. Harhaj NS, Felinski EA, Wolpert EB, Sundstrom JM, Gardner TW, Antonetti DA. VEGF activation of protein kinase C stimulates occludin phosphorylation and contributes to endothelial permeability. *Invest Ophthalm Vis Sci* 2006;47:5106-5115.
33. Huang H, Gandhi JK, Zhong X, et al. TNFalpha is required for late BRB breakdown in diabetic retinopathy, and its inhibition prevents leukostasis and protects vessels and neurons from apoptosis. *Invest Ophthalmol Vis Sci* 2011;52:1336-1344.
34. Qaum T, Xu QW, Joussen AM, et al. VEGF-initiated blood-retinal barrier breakdown in early diabetes. *Invest Ophthalm Vis Sci* 2001;42:2408-2413.
35. Schroder S, Palinski W, Schmid-Schonbein GW. Activated monocytes and granulocytes, capillary nonperfusion, and neovascularization in diabetic retinopathy. *Am J Pathol* 1991;139:81-100.
36. Sfikakis PP, Grigoropoulos V, Emfietzoglou I, et al. Infliximab for diabetic macular edema refractory to laser photocoagulation: a randomized, double-blind, placebo-controlled, crossover, 32-week study. *Diabetes Care* 2010;33:1523-1528.
37. Sfikakis PP, Markomichelakis N, Theodossiadis GP, Grigoropoulos V, Katsilambros N, Theodossiadis PG. Regression of sight-threatening macular edema in type 2 diabetes following treatment with the anti-tumor necrosis factor monoclonal antibody infliximab. *Diabetes Care* 2005;28:445-447.
38. Tsilimbaris MK, Panagiotoglou TD, Charisis SK, Anastasakis A, Krikonis TS, Christodoulakis E. The use of intravitreal etanercept in diabetic macular oedema. *Semin Ophthalmol* 2007;22:75-79.
39. Wu L, Hernandez-Bogantes E, Roca JA, Arevalo JF, Barraza K, Lasave AF. intravitreal tumor necrosis factor inhibitors in the treatment of refractory diabetic macular edema: a pilot study from the Pan-American Collaborative Retina Study Group. *Retina* 2011;31:298-303.

1

2

3

4

5

6

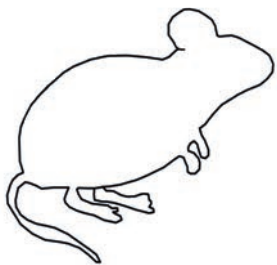
7

8

&



**DEVELOPMENT OF THE BRB
AND THE ROLE OF PLVAP
IN BRB DEVELOPMENT AND
DISRUPTION**



2

Spatial and temporal recruitment of the neurovascular unit during development of the mouse blood-retinal barrier

Anne-Eva van der Wijk,^{1,2} Ilse M.C. Vogels,^{1,2} Henk A. van Veen,³ Cornelis J.F. van Noorden,^{2,4} Reinier O. Schlingemann,^{1,5} Ingeborg Klaassen^{1,2*}

¹ Ocular Angiogenesis Group, Departments of Ophthalmology and ² Medical Biology, Academic Medical Center, University of Amsterdam, Amsterdam, The Netherlands

³ Electron Microscopy Center Amsterdam, Department of Medical Biology, Academic Medical Center, University of Amsterdam, Amsterdam, The Netherlands

⁴ Department of Genetic Toxicology and Cancer Biology, National Institute of Biology, Ljubljana, Slovenia

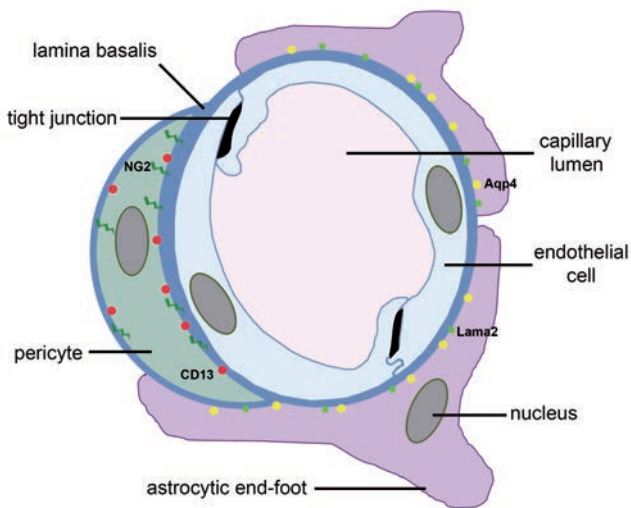
⁵ Department of Ophthalmology, University of Lausanne, Jules-Gonin Eye Hospital, Fondation Asile des Aveugles, Lausanne, Switzerland

Tissue and Cell. (2018) 52: 42-50

ABSTRACT

The inner blood-retinal barrier (BRB) is made up by the neurovascular unit, consisting of endothelial cells, pericytes and glial cells. The BRB maintains homeostasis of the neural retina, but in pathological eye conditions the neurovascular unit is often disrupted, causing BRB loss. Here, we investigated in detail the temporal and spatial recruitment of the neurovascular unit in the neonatal mouse retina from postnatal day (P)3 to P25 employing immunohistochemical staining of the vascular endothelium (isolectin B4), pericytes (α -SMA and NG2) and astrocytes (GFAP). In addition, we investigated gene expression of polarized astrocytic end-feet markers aquaporin-4 and laminin α 2 chain with qPCR. We observed GFAP-positive cells migrating ahead of the retinal vasculature during the first postnatal week, suggesting that the retinal vasculature follows an astrocytic meshwork. From P9 onwards, astrocytes acquired a mature phenotype, with a more stellate shape and increased expression of aquaporin-4. NG2-positive cells and tip cells co-localized at P5 and invaded the retina together as a vascular sprouting front. Together, these data suggest that recruitment of the cell types of the neurovascular unit is a prerequisite for proper retinal vascularization and BRB formation.

The neurovascular unit



1. INTRODUCTION

The neural retina is protected by the inner blood-retinal barrier (BRB), which maintains homeostasis by selectively regulating the entry of molecules into the retina and controlling vascular permeability (Klaassen et al., 2013). The BRB consists of endothelial cells lining the retinal microvessels, pericytes, their basal lamina and glial cells, together forming the neurovascular unit. The presence and crosstalk between these cell types in the neurovascular unit is essential for the maintenance of a tight BRB (Wisniewska-Kruk et al., 2012).

In humans, the retinal vasculature is completed around mid-gestation (Gariano, 2003), but in mice, retinal vascular development starts in the first postnatal week. The retinal vasculature provides oxygen and nutrients to the inner retina, which has several (anatomically tightly-arranged) cellular layers that contain interneurons, ganglion cells and glial cells. Vessels grow from the optic disc into the ganglion cell layer (containing ganglion cells, amacrine cells and (peri-)vascular cells) and radiate outwards to the periphery, that is reached around postnatal day (P) 7. From this superficial vascular plexus, collateral sprouting of capillaries into the inner plexiform layer (where photoreceptor input is processed through bipolar cells, amacrine cells and ganglion cells) and into the inner nuclear layer up to the boundaries of the outer plexiform layer (where photoreceptor cells form connections with bipolar cells and horizontal cells) initiates generation of the interconnected intermediate and deep capillary layers (Fruttiger, 2007). The retinal pigment epithelium and photoreceptors are part of the outer retina and are supplied with oxygen and nutrients by a different vascular bed, the choriocapillaris, which is not discussed here.

Initially, the retinal vasculature lacks a functional barrier during development, as is demonstrated by leakage of plasma proteins and small molecules from the lumen of the vessels (Chow and Gu, 2017; van der Wijk et al., submitted). Recruitment of pericytes and astrocytes to the retina to form the neurovascular unit may be crucial for final maturation of the endothelium and for the formation of a functional BRB.

Previously, it has been shown that astrocytes serve as a meshwork for growing vessels in the retina, thereby guiding endothelial cell migration (Dorrell et al., 2002; O'Sullivan et al., 2017). In addition, pericytes may be involved in the early formation of the BRB by providing a suitable microenvironment for retinal endothelial cells to develop barrier characteristics, as was shown in blood-brain barrier development (Daneman et al., 2010). Moreover, permeability of the blood-brain barrier in neonatal mice inversely correlated with pericyte coverage (Armulik et al., 2010; Daneman et al., 2010), confirming the essence of pericytes in barrier integrity. As the pericyte-to-endothelial ratio is relatively high in the retina (1:1), when compared to brain (1:3) and other microvascular beds (1:10) (Stewart and Tuor, 1994) such a function of pericytes may be particularly important in the BRB.

In the present study, we investigated in detail the temporal and spatial composition of the neurovascular unit in the neonatal mouse retina using gene and protein expression of selected markers of retinal pericytes and astrocytic end-feet.

1

2

3

4

5

6

7

8

&

2. MATERIALS AND METHODS

2.1. Animals

Animal experiments were performed with the approval of the Animal Ethics Committee of the University of Amsterdam and in compliance with the Association for Research in Vision and Ophthalmology (ARVO) Statement for the Use of Animals in Ophthalmic and Vision Research. To study the development of the BRB, neonatal (wildtype) mice were killed on P3, P5, P7, P9, P11, P13, P15, P17 and P25 with an intracardial injection of ketamine-medetomidine-atropine for young mice (until P13), whereas older mice were euthanized with CO₂ asphyxiation. Eyes were enucleated and either snapfrozen in liquid nitrogen (for qPCR or immunohistochemistry) or processed immediately for retinal wholemount staining.

2.2. RNA isolation and mRNA quantification

Retinas (at least 6 to 8 retinas per group) were treated by hypotonic lysis to enrich for retinal vessels (Kowluru et al., 1998). Each retina was incubated in 1 ml sterile water for 2 h at 4 °C. Next, retinas were spun down and sterile water was replaced with sterile water containing 40 µg DNase I (Life Technology, Breda, The Netherlands) and left for 5 min at room temperature. Retinas were spun down, supernatant was removed and the retinal vessels were resuspended in 500 µl TRIzol reagent (Invitrogen, Bleiswijk, The Netherlands) and stored at -20 °C until further processing. Total RNA was isolated according to the manufacturer's protocol and dissolved in RNase-free water. RNA yield was measured using a NanoDrop spectrophotometer (Thermo Scientific, Wilmington, DE) and 1 µg of RNA was treated with DNase-I (Invitrogen) and reverse transcribed into first strand cDNA with a Maxima First Strand cDNA Synthesis Kit (ThermoFisher). Real-time quantitative PCR was performed on 20x diluted cDNA samples using a CFX96 system (Bio-Rad, Hercules, CA) as described previously (Klaassen et al., 2009). Specificity of the primers was confirmed by NCBI BLAST. The presence of a single PCR product was verified by both the presence of a single melting temperature peak and detection of a single band of the expected size on 3% agarose gel. Non-template controls were included to verify the method and the specificity of the primers. Relative gene expression was calculated using the equation: $R = E - Ct$, where E is the mean efficiency of all samples for the gene being evaluated and Ct is the cycle threshold for the gene as determined during real-time PCR. Primer efficiencies (E) were determined with LinRegPCR software (Ruijter et al., 2009) and ranged from 1.631 to 1.973. PCR products that did not show a single melting temperature peak were excluded from analysis. Expression data was normalized by the global mean normalization method (Mestdagh et al., 2009) using expression data of 30 genes in total.

2.3. Retinal wholemount staining

Enucleated mouse eyes were washed in PBS and fixed in 4% paraformaldehyde for 5 min, transferred to 2x PBS for 10 min and retinas were dissected in PBS. Isolated retinas were post-

fixed in methanol and stored in -20 °C until further use. For immunofluorescence staining, retinas were briefly washed in 2x PBS and incubated in wholemount-blocking buffer (1% fetal calf serum, 3% TritonX-100, 0.5% Tween20, 0.2% sodium azide in 2x PBS) for 2 h at room temperature. Next, retinas were incubated overnight with the following antibodies: rabbit anti-gial fibrillary acidic protein (diluted 1:400, Cat # Z0334; GFAP; Dako, Heverlee, Belgium), mouse monoclonal anti-alpha-smooth muscle actin (α -SMA) antibody (diluted 1:200, Cat # C6198; Cy3 labeled, Sigma-Aldrich, Zwijndrecht, The Netherlands), isolectin B4 (diluted 1:30, Cat # I21411; Alexa Fluor-488 labeled, Invitrogen) or rabbit polyclonal anti-NG2 antibody (diluted 1:100, kindly provided by prof. W. Stallcup from the Burnham Institute, La Jolla, CA) diluted in wholemount blocking buffer. GFAP was used as a marker for astrocytes, α -SMA as marker for smooth muscle cells and pericytes, isolectin B4 was used to detect endothelial cells and NG2 was used as marker for pericytes. After 3 wash steps (3 times 30 min in wholemount blocking buffer), secondary antibody was added and wholemounts were incubated for 2-3 h (goat-anti-rabbit Alexa Fluor-633 or goat-anti-rabbit Cy3; Invitrogen, diluted 1:100 in wholemount blocking buffer). After overnight washing in wholemount blocking buffer, retinas were mounted on glass and covered in Vectashield (Vector Laboratories, Burlingame, CA). All staining procedures were performed under gentle agitation at room temperature.

For staining of the cryostat sections, samples were fixed for 10 min using 4% paraformaldehyde, permeabilized for 10 min with 0.2% Triton X-100 and blocked for 1 h with 10% normal goat serum. Staining was done in wholemount blocking buffer with anti-rabbit Apq4 (diluted 1:100, Cat # AB2218; Millipore, Amsterdam, The Netherlands) for 2 h, followed by secondary antibody incubation (goat-anti-rabbit Cy3) for 1 h.

Images of retinal wholemounts were taken at the central retina (at the site of the optic disc), the middle retina and the peripheral retina and were captured using a confocal laser scanning microscope SP8 (Leica Microsystems, Wetzlar, Germany) with a 20x or 63x objective at the Cellular Imaging Core Facility of the Academic Medical Center. Specificity of the staining was checked by absence of fluorescent signal in samples that were stained in the absence of primary antibody.

2.4. Transmission electron microscopy (TEM)

Eyes were harvested and immersion fixed in McDowell fixative in phosphate buffer. To facilitate access of the fixative into the eye, eyes were punctured with a 29 G (which equals diameter of 0.287 mm) needle and the cornea was dissected. Samples were processed for routine TEM, as described previously (Wisniewska-Kruk et al., 2016). Ultrathin sections of 80 nm were examined with a FEI Technai-12 G2 Spirit Biotwin microscope and micrographs were captured with a Veleta TEM camera (Emsis; Münster, Germany) using Radius acquisition software (Emsis) at a magnification of 11.000-30.000 x, at the Electron Microscopy Center of the Academic Medical Center.

1

2

3

4

5

6

7

8

&

3. RESULTS AND DISCUSSION

3.1. Ultrastructure of the neurovascular unit

The close association of endothelial cells and pericytes, which share their basal lamina, and glial cells, which envelope the retinal vessels with their end-feet and a second basal lamina, is referred to as the neurovascular unit of the BRB in the mature retina (Fig. 1A-C). The endothelial cells of the BRB have no fenestrations, few pinocytotic vesicles and a continuous array of inter-endothelial tight junctions, which seal the intercellular space between endothelial cells (Klaassen et al., 2013)(Fig. 1B and b).

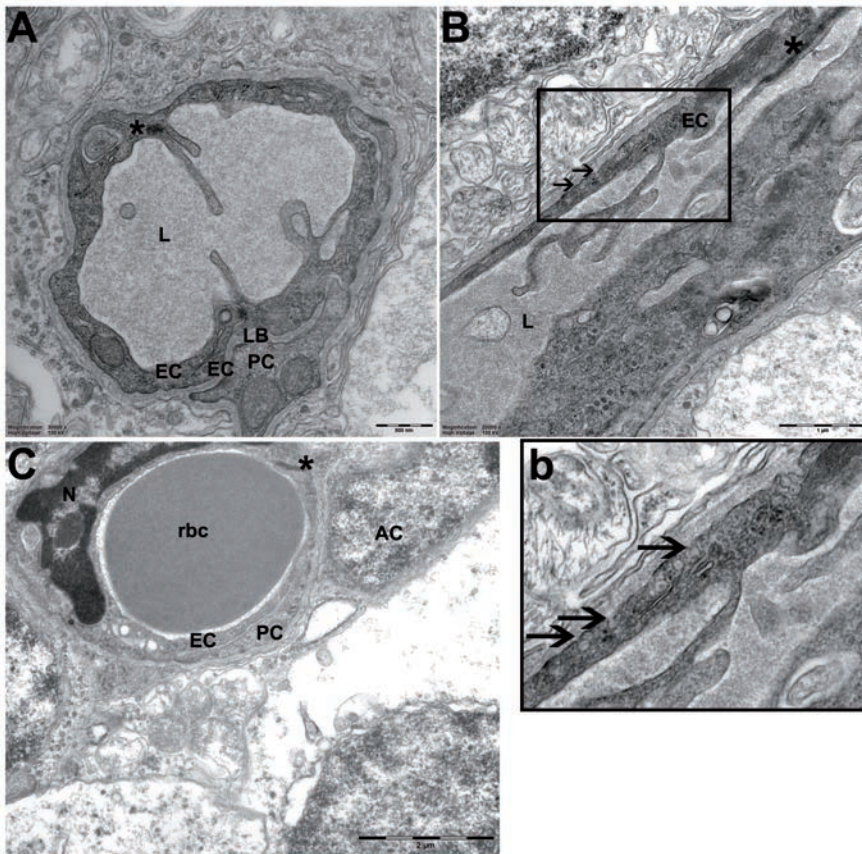


Figure 1. Ultrastructure of the neurovascular unit of the BRB of a mouse at P30. (A) Endothelial cells and pericytes share a basal lamina and are in close association. (B) Endothelial cells of the BRB have few pinocytotic vesicles and tight junctions seal the intercellular space in between endothelial cells, (b) is a magnification of the boxed region in (B). (C) Astrocytic end-feet envelope the retinal vessels and are in contact with pericytes and endothelial cells. EC = endothelial cell, PC = pericyte, AC = astrocyte, LB = basal lamina, L = vessel lumen, N = nucleus, rbc = red blood cell, * = tight junction, black arrow = abluminal caveola. Scale bar = 500 nm (A), 1 μ m (B), 2 μ m (C).

3.2. An astrocytic meshwork precedes the vascular sprouting front during retinal development

Astrocytes have been shown to induce barrier properties of blood-brain barrier and BRB cells *in vitro* (Nakagawa et al., 2009; Wisniewska-Kruk et al., 2012), and they are a major source of VEGF production in conditions with pathological retinal vascularization (West et al., 2005). Confirming previous studies, the retinal vasculature appeared to follow an astrocytic meshwork when forming the superficial vascular plexus during development (Fig. 2A)(Dorrell et al., 2002; Gariano and Gardner, 2005; O'Sullivan et al., 2017), as detected by staining for GFAP in retinal wholemounts. GFAP-positive cells emerged from the optic disc and were found in close contact with retinal vessels in the ganglion cell layer at all time points (Fig. 2A-I), but not in the intermediate and deep capillary layers (data not shown). The time of appearance of glial cells during vascular development is different between retina and brain. In the rat cerebral cortex, angiogenesis begins as early as E12, whereas astrocytes are first generated directly after birth, and physical contact with vessels is made during the first postnatal week (Daneman et al., 2010). In the retina, astrocytes appear before vascularization, and both ablation of astrocytes altogether, or shortly after birth during early postnatal development, resulted in severely impaired retinal vascularization and mispatterning of growing vessels (O'Sullivan et al., 2017), suggesting that the role of astrocytes in vascularization of the retina is more critical than in the brain. In the retina, astrocytes are tightly wrapped around arteries and even more so around veins (Fig. 2C-I), and GFAP expression is stronger in the central retina as compared to the middle and peripheral retina (Fig. 2C). From P9 onwards, the astrocytes had a more stellate shape (Fig. 2D-I), indicating a more mature astrocyte phenotype (West et al., 2005).

Astrocytes make contact with blood vessels through their astrocytic end-feet, which are polarized structures that firmly attach to the abluminal surface of capillaries (Abbott et al., 2006). We investigated the developmental expression pattern of 2 markers for the polarized astrocytic end-feet, aquaporin 4 (Aqp4) and laminin $\alpha 2$ chain (Lama2). Expression of Aqp4, a water channel protein involved in the control of ion concentration and volume regulation (Nagelhus et al., 1998), increased significantly during development. There was very low mRNA expression during the first postnatal week, followed by a steep increase from P9 to P15 (Fig. 2J). This was confirmed at the protein level in retinal cryostat sections, where there was no Aqp4 expression at P5 (data not shown) and only few Aqp4-positive cells around vessels in the ganglion cell layer at P9 (Fig. 2L). At P13 and P25, strong Aqp4 expression was observed around retinal vessels in all the 3 vascular layers (Fig. 2M-O). This pattern may be consistent with astrocyte end-feet, as it coincided with the time point that astrocytes acquire a stellate shape (Fig. 2D), a phenotype which suggests that the cells have become mature and polarized. Aqp4 is also expressed by horizontal cells and Müller cells (Bosco et al., 2005; Hamann et al., 1998), but the staining pattern we observed was not consistent with the localization of these cell types. It has been suggested that the specific Aqp4 localization at the end-feet membrane of astrocytes allows transcellular water redistribution and the maintenance of extracellular osmolality during neuronal activity, without inducing inappropriate volume changes in the extracellular space (Hamann et al.,

1

2

3

4

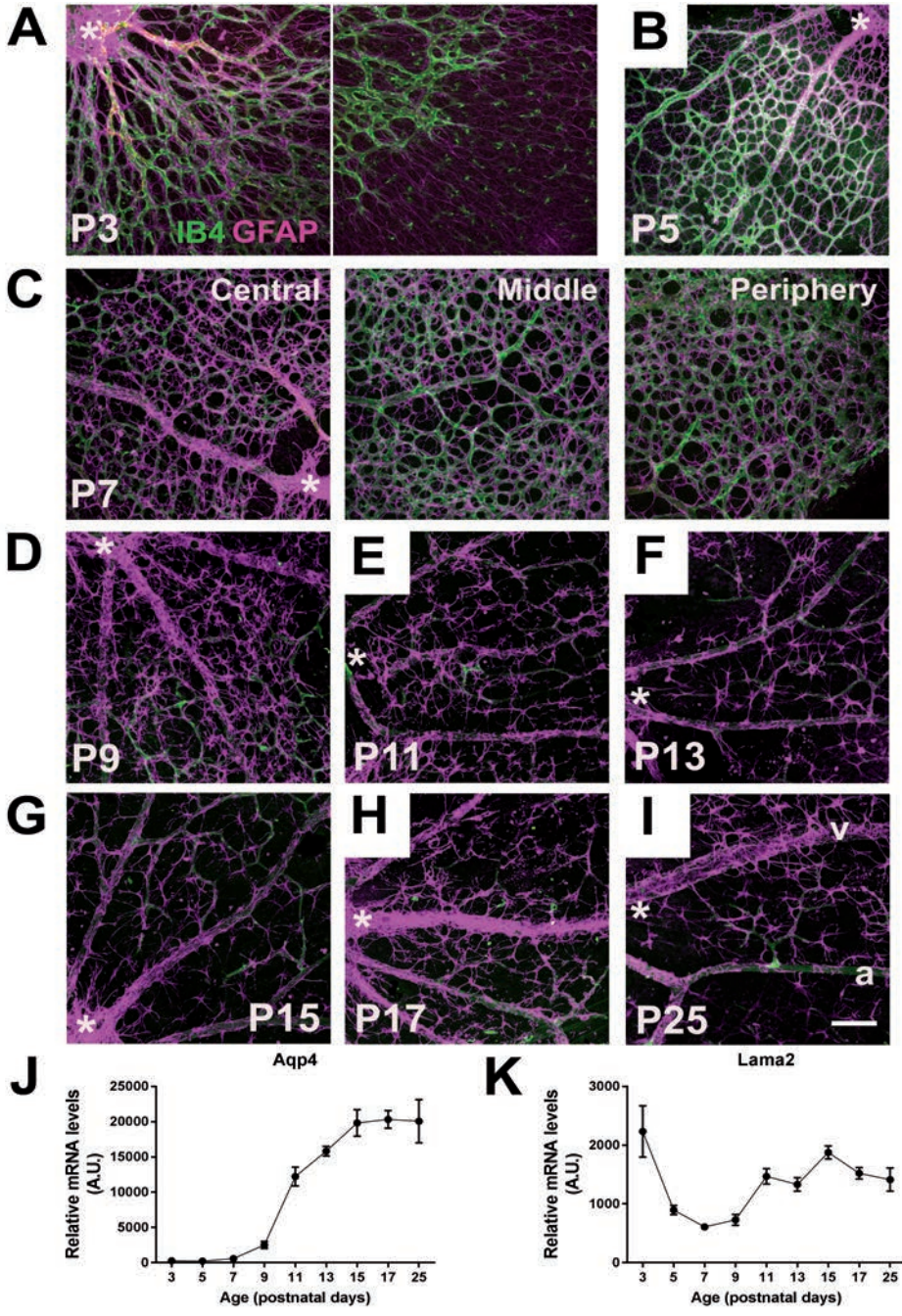
5

6

7

8

&



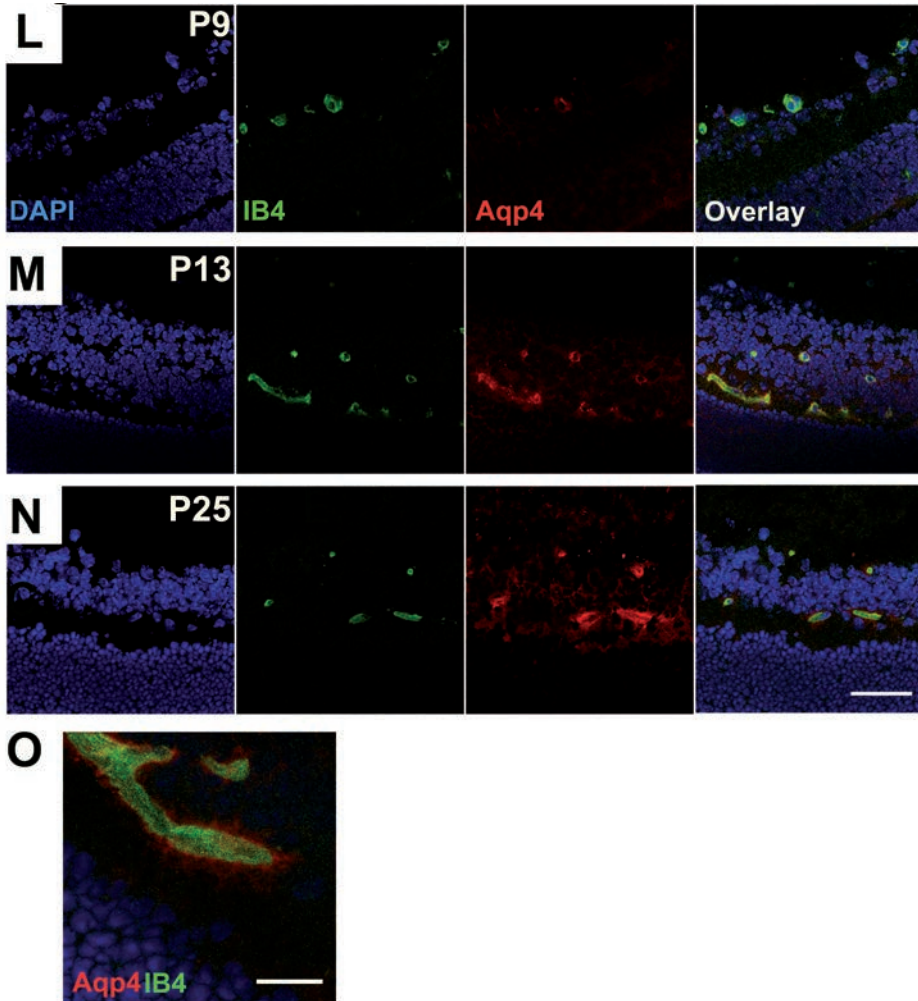


Figure 2. Astrocytes precede the retinal vasculature during development. (A) At P3, astrocytes emerge from the optic disc (indicated by an asterisk) and an astrocytic meshwork was preceding the retinal vasculature, as shown with immunostaining of retinal wholemounts for GFAP (purple). Vasculature is stained by using isolectin B4 (green). GFAP-positive cells are found in close association with retinal vessels in the superficial vascular plexus at (B) P5, (C) P7, (D) P9, (E) P11, (F) P13, (G) P15, (H) P17 and (I) P25. mRNA expression of the marker for polarized astrocytic end-feet Aqp4 (J) increases during development of the retina, whereas (K) Lama2 mRNA levels decrease from P3 to P7-9 and stabilize from P9 onwards. $n=7-11$ for all time points. Data are depicted as mean \pm s.d. At the protein level, we observed a few Aqp4-positive cells in the ganglion cell layer at P9 (L), as shown with retinal cryostat sections. At P13 (M) and P25 (N), there was strong Aqp4 expression around retinal vessels in all the 3 vascular layers. (O) Higher magnification of a retinal vessel which is enveloped by Aqp4-expressing astrocytic end-feet. In (L-O), brightness of the IB4 and Aqp4 signal was enhanced to the same extent at all ages, to improve clarity. IB4 = isolectin B4, GFAP = glial fibrillary acidic protein, Aqp4 = aquaporin 4, a = artery, v = vein, * = optic disc. Scale bar (A-I) = 100 μ m, (L-N) = 50 μ m, (O) = 15 μ m.

1998; Nagelhus et al., 1998). If this is the case, the marked increase in retinal perivascular Aqp4 expression between P9 and P15, in either astrocytes and/or other glial cells, may be related to the opening of the mouse eye (around P14), which is preceded by increased spontaneous retinal waves (i.e., bursts of action potentials among neighboring retinal ganglion cells)(Ackman et al., 2012; Rochefort et al., 2009; Thompson et al., 2017).

Besides the shared basal lamina of endothelial cells and pericytes, astrocytes provide a second basal lamina that is in contact with the retinal endothelial cells (Fig. 1C). Lama2 is an astrocyte-derived basal lamina component, and also a marker of polarized astrocytic end-feet. In the blood-brain barrier, Lama2 expression is critically involved in gliovascular-pericyte interactions (Armulik et al., 2010; Menezes et al., 2014). Moreover, *Lama2*^{-/-} mice had significant vascular abnormalities and a defective (leaky) blood-brain barrier (Menezes et al., 2014). During development, we observed a ~2-fold decrease in Lama2 mRNA expression from P3 to P7-9, and stable Lama2 mRNA expression from P11 onwards (Fig. 2K).

3.3. Expression of alpha-smooth muscle actin (α -SMA) increases during retinal development

The interaction of smooth muscle cells and pericytes with endothelial cells is crucial for vessel stabilization. Unlike pericytes in other parts of the body, pericytes of the central nervous system are considered to originate from the neural crest (reviewed in Armulik et al., 2011). α -SMA is the predominant actin isoform found in smooth muscle cells, and is also expressed by a subset of mature pericytes (Nehls and Drenckhahn, 1991). In the retinal vasculature, expression of α -SMA is associated with smooth muscle cell and pericyte maturation and vessel stability (Benjamin et al., 1998). Smooth muscle cells and pericytes express growth factors that regulate whether vessels are stable or undergo remodeling. Therefore a role has been suggested for these cells in pruning of retinal vessels during the formation of a highly organized vasculature (Uemura et al., 2002). Here, we observed a relative decrease in α -SMA mRNA expression during development (Fig. 3A). However, at P3, α -SMA protein expression was weak and only visible in the most proximal part of vessels of the central retina (Fig. 3B), indicating that there is a proximal-to-distal gradient of maturation in the retinal vessels, as has been reported previously (Fruttiger, 2007; Hughes and Chan-Ling, 2004). α -SMA protein expression increased during maturation of the retinal vasculature (Fig. 3B-J) and this allowed for the identification of arteries and veins, since α -SMA is expressed in higher amounts around arteries (characterized by tightly packed actin filaments) than veins (with a more diffuse and patchy staining, Fig. 3K; (Hughes and Chan-Ling, 2004)), and is not expressed around capillaries (data not shown). Of course, we cannot infer from these data whether α -SMA expression had any effect on the vascular remodeling processes that occur in the 2 weeks after birth. However, in α -SMA null mice, differences in retinal vascular patterning were not observed when compared to wildtype mice, and all vessels were covered by smooth muscle cells and pericytes, suggesting that α -SMA expression is not necessary for the development of a normal retinal vascular pattern (Tomasek et al., 2006). Nevertheless, lack of α -SMA expression resulted in altered BRB

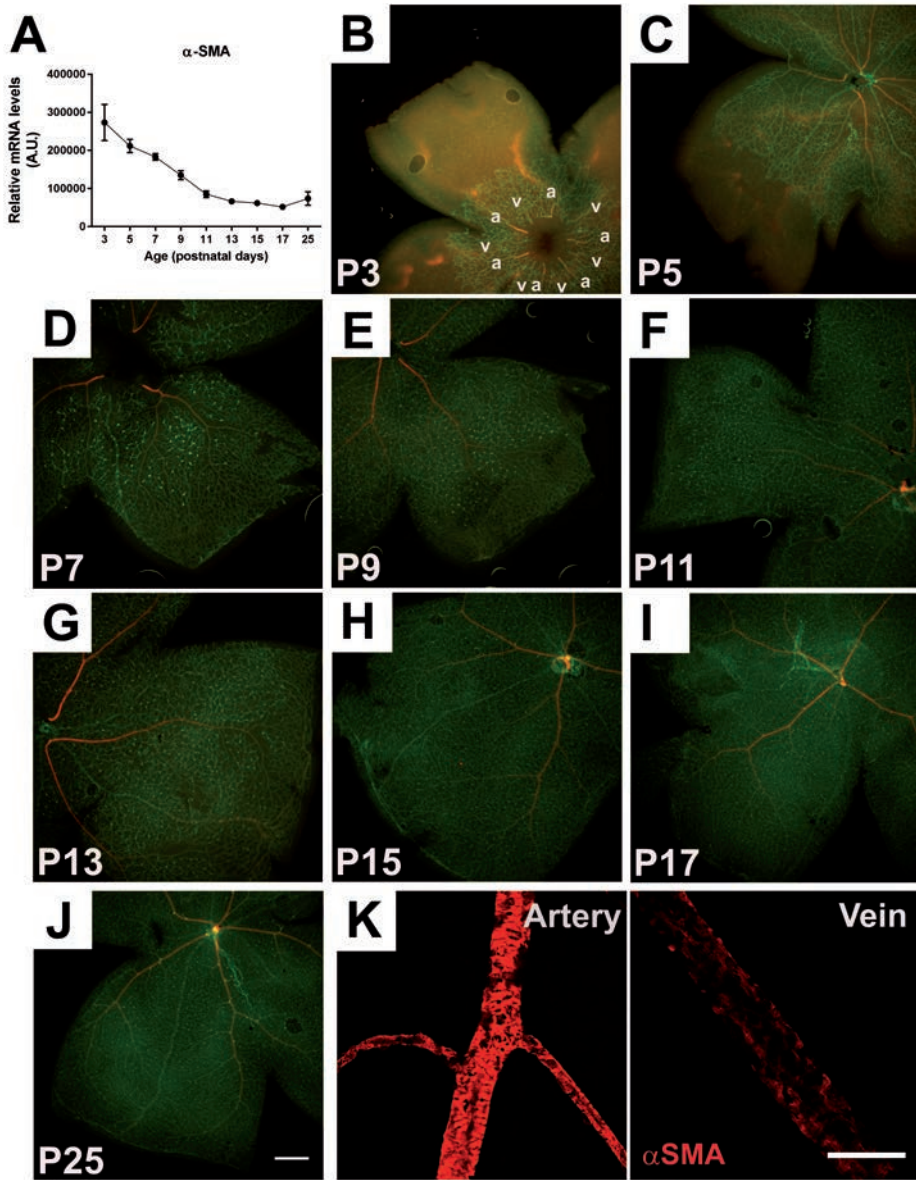


Figure 3. Expression of α -SMA increases during development. (A) mRNA of α -SMA decreases during development. $n=7-11$ for all time points. Data are depicted as mean \pm s.d. (B) At P3, α -SMA expression (red) is weak and only expressed at the most proximal part of vessels in retinal wholemounts. Retinal vessels are stained with isolectin B4 (green). Expression of α -SMA protein increases during development in retinal wholemounts at (C) P5, (D) P7, (E) P9, (F) P11, (G) P13, (H) P15, (I) P17 and (J) P25. In (A-I), green and red levels were adjusted to improve clarity. (K) In arteries, α -SMA expression is strong and characterized by tightly packed actin filaments, whereas α -SMA staining in veins is more diffuse and patchy. IB4 = isolectin B4, α -SMA = alpha-smooth muscle actin, a = artery, v = vein. Scale bar (B-J) $\sim 450 \mu\text{m}$. Scale bar (K) = $50 \mu\text{m}$.

function, including increased BRB permeability and decreased retinal function (Tomasek et al., 2006). Therefore, the presence of α -SMA appears to be crucial for a fully functional BRB.

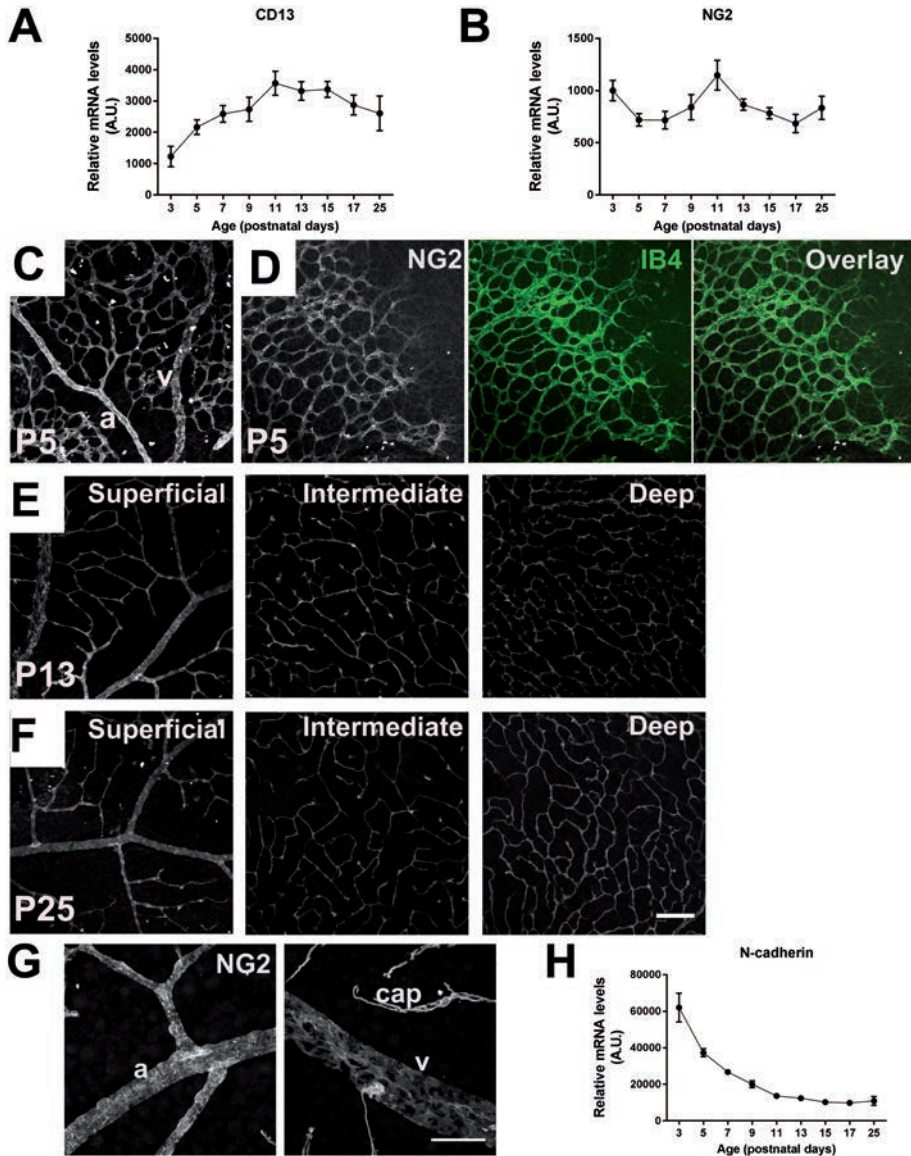


Figure 4. Pericytes precede the vascular sprouting front during retinal development. (A) Expression of CD13 mRNA in the retina increases during development, and stabilizes around P11. (B) Expression of NG2 mRNA is relatively stable during retinal development. $n=7-11$ for all time points. Data are depicted as mean \pm s.d. (C) At P5, NG2 protein expression (white) is visualized in retinal wholemounts

(continued) and show pericytes ensheathing arteries, capillaries and veins. (D) At P5, NG2-positive cells are in close proximity of tip cells in the retinal sprouting front stained with isolectin B4 (green) in the ganglion cell layer. Perivascular NG2 staining is observed in the superficial vascular plexus, and the intermediate and deep capillary layers at P13 (E) and P25 (F). (G) NG2 expression in a retinal artery and vein at higher magnification. (H) mRNA expression of N-cadherin decreased during development. IB4 = isolectin B4, a = artery, cap = capillary, v = vein. Scale bar = 100 μ m.

3.4. NG2-positive pericytes invade the retina together with the vascular sprouting front during retinal development

Pericytes are required for the formation of the blood-brain barrier and are essential for stabilization of mature vessels (Armulik et al., 2010; Daneman et al., 2010). To date, a marker that is entirely pericyte-specific is not known, and the markers that are currently used may differ in expression during different developmental or pathological stages (Armulik et al., 2011). Expression of CD13 mRNA, a type II membrane metalloprotease, that is used to identify brain pericytes (Kunz et al., 1994), increased during development of the retina, and stabilized around P11 (Fig. 4A). NG2 mRNA expression, a chondroitin sulfate proteoglycan that is considered to be one of the most reliable pericyte markers (Hughes and Chan-Ling, 2004; Schlingemann et al., 1990), was relatively stable during development (Fig. 4B). NG2 protein expression was found at all time points and stained pericytes ensheathing arteries, capillaries and veins (Fig. 4C-F). We observed NG2-positive cells in close proximity to the vascular tip cells at P5 (Fig. 4D). Perivascular NG2 staining was observed in the superficial vascular plexus, as well as in the descending intermediate and deep capillary layers (Fig. 4E, F), and was present around all vessel types in the retina (Fig. 4G). mRNA expression of N-cadherin, a cell-adhesion molecule which is involved in endothelial cell – pericyte interactions (Armulik et al., 2011), initially decreased from P3 to P11, the period associated with high angiogenic activity, and stabilized from P11 onwards (Fig. 4H). Together, these data suggest that pericytes are present around endothelial tubes during early vessel formation, and that they localize in the vicinity of tip cells. This is not completely in line with an earlier report by Fruttiger (2002), who showed by in situ hybridization of PDGFR β , in combination with immunofluorescence of collagen type IV in retinal wholemounts, that pericyte recruitment lagged slightly behind the leading edge of the sprouting network (Fruttiger, 2002). However, this discrepancy can be explained by the use of different markers, since PDGFR β -positive cells are co-recruited with angiogenic sprouts when PDGF-B is released by angiogenic endothelial cells (Armulik et al., 2011), whereas NG2-positive cells have been shown to be activated, extramural pericytes (Schlingemann et al., 1990) which may play a role in early stages of angiogenesis (Ruiter et al., 1993). High molecular weight-melanoma associated antigen (HMW-MAA), the previous name of human NG2, has been shown to be a marker of pericytes associated with vascular sprouts and capillaries during angiogenesis (Schlingemann et al., 1990; Ruiter et al., 1993).

By recent work the essential role of pericytes in maintaining the integrity of the blood-brain barrier during development has been well established. Two studies showed that absolute pericyte coverage of brain vessels controls relative blood-brain barrier permeability (Armulik et al., 2010; Daneman et al., 2010), and that recruitment of pericytes to the vessels

1

2

3

4

5

6

7

8

&

temporally correlated with the onset of barrier properties (Daneman et al., 2010). This is not the case in the BRB, where pericytes are already associated with retinal vessels long before the BRB is completely functional, which is, in the mice that we investigated, around P15 (van der Wijk et al., submitted). In addition, a recent study showed that there was no apparent vascular remodeling and leakage after pericyte ablation in the adult retina, whereas during postnatal development, pericyte ablation caused severe vascular defects and BRB disruption (Park et al., 2017). Nevertheless, in pathological conditions such as diabetic retinopathy, early hallmarks are pericyte loss and increased BRB permeability (Hammes, 2005). Thus, in the retina, pericyte recruitment may not be directly and temporally related to barrier genesis, but close association of pericytes with retinal vessels may be essential for BRB formation and function.

4. CONCLUDING REMARKS

Here, we provide a spatio-temporal overview of recruitment and maturation of the neurovascular unit during development of the mouse BRB. Although the BRB closely resembles the blood-brain barrier in terms of function and molecular and cellular composition, there are some differences in vascular and barrier development. In the retina, astrocytes migrate ahead of the vasculature and even provide a template along which the retinal vasculature can grow, which is not the case in the brain. In addition, we observed NG2-positive extramural pericytes in close proximity to vascular tip cells. Moreover, pericytes are associated with retinal vessels before the BRB is functional, whereas the timing of barrier genesis in the brain has been temporally correlated with pericyte recruitment. Considering the astrocytic template, and the fact that the pericyte-to-endothelial ratio is even higher in the retina than it is in the brain (Stewart and Tuor, 1994), we suggest that perivascular cells may be of greater importance in the retina, when compared to the brain. Together, our data indicate that recruitment of all cell types of the neurovascular unit is a prerequisite for proper retinal vascularization, and that a functional BRB is formed after maturation of the neurovascular unit. In the mouse, a functional BRB is completed around the time of eye opening and may be required for the increased sensory input which accompanies vision.

ACKNOWLEDGMENTS

This study was made possible by the financial support of the Diabetes Fonds (Dutch Diabetes Fund, grant 2014.00.1784) and by the following foundations: Landelijke Stichting voor Blinden en Slechtienden, Novartis Fonds and St. MD Fonds, that contributed through UitZicht (Grant UitZicht 2014-33), the Nederlandse Vereniging ter Verbetering van het Lot der Blinden, Rotterdamse Stichting Blindenbelangen (Grant B20140050) and Stichting Blindenhulp. This study was published with financial support from the Edmond en Marianne Blaauw Fonds voor Oogheelkunde. The funding organizations had no role in the design or conduct of this research. They provided unrestricted grants.

Disclosure: A.-E. van der Wijk, None; I.M.C. Vogels, None; H.A. van Veen, none; C.J.F. van Noorden, None; R.O. Schlingemann, None; I. Klaassen, None

AUTHOR CONTRIBUTIONS

AEvdW designed and performed experiments, analyzed data and wrote the manuscript; IMCV performed experiments; HAvV has performed the EM analysis; IK analyzed data, contributed to the study design, discussion, and editing of the manuscript, CJFvN and ROS contributed to the study design, discussion, and editing of the manuscript. All authors have read and approved the final manuscript.

1

2

3

4

5

6

7

8

&

REFERENCES

- Abbott, N.J., Ronnback, L., Hansson, E., 2006. Astrocyte-endothelial interactions at the blood-brain barrier. *Nat Rev Neurosci* 7, 41-53.
- Ackman, J.B., Burbridge, T.J., Crair, M.C., 2012. Retinal waves coordinate patterned activity throughout the developing visual system. *Nature* 490, 219-225.
- Armulik, A., Genove, G., Betsholtz, C., 2011. Pericytes: developmental, physiological, and pathological perspectives, problems, and promises. *Dev Cell* 21, 193-215.
- Armulik, A., Genove, G., Mae, M., Nisancioglu, M.H., Wallgard, E., Niaudet, C., He, L., Norlin, J., Lindblom, P., Strittmatter, K., Johansson, B.R., Betsholtz, C., 2010. Pericytes regulate the blood-brain barrier. *Nature* 468, 557-561.
- Benjamin, L.E., Hemo, I., Keshet, E., 1998. A plasticity window for blood vessel remodelling is defined by pericyte coverage of the preformed endothelial network and is regulated by PDGF-B and VEGF. *Development* 125, 1591-1598.
- Bosco, A., Cusato, K., Nicchia, G.P., Frigeri, A., Spray, D.C., 2005. A developmental switch in the expression of aquaporin-4 and Kir4.1 from horizontal to Muller cells in mouse retina. *Invest Ophthalmol Vis Sci* 46, 3869-3875.
- Chow, B.W., Gu, C.H., 2017. Gradual Suppression of Transcytosis Governs Functional Blood-Retinal Barrier Formation. *Neuron* 93, 1325-+.
- Daneman, R., Zhou, L., Kebede, A.A., Barres, B.A., 2010. Pericytes are required for blood-brain barrier integrity during embryogenesis. *Nature* 468, 562-566.
- Dorrell, M.I., Aguilar, E., Friedlander, M., 2002. Retinal vascular development is mediated by endothelial filopodia, a preexisting astrocytic template and specific R-cadherin adhesion. *Invest Ophthalmol Vis Sci* 43, 3500-3510.
- Fruttiger, M., 2002. Development of the mouse retinal vasculature: angiogenesis versus vasculogenesis. *Invest Ophthalmol Vis Sci* 43, 522-527.
- Fruttiger, M., 2007. Development of the retinal vasculature. *Angiogenesis* 10, 77-88.
- Gariano, R.F., 2003. Cellular mechanisms in retinal vascular development. *Prog Retin Eye Res* 22, 295-306.
- Gariano, R.F., Gardner, T.W., 2005. Retinal angiogenesis in development and disease. *Nature* 438, 960-966.
- Hamann, S., Zeuthen, T., La Cour, M., Nagelhus, E.A., Ottersen, O.P., Agre, P., Nielsen, S., 1998. Aquaporins in complex tissues: distribution of aquaporins 1-5 in human and rat eye. *Am J Physiol* 274, C1332-1345.
- Hammes, H.P., 2005. Pericytes and the pathogenesis of diabetic retinopathy. *Horm Metab Res* 37 Suppl 1, 39-43.
- Hughes, S., Chan-Ling, T., 2004. Characterization of smooth muscle cell and pericyte differentiation in the rat retina in vivo. *Invest Ophthalmol Vis Sci* 45, 2795-2806.
- Klaassen, I., Hughes, J.M., Vogels, I.M., Schalkwijk, C.G., Van Noorden, C.J., Schlingemann, R.O., 2009. Altered expression of genes related to blood-retina barrier disruption in streptozotocin-induced diabetes. *Exp Eye Res* 89, 4-15.
- Klaassen, I., Van Noorden, C.J., Schlingemann, R.O., 2013. Molecular basis of the inner blood-retinal barrier and its breakdown in diabetic macular edema and other pathological conditions. *Prog Retin Eye Res* 34, 19-48.
- Kowluru, R.A., Jirousek, M.R., Stramm, L., Farid, N., Engerman, R.L., Kern, T.S., 1998. Abnormalities of retinal metabolism in diabetes or experimental galactosemia: V. Relationship between protein kinase C and ATPases. *Diabetes* 47, 464-469.
- Kunz, J., Krause, D., Kremer, M., Dermietzel, R., 1994. The 140-kDa protein of blood-brain barrier-associated pericytes is identical to aminopeptidase N. *J Neurochem* 62, 2375-2386.
- Menezes, M.J., McClenahan, F.K., Leiton, C.V., Aranmolate, A., Shan, X., Colognato, H., 2014. The extracellular matrix protein laminin alpha2 regulates the maturation and function of the blood-brain barrier. *J Neurosci* 34, 15260-15280.
- Mestdagh, P., Van Vlierberghe, P., De Weer, A., Muth, D., Westermann, F., Speleman, F., Vandesompele, J., 2009. A novel and universal method for microRNA RT-qPCR data normalization. *Genome Biol* 10, R64.
- Nagelhus, E.A., Veruki, M.L., Torp, R., Haug, F.M., Laake, J.H., Nielsen, S., Agre, P., Ottersen, O.P., 1998. Aquaporin-4 water channel protein in the rat retina and optic nerve: polarized expression in Muller cells and fibrous astrocytes. *J Neurosci* 18, 2506-2519.
- Nakagawa, S., Deli, M.A., Kawaguchi, H., Shimizudani, T., Shiono, T., Kittel, A., Tanaka, K., Niwa, M., 2009. A new blood-brain barrier model using primary rat brain endothelial cells, pericytes and astrocytes. *Neurochem Int* 54, 253-263.
- Nehls, V., Drenckhahn, D., 1991. Heterogeneity of microvascular pericytes for smooth muscle type alpha-actin. *J Cell Biol* 113, 147-154.
- O'Sullivan, M.L., Punal, V.M., Kerstein, P.C., Brzezinski, J.A.t., Glaser, T., Wright, K.M., Kay, J.N., 2017. Astrocytes follow ganglion cell axons to establish an angiogenic template during retinal development. *Glia* 65, 1697-1716.
- Park, D.Y., Lee, J., Kim, J., Kim, K., Hong, S., Han, S., Kubota, Y., Augustin, H.G., Ding, L., Kim, J.W., Kim, H., He, Y., Adams, R.H., Koh, G.Y., 2017. Plastic roles of pericytes in the blood-retinal barrier. *Nat Commun* 8, 15296.
- Rochefort, N.L., Garaschuk, O., Milos, R.I., Narushima, M., Marandi, N., Pichler, B., Kovalchuk, Y., Konnerth, A., 2009. Sparsification of neuronal activity in the

- visual cortex at eye-opening. *Proc Natl Acad Sci U S A* 106, 15049-15054.
- Ruijter, J.M., Ramakers, C., Hoogaars, W.M., Karlen, Y., Bakker, O., van den Hoff, M.J., Moorman, A.F., 2009. Amplification efficiency: linking baseline and bias in the analysis of quantitative PCR data. *Nucleic Acids Res* 37, e45.
- Ruiter, D.J., Schlingemann, R.O., Westphal, J.R., Denijn, M., Rietveld, F.J., De Waal, R.M., 1993. Angiogenesis in wound healing and tumor metastasis. *Behring Inst Mitt*, 258-272.
- Schlingemann, R.O., Rietveld, F.J., de Waal, R.M., Ferrone, S., Ruiter, D.J., 1990. Expression of the high molecular weight melanoma-associated antigen by pericytes during angiogenesis in tumors and in healing wounds. *Am J Pathol* 136, 1393-1405.
- Stewart, P.A., Tuor, U.I., 1994. Blood-eye barriers in the rat: correlation of ultrastructure with function. *J Comp Neurol* 340, 566-576.
- Thompson, A., Gribizis, A., Chen, C., Crair, M.C., 2017. Activity-dependent development of visual receptive fields. *Curr Opin Neurobiol* 42, 136-143.
- Tomasek, J.J., Haakma, C.J., Schwartz, R.J., Vuong, D.T., Zhang, S.X., Ash, J.D., Ma, J.X., Al-Ubaidi, M.R., 2006. Deletion of smooth muscle alpha-actin alters blood-retina barrier permeability and retinal function. *Invest Ophthalmol Vis Sci* 47, 2693-2700.
- Uemura, A., Ogawa, M., Hirashima, M., Fujiwara, T., Koyama, S., Takagi, H., Honda, Y., Wiegand, S.J., Yancopoulos, G.D., Nishikawa, S., 2002. Recombinant angiopoietin-1 restores higher-order architecture of growing blood vessels in mice in the absence of mural cells. *J Clin Invest* 110, 1619-1628.
- West, H., Richardson, W.D., Fruttiger, M., 2005. Stabilization of the retinal vascular network by reciprocal feedback between blood vessels and astrocytes. *Development* 132, 1855-1862.
- Wisniewska-Kruk, J., Hoeben, K.A., Vogels, I.M., Gaillard, P.J., Van Noorden, C.J., Schlingemann, R.O., Klaassen, I., 2012. A novel co-culture model of the blood-retinal barrier based on primary retinal endothelial cells, pericytes and astrocytes. *Exp Eye Res* 96, 181-190.
- Wisniewska-Kruk, J., van der Wijk, A.E., van Veen, H.A., Gorgels, T.G., Vogels, I.M., Versteeg, D., Van Noorden, C.J., Schlingemann, R.O., Klaassen, I., 2016. Plasmalemma Vesicle-Associated Protein Has a Key Role in Blood-Retinal Barrier Loss. *Am J Pathol* 186, 1044-1054.

1

2

3

4

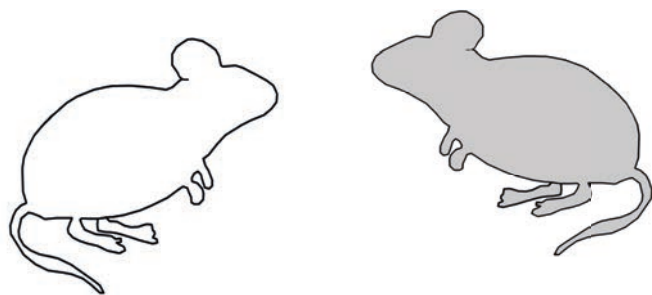
5

6

7

8

&



3

Formation of the retinal vasculature and blood-retinal barrier during early development and the role of Plasmalemma Vesicle-Associated Protein (PLVAP)

Anne-Eva van der Wijk,¹ Joanna Wisniewska-Kruk,¹ Ilse M.C. Vogels,¹ Henk A. van Veen,² Wing Fung Ip,¹ Nicole N. van der Wel,² Cornelis J.F. van Noorden,^{1,3} Reinier O. Schlingemann,^{1,4} Ingeborg Klaassen^{1*}

¹ Ocular Angiogenesis Group, Departments of Ophthalmology and Medical Biology, Academic Medical Center, University of Amsterdam, Amsterdam, The Netherlands

² Electron Microscopy Center Amsterdam, Department of Medical Biology, Academic Medical Center, University of Amsterdam, Amsterdam, The Netherlands

³ Cellular Imaging Core Facility, Department of Medical Biology, Academic Medical Center, University of Amsterdam, Amsterdam, The Netherlands

⁴ Department of Ophthalmology, University of Lausanne, Jules Gonin Eye Hospital, Lausanne, Switzerland

Submitted.

ABSTRACT

Insight into the molecular and cellular processes in blood-retinal barrier (BRB) development, including the contribution of paracellular and transcellular pathways, is still incomplete, but may help to understand the inverse process of BRB loss in pathological eye conditions. In this comprehensive observational study, we describe in detail the formation of the BRB at the molecular level in physiological conditions, using mice from postnatal day (P)3 to P25. Our data indicate that immature vessels already have tight junctions, but that the BRB is functional from P15 onwards. Expression of the endothelial cell-specific protein plasmalemma vesicle-associated protein (PLVAP), that is known to be involved in transcellular transport and associated with BRB permeability, decreased during development and was absent when a functional barrier was formed. Moreover, with the use of transgenic heterozygous *Plvap* mice, we show that PLVAP is involved in the formation of both the retinal vasculature and the BRB.

INTRODUCTION

Homeostasis of the neural retina is maintained by the blood-retinal barrier (BRB), formed by the neurovascular unit consisting of endothelial cells of the retinal capillaries, pericytes and glial cells (1, 2). In humans, the retinal vasculature develops around mid-gestation (3). Initially, this vasculature lacks a functional BRB, which is formed during further differentiation to mature endothelium. In pathological conditions such as diabetic macular edema, the acquired BRB properties are lost in the adult retina (4), causing blindness. The molecular and cellular events in BRB development are poorly understood, but may help to understand the events in BRB loss. In fact, such understanding may even enable the development of alternative treatment strategies for pathological eye conditions involving BRB loss.

We have previously identified a specific set of genes that is associated with BRB integrity (5). The most important were either genes involved in paracellular transport (claudin-5 and occludin), or vesicular/transcellular transport-related genes caveolin-1 and plasmalemma vesicle associated protein (PLVAP, or PV-1). In the brain, expression of the endothelial cell-specific protein PLVAP is negatively correlated with blood-brain barrier (BBB) function (6, 7), and PLVAP protein is not detected when a functional BBB is formed (8, 9). PLVAP is also absent in mature barrier endothelium of the BRB and the testis (10, 11). Conversely, PLVAP is upregulated in monkey retina after intravitreal injections of vascular endothelial growth factor (VEGF), a major inducer of BRB breakdown (12, 13). Moreover, increased PLVAP expression in capillaries is associated with loss of the BBB in brain tumors (7, 14) and of the BRB in human patients with diabetic retinopathy (15).

PLVAP is a structural component of fenestral and stomatal diaphragms on fenestrae, caveolae and trans-endothelial channels (16). Recent generation of *Plvap*-deficient mice highlighted the structural role of PLVAP in the maintenance of size-selective permeability in fenestrated endothelia (17, 18). In fact, *Plvap*-deficient mice that survive postnatally, showed growth retardation and anemia (17), and selective loss of plasma proteins with subsequent edema and dyslipidemia, eventually leading to a lethal, protein-losing enteropathy (18). Crucially, a human form of PLVAP deficiency caused by a nonsense mutation in the *Plvap* gene resulted in a nearly identical disease profile to that observed in *Plvap*-deficient mice, and was characterized by hypoproteinemia, hypoalbuminemia, and hypertriglyceridemia (19). These observations indicate that in non-barrier endothelium, PLVAP prevents excessive protein leakage into tissues, a function that is apparently not needed in a patent BBB or BRB. In addition to this structural role of PLVAP in non-barrier vessels, our group has demonstrated that PLVAP is actively involved in BRB loss (20), and also has a key role in physiological and pathological angiogenesis (manuscript in preparation).

In the present observational study, we give a comprehensive overview of the development of the BRB in mice, with respect to paracellular and transcellular transport and VEGF signaling. Moreover, we focus on the role of PLVAP in this process and with the use of transgenic heterozygous *Plvap* mice (*Plvap*^{+/-}), we show that PLVAP is involved in the formation of the retinal vasculature and the BRB.

MATERIALS AND METHODS

Generation of transgenic mice

Animal experiments were performed with the approval of the Animal Ethics Committee of the University of Amsterdam and in compliance with the Association for Research in Vision and Ophthalmology (ARVO) Statement for the Use of Animals in Ophthalmic and Vision Research.

Plvap^{+/-} mice were generated by targeting exon 1 on the *Plvap* locus by homologous recombination in strain 129/SvEvBrd-derived embryonic stem cells. The chimeric mice were bred to C57BL/6-Tyr^{c-Brd} albino mice to generate F1 heterozygous animals. This progeny was intercrossed to generate F2 wildtype, heterozygous, and homozygous mutant progeny. The B6;129S5-*Plvap*^{tm1LEX}/Mmucd mice were imported from the Mutant Mouse Regional Resource Center (MMRRC; Davis, CA) and further bred in the animal facility at the Animal Research Institute of the Academic Medical Center (ARIA). Because complete knockout of *Plvap* results in the majority of cases in *in utero* and perinatal mortality, and the homozygous *Plvap* mice that do survive showed postnatally a very strong phenotype and died within 2 to 4 weeks, we used heterozygous *Plvap* mice (*Plvap*^{+/-}), which have significantly decreased *Plvap* expression (Fig. S1), and no apparent systemic phenotype (17, 18).

To study the development of the BRB, neonatal (wildtype) mice were killed on postnatal days (P)3, P5, P7, P9, P11, P13, P15, P17, P25 with an intracardial injection of ketamine-medetomidine-atropine for young mice (until P13), older mice were euthanized with CO₂ asphyxiation. Heterozygous littermates were killed on P5, 9, 13 and 25. Eyes were enucleated and either snapfrozen in liquid nitrogen (for qPCR or immunohistochemistry) or processed immediately for retinal wholemount staining.

Genotyping

Genotyping was performed by PCR analysis, using Fw and Rv primers (5' - TCCTCTTCGTGTCGCTCATT CAG and 5' - CTTACCAGGTCGCCTTGGCAC), resulting in a 289 bp PCR fragment for the wildtype allele and Fw and Rv primers (5' - GTTGCATGTACTACACCAGG and 5' - GCAGCGCATCGCCTTCTATC), resulting in a 395 bp fragment for the targeted allele. Genomic DNA was obtained from toes. Genomic DNA was isolated using the quick and dirty protocol according to Truett *et al.* (21). PCR analysis was performed with GoTaq[®] Hot Start Green Master Mix (Promega, Leiden, The Netherlands) containing GoTaq[®] Hot Start Polymerase, dNTPs, MgCl₂ and reaction buffers in 25 µl reaction volumes. The cycling conditions consisted of hot start initiation at 94 °C for 5 min, followed by denaturation for 15 sec at 94 °C, annealing for 30 sec at 60 °C and elongation for 40 sec at 72 °C, for 40 cycles.

Western blot analysis

Protein was extracted from kidney samples on ice by homogenizing the tissue in RIPA

buffer (ThermoFisher, Landsmeer, The Netherlands) supplemented with protease inhibitors. Insoluble constituents were removed by centrifugation for 10 min at 4 °C, at maximum speed. For western blot analysis, 50 µg protein was subjected to SDS-PAGE on a precast gradient gel (Bio-Rad, Veenendaal, The Netherlands) and transferred to a PVDF membrane (Merck Millipore, Amsterdam, The Netherlands) by wet blotting. After blocking for 1 h with 5% BSA in tris-buffered saline with 0.05% Tween20 (TBS-T), membranes were incubated overnight at 4 °C with rat anti-pan ECA (MECA-32) IgG_{2a} antibody (Santa Cruz Biotechnology, Santa Cruz, CA), diluted 1:500 in 5% BSA in TBS-T. After washing in TBS-T, membranes were incubated for 1 h at room temperature with rabbit anti-rat-HRP (Dako, Heverlee, Belgium), diluted 1:10.000 in 0.5% BSA in TBS-T. Membranes were washed twice in TBS-T and once in TBS, incubated for 5 min with chemiluminescent substrate (SuperSignal™ West Pico Chemiluminescent Substrate, ThermoFisher) and visualized on an ImageQuant™ LAS 4000 Imager (GE Healthcare, Eindhoven, The Netherlands).

RNA isolation and mRNA quantification

Retinas (at least 6 to 8 retinas per group) were treated by hypotonic lysis to enrich for retinal vessels (22). Each retina was incubated in 1 ml sterile water for 2 h at 4 °C. Next, retinas were spun down and sterile water was replaced with sterile water containing 40 µg DNase I (Life Technology, Breda, The Netherlands) and left for 5 min at room temperature. Retinas were spun down, supernatant was removed and the retinal vessels were resuspended in 500 µl TRIzol reagent (Invitrogen, Bleiswijk, The Netherlands) and stored in -20 °C until further processing. Total RNA was isolated according to the manufacturer's protocol and dissolved in RNase-free water. RNA yield was measured using a NanoDrop spectrophotometer (Thermo Scientific, Wilmington, DE) and 1 µg of RNA was treated with DNase-I (Invitrogen) and reverse transcribed into first strand cDNA with Maxima First Strand cDNA Synthesis Kit (ThermoFisher). Real-time quantitative PCR was performed on 20x diluted cDNA samples using a CFX96 system (Bio-Rad, Hercules, CA) as described previously (5). Specificity of the primers was confirmed by NCBI BLAST. The presence of a single PCR product was verified by both the presence of a single melting temperature peak and detection of a single band of the expected size on 3% agarose gel. Non-template controls were included to verify the method and the specificity of the primers. Relative gene expression was calculated using the equation: $R = E^{-Ct}$, where E is the mean efficiency of all samples for the gene being evaluated and Ct is the cycle threshold for the gene as determined during real-time PCR. Primer efficiencies (E) were determined with LinRegPCR software (23) and ranged from 1,817 to 1,979. PCR products that did not show a single melting temperature peak were excluded from analysis. Expression data was normalized by the global mean normalization method using expression data of all tested genes (24).

Retinal wholemount and cryostat section staining

Enucleated mouse eyes were washed in PBS and fixed in 4% paraformaldehyde for 5 min, transferred to 2x PBS for 10 minutes and retinas were dissected in PBS. Isolated retinas were post-fixed in methanol and stored in -20 °C until further use. For immunofluorescent

staining, retinas were briefly washed in 2x PBS and incubated in wholemount-blocking buffer (1% fetal calf serum, 3% TritonX-100, 0.5% Tween20, 0.2% sodium azide in 2x PBS) for 2 h at room temperature. Next, retinas were incubated overnight with the following antibodies: rabbit-anti-claudin-5 (diluted 1:250, Cat # 34-1600, ThermoFisher), Isolectin B4 (Alexa Fluor-488 labeled, diluted 1:30, Cat # I21411, Invitrogen) or rat-anti-MECA-32 (diluted 1:100, Cat # 553849, BD Pharmingen, Breda, The Netherlands) diluted in wholemount blocking buffer. After 3 wash steps (3 times 30 min in wholemount blocking buffer), secondary antibody was added for 2-3 h (diluted 1:100, goat-anti-rabbit Alexa Fluor-633, goat-anti-rabbit Cy3 or goat-anti-rat Cy3; Invitrogen) diluted in wholemount blocking buffer. When retinas were stained with rat-anti-MECA-32, 2% normal mouse serum was added to the secondary antibody mix. After overnight washing in wholemount blocking buffer, retinas were mounted on glass and covered in Vectashield (Vector Laboratories, Burlingame, CA). All staining procedures were performed under gentle agitation at room temperature. For staining of the cryostat sections, the samples were fixed for 10 min with 4% paraformaldehyde, permeabilized for 10 min with 0.2% TritonX-100 and blocked for 1 h with 10% normal goat serum. Staining was done in wholemount blocking buffer with rabbit-anti-mouse IgG (Dako) or rabbit-anti-fibrinogen (Abcam) for 2 h, followed by secondary antibody incubation (goat-anti-rabbit Cy3) for 1 h.

Images of wholemounts were taken at the central (at the site of the optic nerve head), middle and peripheral retina and were recorded using a confocal laser scanning microscope SP8 (Leica Microsystems, Wetzlar, Germany) with a 20x or 63x objective at the Cellular Imaging Core Facility of the Academic Medical Center. Specificity of the staining was checked by absence of fluorescent signal in samples where primary antibody was omitted.

For quantification of vascular density, x-y-sections at the superficial, intermediate and deep layer were taken at 4 regions around the central retina (starting at the optic nerve head) and measurements of these regions were averaged per retina. Images were thresholded and binarized with Matlab (version R2015a; MathWorks, Natick, MA) from which vascular coverage was determined (ratio of black pixels to total amount of pixels).

Modified Miles' assay in the skin

Mice (n=5 per group) were anesthetized with an intraperitoneal (i.p.) injection of ketamine-medetomidine-atropine mix, directly followed by an i.p. injection with 150 μ l Evans Blue dye (EB; 30 mg/ml; Sigma Aldrich, Zwijndrecht, The Netherlands). The back skin was shaved, EB was allowed to circulate for 20 min and then mrVEGF₁₆₄ (200 ng; Sanquin, Amsterdam, The Netherlands) and histamine (500 ng; Sigma Aldrich) in 25 μ l PBS were injected intradermally into flank skin. PBS (25 μ l) was used as negative control and injections were performed in duplo. After 20 min, mice were euthanized with an overdose of pentobarbital (250 mg/kg) and the tissue containing extravasated EB dye was harvested with an 8 mm biopsy puncher and incubated for 18 h in 200 μ l formamide at 70 °C. Extracted EB was quantified using a spectrophotometer (BMG POLARstar; MTX Lab Systems, Bradenton, FL) set at 650 nm. Measurements from skin were normalized to EB circulating in the bloodstream taken from a cardiac puncture. To correct for differences

between the experiments, factor correction was applied using Factor Correction software v2015.2.0.0 (25).

Transmission electron microscopy (TEM) of mouse eyes

Eyes were harvested and immersion fixed in McDowell phosphate buffer. To facilitate entry of the fixative into the eye, eyes were punctured with a 29 gauge needle and the cornea was cut off. Samples were processed for routine TEM, as described in Wisniewska-Kruk et al., 2016. Ultrathin sections of 80 nm were examined with a FEI Technai-12 G2 Spirit Biotwin microscope and micrographs were taken with a Veleta TEM camera (Emsis; Münster, Germany) using Radius acquisition software (Emsis) at a magnification of 30.000x at the Cellular Imaging Core Facility of the Academic Medical Center. The images were quantified with iTEM software (Olympus Soft Imaging Solutions; Olympus, Tokyo, Japan). The number of caveolae in endothelial cells was manually counted on the luminal and abluminal side in retinal capillaries in the inner or outer plexiform layer, and expressed per μm endothelial cell wall. A total of 54 capillaries was analyzed for WT mice (n=2), and 49 capillaries for HET mice (n=4).

Statistics

Data are depicted as mean \pm standard deviation (s.d.). Differences between groups were tested using a Mann-Whitney U test for nonparametric data or ANOVA with post-hoc Bonferroni's test, where appropriate. Differences were considered statistically significant when $P \leq 0.05$. Statistical analyses and graphing were performed using GraphPad Prism 6 (GraphPad Software Inc., La Jolla, CA) software.

RESULTS

Development of the murine retinal vasculature

As previously described (26), retinal vascularization in the murine eye started with the growth of a superficial vascular network in the ganglion cell layer. Vascularization started at the optic nerve head and grew radially outwards where it reached the periphery of the retina around P7 (Fig. S2A-C). The intermediate and deep capillary layers in the inner and outer plexiform layers developed by sprouting angiogenesis from the capillaries around retinal veins in the superficial plexus, starting around P7 (Fig. S2C, D-G). In the first 2 weeks after birth, the superficial vasculature remodeled from a very dense capillary-like meshwork to a highly organized hierarchical patterning of arteries, capillaries and veins. The deep capillary plexus was more or less formed and connected at P13, whereas the intermediate layer was still in the process of connecting at that time point (Fig. S2E). At P25, all 3 vascular layers were formed and connected (Fig. S2F, H).

1
2
3
4
5
6
7
8
&

A functional BRB is formed around P15

To assess at what time point the BRB was functional, we performed an immunohistochemical staining for plasma protein IgG, as an endogenous marker of protein leakage, on cryostat sections of mouse eyes at different postnatal ages. In mature and functional barrier endothelium, plasma proteins are confined to the lumen of the vessels, whereas extravasation of plasma proteins indicates an immature or leaky barrier (12). In the first postnatal weeks, IgG was localized in and around the superficial vessels in the ganglion cell layer, indicating leakage of the protein out of the vessels (Fig.1). At P13, there were still vessels with IgG around them, but also vessels where IgG was confined to the vessel lumen. In contrast, from P15 onwards IgG was confined to the vessels in the inner retina, which suggests that at this time point, the BRB was closed and hence, functional (Fig.1). Similar results were obtained with fibrinogen (data not shown). Staining of IgG in the choriocapillaris can be regarded as a positive control of plasma protein leakage at all time points (Fig.1), since the choriocapillaris consists of fenestrated endothelium and is known to be highly permeable (10).

Endothelial junction gene expression is sequentially regulated during BRB formation

Endothelial cells of the BBB and BRB are known to form a tight barrier with limited paracellular and transcellular transport, to strictly maintain homeostasis of the neural tissue. In pathological BRB loss, increased paracellular leakage through disruption of tight and adherens junctions is one of the known mechanisms (4, 27). In line with this, during development, expression of VE-cadherin (VE-cad), occludin and claudin-5 mRNA levels increased in retinal vessels from neonatal mice (Fig. 2A). VE-cad and occludin mRNA levels almost doubled from P3 to P5, and VE-cad levels increased until P11, from where it showed a marked decrease. Occludin peaked at P17 and was almost 5-fold higher as compared to P3. Claudin-5 started to increase from P5 onwards and peaked at P15. mRNA levels of ZO-1 and β -catenin, which is involved in Wnt-signaling but also part of adherens junctions, showed a relative decrease over time. When comparing the abundance of the tight and adherens junction components (based on arbitrary units, see Methods section), claudin-5, ZO-1 and β -catenin were present at relatively high levels already at P3, whereas VE-cad and occludin were less abundant (Fig. 2A). Moreover, staining of retinal vessels in wholemounts confirmed that claudin-5 protein was present at all time points (Fig. 2B) and in all 3 vascular plexi (data not shown). At P5, claudin-5 protein was localized at the cell membranes and in the cytoplasm. The cell membrane localization appeared less pronounced as compared to later time points (Fig. 2C). These data indicate that expression of tight and adherens junctions is temporally regulated, and that already at P5 the immature vessels have tight junctions, before a functional BRB is formed.

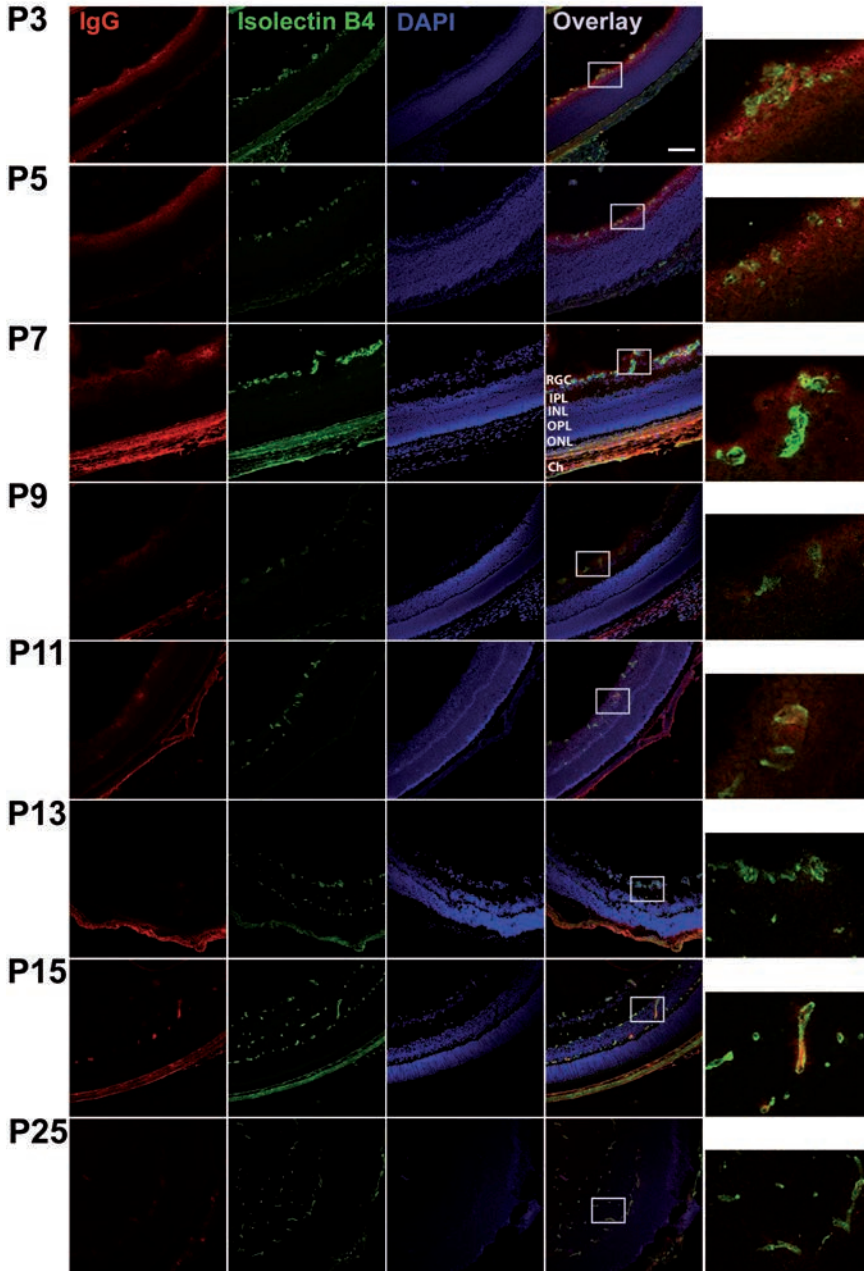


Figure 1. Leakage of the plasma protein IgG in the retina during BRB development. Retinal cryostat sections were stained for IgG (red), endothelial cells (isolectin B4; green) and nuclei (DAPI; blue). In the first postnatal weeks, leakage of IgG from the vessels occurred in the retinal ganglion cell layer, whereas at P15, IgG was confined to the lumen of blood vessels. RGC = retinal ganglion cell layer, IPL = inner plexiform layer, INL = inner nuclear layer, OPL = outer plexiform layer, ONL = outer nuclear layer, Ch = choriocapillaris. Scale bar = 100 μ m.

1
2
3
4
5
6
7
8
&

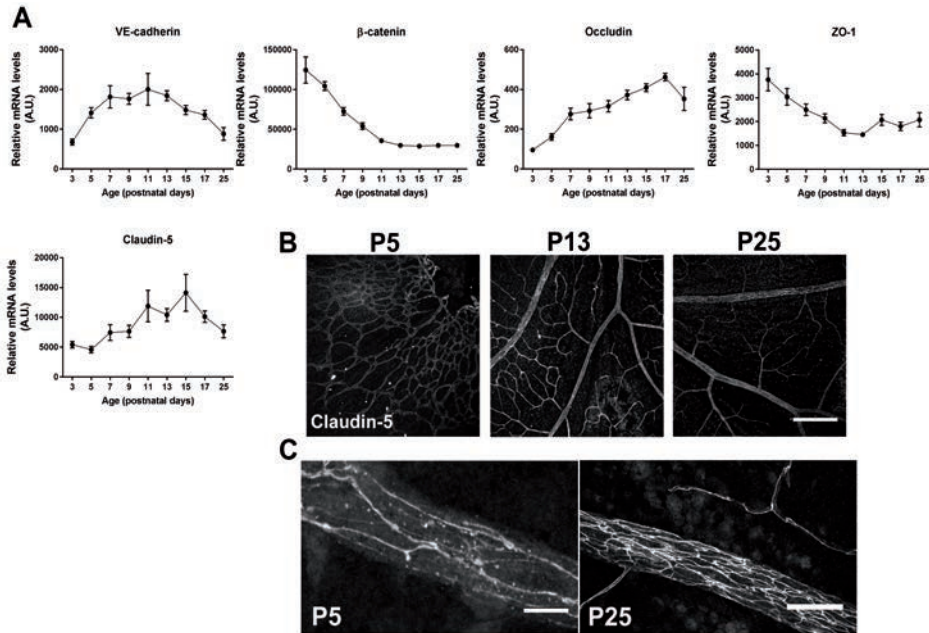


Figure 2. Expression of tight junctions increases during BRB development. (A) mRNA levels of VE-cadherin, β -catenin, occludin, ZO-1 and claudin-5 in the retinal vasculature from P3 to P25. $n=7-11$ for all time points. Data are depicted as mean \pm s.d. (B) Protein expression of claudin-5 (grey) in retinal wholemounts was present at all ages. Scale bar = 200 μ m. (C) At P5, claudin-5 was localized at the cell membrane, and its membrane expression increased on later time points. Retinal veins are shown. Scale bar = 10 μ m (P5) and 50 μ m (P25).

PLVAP expression in the retinal vasculature decreases during BRB development

During BRB development, we observed a decrease in *Plvap* mRNA levels over time, with a significant decrease from P3 to P9, and virtually no expression from P9 onwards (Fig. 3A). Immunolocalization of PLVAP protein was visualized using the monoclonal MECA-32 antibody in retinal wholemounts. PLVAP protein expression followed a similar pattern as *Plvap* mRNA transcript levels over time (Fig. 3B). PLVAP expression was high at P3 and P5 and decreased until immunoreactivity of PLVAP protein was absent in retinal wholemounts at P17 and P25. At early time points, PLVAP was expressed in all retinal vessels, *i.e.* arteries, capillaries and veins. However, PLVAP was not expressed in the filopodia of tip cells at the vascular sprouting front (Fig. 3C). Expression was highest in the superficial vascular plexus and a low signal was observed in the deep capillary plexus at P9 (data not shown). These data indicate a negative relationship between PLVAP expression and formation of the barrier.

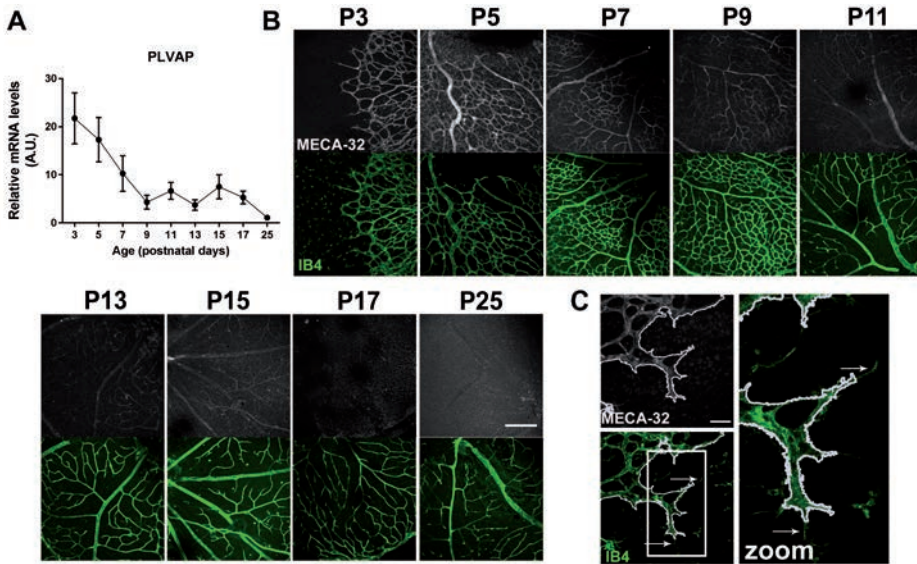


Figure 3. Retinal Plvap expression decreases during BRB development. (A) Plvap mRNA levels were highest at P3 in the retinal vasculature and decreased from P3 to P25; $n=7-11$ for all time points. Data are depicted as mean \pm s.d. (B) Immunolocalization of PLVAP protein was visualized using MECA-32 antibody (grey) in retinal wholemounts. Isolectin B4 (IB4, green) was used to stain the retinal vessels. PLVAP expression decreased over time. Scale bar = 200 μ m. (C) PLVAP was not expressed in the filopodia of tip cells. White line outlines MECA-32 expression (outlined with magic wand tool in ImageJ) and white arrows indicate filopodia. Images are captured of a retina at P3. Scale bar = 40 μ m.

Reduced PLVAP expression delays retinal vascularization at P5, but does not affect retinal vascular density at later time points

To further investigate the role of PLVAP in barrier endothelium, we made use of transgenic *Plvap* mice. To confirm that *Plvap*^{+/-} mice have less PLVAP, we checked mRNA and protein levels in kidneys, and observed significantly reduced PLVAP expression in *Plvap*^{+/-} mice as compared to wildtype (Fig. S1A-C). We assessed whether PLVAP is necessary for the formation of the vascular network in the retina by comparing retinal vascularization at P5, P9, P13 and P25 in wildtype and *Plvap*^{+/-} mice. We recently observed that decreased expression of PLVAP leads to reduced migration, sprouting and tip cell numbers in vitro, and that sprouting endothelial cells in the retina in *Plvap*^{+/-} mice have less filopodia at P5 as compared to wildtype controls (manuscript in preparation). In the present study, we found that retinal vascularization was delayed in *Plvap*^{+/-} mice at P5, with 58.0 \pm 10.1% of the retina vascularized in wildtype animals, versus 44.0 \pm 9.3% in *Plvap*^{+/-} mice ($P<0.05$; Fig. S3A-C). Despite this delay at P5, vascularization of the *Plvap*^{+/-} retina followed essentially the same pattern as that of wildtype mice, with a fully vascularized retina at P25 (Fig. S3D-G). Quantification in the central retina showed that vascular density of the superficial, intermediate and deep layers was not affected by reduced PLVAP expression at P9 and P13

1
2
3
4
5
6
7
8
&

(Fig. S4A, B). There was a trend towards a less dense vasculature in *Plvap*^{+/-} mice at P25, but this did not reach statistical significance (Fig. S4C). However, a closer examination of the fully vascularized retinas (\geq P25) revealed that, instead of capillaries branching off of veins in the superficial vascular plexus to form the parallel intermediate and deep capillary layers, the retinal vein itself traversed across the different retinal layers in a number of eyes, ending in the deep capillary layer. This was more often the case in *Plvap*^{+/-} mice (20.6% of veins, 2.7% of arteries) than in wildtype mice (9.8% of veins, 3.3% of arteries; Table S1, Video S1). Taken together, these data indicate that reduced PLVAP expression during development does not affect vascular density in the retina eventually, but does have a temporary effect on vascular growth, and on the spatial distribution of veins in the fully developed retina.

Reduced PLVAP expression affects retinal tight junctions

To determine whether reduced PLVAP expression during development affects BRB formation, we selected 3 crucial time points (P5, P13 and P25), to compare expression of BRB-specific components of wildtype and *Plvap*^{+/-} mice. At P5, the superficial retinal vasculature was still extending from the central retina to the periphery. At P13, the deep capillary layer was formed, and at P25, the formation of all 3 vascular plexi was complete. At all ages, no *Plvap* mRNA was detected in the retinal vasculature of *Plvap*^{+/-} mice (Fig. 4A), whilst PLVAP protein was present at P5, but not at P13 and P25 (Fig. 4B).

The mRNA expression of tight and adherens junction genes followed the same pattern over time in wildtype and *Plvap*^{+/-} mice, e.g., VE-cad increased from P5 to P13, but then decreased again between P13 and P25, and occludin expression increased (Fig. 4C-F). However, when compared to wildtype mice, VE-cad mRNA levels were lower in *Plvap*^{+/-} mice at all time points (Fig. 4C), and there were no differences in β -catenin expression levels between wildtype and *Plvap*^{+/-} mice (data not shown). In contrast, occludin mRNA levels at all three time points, and ZO-1 at P25 were higher in *Plvap*^{+/-} mice (Fig. 4D, E). Whereas claudin-5 mRNA levels were lower at all time points in *Plvap*^{+/-} mice (Fig. 4F), protein expression of claudin-5 at P5 and P25 did not appear much different (Fig. 4G, H). These data indicate that PLVAP directly or indirectly affects gene expression of endothelial junctions, which may affect paracellular permeability.

Reduced PLVAP expression affects BRB transport mechanisms

PLVAP is a structural component of caveolae (16), and is involved in transcellular transport (20). The levels of caveolin-1, the primary structural protein of caveolae (28), increased over time in the retinal vasculature, but levels were similar in *Plvap*^{+/-} and wildtype mice, both at the mRNA (Fig. 5A) and protein level (Fig. 5B). However, several other molecules involved in transcellular (caveolar) transport were increased in *Plvap*^{+/-} mice. Dynamin-1 and -2, essential for the fission of plasma membrane caveolae to form free transport vesicles (29) and Pacsin2, involved in the formation of caveolae (30), were increased in *Plvap*^{+/-} mice at P25 (Fig. 5C, D, E). Expression of flotillin-1 and -2 (Flot1 and -2, respectively), 2 membrane-associated proteins involved in endocytosis that are expressed in the mouse retina (5, 31), also showed higher mRNA expression at P5 (*Flot1*) or all time points (*Flot2*) as compared

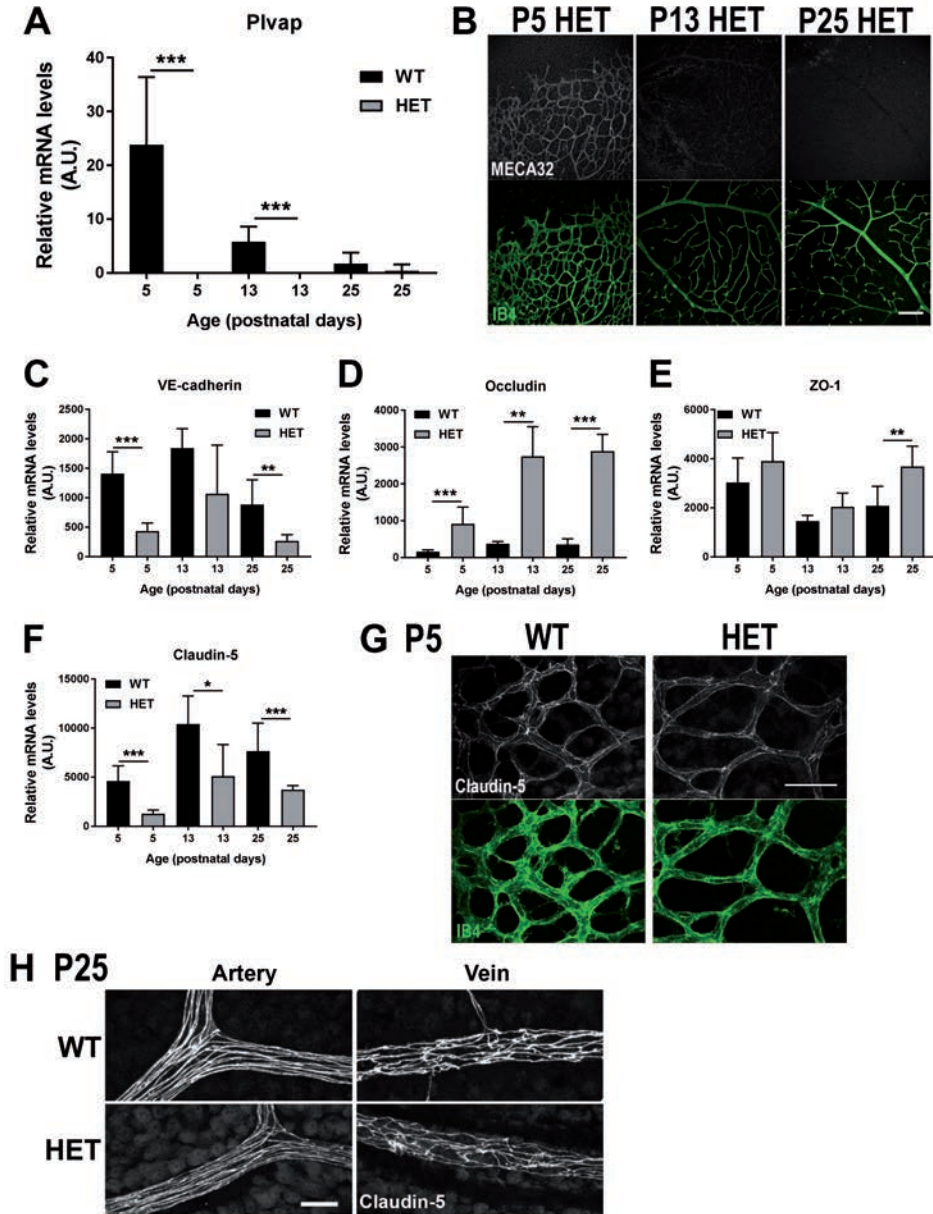


Figure 4. Reduced PLVAP expression affects retinal tight junctions. (A) Plvap mRNA was not detected in retinal vasculature of Plvap^{-/-} mice (HET), whereas expression levels were significantly higher in wildtype mice (WT) at P5 and P13. (B) PLVAP protein expression was visualized in retinal wholemounts of HET mice using MECA-32 (grey) and isolectin B4 (IB4, green) at P5, P13 and P25. Scale bar = 100 μ m. mRNA levels of VE-cadherin (C), occludin (D), ZO-1 (E) and claudin-5 (F) in the retinal vasculature in WT and HET mice at P5, P13 and P25; n=7-8 for both groups at each time point. Data are depicted as mean \pm s.d. *P<0.05, **P<0.01, ***P<0.001. Protein expression of claudin-5 (grey) in retinal wholemounts of WT and HET mice at P5 (G) and P25 (H). Scale bar = 50 μ m (P5 and P25).

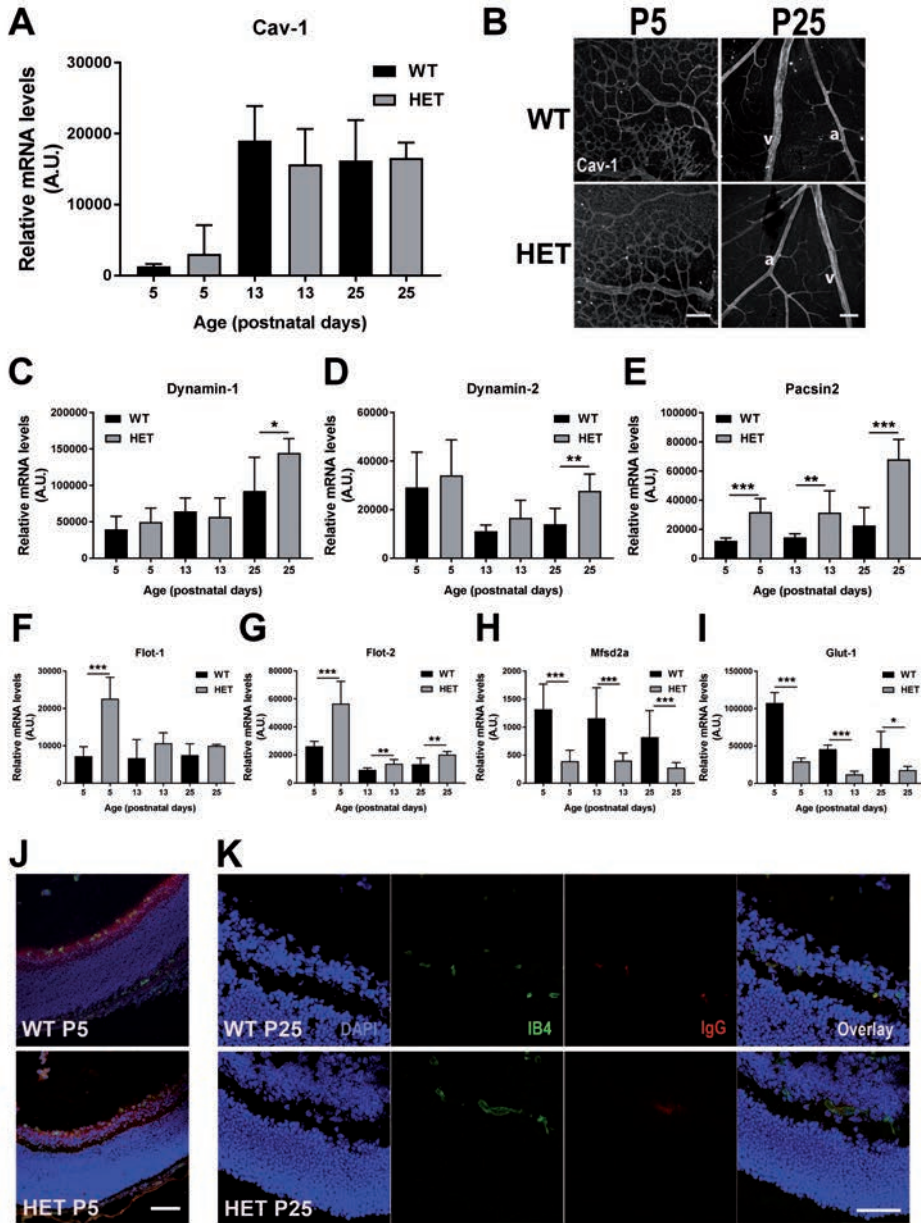


Figure 5. Reduced PLVAP expression affects BRB transport mechanisms. (A) mRNA levels of caveolin-1 in the retinal vasculature of *Plvap*^{+/-} (HET) and wildtype (WT) mice. (B) Caveolin-1 protein expression (grey) was similar in retinal wholemounts of HET and WT mice at P5 and P25. a = artery, v = vein. Scale bar = 100 μ m. mRNA levels of flot-1 (C), flot-2 (D), dynamin-1 (E), dynamin-2 (F), pacsin-2 (G), *mfsd2a* (H), and Glut-1 (I) in the retinal vasculature of WT and HET mice of P5, P13 and P25; n=7-8 for both groups at each time point. * $P < 0.05$, ** $P < 0.01$, *** $P < 0.001$. Data are depicted as mean \pm s.d. Leakage of IgG from retinal vessels at P5 (J) and P25 (K) was similar in WT and HET mice. Scale bar = 100 μ m (P5) and 50 μ m (P25).

to wildtype mice (Fig. 5F, G). In contrast, *Msf2a*, a known suppressor of transcytosis in BBB and BRB formation (32, 33), was significantly less expressed in *Plvap*^{+/-} mice at all time points (Fig. 5H). In addition, mRNA levels of the glucose transporter *Glut1* (an indicator of BBB function and development; 34), were significantly lower in *Plvap*^{+/-} mice at all time points (Fig. 5I). Although above results suggest a compromised transcellular transport, IgG staining in retinal cryostat sections was similar in wildtype and *Plvap*^{+/-} mice at P5 and P25 (Fig. 5J, K). Together, these data indicate that decreased PLVAP levels during development lead to altered expression of molecules involved in (caveolar) transport, without functional changes in protein permeability as shown by IgG leakage patterns.

PLVAP expression does not affect the number of caveolae in the retina

Given the changes in components of caveolae-dependent transport in *Plvap*^{+/-} mice, we compared retinal capillaries in the inner and outer plexiform layer of wildtype and *Plvap*^{+/-} mice at the ultrastructural level. In human retinal explants, we previously showed that knockdown of PLVAP expression blocked the formation of caveolae after VEGF stimulation, but that basal levels of caveolae in endothelial cells were not affected (20). In line with this, we did not find any differences in the number of abluminal and/or luminal caveolae between wildtype and *Plvap*^{+/-} mice (Fig. 6A-C). In both groups, there was a paucity of endothelial caveolae, and there were more located on the abluminal side as compared to the luminal side (Fig. 6C).

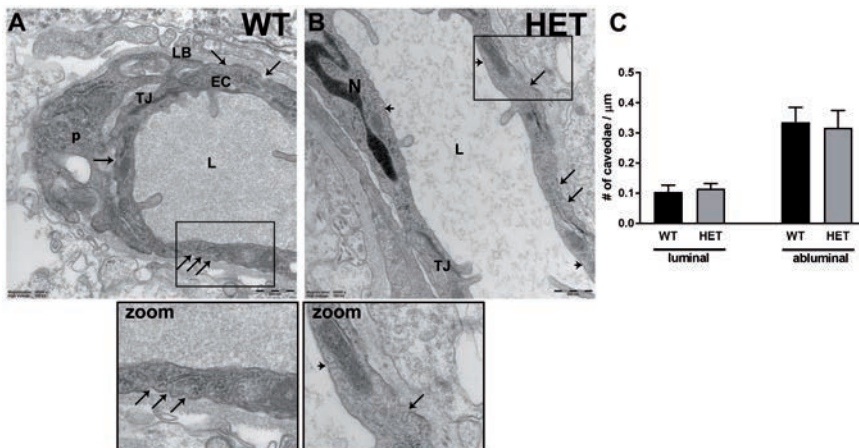


Figure 6. PLVAP expression does not affect the number of caveolae in the retina. Caveolae were observed at the abluminal and luminal side of endothelial cells in wildtype (WT) (A) and *Plvap*^{+/-} (HET) (B) mice at P30, as shown on the ultrastructural level with transmission electron microscopy. (C) Quantification of the number of caveolae per μm in retinal capillaries at the luminal and abluminal side in WT and HET mice. Data are depicted as mean \pm s.d. *** $P < 0.001$. EC = endothelial cell, p = perivascular cell, LB = lamina basalis, TJ = tight junction, L = lumen, N = nucleus, large arrow = abluminal caveolae, small arrow = luminal caveolae. Scale bar = 500 nm.

VEGFR expression during retinal vascularization

VEGF signaling is a main driver of angiogenesis during development and of neovascularization in pathological conditions, such as proliferative diabetic retinopathy (1). In addition, PLVAP expression is regulated by VEGF in a VEGF receptor 2 (VEGFR2)-dependent manner (35). In developing retinal vessels of wildtype mice, we found similar patterns of mRNA levels of VEGFR2 (*Kdr*) and its co-receptors *Nrp1* and *Nrp2*, with high expression at P3 and a decrease over time (Fig. 7C,G,I), and this pattern matched the pattern of *Plvap* expression (Fig. 3A). In contrast, VEGFR1 (*Flt1*) expression was low at P3 but showed a steep increase over time, with high expression at P25 (Fig. 7A). VEGFR3 (*Flt4*) expression was more capricious, starting low at P3 but increasing erratically over time (Fig. 7E). mRNA levels of *Vegfa* started off high and decreased over time in the retinal vasculature of wildtype mice (Fig. 7K). The expression patterns of VEGFR1, -2, -3, *Nrp1* and -2, and *Vegfa* were similar in *Plvap*^{+/-} and wildtype mice (Fig. 7B,D,E,H,J,L). However, at P25, *Vegfa* expression was significantly higher in retinal vessels of *Plvap*^{+/-} mice, whereas VEGFR2 and -3 (at P5 and P13) and *Nrp1* expression (at all time points) were lower. This suggests that during development VEGF signaling is different in *Plvap*^{+/-} mice as compared to wildtype mice.

Reduced PLVAP levels protect against VEGF- and histamine-induced vascular leakage in continuous endothelium

Previously, we have shown that knockdown of PLVAP prevents both VEGF-induced permeability in an *in vitro* model of the BRB, and hypoxia-induced retinal vascular leakage in an *in vivo* mouse model (20). To assess whether reduced PLVAP expression protects *Plvap*^{+/-} mice from VEGF-induced vascular leakage, we performed a modified Miles assay using the dorsal skin, which has continuous, non-fenestrated endothelium, but contains caveolae with stomatal diaphragms (17). Evans Blue extravasation under basal (PBS-injected) conditions was similar in wildtype and *Plvap*^{+/-} mice (Fig. 8A, B). Histamine, a known inducer of vascular leakage (36) but not of PLVAP expression, was used as a positive control. In wildtype mice, VEGF (200 ng) and histamine (500 ng) both caused increased extravasation of Evans Blue, although this increase did not reach statistical significance for VEGF (P=0.06). In accordance with our previous results, VEGF injections did not result in increased vascular leakage in *Plvap*^{+/-} mice (Fig. 8A, B), confirming the necessity of PLVAP in VEGF-induced vascular leakage. Unexpectedly, histamine-induced vascular leakage was also decreased in *Plvap*^{+/-} mice (Fig. 8A, B), indicating that PLVAP may also be downstream of histamine signaling, and that PLVAP is necessary for histamine-induced leakage.

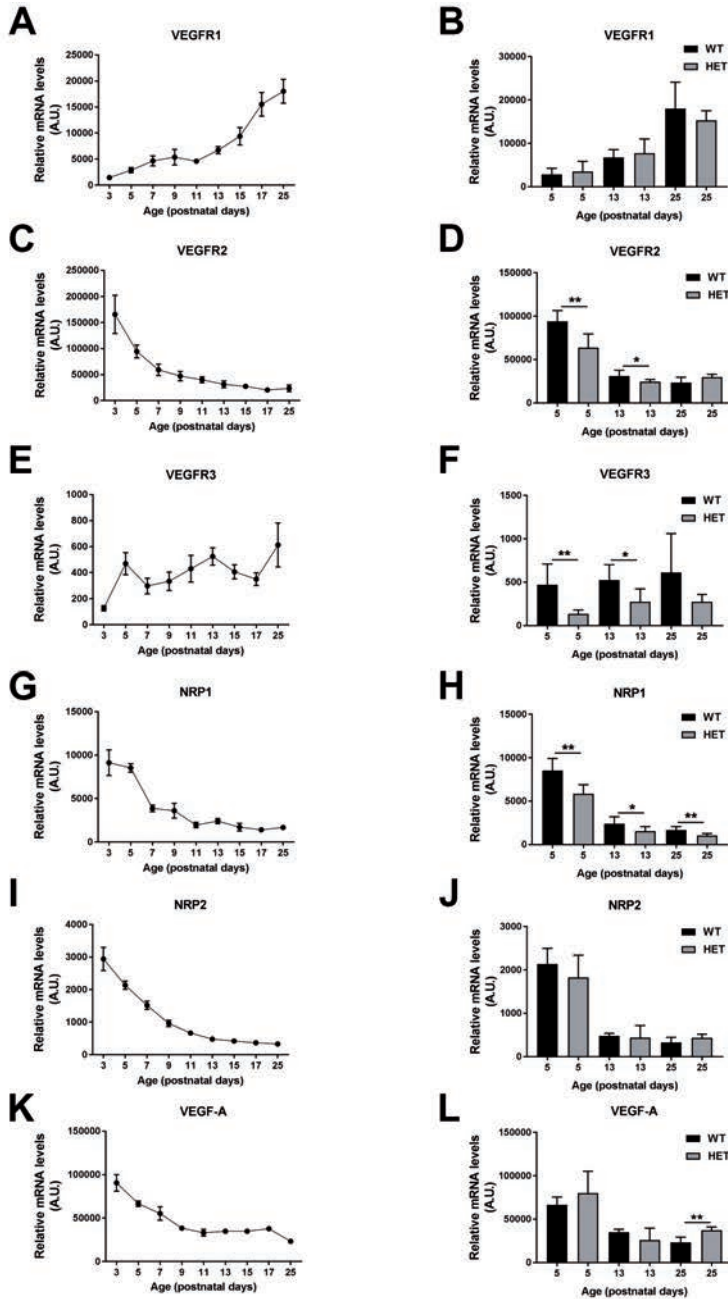


Figure 7. Expression of VEGFR1, -2, -3, NRP1, -2 and VEGF-A during retinal vascularization in wildtype (WT) and *Plvap*^{+/-} (HET) mice. mRNA levels of VEGFR1 (A), VEGFR2 (C), VEGFR3 (E), NRP1 (G), NRP2 (I) and VEGF-A (K) in the retinal vasculature of WT mice from P3 to P25; n=7-11 for all ages. mRNA levels of VEGFR1 (B), VEGFR2 (D), VEGFR3 (F), NRP1 (H), NRP2 (J) and VEGF-A (L) in the retinal vasculature of WT and HET mice at P5, P13 and P25; n=7-8 for both groups at each time point. *P<0.05, **P<0.01. Data are depicted as mean±s.d.

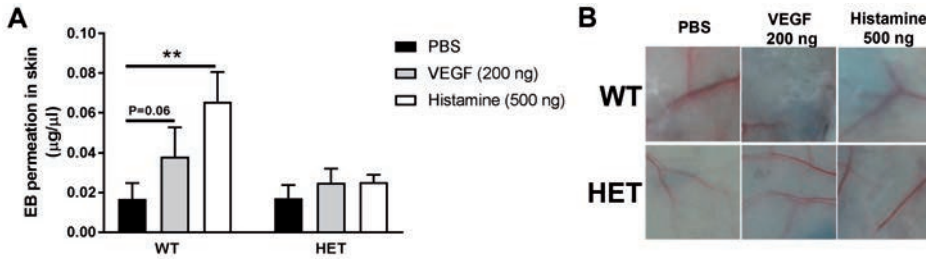


Figure 8. Reduced PLVAP levels protect against VEGF- and histamine-induced vascular leakage. A modified Miles assay was performed in the dorsal skin of *Plvap*^{+/-} (HET, n=5) and wildtype (WT, n=5) mice treated with VEGF (200 ng), histamine (500 ng) and PBS as a control. (A) In WT mice, histamine and VEGF caused increased extravasation of Evans Blue (EB), which was not the case in HET mice. ***P*<0.01. Data are depicted as mean±s.d. (B) Representative images of skin injected with PBS, VEGF or histamine in WT and HET mice.

DISCUSSION

Here, we conducted a comprehensive study using neonatal mice from P3 to P25 to describe all aspects of BRB development, with a special focus on PLVAP. We show that PLVAP expression decreases during BRB formation, and that it is absent when a functional barrier is formed. Moreover, using *Plvap*^{+/-} mice, we show that PLVAP is necessary for retinal vascularization during early development and that vascular permeability mechanisms and VEGF signaling are affected in *Plvap*^{+/-} mice.

One of the limitations of this study is that we report mainly data on mRNA expression, which may not necessarily result in differences in protein levels and cannot be readily correlated to functional differences. For instance, mRNA levels at P5 and P25 for claudin-5 were more or less similar, whereas there was still IgG extravasation in the retina at P5, but not at P25 and thus, mRNA levels cannot be correlated to IgG leakage. In addition, claudin-5 protein was already clearly present at P5, and located at the tight junctions. Furthermore, our study is largely observational and descriptive in nature. However, since our knowledge of cellular and molecular development of the BRB is still incomplete, exploratory research as this study is needed in order to design subsequent studies focused on the mechanisms at play. Lastly, we have made use of genetically modified mice, in which the full knockout condition has a major systemic phenotype and is often embryonically lethal. Therefore, we used heterozygous mice for our experiments, which has the advantage that these mice, to our knowledge, do not have systemic defects (Stan et al., 2012; Herrnberger et al., 2012). Heterozygous mice express PLVAP during development, albeit much less than wildtype mice, therefore the effects we observed may be even greater when PLVAP is completely ablated. However, a conditional PLVAP knockout in which PLVAP expression can be temporally silenced would be even more valuable to further study the role of PLVAP in barrier endothelium, as systemic and compensatory effects can be minimized in such a model.

Taking a closer look at the maturation of the BRB, we found that mRNA levels of the tight junction genes claudin-5 and occludin increased over time. From our analyses, it appeared that claudin-5 and occludin expression stabilized in the third postnatal week, confirming previous studies (37). In contrast, ZO-1 and β -catenin showed a decrease over time, and VE-cad peaked around P11 and then decreased as well. This points towards temporal differences in the recruitment of different components to form the tight and adherens junctions. Indeed, it has been shown that adherens junctions precede tight junctions at intercellular contacts, and that adherens junctions influence tight junction organization (38). Protein expression of claudin-5 was already clearly present and localized at the cell membranes from P5 and onwards. This suggests that immature vessels already have tight junctions, confirming 2 recent reports that angiogenesis occurs simultaneously with barrier genesis in the BBB (34) and that the tight junctions in retinal vessels in mice are functional as early as P1 (33).

To our knowledge, this is the first study to follow the time course of PLVAP and BRB gene expression in detail during BRB development. PLVAP is regularly used as a marker of immature or leaky retinal vessels, and in addition to VEGF, is transcriptionally regulated by canonical Wnt/ β -catenin signaling during development (39). When inactivating different components of the Wnt signaling pathway (*e.g.* Wnt-receptor ligands, receptors or co-receptors), *Plvap* is upregulated and vessels become leaky, also in adult mice (40). In these studies, PLVAP was expressed in wildtype mice at P7 and P8 (41, 42), but not at P15 (43). Using mice from postnatal day 3 to 25, our study confirms and expands these observations, showing a gradual decrease in *Plvap* expression. Expression of β -catenin mRNA also decreased during development, but considering the dual role of β -catenin in endothelium (adherens junctions and Wnt signaling), we cannot conclude anything about β -catenin mRNA levels in relation to PLVAP expression. PLVAP protein expression was found in all retinal vessels (arteries, capillaries and veins), which is in agreement with an earlier report using the monoclonal MECA-32 antibody in mouse brain tissue (6). While the MECA-32 antibody specifically recognizes murine PLVAP, these results contrast with other studies, because antibodies against human PLVAP (PAL-E, 174/2) do not stain arterioles, arteries and large veins (44, 45).

With the generation of *Plvap*-deficient mice, large steps have been taken towards unraveling the function of PLVAP in fenestrated and continuous endothelia of peripheral organs by 2 independent research groups (17, 18). However, in mature barrier endothelium PLVAP is normally absent, except in pathological conditions like diabetic retinopathy (15), brain tumors (7, 14) and ischemic brain tissue (46, 47). Using *Plvap*^{+/-} mice, we tried to elucidate the role of PLVAP in barrier endothelium. Our data suggest that, in addition to its role in transcellular permeability, PLVAP may also affect paracellular permeability via effects on endothelial junctions. Expression levels of ZO-1 and particularly occludin were higher in *Plvap*^{+/-} animals, whereas claudin-5 and VE-cad were lower, although this was not apparent for claudin-5 protein expression using retinal wholemounts. Whether these differences are caused by direct or indirect effects of reduced PLVAP expression requires further investigation. However, in our previous studies *in vitro*, we observed a modest

beneficial effect of *Plvap* inhibition on junctions of bovine retinal endothelial cells, but no differences in permeability to a small molecular tracer (20), making a direct effect of PLVAP on paracellular permeability less likely.

By immunostaining of endogenous markers of protein leakage in retinal cryostat sections, we found signs of extravasation of plasma proteins during the first postnatal weeks, whereas the barrier was closed at P15 in wildtype mice. These observations support our hypothesis that the absence of PLVAP is a prerequisite for the BRB to be functional, as PLVAP protein expression was still present from P3 to P15, but virtually absent at later time points. However, reduced PLVAP levels during development in *Plvap*^{+/-} mice had some unexpected effects on the expression of components of the transcellular transport pathway. *Plvap*^{+/-} mice had increased mRNA expression of Flot1, Flot2, Pacsin2, and dynamin-1 and -2, which are all proteins involved in caveolar transport. In addition, *Mfsd2a*, a recently described suppressor of transcytosis in the BBB (32) and BRB (33), was significantly downregulated in *Plvap*^{+/-} mice, suggesting that these mice may have impaired inhibition of transcytosis. Nevertheless, expression of caveolin-1, the key structural protein of caveolae, was similar in wildtype and *Plvap*^{+/-} retinal vessels, as was the number of endothelial caveolae. In addition, large differences in IgG extravasation were not observed between wildtype and *Plvap*^{+/-} mice. In fact, in the few homozygous knockout (*Plvap*^{-/-}) mice that we were able to obtain, we also did not find leakage of IgG from the retinal vessels at P15. This suggests that despite the increased expression of the vesicular transcellular transport machinery and downregulation of *Mfsd2a*, there is no obvious increase in transcytosis under basal conditions in the retinal vessels of these mice. Considering these data and the fact that the absence, rather than the presence, of PLVAP is needed for a functional BRB, it seems that the course of barrier formation in *Plvap*^{+/-} mice may differ from the wildtype situation, but that the final result is the same, i.e. a highly restrictive barrier with very limited transport. However, it should be noted that staining for serum proteins in fixed retinal sections is suboptimal, as it does not cover leakage in the entire retina. Therefore, it would be interesting to confirm our results of BRB permeability status with other functional assays, like Evans Blue tracer extravasation or HRP tracer combined with EM in future experiments, to study this aspect in more detail.

Although we did not observe differences in basal retinal permeability between wildtype and *Plvap*^{+/-} mice, we have shown before that knockdown of PLVAP prevented hypoxia- and VEGF-driven increases in retinal permeability (20). In contrast, knockdown of PLVAP in fenestrated endothelium caused a size-selective increase in permeability, but did not appear to have an effect on permeability in continuous endothelium (17, 18). In line with this, we did not observe differences in basal permeability between wildtype and *Plvap*^{+/-} mice in continuous endothelium of the dorsal skin. However, reduced PLVAP levels prevented VEGF- and histamine-induced permeability. Thus, the role of PLVAP in basal permeability may be more structural (acting as a size-selective molecular 'sieve'), whereas in pathological (VEGF- or hypoxia-induced) permeability conditions, the role of PLVAP may be more active, e.g. by enhancing the VEGF signal to the endothelium. Alternatively, lack of PLVAP could render the continuous endothelium with a more barrier-like endothelium status,

limiting permeability to a minimum. This is in line with our previous findings, in which human umbilical vein endothelial cells had increased trans-endothelial electric resistance and decreased permeability after PLVAP knockdown (Wisniewska-Kruk et al., 2016).

Our group and others (46, 47) have found strong indications that PLVAP is not only a marker of vascular permeability, but is also actively involved in angiogenesis. In the present study, we observed that vascularization of *Plvap*^{+/-} retinas was delayed during early development at P5, whereas the vasculature was normalized at P13. We were able to obtain a retinal wholemount and frozen tissue of one *Plvap*^{-/-} mouse at P5, showing an even more severe delay in vascularization (Fig. S5A-C, n=1 for *Plvap*^{-/-}). To our surprise, even in *Plvap*^{-/-} mice, the retinal vasculature at P15 and P32 was more or less similar as in wildtype and *Plvap*^{+/-} mice (Fig. S5D-G, n=1 for *Plvap*^{+/-} for both time points). Based on these findings, we conclude that PLVAP is necessary for initial retinal developmental angiogenesis, but that compensatory mechanisms eventually ensure development of a normal vasculature. This is corroborated by the fact that we did not find significant differences between wildtype and *Plvap*^{+/-} mice when quantifying vessel density at time points beyond P5.

In the retina, development of the superficial vascular plexus is driven by a physiological hypoxia-driven upregulation of VEGF (26). Moreover, migration of angiogenic sprouts is dependent on signaling via VEGFR2, located on the tip cell filopodia (48), and VEGFR2 expression in activated endothelium correlates strongly with expression of VEGF-A (49). In the current study, we found that VEGFR1 expression increased over time, whereas VEGFR2 was initially high, but decreased and stabilized with low expression at later time points. These data are in line with a report showing that in control human eyes and PBS-injected monkey eyes, retinal vessels stained positively for VEGFR1, but expression of VEGFR2 and VEGFR3 was low or absent (50) and indicates that in quiescent retinal endothelium there is constitutive expression of VEGFR1, but not of VEGFR2 and -3. In contrast, in the majority of diabetic human eyes and VEGF-injected monkey eyes, expression of all 3 VEGF-receptors was observed, and VEGFR2 expression coincided with PLVAP expression in leaky retinal microvessels (50). We have found recently that PLVAP directly or indirectly regulates VEGFR2 transcription (manuscript in preparation). Here, we observed that VEGFR2 expression in the retinal vasculature followed the same expression pattern as *Plvap*, and as expression of its co-receptors *Nrp1* and *Nrp2*. Only at P5, we found that VEGFR2 transcript levels were decreased in *Plvap*^{+/-} retinas. This was also the only time point at which we observed a delay in retinal vascularization in *Plvap*^{+/-} mice. These observations suggest that during early retinal vascular development, reduced PLVAP levels result in diminished angiogenesis, possibly via reduced VEGFR2-mediated signaling. At later time points, this defect is overcome and vascularization proceeds normally, despite some resulting venous anomalies that we report here. The higher incidence of aberrant retinal veins, traversing from the ganglion cell layer all the way to the outer plexiform layer, may also relate to this defective VEGF-signaling in *Plvap*^{+/-} mice, e.g. by not conveying the cues to halt migration and growth of endothelial sprouts at the right location.

In conclusion, in this comprehensive study we showed that during BRB formation, expression of tight and adherens junctions is temporally regulated and that immature

vessels already have tight junctions. In addition, we specified the role of PLVAP in barrier endothelium by demonstrating, with the use of *Plvap*^{+/-} mice, that PLVAP is essential in the retina during early development for proper retinal vascularization. These data confirm a role for PLVAP in angiogenesis, likely mediated by VEGF signaling. Moreover, we suggest that in differentiated barrier endothelium, the absence of PLVAP appears to be a prerequisite for a functional BRB, since there is retinal vascular leakage at times when PLVAP expression is high, and PLVAP is absent when the barrier was intact. Taken together, our data indicate that PLVAP expression may be permissive for vascular leakage as part of the transcytosis machinery, rather than it having a regulatory role.

ACKNOWLEDGEMENTS

The authors thank Dr. R.A. Hoebe of the Cellular Imaging Core Facility for his advice with respect to quantification of vascular density and help with making the supplemental video. The mouse strain used for this research project, B6;129S5-*Plvap*^{tm1Lex}/Mmucd, identification number 032525-UCD, was obtained from the Mutant Mouse Regional Resource Center (MMRRC), a NIH funded strain repository, and was donated to the MMRRC by Genentech.

This study was made possible by the financial support of the Diabetes Fonds (Dutch Diabetes Fund, grant 2014.00.1784) and by the following foundations: Landelijke Stichting voor Blinden en Slechtienden, Novartis Fonds and St. MD Fonds, that contributed through UitZicht (Grant UitZicht 2014-33), the Nederlandse Vereniging ter Verbetering van het Lot der Blinden, Rotterdamse Stichting Blindenbelangen (Grant B20140050) and Stichting Blindenhulp. This study was published with the help of Edmond en Marianne Blaauw Fonds voor Oogheelkunde. The funding organizations had no role in the design or conduct of this research. They provided unrestricted grants.

Disclosure: None of the authors disclosed any relevant financial relationships.

AUTHOR CONTRIBUTIONS

AEvdW designed and performed experiments, analyzed data and wrote the manuscript; JWK designed and performed experiments; IMCV and WFI performed experiments; HAvV and NNvdW were involved in the EM study; IK analyzed data, contributed to the study design, discussion, and editing of the manuscript, CJFvN and ROS contributed to the study design, discussion, and editing of the manuscript.

REFERENCES

1. Antonetti, D. A., Klein, R., and Gardner, T. W. (2012) Diabetic retinopathy. *N Engl J Med* **366**, 1227-1239
2. van der Wijk, A. E., Vogels, I. M., van Veen, H. A., van Noorden, C. J., Schlingemann, R. O., and Klaassen, I. (2018) Spatial and temporal recruitment of the neurovascular unit during development of the mouse blood-retinal barrier. *Tissue and Cell* **52**, 42-50
3. Gariano, R. F. (2003) Cellular mechanisms in retinal vascular development. *Prog Retin Eye Res* **22**, 295-306
4. Klaassen, I., Van Noorden, C. J., and Schlingemann, R. O. (2013) Molecular basis of the inner blood-retinal barrier and its breakdown in diabetic macular edema and other pathological conditions. *Prog Retin Eye Res* **34**, 19-48
5. Klaassen, I., Hughes, J. M., Vogels, I. M., Schalkwijk, C. G., Van Noorden, C. J., and Schlingemann, R. O. (2009) Altered expression of genes related to blood-retina barrier disruption in streptozotocin-induced diabetes. *Exp Eye Res* **89**, 4-15
6. Hallmann, R., Mayer, D. N., Berg, E. L., Broermann, R., and Butcher, E. C. (1995) Novel mouse endothelial cell surface marker is suppressed during differentiation of the blood brain barrier. *Dev Dyn* **202**, 325-332
7. Schlingemann, R. O., Bots, G. T. A. M., Van Duinen, S. G., and Ruiters, D. J. (1988) Differential Expression of Endothelium-specific Antigen PAL-E in Vasculature of Brain Tumors and Preexistent Brain Capillaries. *Annals of the New York Academy of Sciences* **529**, 111-114
8. Risau, W., and Wolburg, H. (1990) Development of the blood-brain barrier. *Trends Neurosci* **13**, 174-178
9. Saunders, N. R., Liddelow, S. A., and Dziegielewska, K. M. (2012) Barrier mechanisms in the developing brain. *Front Pharmacol* **3**, 46
10. Schlingemann, R. O., Hofman, P., Anderson, L., Troost, D., and van der Gaag, R. (1997) Vascular expression of endothelial antigen PAL-E indicates absence of blood-ocular barriers in the normal eye. *Ophthalmic Res* **29**, 130-138
11. Stan, R. V., Ghitescu, L., Jacobson, B. S., and Palade, G. E. (1999) Isolation, cloning, and localization of rat PV-1, a novel endothelial caveolar protein. *J Cell Biol* **145**, 1189-1198
12. Hofman, P., Blaauwgeers, H. G., Tolentino, M. J., Adamis, A. P., Nunes Cardozo, B. J., Vrensen, G. F., and Schlingemann, R. O. (2000) VEGF-A induced hyperpermeability of blood-retinal barrier endothelium in vivo is predominantly associated with pinocytotic vesicular transport and not with formation of fenestrations. Vascular endothelial growth factor-A. *Curr Eye Res* **21**, 637-645
13. Hofman, P., Blaauwgeers, H. G., Vrensen, G. F., and Schlingemann, R. O. (2001) Role of VEGF-A in endothelial phenotypic shift in human diabetic retinopathy and VEGF-A-induced retinopathy in monkeys. *Ophthalmic Res* **33**, 156-162
14. Leenstra, S., Troost, D., Das, P. K., Claessen, N., Becker, A. E., and Bosch, D. A. (1993) Endothelial cell marker PAL-E reactivity in brain tumor, developing brain, and brain disease. *Cancer* **72**, 3061-3067
15. Schlingemann, R. O., Hofman, P., Vrensen, G. F., and Blaauwgeers, H. G. (1999) Increased expression of endothelial antigen PAL-E in human diabetic retinopathy correlates with microvascular leakage. *Diabetologia* **42**, 596-602
16. Stan, R. V. (2004) Multiple PV1 dimers reside in the same stomatal or fenestral diaphragm. *Am J Physiol Heart Circ Physiol* **286**, H1347-1353
17. Herrnberger, L., Seitz, R., Kuespert, S., Bosl, M. R., Fuchshofer, R., and Tamm, E. R. (2012) Lack of endothelial diaphragms in fenestrae and caveolae of mutant Plvap-deficient mice. *Histochem Cell Biol* **138**, 709-724
18. Stan, R. V., Tse, D., Deharvengt, S. J., Smits, N. C., Xu, Y., Luciano, M. R., McGarry, C. L., Buitendijk, M., Nemani, K. V., Elgueta, R., Kobayashi, T., Shipman, S. L., Moodie, K. L., Daghlian, C. P., Ernst, P. A., Lee, H. K., Suriawinata, A. A., Schned, A. R., Longnecker, D. S., Fiering, S. N., Noelle, R. J., Gimi, B., Shworak, N. W., and Carriere, C. (2012) The diaphragms of fenestrated endothelia: gatekeepers of vascular permeability and blood composition. *Dev Cell* **23**, 1203-1218
19. Elkadri, A., Thoeni, C., Deharvengt, S. J., Murchie, R., Guo, C., Stavropoulos, J. D., Marshall, C. R., Wales, P., Bandsma, R., Cutz, E., Roifman, C. M., Chitayat, D., Avitzur, Y., Stan, R. V., and Muise, A. M. (2015) Mutations in Plasmalemma Vesicle Associated Protein Result in Sieving Protein-Losing Enteropathy Characterized by Hypoproteinemia, Hypoalbuminemia, and Hypertriglyceridemia. *Cell Mol Gastroenterol Hepatol* **1**, 381-394 e387
20. Wisniewska-Kruk, J., van der Wijk, A. E., van Veen, H. A., Gorgels, T. G., Vogels, I. M., Versteeg, D., Van Noorden, C. J., Schlingemann, R. O., and Klaassen, I. (2016) Plasmalemma Vesicle-Associated Protein Has a Key Role in Blood-Retinal Barrier Loss. *Am J Pathol* **186**, 1044-1054
21. Truett, G. E., Heeger, P., Mynatt, R. L., Truett, A. A., Walker, J. A., and Warman, M. L. (2000) Preparation of PCR-quality mouse genomic DNA with hot sodium hydroxide and tris (HotSHOT). *Biotechniques* **29**, 52, 54
22. Kowluru, R. A., Jirousek, M. R., Stramm, L., Farid, N., Engerman, R. L., and Kern, T. S. (1998) Abnormalities of retinal metabolism in diabetes or experimental galactosemia: V. Relationship between protein kinase C and ATPases. *Diabetes* **47**, 464-469
23. Ruijter, J. M., Ramakers, C., Hoogaars, W. M., Karlen, Y., Bakker, O., van den Hoff, M. J., and Moorman, A. F. (2009) Amplification efficiency: linking baseline and

- bias in the analysis of quantitative PCR data. *Nucleic Acids Res* **37**, e45
24. Mestdagh, P., Van Vlierberghe, P., De Weer, A., Muth, D., Westermann, F., Speleman, F., and Vandesompele, J. (2009) A novel and universal method for microRNA RT-qPCR data normalization. *Genome Biol* **10**, R64
 25. Ruijter, J. M., Thygesen, H. H., Schoneveld, O. J., Das, A. T., Berkhout, B., and Lamers, W. H. (2006) Factor correction as a tool to eliminate between-session variation in replicate experiments: application to molecular biology and retrovirology. *Retrovirology* **3**, 2
 26. Fruttiger, M. (2007) Development of the retinal vasculature. *Angiogenesis* **10**, 77-88
 27. Felinski, E. A., and Antonetti, D. A. (2005) Glucocorticoid regulation of endothelial cell tight junction gene expression: novel treatments for diabetic retinopathy. *Curr Eye Res* **30**, 949-957
 28. Stan, R. V. (2005) Structure of caveolae. *Biochim Biophys Acta* **1746**, 334-348
 29. Macia, E., Ehrlich, M., Massol, R., Boucrot, E., Brunner, C., and Kirchhausen, T. (2006) Dynasore, a cell-permeable inhibitor of dynamin. *Dev Cell* **10**, 839-850
 30. Shvets, E., Ludwig, A., and Nichols, B. J. (2014) News from the caves: update on the structure and function of caveolae. *Curr Opin Cell Biol* **29**, 99-106
 31. Lang, D. M., Lommel, S., Jung, M., Ankerhold, R., Petrausch, B., Laessing, U., Wiechers, M. F., Plattner, H., and Stuermer, C. A. (1998) Identification of reggie-1 and reggie-2 as plasmamembrane-associated proteins which cluster with activated GPI-anchored cell adhesion molecules in non-caveolar micropatches in neurons. *J Neurobiol* **37**, 502-523
 32. Ben-Zvi, A., Lacoste, B., Kur, E., Andreone, B. J., Mayshar, Y., Yan, H., and Gu, C. H. (2014) Mfsd2a is critical for the formation and function of the blood-brain barrier. *Nature* **509**, 507-511
 33. Chow, B. W., and Gu, C. H. (2017) Gradual Suppression of Transcytosis Governs Functional Blood-Retinal Barrier Formation. *Neuron* **93**, 1325-+
 34. Umans, R. A., Henson, H. E., Mu, F., Parupalli, C., Ju, B., Peters, J. L., Lanham, K. A., Plavicki, J. S., and Taylor, M. R. (2017) CNS angiogenesis and barrierogenesis occur simultaneously. *Dev Biol* **425**, 101-108
 35. Strickland, L. A., Jubb, A. M., Hongo, J. A., Zhong, F., Burwick, J., Fu, L., Frantz, G. D., and Koeppen, H. (2005) Plasmalemmal vesicle-associated protein (PLVAP) is expressed by tumour endothelium and is upregulated by vascular endothelial growth factor-A (VEGF). *J Pathol* **206**, 466-475
 36. Gardner, T. W., Leshner, T., Khin, S., Vu, C., Barber, A. J., and Brennan, W. A., Jr. (1996) Histamine reduces ZO-1 tight-junction protein expression in cultured retinal microvascular endothelial cells. *Biochem J* **320** (Pt 3), 717-721
 37. Luo, Y., Xiao, W., Zhu, X., Mao, Y., Liu, X., Chen, X., Huang, J., Tang, S., and Rizzolo, L. J. (2011) Differential expression of claudins in retinas during normal development and the angiogenesis of oxygen-induced retinopathy. *Invest Ophthalmol Vis Sci* **52**, 7556-7564
 38. Taddei, A., Giampietro, C., Conti, A., Orsenigo, F., Breviaro, F., Pirazzoli, V., Potente, M., Daly, C., Dimmeler, S., and Dejana, E. (2008) Endothelial adherens junctions control tight junctions by VE-cadherin-mediated upregulation of claudin-5. *Nat Cell Biol* **10**, 923-934
 39. Liebner, S., Corada, M., Bangsow, T., Babbage, J., Taddei, A., Czupalla, C. J., Reis, M., Felici, A., Wolburg, H., Fruttiger, M., Takeeto, M. M., von Melchner, H., Plate, K. H., Gerhardt, H., and Dejana, E. (2008) Wnt/beta-catenin signaling controls development of the blood-brain barrier. *J Cell Biol* **183**, 409-417
 40. Zhou, Y., Wang, Y., Tischfield, M., Williams, J., Smallwood, P. M., Rattner, A., Takeeto, M. M., and Nathans, J. (2014) Canonical WNT signaling components in vascular development and barrier formation. *J Clin Invest* **124**, 3825-3846
 41. Chen, J., Stahl, A., Krahe, N. M., Seaward, M. R., Joyal, J. S., Juan, A. M., Hatton, C. J., Aderman, C. M., Dennison, R. J., Willett, K. L., Sapieha, P., and Smith, L. E. (2012) Retinal expression of Wnt-pathway mediated genes in low-density lipoprotein receptor-related protein 5 (Lrp5) knockout mice. *PLoS One* **7**, e32020
 42. Schafer, N. F., Luhmann, U. F., Feil, S., and Berger, W. (2009) Differential gene expression in Ndpk-knockout mice in retinal development. *Invest Ophthalmol Vis Sci* **50**, 906-916
 43. Junge, H. J., Yang, S., Burton, J. B., Paes, K., Shu, X., French, D. M., Costa, M., Rice, D. S., and Ye, W. (2009) TSPAN12 regulates retinal vascular development by promoting Norrin- but not Wnt-induced FZD4/beta-catenin signaling. *Cell* **139**, 299-311
 44. Schlingemann, R. O., Dingjan, G. M., Emeis, J. J., Blok, J., Warnaar, S. O., and Ruiters, D. J. (1985) Monoclonal antibody PAL-E specific for endothelium. *Lab Invest* **52**, 71-76
 45. Niemela, H., Elima, K., Henttinen, T., Irjala, H., Salmi, M., and Jalkanen, S. (2005) Molecular identification of PAL-E, a widely used endothelial-cell marker. *Blood* **106**, 3405-3409
 46. Carson-Walter, E. B., Hampton, J., Shue, E., Geynisman, D. M., Pillai, P. K., Sathanoori, R., Madden, S. L., Hamilton, R. L., and Walter, K. A. (2005) Plasmalemmal vesicle associated protein-1 is a novel marker implicated in brain tumor angiogenesis. *Clin Cancer Res* **11**, 7643-7650
 47. Shue, E. H., Carson-Walter, E. B., Liu, Y., Winans, B. N., Ali, Z. S., Chen, J., and Walter, K. A. (2008) Plasmalemmal vesicle associated protein-1 (PV-1) is a marker of blood-brain barrier disruption in rodent models. *BMC Neurosci* **9**, 29

48. Gerhardt, H., and Betsholtz, C. (2005) How do endothelial cells orientate? *EXS*, 3-15
49. Kremer, C., Breier, G., Risau, W., and Plate, K. H. (1997) Up-regulation of flk-1/vascular endothelial growth factor receptor 2 by its ligand in a cerebral slice culture system. *Cancer Res* 57, 3852-3859
50. Witmer, A. N., Blaauwgeers, H. G., Weich, H. A., Alitalo, K., Vrensen, G. F., and Schlingemann, R. O. (2002) Altered expression patterns of VEGF receptors in human diabetic retina and in experimental VEGF-induced retinopathy in monkey. *Invest Ophthalmol Vis Sci* 43, 849-857

1
2
3
4
5
6
7
8
&

SUPPLEMENTAL INFORMATION

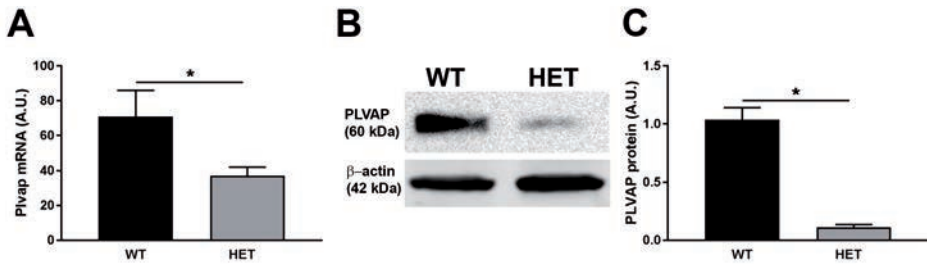
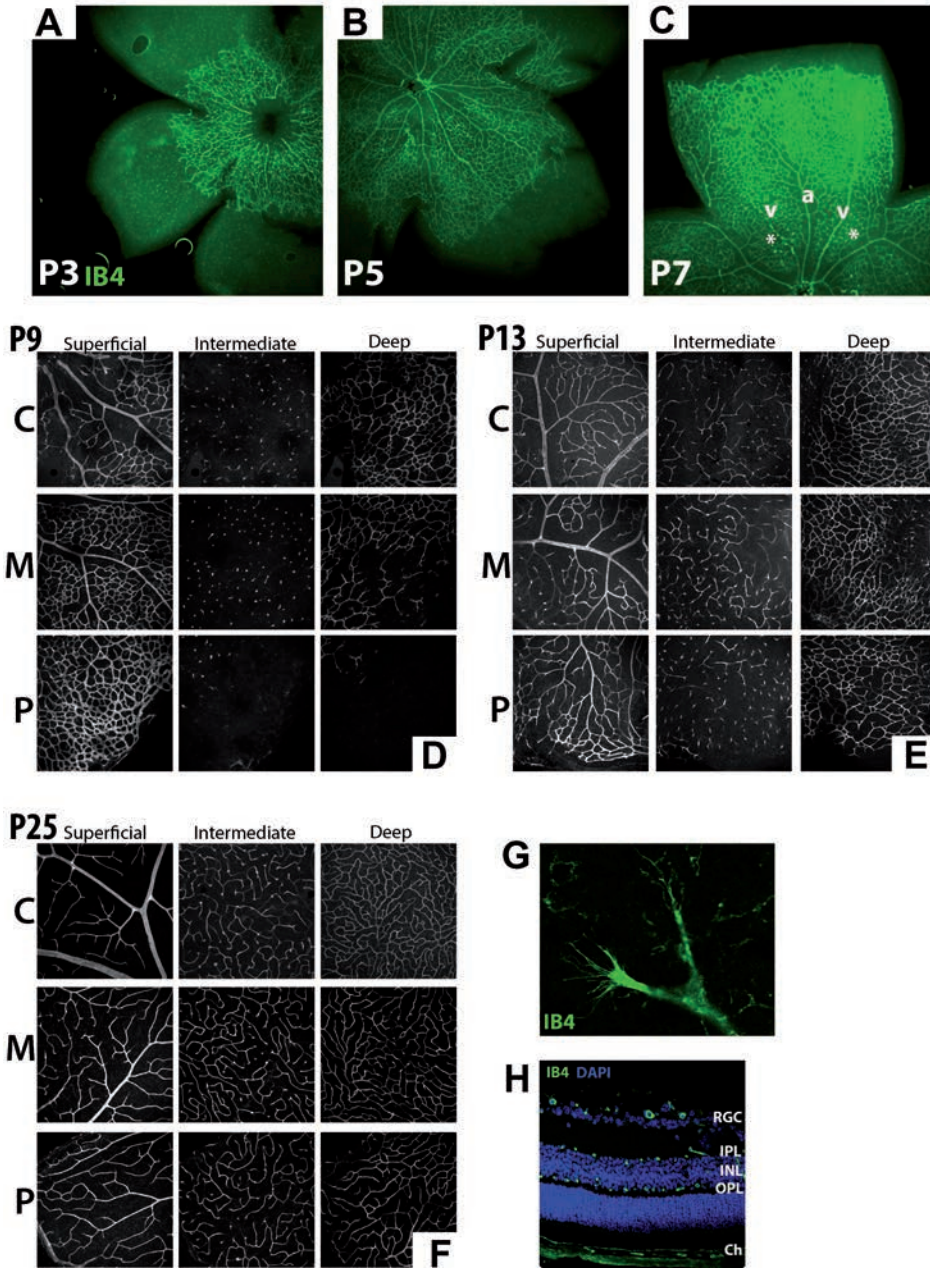


Figure S1. PLVAP expression in wildtype and *Plvap*^{+/-} mice. (A) *Plvap*^{+/-} mice (HET) showed significantly lower *Plvap* mRNA expression levels in kidney as compared to wildtype (WT) mice. Also on the protein level, there was significantly less PLVAP expression in kidneys from HET mice, as compared to WT (B). (C) Quantification of PLVAP expression from kidney samples of WT and HET mice. **P*<0.05. Data are depicted as mean \pm s.d.

Figure S2. (right page) Vascularization of wildtype retinas. Retinal vascularization of the mouse eye was imaged in retinal wholemounts using isolectin B4 (green) at postnatal (P) age 3 (A), P5 (B) and P7 (C). (D) At P9, the superficial vascular plexus reached the periphery, and the intermediate and deep capillary plexi started to be generated. (E) At P13, the deep capillary plexus was connected, whereas the intermediate capillary plexus was still being generated. (F) At P25, all 3 vascular plexi were generated and connected. (G) Formation of the intermediate and deep capillary plexi were initiated through sprouting angiogenesis from the superficial vascular plexus. Image shows a sprouting vessel from the superficial into the intermediate layer at P13. (H) Confocal image of a retinal cryostat section at P25, showing 3 parallel vascular plexi in the retinal ganglion cell layer and the inner and outer plexiform layers. Nuclei are stained with DAPI (blue). IB4 = isolectin B4, v = vein, a = artery, asterisks (*) indicate veins from which capillaries sprout into the intermediate and deep capillary layers shown as bright green dots, C = central retina, M = middle retina, P = peripheral retina, RGC = retinal ganglion cell layer, IPL = inner plexiform layer, INL = inner nuclear layer, OPL = outer plexiform layer, Ch = choriocapillaris.



1
2
3
4
5
6
7
8
&

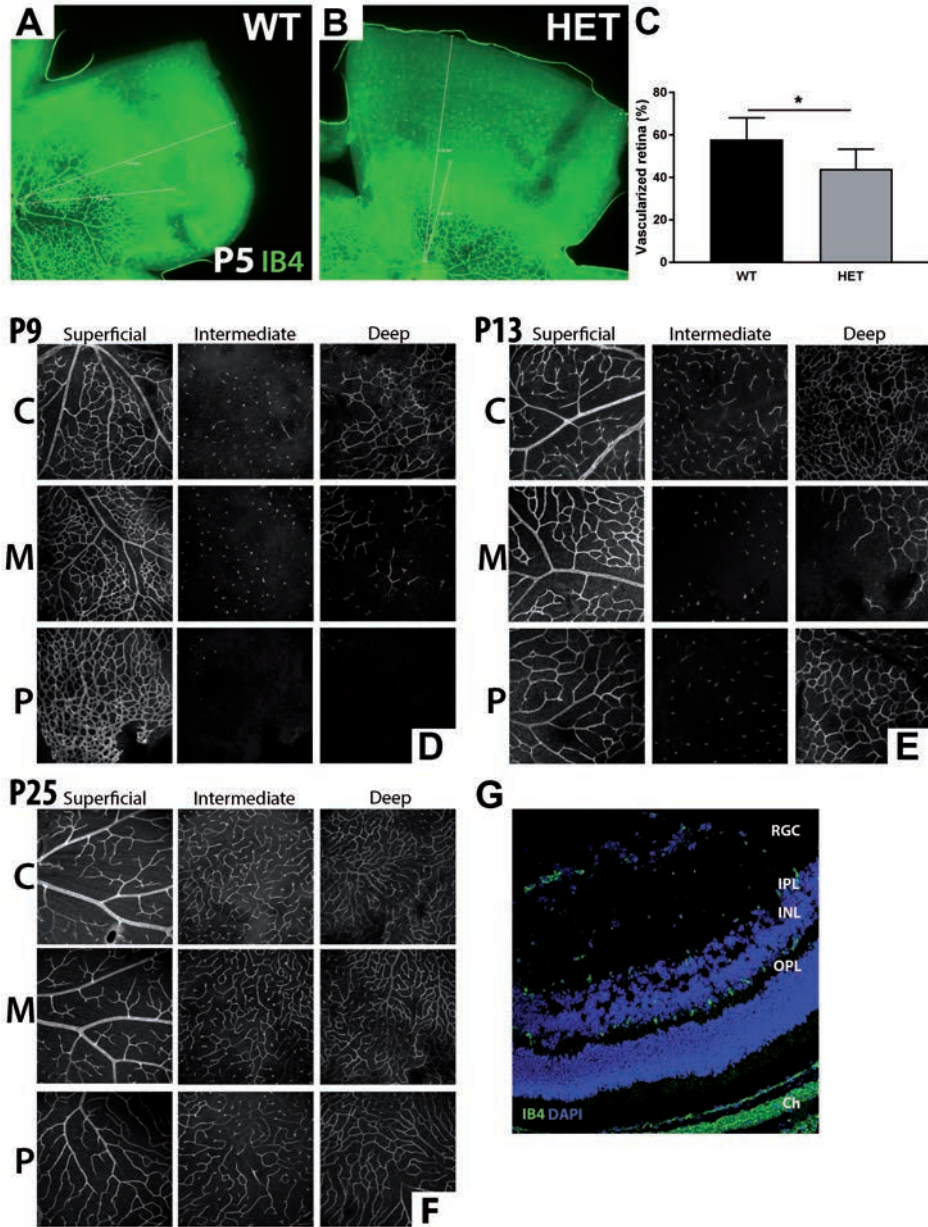


Figure S3. Vascularization of the *Plvap*^{-/-} (HET) retina. Retinal vascularization was imaged in retinal wholemounts using isolectin B4 (green) at P5, P9, P13 and P25. At P5, retinal vascularization was delayed in HET mice (B), when compared to WT mice (A). (C) Quantification of retinal vascularization at P5. (D) At P9, the superficial vascular plexus reached the periphery, and the intermediate and deep capillary plexi started to be generated. (E) At P13, the deep capillary plexus was connected, whereas the intermediate capillary plexus was still being generated. (F) At P25, all 3 vascular plexi were generated and connected. (G) Confocal image of a retinal cryostat section at P25, showing 3 parallel vascular plexi in the retinal ganglion cell layer and the inner and outer plexiform layers.

(continued) Nuclei are stained with DAPI (blue). IB4 = isolectin B4, C = central retina, M = middle retina, P = peripheral retina, RGC = retinal ganglion cell layer, IPL = inner plexiform layer, INL = inner nuclear layer, OPL = outer plexiform layer, Ch = choriocapillaris.

1
2
3
4
5
6
7
8
&

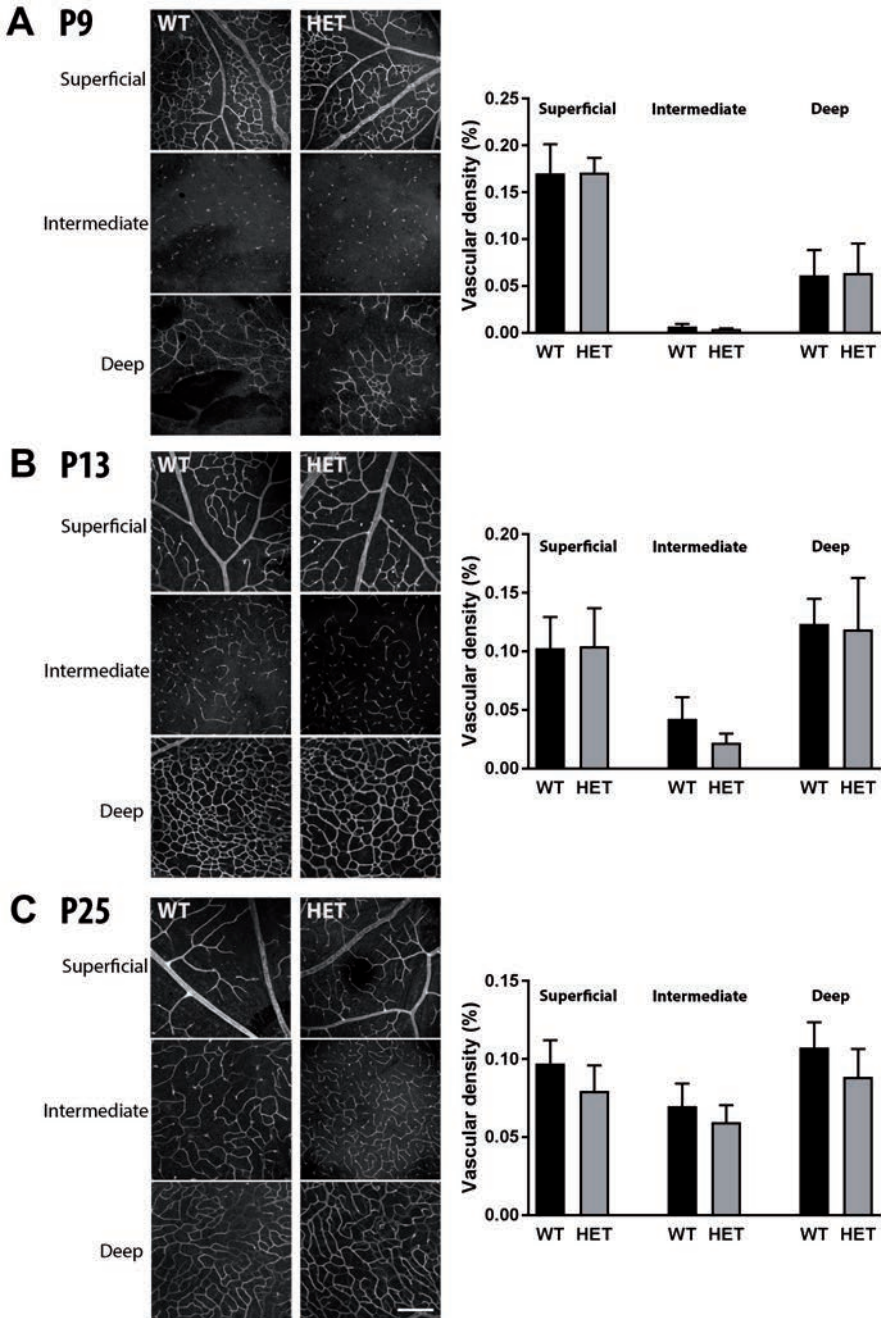


Figure S4. Reduced PLVAP expression does not alter vascular density. Vascular density of the retina was visualized with isolectin B4 in wildtype (WT) and *Plvap*^{+/-} mice (HET) at P9 (A), P13 (B) and P25 (C) and quantified in the central retina, using Matlab software; n=3-5 per time point for HET and n=4-8 per time point for WT. Scale bar = 200 μ m. Data are depicted as mean \pm s.d.

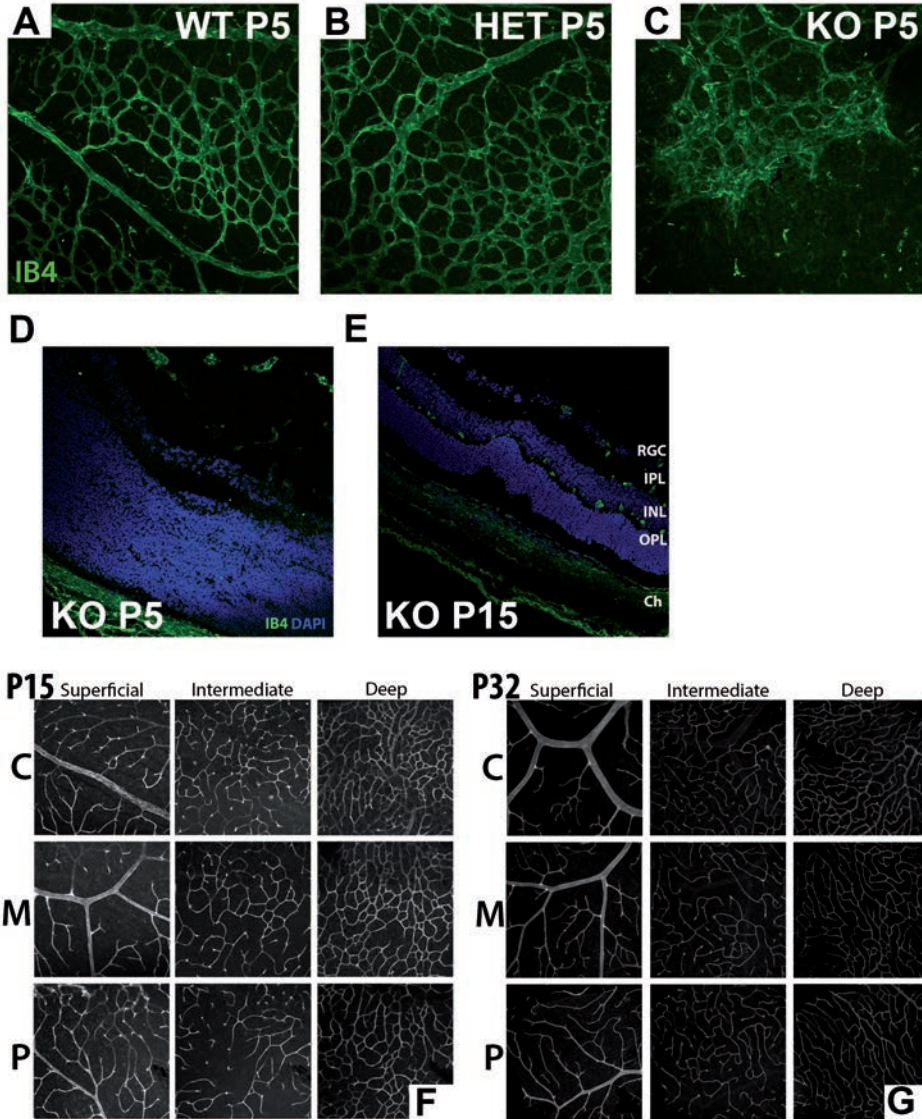
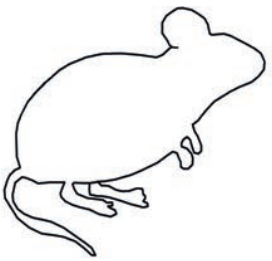


Figure S5. Vascularization of the *Plvap*^{-/-} (KO) retina. Retinal vascularization at P5 was visualized in retinal wholemounts using isolectin B4 (green). In KO mice, the retinal vasculature at P5 was significantly delayed as compared to wildtype (WT) and *Plvap*^{+/-} (HET) mice (A-C). Confocal images of a retinal cryostat section at P5 (D) and P15 (E) in *Plvap*^{-/-} mice. At P15, 3 parallel vascular layers were formed. Nuclei are stained with DAPI (blue). (F) At P15, the deep capillary plexus was connected, whereas the intermediate capillary plexus was still being generated. (G) At P32, all 3 vascular plexi were formed and connected. The retinal vasculature was similar as in WT and HET mice, although there may be less arteries, which was compensated for by more arterial branching in the central retina. IB4 = isolectin B4, C = central retina, M = middle retina, P = peripheral retina, RGC = retinal ganglion cell layer, IPL = inner plexiform layer, INL = inner nuclear layer, OPL = outer plexiform layer, Ch = choriocapillaris.

Table S1. Number of veins and arteries traversing from the superficial plexus to the deep capillary layer in retinas from wildtype (WT; n=14) and *Plvap^{+/-}* (HET; n=17) mice.

	Veins imaged (n)	Veins traversing (n)	Veins traversing (% of imaged)	Arteries imaged (n)	Arteries traversing (n)	Arteries traversing (% of imaged)
WT (n=14)	61	6	9.8	92	3	3.3
HET (n=17)	68	14	20.6	111	3	2.7

Video S1. Traversing retinal veins in the retina of a *Plvap^{+/-}* (HET) mouse. A 3D image of the retinal vasculature was generated from a confocal z-stack of a retinal wholemount. The vasculature is depth coded (red = superficial vascular plexus, green/yellow = intermediate capillary layer, blue = deep capillary layer). The artery in the middle grows into the superficial vascular plexus, with capillaries branching off to generate the parallel intermediate and deep capillary layers. The 2 retinal veins (indicated by the white drawing pins) grow from the optic nerve head into the superficial vascular plexus, but traverse the retinal layers, ending in the deep capillary layer.



4

Plasmalemma Vesicle-Associated Protein has a key role in blood-retinal barrier loss

Joanna Wisniewska-Kruk,^{*} Anne-Eva van der Wijk,^{*} Henk A. van Veen,^y Theo G.M.F. Gorgels,^z Ilse M.C. Vogels,^{*} Danielle Versteeg,^x Cornelis J.F. Van Noorden,^{*y} Reinier O. Schlingemann,^{*} and Ingeborg Klaassen^{*}

Ocular Angiogenesis Group,^{*} Departments of Ophthalmology and Cell Biology and Histology, and the Core Facility Cellular Imaging,^y Department of Cell Biology and Histology, Academic Medical Center, University of Amsterdam, Amsterdam

University Eye Clinic Maastricht,^z Maastricht University Medical Center, Maastricht

Hubrecht Laboratory and Interuniversity Cardiology Institute Netherlands,^x Royal Netherlands Academy of Arts and Sciences, Utrecht, the Netherlands

R.O.S. and I.K. contributed equally to this work as senior authors.

Am J Pathol. (2016) 186(4): 1044-1054

ABSTRACT

Loss of blood-retinal barrier (BRB) properties induced by vascular endothelial growth factor (VEGF) and other factors is an important cause of diabetic macular edema. Previously, we found that the presence of plasmalemma vesicle-associated protein (PLVAP) in retinal capillaries associates with loss of BRB properties and correlates with increased vascular permeability in diabetic macular edema. In this study, we investigated whether absence of PLVAP protects the BRB from VEGF-induced permeability. We used lentiviral-delivered shRNA or siRNA to inhibit PLVAP expression. The barrier properties of in vitro BRB models were assessed by measuring transendothelial electrical resistance, permeability of differently sized tracers, and the presence of endothelial junction complexes. The effect of VEGF on caveolae formation was studied in human retinal explants. BRB loss in vivo was studied in the mouse oxygen-induced retinopathy model. The inhibition of PLVAP expression resulted in decreased VEGF-induced BRB permeability of fluorescent tracers, both in vivo and in vitro. PLVAP inhibition attenuated transendothelial electrical resistance reduction induced by VEGF in BRB models in vitro and significantly increased transendothelial electrical resistance of the nonbarrier human umbilical vein endothelial cells. Furthermore, PLVAP knockdown prevented VEGF-induced caveolae formation in retinal explants but did not rescue VEGF-induced alterations in endothelial junction complexes. In conclusion, PLVAP is an essential cofactor in VEGF-induced BRB permeability and may become an interesting novel target for diabetic macular edema therapy.

INTRODUCTION

Diabetic macular edema (DME) is the most frequent cause of vision loss among patients with diabetic retinopathy (DR). DME is a complex disease that has been associated with increased vascular permeability due to loss of the inner blood-retinal barrier (BRB).¹ Disruption of the BRB leads to abnormal inflow of proteins and fluids into retinal tissue, which results in thickening of the central fovea and loss of visual acuity. Vascular endothelial growth factor (VEGF)-A, a potent inducer of vasopermeability and angiogenesis, is a major mediator in this process.²⁻⁴ The inner BRB is composed of endothelial cells, pericytes, and astrocytes, which form the neurovascular unit.^{1,5} The robust interactions among these BRB components are crucial for formation and maintenance of a physical and biochemical barrier between the retina and the vasculature.⁶⁻⁸ Despite the fact that the mechanisms of BRB breakdown in DR are multifactorial⁹ and affect all components of the neurovascular unit,¹⁰⁻¹² the most prominent pathologic changes are observed in endothelial cells.¹³⁻¹⁵ To date, two mechanisms are known to contribute to VEGF-induced endothelial cell permeability: increased paracellular transport that involves changes in endothelial junction integrity and increased transcellular transport in endothelial cells mediated by caveolae.^{10,13-15} The effects of VEGF on altered tight junction integrity and decreased junctional protein expression have been extensively studied,^{5,10,13,16,17} but the effect of augmented caveolae formation in endothelium on BRB permeability remains not fully understood.

Plasmalemma vesicle-associated protein (PLVAP, PV-1) is an endothelial cell-specific protein^{18,19} that is known to be a structural component of caveolae, transendothelial channels, and fenestrae.^{20,21} PLVAP is widely expressed in capillaries and the venous vasculature but is absent in intact BRB and blood-brain barrier (BBB) endothelia.²²⁻²⁷ However, in pathologic conditions, such as DR,^{22,23,28} ischemia, or cancer,^{24,26,27} PLVAP expression in the BRB and BBB is highly upregulated and associated with increased barrier permeability.^{23,25} In addition, PLVAP expression has been described to be present in immature and incompletely developed vasculature of the BRB and BBB.²⁹⁻³² Recently, we studied the Akimba mouse, a model of advanced DR with hyperglycemia and high levels of intraocular VEGF, in which we found a correlation between *Plvap* mRNA levels and the degree of fluorescein leakage.¹⁰ PLVAP expression in endothelium is triggered by VEGF^{6,13,26,28,33} in a VEGF receptor (VEGFR)-2-dependent manner.²⁶ Therefore, PLVAP may be involved in VEGF-induced BRB loss in DR.

Although PLVAP expression has been associated with BRB loss, a functional contribution of this protein to increased vascular permeability has not yet been found. This study examines the role of PLVAP in BRB loss in vivo and in vitro. To this end, we have assessed the changes that occur in permeability and in endothelial junctions and caveolae formation after knocking down PLVAP to elucidate the mechanisms that underlie the regulatory role of PLVAP in vascular permeability.

MATERIALS AND METHODS

Lentiviral constructs

For knockdown of PLVAP expression, shRNA lentiviral pLKO.1 constructs (SIGMA/TRC; Sigma-Aldrich, Zwijndrecht, the Netherlands) were used. Control cells were transduced with nontargeting shRNA (MISSION Non-Target shRNA Control Vector; Sigma-Aldrich). Virus particles were generated by co-transfecting the constructs with three packaging plasmids, pMDLg/pRRE, pMD2G, and RSV-Rev (Addgene, Cambridge, MA), into 293T cells. The sequences of PLVAP shRNA and Non-Target shRNA were 5'-CCGGCCCTTT CACACACACTTTCTACTCGAGTA-GAAAGTGTGTGTGAAAGGGTTTTTTG-3' and 5'-CCGGCAACAAGATGAAGAGC-ACCAACTCGAGTTGGTGCTCTTCATCTTGTG TTTTT-3', respectively.

In vitro BRB model

Cells were isolated as described previously.⁶ Three different models were assembled to study endothelial barrier permeability, including i) a bovine retinal endothelial cell (BREC) monolayer, ii) a triple co-culture model with BRECs, pericytes, and astrocytes, and iii) human umbilical vein endothelial cells (HUVECs). In the triple co-culture model, BRECs were seeded on top of the Transwell filter, primary rat astrocytes were seeded on the reverse side of the Transwell filters, and bovine primary pericytes were cultured on the bottom of a 24-well plate in which a Transwell filter was placed, as described previously.⁶ Three independent experiments were performed for each model (n=11).

Permeability assay

Three days after assembling each of the models, shRNA lentiviral particles (50 pg/mL) were added to the cells. After 24 hours, cells were stimulated apically with 200 ng/mL human recombinant VEGF-A (Sanquin, Amsterdam, the Netherlands). Permeability was measured 72 hours after stimulation by adding 766 Da Cy3 (GE Healthcare, Eindhoven, the Netherlands) and 70 kDa of fluorescein isothiocyanate (FITC)-dextran (FD; Sigma-Aldrich). Concentrations of the tracer molecules were determined using a fluorescence plate reader (BMG POLARstar; MTX Lab Systems, Vienna, VA), as described previously.⁶ Transendothelial electrical resistance (TEER) was measured in real time with the CellZscope system (NanoAnalytics, Münster, Germany) and expressed as Ωcm^2 . In all experimental conditions, data were collected in quadruplicate. Three independent experiments were performed for each model.

RNA isolation and Real-Time PCR

Total RNA was isolated using TRIzol reagent (Life Technologies, Bleiswijk, the Netherlands) following the manufacturer's protocol. Total RNA (1 μg) was treated with DNase I (Amplification Grade; Life Technologies) and reverse transcribed into first-strand cDNA using a Maxima First Strand cDNA Synthesis Kit (Thermo Scientific, Roskilde,

Denmark).⁶ Real-time PCR was performed using a CFX96 system (Bio-Rad; Hercules, CA) as described previously.¹³ Expression data were normalized by the geometric mean of the two most stable housekeeping genes (ACTG1 and GAPDH), as determined by NormFinder.³⁴ Three independent experiments were performed for each model (n=6). Primer sequences for bovine PLVAP were described previously.¹³ The primer sequences for ACTG1 and GAPDH were as follows: ACTG1, forward 5'-GATCTGGCACCACACCTTTT-3', reverse 5'-CCACATACATGGCAGGAGTG-3'; GAPDH, forward 5'-GGCGTGAACCACGAGAA-GTATAA-3', reverse 5'-CCCTCCACGATGCCAAAGT-3'.

Oxygen-induced retinopathy mouse model

Animal experiments were performed with the approval of the Animal Ethics Committee of the University of Amsterdam and in compliance with the Association for Research in Vision and Ophthalmology statement for the Use of Animals in Ophthalmic and Vision Research. From postnatal day 7 (P7), C57BL/6 mice were exposed to 75% oxygen for 5 days.³⁵ At P12, pups were divided randomly, anesthetized, and injected intraocularly with 1 μ L of 50 μ M anti-Plvap siRNA (Accell SMARTpool; Thermo Scientific), treated with control siRNA (Accell Green Non-targeting siRNA; Thermo Scientific), or remained untreated. Pups were then returned to room air. At P17, fluorescein angiography was performed, and alternatively, eyes were analyzed for PLVAP expression and vascular leakage indicated by IgG extravasation into retinal tissue. Two independent experiments were performed (n=6).

For evaluation of blood vessel tortuosity, retinas were flat mounted and stained with isolectin IB4 probe conjugated with Alexa-647 (Life Technologies). A minimum total of four blood vessels (arterioles and venules) were measured per retina (n=8 per group) using ImageJ version 1.48v (NIH, Bethesda, MD; <http://imagej.nih.gov/ij>). The tortuosity index was expressed as a quotient: vessel curve length (mean length, 788 μ m) over the line distance between the two ends.

Fluorescein angiography

At P17, oxygen-induced retinopathy (OIR) mice were anesthetized. The pupils of the mouse eyes were dilated with tropicamide eye drops (Mydracil; Alcon Laboratories, Fort Worth, TX). A plano contact lens (Cantor + Nissel, Brackley, UK) was placed on the mouse eye to prevent dehydration of the cornea. Next, mice were injected intracardially with a mixture of 70 kDa FD (10 mg/mL; Sigma-Aldrich) and sodium fluorescein [approximately 4 kDa, 10% in phosphate-buffered saline (PBS); Sigma-Aldrich]. Immediately after injections, image acquisition was started using the scanning laser ophthalmoscope HRA2 (Heidelberg Engineering, Heidelberg, Germany). The HRA2 was operated in the fluorescence mode with the excitation light provided by a 488-nm Argon laser. All images were acquired by using the automatic real-time mode. Eyes were enucleated 20 minutes after perfusion of tracers, dissected, and fixed in 4% paraformaldehyde for 4 hours at 4°C. Next, retinas were washed in PBS to remove sodium fluorescein from the tissue and flat mounted. Images of retinas were recorded using a wide-field fluorescence microscope (Leica, Mannheim, Germany).

The images were processed in GIMP software version 2.8v (GNU Image Manipulation Program; GNOME Foundation, Cambridge, MA; <http://www.gimp.org>).

Fluorescence immunohistochemistry

Mouse retinas were permeabilized with 0.5% Triton X-100 for 30 minutes and incubated for 1 hour with 2% normal goat serum (Dako, Glostrup, Denmark). Subsequently, retinas were incubated overnight at 4°C with isolectin IB4 (Alexa-546 conjugated; Invitrogen), anti-PLVAP antibody (rat monoclonal, MECA-32; Abcam, Cambridge, UK), or anti-mouse IgG antibody (Dako). Next, retinas were washed three times for 30 minutes in PBS, and Cy3-, Cy5-, FITC-, or Alexa-488-conjugated secondary antibodies (Jackson Immuno- Research, Suffolk, UK) were added. After 2 hours of incubation, retinas were washed three times for 30 minutes in PBS. Finally, retinas were flat mounted and covered with fluorescence mounting medium (Dako).

BRECs or HUVECs were cultured on collagen- or gelatin- coated plastic coverslips (Nunc, Thermo Scientific), respectively. Cells were fixed and stained as described previously.⁶ The following antibodies were used: anti-claudin-5 (rabbit polyclonal; Life Technologies), anti-vascular endothelial cadherin (rabbit polyclonal; Abcam), anti-zonula occludens protein 1 (rabbit polyclonal; Life Technologies), anti-VEGFR2 (rabbit polyclonal; Abcam), phalloidin (Texas Red-X; Invitrogen, Life Technologies), and anti-PLVAP (174/2; Abcam). Nuclei were stained using 1 µg/mL Hoechst dye (Life Technologies). Images were recorded using a confocal laser scanning microscope SP8 (Leica). In all experiments, specificity of the staining was tested by omitting primary antibody. Three independent experiments were performed (n=8).

To quantify actin stress fibers, GIMP software was used. Images of BRECs stained with phalloidin probe were converted to gray scale images with three shades of gray. Stress fibers were assessed by quantifying only the brightest pixels divided by the total amount of gray pixels, representing the amount of total fiber.

Cell-based enzyme-linked immunosorbent assay

BRECs were seeded in a 96-well plate (Corning, Canton, MA). After reaching confluence, cells were transduced with lentiviral constructs and 24 hours later stimulated with 200 ng/mL human recombinant VEGF. Cells were fixed with 4% paraformaldehyde and stained as described previously.⁶ The following primary antibodies were used: anti-claudin-5 (rabbit polyclonal; Life Technologies), anti-vascular endothelial cadherin (rabbit polyclonal; Abcam), and anti-occludin (mouse monoclonal; Life Technologies). Primary antibodies were detected using horseradish peroxidase-conjugated antibody (rabbit anti-mouse and swine anti-rabbit antibody; Dako). Next 3,3',5,5'-tetramethylbenzidine (Merck, Whitehouse Station, NJ) was added. The reaction was stopped with 1M H₂SO₄ (Merck). The absorbance was measured on a plate reader (Bio-Rad) with excitation at 450 nm and emission at 655 nm. Two independent experiments were performed (n=7).

Electron microscopy

Human donor eyes were provided by the Euro Cornea Bank (Beverwijk, The Netherlands) after removal of corneal buttons for transplantation. The use of human material was in accordance with the international declaration of Helsinki. The Euro Cornea Bank obtained permission from the donors for eye autopsy and the use of clinical information for research purposes. Retinas were dissected from donor eyes (57-year-old man and 62-year-old woman, with no clinical manifestations of diabetes or DR) and sampled using an 8-mm biopsy puncher (Stiefel, Watford, UK). Retinas were cultured in neurobasal medium (Gibco, Life Technologies) supplemented with B27 Serum Free Supplement (Gibco) and antibiotics (1% penicillin streptomycin; Life Technologies). After overnight incubation with lentiviral shRNA constructs (short hairpin control and PLVAP), retinas were stimulated after 72 hours with 100 ng/mL human recombinant VEGF, and samples were fixed and stored in McDowell phosphate buffer.³⁶ After fixation, the samples were washed in 0.1 M phosphate buffer followed by washing in distilled water, osmication for 75 minutes in 1% OsO₄ in water, and additional washing in distilled water. For contrast enhancement in the electron microscope, biopsy specimens were block stained overnight in 1.5% aqueous uranyl acetate and then dehydrated through incubation in ethanol and embedded in epon 812 (Electron Microscopy Sciences, Hatfield, PA). The resin blocks were polymerized for 48 hours at 60°C. Ultrathin sections of 90 nm were cut on a Reichert EM UC6 (Leica) with a diamond knife, collected on Formvar (Structure Probe Inc., West Chester, PA) coated grids, and stained with uranyl acetate and lead citrate. Micrographs were taken with a Veleta Transmission Electron Microscopy camera (Olympus, Soft Imaging Solutions, Münster, Germany). The images were masked and analyzed using iTEM software version 6076 (Olympus Soft Imaging Solutions). The number of caveolae in endothelial cells was assessed by counting the caveolae-like membrane invaginations on the luminal and abluminal side in retinal blood vessel. A mean of 28.5 μm of endothelium, including luminal (mean = 13.3 μm) and abluminal (mean = 15.2 μm) linear length of blood vessel, was evaluated for the presence of caveolae (n = 15 from two different donors).

Statistical analysis

One-way analysis of variance followed by Bonferroni's multiple comparison test were used to evaluate the statistical significance of the data. Results are expressed as mean \pm SEM. $P < 0.05$ was considered significant.

RESULTS

PLVAP inhibition reduces VEGF-induced BRB permeability in vitro

The endothelial barrier in our in vitro BRB model is formed by BRECs. The basal PLVAP expression in these cells is low, but stimulation with 200 ng/mL VEGF for 72 hours leads to significant induction of PLVAP expression, both at the mRNA (Figure 1A) and protein level (Figure 1B). Knocking down PLVAP significantly blocked VEGF-induced PLVAP

expression (Figure 1, A and B), thus confirming an efficient inhibition by shRNA.

To study whether increased PLVAP expression in retinal capillaries is necessary for loss of BRB integrity, we knocked down PLVAP expression in BRECs and induced BRB breakdown using 200 ng/mL VEGF. As expected, stimulation of BRECs with VEGF resulted in a clear decrease in TEER values, which reflects the loss of endothelial barrier properties (Figure 1C). Knockdown of PLVAP expression in BRECs before VEGF stimulation considerably diminished the decrease in TEER values (Figure 1C), suggesting that the absence of PLVAP in endothelial cells has a protective effect on VEGF-induced BRB breakdown. Consistently, knockdown of PLVAP expression in BREC monolayers prevented VEGF-induced permeability for small 766-Da (Figure 1D) and large 70-kDa (Figure 1E) fluorescent tracers 72 hours after stimulation. Given the fact that the BRB is formed by endothelial cells, pericytes, and astrocytes,¹ we further investigated the effect of knocking down PLVAP on VEGF-induced permeability in the triple co-culture BRB model. Knockdown of PLVAP in the triple co-culture BRB model did not significantly reduce VEGF-induced permeability for 766-Da tracers (Figure 1F) but significantly inhibited the permeability for 70-kDa molecules 72 hours after stimulation (Figure 1F). Overall, these data indicate that PLVAP is necessary for VEGF-induced BRB loss.

Effect of PLVAP inhibition on endothelial junction protein expression and integrity

On the basis of TEER and permeability measurements of BRECs cultured on Transwell filters in the presence of increasing doses of VEGF (data not shown), we decided to use a dose of 200 ng/mL for subsequent *in vitro* experiments. VEGF stimulation of BRECs for 12 hours resulted in endothelial junction disorganization along the cell periphery and increased cytoplasmic staining of claudin-5, zonula occludens protein 1, and vascular endothelial cadherin protein (Figure 2A), as determined by immunofluorescence. Furthermore, by using cell-based enzyme-linked immunosorbent assay, we found that VEGF induces a downregulation of vascular endothelial cadherin and occludin expression in BRECs (Figure 2B). Knockdown of PLVAP expression had only a modest positive effect on the preservation of endothelial junction integrity (Figure 2A) and did not rescue them from VEGF-induced degradation (Figure 2B).

In our previous study, we found that VEGF-induced stress fiber formation in endothelial cells leads to the formation of gaps between endothelial cells, which may directly contribute to increased barrier permeability.⁶ A significant reduction in stress fiber formation after inhibition of PLVAP expression was observed in VEGF-stimulated BRECs (Figure 2C), which may contribute to the maintenance of the contact between endothelial cells and the barrier integrity.

Knockdown of PLVAP reduces the number of endothelial caveolae in human retinal explants after VEGF stimulation

To investigate the potential role of PLVAP in increased endothelial cell permeability via induction of caveolae-mediated transcellular transport in these cells, *ex vivo* cultured

human retinas were transduced with shRNA and cultured in the presence or absence of 100 ng/mL VEGF. In control samples incubated with VEGF, a significantly increased number of caveolae was observed in endothelial cells (Figure 3A). Knockdown of PLVAP expression significantly blocked this VEGF-induced formation of caveolae (Figure 3B) but did not alter the basal levels of caveolae in endothelial cells. No differences in the ratio between luminal and abluminal number of caveolae were observed among all investigated conditions (data not shown).

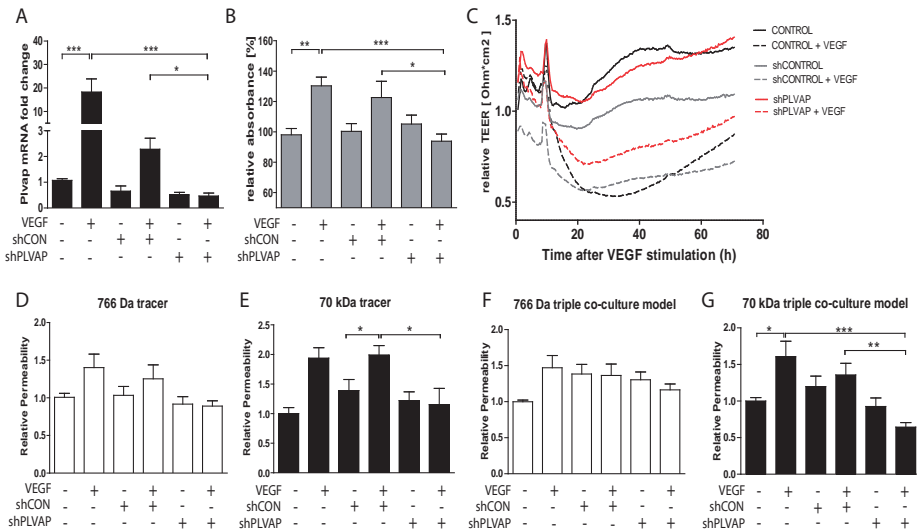


Figure 1. Inhibition of plasmalemma vesicle-associated protein (PLVAP) expression reduces vascular endothelial growth factor (VEGF)induced permeability in the in vitro blood-retinal barrier (BRB) model. Relative PLVAP mRNA (A) and protein (B) levels in control and shRNA transduced bovine retinal endothelial cells (BRECs) that were cultured in the presence or absence of VEGF. mRNA expression was measured using real-time PCR, and protein levels were quantified using cell-based enzyme-linked immunosorbent assay. Lentiviral delivered shPLVAP constructs significantly block VEGF-induced PLVAP expression, both at the mRNA and protein levels. C: Changes in real-time transendothelial electrical resistance (TEER) in control (shCON) and shRNA (shPLVAP) expressing BRECs, cultured in the presence or absence of VEGF. Knockdown of PLVAP expression reduces the VEGF-induced decrease in TEER values. D and E: Relative permeability after knocking down PLVAP expression of 767-Da Cy3 (D) and 70-kDa dextran tracer (E) was measured in BREC monolayers. F and G: Relative permeability in the triple co-culture BRB model of 767-Da Cy3 (F) and 70-kDa dextran (G) after knocking down PLVAP in endothelial cells. Endothelial permeability in all BRB models was induced by 200 ng/mL VEGF for 72 hours. *P < 0.05, **P < 0.01, and ***P < 0.001.

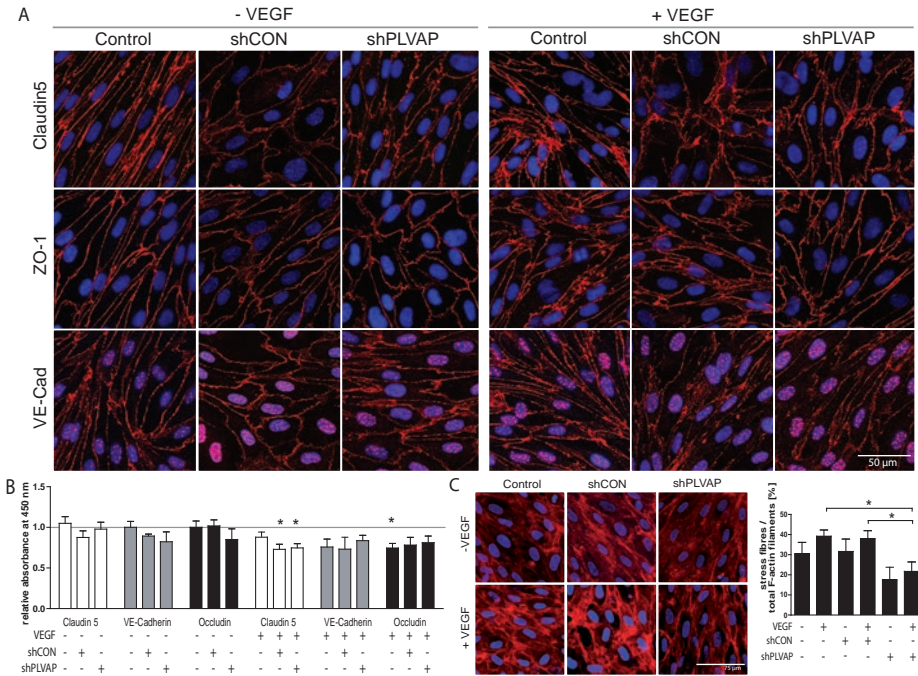


Figure 2. Knockdown of plasmalemma vesicle-associated protein (PLVAP) expression does not prevent vascular endothelial growth factor (VEGF)-induced alterations in tight junction complexes. A: The presence of 200 ng/mL VEGF leads to loss of tight junction integrity in bovine retinal endothelial cells (BRECs). Tight junction staining is presented in red and nuclear staining in blue. B: Inhibition of PLVAP expression has a modest effect on the preservation of the tight junction integrity and does not prevent downregulation of tight junction protein expression in BRECs after VEGF stimulation (200 ng/mL), as determined by cell-based enzyme-linked immunosorbent assay. Protein levels and statistical comparisons are relative to untreated controls. C: Silencing of PLVAP expression in BRECs reduces VEGF-induced stress fiber formation. F-actin filaments were stained using the phalloidin probe. Stress fibers were selected on the basis of on staining intensity (as described in Materials and Methods). Images were recorded using confocal microscopy. Data is presented as means \pm SD. *P < 0.05. VE-Cad, vascular endothelial cadherin; ZO-1, zonula occludens protein 1.

Knockdown of PLVAP reduces hypoxia-induced retinal vascular leakage in vivo

To confirm the functional role of PLVAP in retinal vascular permeability in vivo, we evaluated the effects of knocking down Plvap expression in the mouse OIR model. In this model, P7 mouse pups are exposed to 75% oxygen until P12, which results in large capillary obliteration. Next, pups are removed from the hyperoxia and placed in normoxia, which leads to onset of hypoxia and an overexpression of hypoxia-induced growth factors, such as VEGF, which is a potent inducer of angiogenesis and vessel permeability.

In the OIR model, we observed both high PLVAP protein expression in endothelium and vascular leakage in the retina, as indicated by extravasation of endogenous IgG

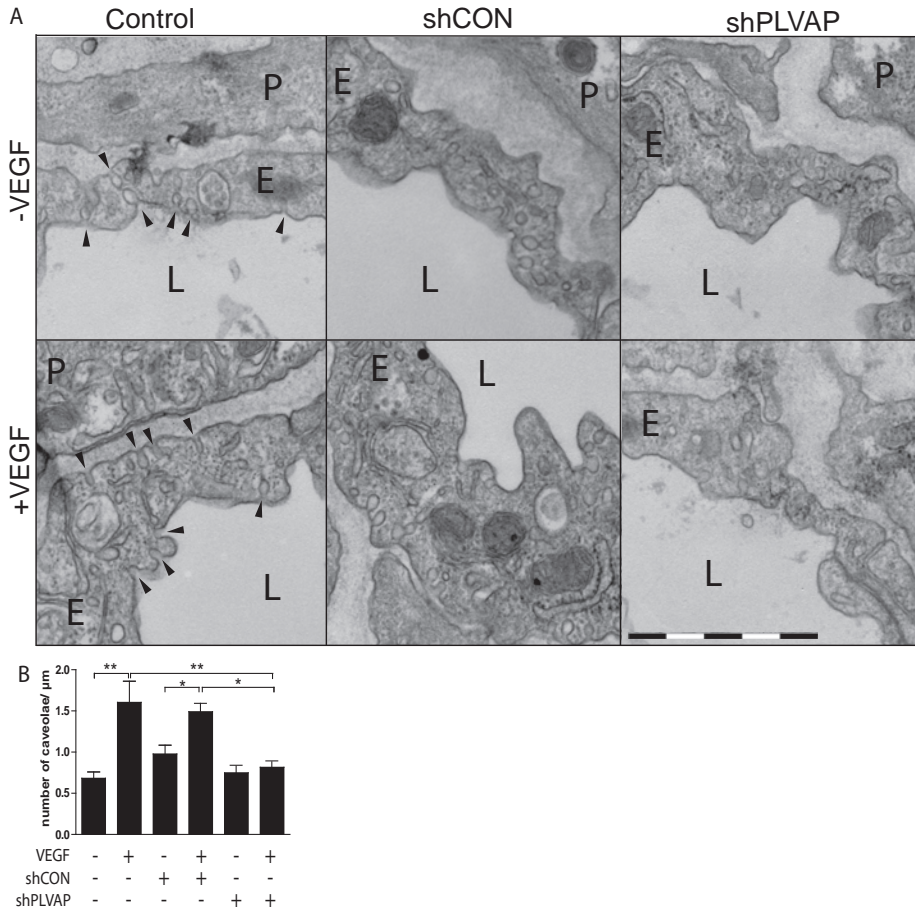


Figure 3. Inhibition of plasmalemma vesicle-associated protein (PLVAP) expression in human retinal explants blocks vascular endothelial growth factor (VEGF)-induced caveolae formation in endothelial cells. **A:** Human retinal explants were transduced with shRNA constructs [control (shCON) and shRNA (shPLVAP)] and cultured in the presence or absence of 100 ng/mL VEGF for 72 hours. VEGF stimulation induced caveola formation in endothelial cells, whereas inhibition of PLVAP expression significantly blocked this process. Only caveolae-like invaginations on the luminal and abluminal side in retinal blood vessel were scored per linear micrometer of endothelium. Examples of caveolae are marked by black arrowheads. **B:** Quantification of caveolae in endothelial cells of blood vessels present in human retinal explants. * $P < 0.05$, ** $P < 0.01$. Scale bar = 1 μm . E, endothelial cell; L, lumen of a blood vessel; P, pericyte.

molecules (Figure 4A). In most samples, PLVAP expression was visibly upregulated in the neovascular tufts, which are a hallmark of the OIR model. Immunofluorescence analysis of OIR retinas revealed that intraocular treatment with *Plvap*-targeting siRNA resulted in decreased PLVAP protein expression in retinal blood vessels at P17 compared with eyes treated with control siRNA (Figure 4B). Furthermore, knockdown of *Plvap* expression in OIR eyes significantly reduced retinal vascular leakage of 70-kDa FITC-labeled dextran

(Figure 4, C and D) and tortuosity of blood vessels (Figure 4, E and F) compared with untreated eyes and eyes treated with control siRNA. Fluorescein angiography images of live animals revealed diffuse leakage of fluorescently labeled tracers (4 and 70 kDa) from preexisting retinal blood vessels with no significant differences among all experimental conditions (Figure 4C). Overall, these results indicate that PLVAP plays a critical role in hypoxia-driven increased vascular permeability and vascular tortuosity in the OIR model.

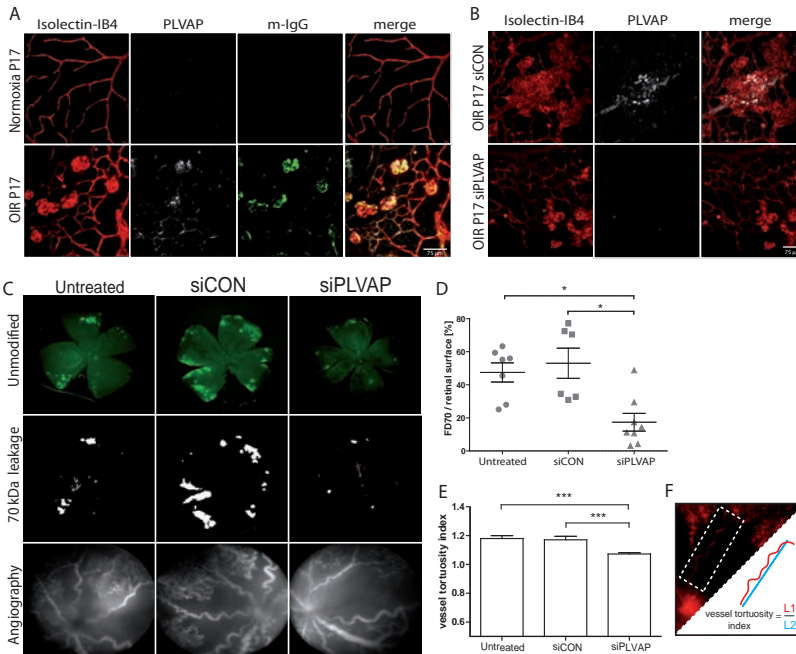


Figure 4. Knockdown of plasmalemma vesicle-associated protein (PLVAP) expression reduces blood-retinal barrier (BRB) leakage and tortuosity of blood vessels in oxygen-induced retinopathy (OIR). **A:** PLVAP expression and extravasation of endogenous mouse IgG (m-IgG), a marker of BRB permeability, increase in OIR retinas. Note the formation of vascular tufts as a result of pathological angiogenesis triggered by retinal hypoxia. **B:** Intraocular treatment with siRNA targeting Plvap results in significantly reduced PLVAP protein expression in the retinal vasculature in OIR compared with control nontargeting siRNA treatment (siCON). Images were recorded using confocal microscopy. **C:** Inhibition of Plvap expression in OIR retinas results in decreased extravasation of fluorescently labeled tracers into the retina (top row). Images were recorded using wide-field fluorescence microscopy. Examples of images representing tracer leakage are shown in the middle row. In addition, vascular leakage in OIR retinas was visualized by fluorescence angiography (bottom row). Images are representative for each experimental group. **D:** Quantification of fluorescently labeled tracers that leaked into the retina. The extravasation of the 70-kDa tracer into retinal tissue was quantified using graphic software. **E:** Inhibition of Plvap expression in OIR retinas results in decreased tortuosity of blood vessels. **F:** Blood vessel tortuosity index is expressed as a quotient: length of curved blood vessel over linear distance between ends. * $P < 0.05$, *** $P < 0.001$. Scale bar = 100 μm (B).

PLVAP knockdown induces barrier properties in HUVECs

In physiological conditions, PLVAP protein expression is absent from barrier endothelium,^{22,23,28} but it is widely expressed in other endothelia of the vascular system.^{18,37} Therefore, we hypothesized that inhibition of PLVAP expression in a nonbarrier type of endothelium, such as HUVECs, results in the formation of an endothelial barrier. HUVECs express considerable levels of PLVAP (Figure 5A) and form a relatively permeable barrier, as indicated by low TEER values (Figure 5B). Knockdown of PLVAP expression in HUVECs resulted in a twofold increase in TEER value (Figure 5B) and significantly reduced permeability for 766-Da (Figure 5C) and 70-kDa fluorescent tracers (Figure 5D) compared with untreated HUVECs. These results indicate that PLVAP expression in nonbarrier endothelium is a prerequisite for a permeable endothelial functional barrier phenotype.

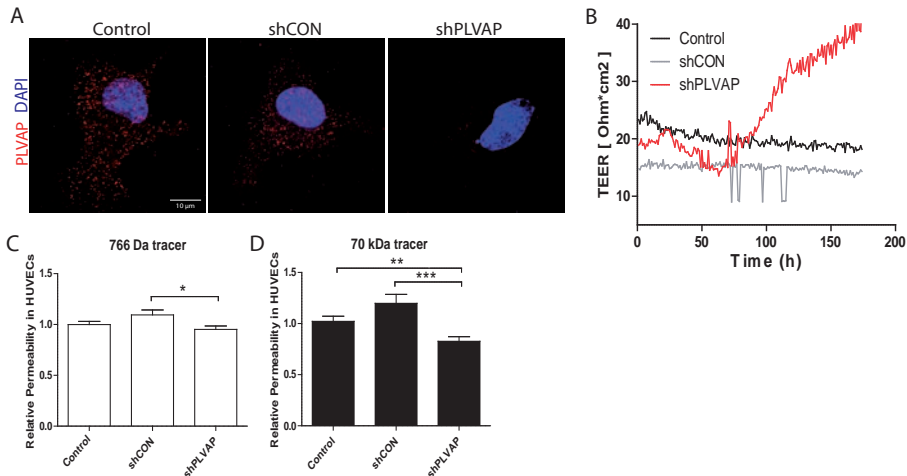


Figure 5. Blocking plasmalemma vesicle-associated protein (PLVAP) expression leads to barrier formation in nonbarrier type of endothelium. A: PLVAP protein expression in human umbilical vein endothelial cells (HUVECs). Images were recorded using confocal microscopy. B-D: Knockdown of PLVAP expression in HUVEC induces increased transendothelial electrical resistance (TEER) values (B) and decreased permeability for 766-Da (C) and 70-kDa (D) tracers. Permeability of HUVEC monolayers was measured 72 hours after lentiviral delivery of shRNA constructs. * $P < 0.05$, ** $P < 0.01$, and *** $P < 0.001$.

DISCUSSION

Disruption of the BRB in patients with DR leads to leakage of plasma proteins and fluid from the microvasculature and subsequent retinal edema. Although the mechanisms responsible for BRB loss in DR are not completely understood, VEGF is one of the key mediators in this process.^{2,4} High VEGF levels induce PLVAP expression,^{26,28} which in physiological conditions is absent from the intact BRB.^{18,19,22,23} In organs with blood-tissue barriers, such

as the brain and eye, the presence of PLVAP indicates the lack of a blood-tissue barrier^{22,25} and correlates with increased microvascular permeability in pathologic conditions, such as brain tumors,^{24,26,27} brain ischemia,²⁵ and DR.^{23,28,38}

We observed a significant reduction of VEGF-induced BRB permeability *in vitro* and of BRB loss *in vivo* after knockdown of PLVAP expression. VEGF disrupts the endothelial barrier by inducing tight junction phosphorylation and degradation^{6,13-16,39} and increasing transendothelial transport mediated by caveolae.^{13,40-42} We hypothesized that PLVAP knockdown would mainly have an effect on transcellular transport because it is a structural component of caveolar diaphragms.²¹ Indeed, we observed *in vitro* the most prominent effect of PLVAP silencing on VEGF-induced permeability for large fluorescent tracers (70 kDa), which we hypothesize to preferentially cross the endothelium via the transcellular pathway. Similarly, we observed in *in vivo* studies a significantly reduced leakage of the 70-kDa tracer, whereas no effect on leakage of the small molecule sodium fluorescein (approximately 4 kDa) was observed in mice injected with siRNA against Plvap in the OIR model. Furthermore, this finding is consistent with the finding that inhibition of PLVAP prevented the induction of caveolae by VEGF in human retinal explants. Our data on tight junction integrity further support the idea that inhibition of PLVAP mainly affects the transcellular pathway because VEGF-induced disruption of tight junctions could not be prevented by inhibition of PLVAP, despite a reduction in stress fiber formation.

Knockdown of PLVAP expression in human retinal explants blocked VEGF-induced caveolae formation but did not alter the basal levels of caveolae, which is in agreement with previous reports.⁴³ This finding suggests that PLVAP is necessary for the formation of new caveolae in conditions with increased permeability. The finding that inhibition of PLVAP has a similar effect on caveolae formation and permeability in the presence of VEGF suggests that the effects of PLVAP on vascular permeability are explained by its structural role in caveolae. In our previous studies, we found that intraocular injections of VEGF in cynomolgus monkeys not only increased the expression of PLVAP protein²⁸ but also caused a shift in the distribution of caveolae from a predominantly abluminal localization to a predominantly luminal localization, similar to the situation in nonbarrier endothelium.⁴²

VEGFR2 is the key mediator of VEGF signaling in endothelial cells^{2,44} and is localized in caveolae.⁴⁵ Therefore, reduced numbers of caveolae may alter VEGF signaling. Co-regulated expression of VEGFR2 and PLVAP was observed in previous studies.³⁸ In healthy patients, in which the BRB is intact, low numbers of caveolae and low VEGFR2 and PLVAP protein levels were found. On the other hand, in DR both VEGFR2 and PLVAP are expressed in retinal capillaries with BRB loss as demonstrated by leakage of endogenous plasma proteins.^{23,33,38} Besides VEGFR2, caveolae harbor many other receptors involved in vascular permeability, including transforming growth factor- β receptors,⁴⁶ that may be reduced as well in the absence of PLVAP in endothelial cells. Consistent with this notion, we found in the present study that nonbarrier endothelial cells (HUVECs), which have constitutive expression of PLVAP, form a tighter endothelial barrier after knockdown of PLVAP expression. Hence, absence of PLVAP expression in physiologic conditions in the retina seems to be essential for maintaining BRB properties.

Outside the eye and brain, PLVAP is expressed in large and medium-sized veins and in continuous and fenestrated endothelia.¹⁸ In these fenestrations, PLVAP forms diaphragms that may work as a sieve to regulate nonspecific transport of plasma proteins. In PLVAP knockouts, increased vascular leakage⁴⁰ may be explained by the absence of these fenestral sieves, whereas in VEGF-induced conditions, PLVAP may also regulate VEGFR2 availability and therefore also facilitate a VEGF-induced decrease in endothelial junctions.⁴⁷ This finding may explain why plasma proteins in normal vascular beds and tumors have occasionally been found to extravasate paracellularly.⁴⁸

Although our present and previous data clearly indicate a function of caveolae in VEGF-induced vascular permeability,^{1,10,13,42} the exact molecular function of caveolae in relation to PLVAP in BRB permeability remains incompletely understood and needs to be addressed in future studies. Our results indicate that PLVAP can be an interesting novel therapeutic target for the treatment of DME. This finding is further supported by our recent study in the Akimba mouse,¹⁰ a model that presents many clinical features of DR, including DME,¹¹ in which we found a correlation between PLVAP levels and the degree of fluorescein leakage in the retina. The Akimba mouse was generated by crossing the Kimba mouse, which has high levels of intraocular VEGF, and the Akita mouse, which spontaneously develops diabetes.¹¹ In the Kimba mouse, we found a strong but statistically insignificant correlation between PLVAP levels and the degree of fluorescein leakage, suggesting that other factors other than VEGF play a role in the induction of PLVAP.

The currently available clinical approaches to treat DR are laser surgery, corticosteroids, and anti-VEGF therapy. Because VEGF is involved in many physiological processes in the retina, such as neurogenesis, neuroprotection, glial growth, and endothelial cell survival,⁴⁹ the long-term use of anti-VEGF compounds may potentially lead to serious adverse effects, such as photoreceptor degeneration¹¹ and Müller cell death.⁵⁰ In addition, VEGF-neutralizing antibodies in proliferative DR may shift the balance between VEGF and connective tissue growth factor concentrations in the eye, which can result in fibrosis, retinal detachment, and vision loss.^{51,52} Therefore, knockdown of PLVAP expression, which attenuates caveolae formation and moderates hypoxia-induced vascular tortuosity, may provide a safer, endothelium-specific approach for DR and DME therapy. However, systemic inhibition of PLVAP potentially interferes with crucial functions of PLVAP in organ homeostasis.^{18,37,43} Because the eye has limited fluid exchange with other parts of the body, the preferred route for delivery of inhibitors of PLVAP would therefore be intravitreally by injection or implantation of slow-release drug delivery systems.

In conclusion, our study presents the first functional evidence that PLVAP plays a key role in BRB loss induced by VEGF and other factors and suggests that PLVAP regulates permeability in nonbarrier endothelia.

ACKNOWLEDGMENTS

We thank Vincent Everts, Ph.D., (Academic Medical Center) for his assistance in electron microscopy, suggestions, and comments.

This study was supported by Landelijke Stichting voor Blinden en Slechtzienden, Stichting Oogfonds Nederland, Stichting Winckel Sweep, UitZicht grant 2012-16, Nederlandse Vereniging ter Verbetering van het Lot der Blinden, Rotterdamse Stichting Blindenbelangen grant B20120030, Stichting Blindenhulp, and Stichting Nederlands Oogheelkundig Onderzoek grant 2012-05. This study was published with the help of Edmond en Marianne Blaauw Fonds voor oogheelkunde (Edmond and Marianne Blaauw fund for ophthalmology).

Disclosures: None declared.

AUTHOR CONTRIBUTIONS

J.W.-K. designed and performed experiments, analyzed data, and wrote the manuscript; A.-E.v.d.W. performed experiments and edited the manuscript, I.M.C.V. performed experiments; I.K.; T.G.M.F.G., and D.V. contributed to the FA study; H.A.v.V. contributed to the EM study; I.K., C.J.F.V.N. and R.O.S. contributed to study design, discussion, and editing of the manuscript. I.K. is the guarantor of this work and, as such, had full access to all of the data in the study and takes responsibility for the integrity of the data and the accuracy of the data analysis.

REFERENCES

1. Klaassen I, Van Noorden CJ, Schlingemann RO: Molecular basis of the inner blood-retinal barrier and its breakdown in diabetic macular edema and other pathological conditions. *Prog Retin Eye Res* 2013, 34: 19e48
2. Witmer AN, Vrensen GF, Van Noorden CJ, Schlingemann RO: Vascular endothelial growth factors and angiogenesis in eye disease. *Prog Retin Eye Res* 2003, 22:1e29
3. Schlingemann RO, van Hinsbergh VW: Role of vascular permeability factor/vascular endothelial growth factor in eye disease. *Br J Ophthalmol* 1997, 81:501e512
4. Qaum T, Xu Q, Joussen AM, Clemens MW, Qin W, Miyamoto K, Hassessian H, Wiegand SJ, Rudge J, Yancopoulos GD, Adamis AP: VEGF-initiated blood-retinal barrier breakdown in early diabetes. *Invest Ophthalmol Vis Sci* 2001, 42:2408e2413
5. Abbott NJ, Ronnback L, Hansson E: Astrocyte-endothelial interactions at the blood-brain barrier. *Nat Rev Neurosci* 2006, 7: 41e53
6. Wisniewska-Kruk J, Hoeben KA, Vogels IM, Gaillard PJ, Van Noorden CJ, Schlingemann RO, Klaassen I: A novel co-culture model of the blood-retinal barrier based on primary retinal endothelial cells, pericytes and astrocytes. *Exp Eye Res* 2012, 96: 181e190
7. Armulik A, Genove G, Mae M, Nisancioglu MH, Wallgard E, Niaudet C, He L, Norlin J, Lindblom P, Strittmatter K, Johansson BR, Betsholtz C: Pericytes regulate the blood-brain barrier. *Nature* 2010, 468:557e561
8. Gesuete R, Orsini F, Zanier ER, Albani D, Deli MA, Bazzoni G, De Simoni MG: Glial cells drive preconditioning-induced blood-brain barrier protection. *Stroke* 2011, 42:1445e1453
9. Romero-Aroca P: Targeting the pathophysiology of diabetic macular edema. *Diabetes Care* 2010, 33:2484e2485
10. Wisniewska-Kruk J, Klaassen I, Vogels IM, Magno AL, Lai CM, Van Noorden CJ, Schlingemann RO, Rakoczy EP: Molecular analysis of blood-retinal barrier loss in the Akimba mouse, a model of advanced diabetic retinopathy. *Exp Eye Res* 2014, 122:123e131
11. Rakoczy EP, Ali Rahman IS, Binz N, Li CR, Vagaja NN, de Pinho M, Lai CM: Characterization of a mouse model of hyperglycemia and retinal neovascularization. *Am J Pathol* 2010, 177:2659e2670
12. Hammes HP, Feng Y, Pfister F, Brownlee M: Diabetic retinopathy: targeting vasoregression. *Diabetes* 2011, 60:9e16
13. Klaassen I, Hughes JM, Vogels IM, Schalkwijk CG, Van Noorden CJ, Schlingemann RO: Altered expression of genes related to blood-retina barrier disruption in streptozotocin-induced diabetes. *Exp Eye Res* 2009, 89:4e15
14. Argaw AT, Gurfein BT, Zhang Y, Zameer A, John GR: VEGF-mediated disruption of endothelial CLN-5 promotes blood-brain barrier breakdown. *Proc Natl Acad Sci U S A* 2009, 106:1977e1982
15. Murakami T, Frey T, Lin C, Antonetti DA: Protein kinase c beta phosphorylates occludin regulating tight junction trafficking in vascular endothelial growth factor-induced permeability in vivo. *Diabetes* 2012, 61:1573e1583
16. Antonetti DA, Barber AJ, Hollinger LA, Wolpert EB, Gardner TW: Vascular endothelial growth factor induces rapid phosphorylation of tight junction proteins occludin and zonula occluden 1. A potential mechanism for vascular permeability in diabetic retinopathy and tumors. *J Biol Chem* 1999, 274:23463e23467
17. Wang W, Dentler WL, Borchardt RT: VEGF increases BMEC monolayer permeability by affecting occludin expression and tight junction assembly. *Am J Physiol Heart Circ Physiol* 2001, 280: H434eH440
18. Schlingemann RO, Dingjan GM, Emeis JJ, Blok J, Warnaar SO, Ruiter DJ: Monoclonal antibody PAL-E specific for endothelium. *Lab Invest* 1985, 52:71e76
19. Niemela H, Elima K, Henttinen T, Irjala H, Salmi M, Jalkanen S: Molecular identification of PAL-E, a widely used endothelial-cell marker. *Blood* 2005, 106:3405e3409
20. Stan RV, Tkachenko E, Niesman IR: PV1 is a key structural component for the formation of the stomatal and fenestral diaphragms. *Mol Biol Cell* 2004, 15:3615e3630
21. Stan RV: Structure of caveolae. *Biochim Biophys Acta* 2005, 1746: 334e348
22. Schlingemann RO, Hofman P, Anderson L, Troost D, van der Gaag R: Vascular expression of endothelial antigen PAL-E indicates absence of blood-ocular barriers in the normal eye. *Ophthalmic Res* 1997, 29:130e138
23. Schlingemann RO, Hofman P, Vrensen GF, Blaauwgeers HG: Increased expression of endothelial antigen PAL-E in human diabetic retinopathy correlates with microvascular leakage. *Diabetologia* 1999, 42:596e602
24. Carson-Walter EB, Hampton J, Shue E, Geynisman DM, Pillai PK, Sathanoori R, Madden SL, Hamilton RL, Walter KA: Plasmalemmal vesicle associated protein-1 is a novel marker implicated in brain tumor angiogenesis. *Clin Cancer Res* 2005, 11:7643e7650
25. Shue EH, Carson-Walter EB, Liu Y, Winans BN, Ali ZS, Chen J, Walter KA: Plasmalemmal vesicle associated protein-1 (PV-1) is a marker of blood-brain barrier disruption in rodent models. *BMC Neurosci* 2008, 9:29
26. Strickland LA, Jubb AM, Hongo JA, Zhong F, Burwick J, Fu L, Frantz GD, Koeppen H: Plasmalemmal vesicle-associated protein (PLVAP) is expressed by tumour endothelium and is upregulated by vascular endothelial growth factor-A (VEGF). *J Pathol* 2005, 206: 466e475

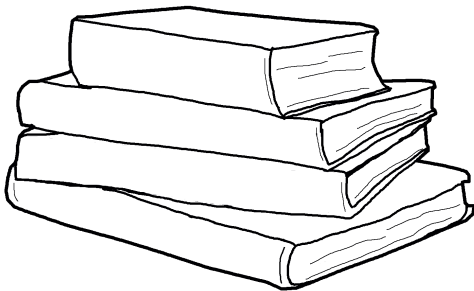
27. Schlingemann RO, Bots GTAM, Van Duinen SG, Ruiters DJ: Differential expression of endothelium-specific antigen PAL-E in vasculature of brain tumors and preexistent brain capillaries. *Ann N Y Acad Sci* 1988, 529:111e114
28. Hofman P, Blaauwgeers HG, Vrensen GF, Schlingemann RO: Role of VEGF-A in endothelial phenotypic shift in human diabetic retinopathy and VEGF-A-induced retinopathy in monkeys. *Ophthalmic Res* 2001, 33:156e162
29. Junge HJ, Yang S, Burton JB, Paes K, Shu X, French DM, Costa M, Rice DS, Ye W: TSPAN12 regulates retinal vascular development by promoting Notch1 but not Wnt-induced FZD4/beta-catenin signaling. *Cell* 2009, 139:299e311
30. Wang Y, Rattner A, Zhou Y, Williams J, Smallwood PM, Nathans J: Notch1/Frizzled4 signaling in retinal vascular development and blood brain barrier plasticity. *Cell* 2012, 151:1332e1344
31. Liebner S, Corada M, Bangsow T, Babbage J, Taddei A, Czupalla CJ, Reis M, Felici A, Wolburg H, Fruttiger M, Taketo MM, von Melchner H, Plate KH, Gerhardt H, Dejana E: Wnt/beta-catenin signaling controls development of the blood-brain barrier. *J Cell Biol* 2008, 183:409e417
32. Daneman R, Zhou L, Kebede AA, Barres BA: Pericytes are required for blood-brain barrier integrity during embryogenesis. *Nature* 2010, 468:562e566
33. Witmer AN, van Blijswijk BC, van Noorden CJ, Vrensen GF, Schlingemann RO: In vivo angiogenic phenotype of endothelial cells and pericytes induced by vascular endothelial growth factor-A. *J Histochem Cytochem* 2004, 52:39e52
34. Andersen CL, Jensen JL, Orntoft TF: Normalization of real-time quantitative reverse transcription-PCR data: a model-based variance estimation approach to identify genes suited for normalization, applied to bladder and colon cancer data sets. *Cancer Res* 2004, 64:5245e5250
35. Smith LE, Wesolowski E, McLellan A, Kostyk SK, D'Amato R, Sullivan R, D'Amore PA: Oxygen-induced retinopathy in the mouse. *Invest Ophthalmol Vis Sci* 1994, 35:101e111
36. McDowell EM, Trump BF: Histologic fixatives suitable for diagnostic light and electron microscopy. *Arch Pathol Lab Med* 1976, 100:405e414
37. Stan RV, Arden KC, Palade GE: cDNA and protein sequence, genomic organization, and analysis of cis regulatory elements of mouse and human PLVAP genes. *Genomics* 2001, 72:304e313
38. Witmer AN, Blaauwgeers HG, Weich HA, Alitalo K, Vrensen GF, Schlingemann RO: Altered expression patterns of VEGF receptors in human diabetic retina and in experimental VEGF-induced retinopathy in monkey. *Invest Ophthalmol Vis Sci* 2002, 43:849e857
39. Murakami T, Felinski EA, Antonetti DA: Occludin phosphorylation and ubiquitination regulate tight junction trafficking and vascular endothelial growth factor-induced permeability. *J Biol Chem* 2009, 284:21036e21046
40. Feng Y, Venema VJ, Venema RC, Tsai N, Behzadian MA, Caldwell RB: VEGF-induced permeability increase is mediated by caveolae. *Invest Ophthalmol Vis Sci* 1999, 40:157e167
41. Lin ZX, Yang LJ, Huang Q, Lin JH, Ren J, Chen ZB, Zhou LY, Zhang PF, Fu J: Inhibition of tumor-induced edema by antisense VEGF is mediated by suppressive vesiculo-vacuolar organelles (VVO) formation. *Cancer Sci* 2008, 99:2540e2546
42. Hofman P, Blaauwgeers HG, Tolentino MJ, Adams AP, Nunes Cardozo BJ, Vrensen GF, Schlingemann RO: VEGF-A induced hyperpermeability of blood-retinal barrier endothelium in vivo is predominantly associated with pinocytotic vesicular transport and not with formation of fenestrations. *Vascular endothelial growth factor-A. Curr Eye Res* 2000, 21:637e645
43. Stan RV, Tse D, Deharvengt SJ, Smits NC, Xu Y, Luciano MR, McGarry CL, Buitendijk M, Nemani KV, Elgueta R, Kobayashi T, Shipman SL, Moodie KL, Daglian CP, Ernst PA, Lee HK, Suriawinata AA, Schned AR, Longnecker DS, Fiering SN, Noelle RJ, Gimi B, Shworak NW, Carrière C: The diaphragms of fenestrated endothelia: gatekeepers of vascular permeability and blood composition. *Dev Cell* 2012, 23:1203e1218
44. Olsson AK, Dimberg A, Kreuger J, Claesson-Welsh L: VEGF receptor signalling - in control of vascular function. *Nat Rev Mol Cell Biol* 2006, 7:359e371
45. Tahir SA, Park S, Thompson TC: Caveolin-1 regulates VEGF-stimulated angiogenic activities in prostate cancer and endothelial cells. *Cancer Biol Ther* 2009, 8:2286e2296
46. Santibanez JF, Blanco FJ, Garrido-Martin EM, Sanz-Rodriguez F, del Pozo MA, Bernabeu C: Caveolin-1 interacts and cooperates with the transforming growth factor-beta type I receptor ALK1 in endothelial caveolae. *Cardiovasc Res* 2008, 77:791e799
47. Dejana E, Orsenigo F, Lampugnani MG: The role of adherens junctions and VE-cadherin in the control of vascular permeability. *J Cell Sci* 2008, 121:2115e2122
48. Nagy JA, Dvorak AM, Dvorak HF: Vascular hyperpermeability, angiogenesis, and stroma generation. *Cold Spring Harb Perspect Med* 2012, 2:a006544
49. Carmeliet P, Storkebaum E: Vascular and neuronal effects of VEGF in the nervous system: implications for neurological disorders. *Semin Cell Dev Biol* 2002, 13:39e53
50. Saint-Geniez M, Maharaj AS, Walshe TE, Tucker BA, Sekiyama E, Kurihara T, Darland DC, Young MJ, D'Amore PA: Endogenous VEGF is required for visual function: evidence for a survival role on muller cells and photoreceptors. *PLoS One* 2008, 3:e3554
51. Kuiper EJ, Van Nieuwenhoven FA, de Smet MD, van Meurs JC, Tanck MW, Oliver N, Klaassen I, Van

- Noorden CJ, Goldschmeding R, Schlingemann RO: The angio-fibrotic switch of VEGF and CTGF in proliferative diabetic retinopathy. *PLoS One* 2008, 3:e2675
52. Van Geest RJ, Lesnik-Oberstein SY, Tan HS, Mura M, Goldschmeding R, Van Noorden CJ, Klaassen I, Schlingemann RO: A shift in the balance of vascular endothelial growth factor and connective tissue growth factor by bevacizumab causes the angio-fibrotic switch in proliferative diabetic retinopathy. *Br J Ophthalmol* 2012, 96:587e590

1
2
3
4
5
6
7
8
&



THE ROLE OF INFLAMMATION AND THERAPEUTIC INTERVENTIONS IN BRB DISRUPTION



5

Is leukostasis a crucial step or epiphenomenon in the pathogenesis of diabetic retinopathy?

Anne-Eva van der Wijk,^{*,†,1} John M. Hughes,^{*,†,1} Ingeborg Klaassen,^{*,†} Cornelis J. F. Van Noorden,^{*,†,‡} and Reinier O. Schlingemann^{*,†}

Ocular Angiogenesis Group, Departments of ^{*}Ophthalmology and [†]Medical Biology, and [‡]Cellular Imaging Core Facility, Department of Medical Biology, Academic Medical Center, University of Amsterdam, Amsterdam, The Netherlands

¹These authors contributed equally to this work.

J Leukoc Biol. (2017) 102(4): 993-1001.

ABSTRACT

Leukostasis in the retinal microvasculature in animal model studies of diabetes is associated with the development of diabetes-like retinopathy. Therefore, it is generally assumed that adhesion of leukocytes is a central event inciting a chronic, low-grade form of inflammation that causes the vascular abnormalities that are specific for the early stages of diabetic retinopathy (DR), which culminate in diabetic macular edema, proliferative DR, and vision loss in humans. Here, we review the literature critically with respect to leukostasis and assess its pathologic consequences in the human diabetic retina. First, we review the pathologic processes that are known to be involved in the development of human DR. Then, we summarize experimental evidence for the role of leukostasis in the development of DR and the mechanisms involved in leukostasis in the retina. Based on our critical review, we conclude that leukostasis may be an epiphenomenon of the diabetic retinal milieu, rather than a crucial, specific step in the development of human DR.

INTRODUCTION

DR is a leading cause of blindness in working-age individuals in developed countries [1]. The earliest clinical changes in the diabetic retina occur in the microvasculature and, as such, DR has traditionally been considered a vascular disease. Pericyte loss, thickening of the vascular basal lamina (or LB), breakdown of the BRB, and acellular capillaries are preclinical phenomena that are considered hallmarks of the early stages of DR [2]. As the disease progresses, saccular microaneurysms and hemorrhages appear and increasingly larger areas of nonperfused capillaries become evident. This nonperfusion, in combination with the loss of BRB, facilitates the formation of retinal exudates and retinal edema in the macula with loss of vision. In more-advanced disease, when the areas of nonperfused retina become large enough, neovascularization may develop, which leads to vitreal hemorrhaging, scarring, and retinal detachment with subsequent severe vision loss. Although each of these individual signs of DR may also be observed in other ischemic retinopathies, the usual constellation of these findings in the fundus of a patient with DR is so specific that no other diagnosis is possible. Therefore, DR is a unique disease of the retina, which only develops in patients with diabetes, and is initiated by hyperglycemia or other factors related to the diabetic milieu. It develops independently of other diabetic microvascular complications, but the local cause of the specific sensitivity of the retina to the diabetic milieu is still a matter of debate [3]. Therefore, the major questions in DR research are 1) how does diabetes cause the onset and progression of DR, and 2) why is the retina specifically sensitive to diabetes? Here, we review and discuss the possible role of leukostasis and associated low-grade inflammation in DR in the context of those questions.

LEUKOSTASIS IN ANIMAL MODELS OF THE DIABETIC RETINA

Leukostasis in situ

The phenomenon of leukostasis in the vasculature of retinas of diabetic rats was first described by Schröder et al. [4]. In their histochemical study of retinal whole mounts obtained from perfusion-fixed diabetic rats, significantly more capillary-occluding monocytes and granulocytes were observed as compared with control rats. These capillary-occluding leukocytes also displayed a strong spatial correlation with focal endothelial swelling, capillary loss, and formation of intraretinal microvascular abnormalities. Because the leukocytes were found to be activated in the diabetic rats and because of their known ability to induce cellular damage by releasing cytotoxic products, it was speculated that occluding leukocytes have a causal role in the pathogenesis of DR through the induction of direct damage to the endothelium and surrounding tissue [4].

Some 10 years later, strong support for that hypothesis was presented by Jousset et al. [5], who observed high numbers of propidium iodide-stained retinal endothelial cells, indicating increased numbers of dead or dying cells in mice with 11 mo of STZ-induced diabetes or 22 mo of galactosemia. This was not the case in nondiabetic controls

or in transgenic diabetic ICAM-1^{-/-} and CD18^{-/-} mice, in which less retinal leukostasis was observed. These transgenic mice also displayed reduced DR-associated retinal vascular pathology, including BRB breakdown, endothelial cell and pericyte loss, and acellular capillaries. The authors concluded that in long-term diabetes in rodents, a chronic, low-grade inflammation, initiated by leukostasis, induced the specific abnormalities of PCDR. These early abnormalities are considered to cause the initiation of more-advanced disease and vision loss in human DR and hence, the hypothesis that human DR is an inflammatory disease was born [6].

Recently, additional evidence for a causal role of leukocyte- induced vascular damage in PCDR in rodents was reported by various research groups, who demonstrated that after several intervention methods, decreased leukostasis led to decreased diabetic sequelae in diabetic animal models [5, 7–10], which will be further discussed in the “Experimental evidence for the role of leukostasis in the development of vascular pathology in DR” section

Leukostasis in vitro

In vitro studies using isolated retinal microvascular endothelial cells have been performed to further elucidate the specific effects of the hyperglycemic milieu on leukostasis. In one study, BRECs were exposed to high concentrations (20–100 mM) of D-glucose. This resulted in a dose-dependent increase in leukocyte adhesion. However, similar effects were obtained when BRECs were incubated in the presence of the same concentrations of mannitol instead of D-glucose, indicating that increased leukocyte adhesion was due to hyperosmolarity, rather than to the specific effect of excess D-glucose levels [11]. A similar experiment was performed with human retinal endothelial cells, which showed elevated leukocyte adhesion in the presence of high D-glucose concentrations (46 mM), whereas that effect was not observed when mannitol (30 mM) or L-glucose (30 mM) was used [12], suggesting that increased leukocyte adhesion to human retinal endothelial cells is a D-glucose-specific reaction and not a nonspecific reaction to a hyperosmotic environment. This interexperimental variation illustrates the difficulty of using in vitro models to study a complex systemic human disease, such as diabetes.

Leukostasis in vivo

Nishiwaki et al. [13] developed a technique to analyze leukocyte dynamics in the retinal microvasculature of laboratory animals in vivo. Leukocytes were labeled by an i.v. injection of acridine orange and were then visualized in the retinal microvasculature using a scanning laser ophthalmoscope. In various animal models, increased leukostasis in the retinal microvasculature was reported after short- and long-term diabetes using this technique [14–16]. On the other hand, in rhesus monkeys with spontaneous diabetes type 2 [17], static leukocytes in retinas with histologic evidence of DR were not different from those in retinas without signs of DR. Moreover, the db/db mouse, a model for diabetic dyslipidemia, did not show increased leukostasis in the retina [18].

Unfortunately, the toxic nature of acridine orange prevents the study of leukostasis in the retinal vasculature of humans with diabetes. A safe technique for visualizing leukocytes

in humans has yet to be developed. Therefore, the study of leukostasis in human retinal vasculature is not yet possible, and as a consequence, most of the current data on retinal leukostasis is derived from animal models of DR.

PROPOSED MECHANISMS OF LEUKOSTASIS

There are 3 mechanisms that have been proposed to lead to increased leukostasis in the retina during the development of DR: 1) decreased retinal blood flow or perfusion pressure; 2) narrowing of capillary lumina; and 3) increased leukocyte–endothelium adhesion.

Decreased retinal blood flow and perfusion pressure

The state of retinal blood flow in diabetes is controversial, with studies reporting both decreased and increased blood flow in the diabetic retina [19, 20]. One study of retinal hemodynamics showed that the number of static leukocytes increased in diabetic rats, whereas leukocyte passage time through retinal capillaries was similar to that in controls [15]. In contrast, Abiko et al. [14] showed that increased leukostasis in Zucker diabetic fatty rats was accompanied by reduced retinal blood flow. However, treatment of diabetic rats with the antioxidant α -lipoic acid prevented the occurrence of leukostasis but did not normalize retinal blood flow. Therefore, it seems unlikely that decreased retinal blood flow or perfusion pressure is the mechanism of retinal leukostasis.

Narrowing of capillaries

Luminal narrowing of retinal capillaries has been observed in diabetic OLETF rats [21] and primates with VEGF-induced retinopathy [22]. The exact mechanisms by which the narrowing occurs are largely unknown. In primates with VEGF-induced retinopathy, hypertrophy of the endothelial cells has been shown to cause lumen narrowing in retinal capillaries [22]. Vascular constriction has been proposed as a mechanism of leukostasis through capillary narrowing because expression of the vasoconstrictor ET-1 was found to be increased in the retinal vasculature of diabetic rats [23, 24], whereas the expression of ET-1 receptors on retinal pericytes was also found to be increased [24]. ET-1 receptor antagonists limited leukostasis in the retinas of rats with STZ-induced diabetes, but that effect was attributed to decreased VEGF production, rather than to vasoconstriction [25]. Therefore, the evidence is minimal at best that capillary constriction is a cause of leukostasis in the diabetic retina.

Vascular compression from LB thickening has also been suggested to cause lumen narrowing [26]. LB thickening is a well-established, histopathologic feature of DR [27, 28], but it has not been shown to cause lumen narrowing or leukostasis in retinal capillaries [29]. Furthermore, there is no spatial correlation between the vascular complications attributed to increased leukostasis, which occur nonuniformly throughout the retina of patients with diabetes, whereas LB thickening occurs uniformly, making LB thickening a less-likely cause of leukostasis [30].

Lumen narrowing has yet to be demonstrated in retinal capillaries of humans, but a number of findings support the feasibility that it causes leukostasis in humans. First, leukocytes isolated from patients with diabetes have decreased elasticity [31]. Because the diameter of most leukocytes is roughly twice that of the average retinal capillary, adequate elasticity is crucial for leukocyte passage. Second, vessels in the diabetic retina have been shown to be more tortuous compared with nondiabetic retinas in both rodents [21, 32] and humans [33]. Therefore, more-rigid leukocytes can become trapped at tortuous sites when blood flow is hampered in retinas of patients with diabetes. However, to date, no direct evidence exists for this mechanism of leukostasis in the human diabetic retina.

Increased leukocyte-endothelium adhesion

Considerably more evidence has been generated in both animal models and patients that implicate low-grade, chronic inflammation in inducing leukocyte-endothelial adhesion as a major mechanism of increased leukostasis in diabetic retinas [5]. Leukocytes isolated from diabetic rats and humans show increased adhesion to endothelial cells in vitro [34, 35]. Additionally, leukocytes from diabetic rats and patients express increased levels of the β_2 -integrins CD11a, CD11b, and CD18 [34, 36]. These adhesion molecules, in conjunction with their endothelial counterparts ICAM-1 and VCAM-1, have a crucial role in inflammation because they are required for firm leukocyte-endothelial cell adhesion. Abs against CD11a, CD11b, and CD18 prevented adhesion in vitro, and CD18 blockade suppressed leukocyte adhesion in retinal capillaries of diabetic rats in vivo [34]. Furthermore, activated leukocytes that were injected into healthy mice were shown to interact with retinal endothelium in association with increased ICAM-1 staining [37]. That indicates that activated leukocytes have the capacity to locally upregulate endothelial ICAM-1 expression. Administration of anti-ICAM-1 Abs significantly reduced leukostasis in diabetic rats [38]. Moreover, leukostasis did not occur in ICAM-1- or CD18-deficient mice at 11 mo of STZ-induced diabetes or 22 mo of galactosemia [5].

In the diabetic human retina, the relevance of ICAM-1 expression has not yet been established. Both increased and unaltered ICAM-1 expression has been found [39, 40]. The different results of these 2 studies may be explained by the size of the control groups. One study used a small group of 6 control retinas, 4 of which were devoid of ICAM-1 staining, whereas 2 were not [40]. The other study included a control group equal in size to the diabetic groups that were studied ($n = 19$). In that study, most of the control retinas exhibited low to moderate ICAM-1 staining that was similar to that in diabetic retinas [39].

In agreement with the latter study, moderate, constitutive, endothelial ICAM-1 expression has been reported in human retinal capillaries in vivo [41] and in human retinal endothelial cells in vitro [42, 43]. Moreover, the adhesion molecules VCAM-1, E-selectin, and P-selectin, which are important in the inflammatory process through their tethering of leukocytes to the endothelium, have not been found expressed in the healthy or diabetic human retinal microvasculature [39, 40].

CURRENT PARADIGM OF LEUKOCYTE-INDUCED VASCULAR PATHOLOGY LEADING TO DR

In this section, we present a synopsis of data regarding the molecular processes that lead to leukostasis and PCDR, as observed in diabetic animal models. Furthermore, we attempt to incorporate those processes into a simplified chain of events that represents the theory of how leukostasis and low-grade inflammation lead to the specific vascular pathology of DR.

Many biologic factors and conditions have been shown to modulate retinal leukostasis. Tables 1 and 2 contain a comprehensive list of factors and conditions that either induce or reduce leukocyte adhesion in the retinal circulation in experimental models. The hyperglycemic state induced by diabetes has been proposed to lead to DR through 3 major pathologic biochemical processes: 1) increased flux of glucose metabolites through the polyol pathway [56], 2) nonenzymatic protein glycosylation and the resulting accumulation of AGEs [57, 58], and 3) increased oxidative stress from accumulation of ROS [43, 59, 60]. These latter 2 processes have also been implicated in increased retinal leukostasis. Systemic administration of AGEs leads directly to increased retinal leukostasis in mice [48], whereas various antioxidant therapies neutralize the diabetes-induced increase in leukostasis [14, 61].

Table 1. Factors known to increase retinal leukostasis

Factors increasing leukostasis	Fold increase*
Diabetes	1.9 [44]–4.8 [17]
Increased glucose	1.9 [12]
Hyperosmolarity	1.6 [11]
VEGF	4.8 [45]–14.5 [46]
TNF- α	13–92 [46, 47]
IL-1 β	4.5 [46]
Platelet-activating factor	13.6 [46]
AGEs	2.7 [48]
Insulin	2.5 [49]
Hypertension	2–2.7 [50]
Hypercholesterolemia	2.1 [51]

*Fold increase relative to control experiments.

Hyperglycemia itself may also directly lead to increased leukostasis through PKC- β activation, likely via de novo synthesis of diacylglycerol [62]. AGEs and ROS also lead to activation of PKC- β [14, 63]. As such, it is conceivable that PKC- β activation is a common mechanism through which AGEs, ROS, and hyperglycemia lead to leukostasis and DR. Activation of PKC- β leads to increased transcription of various proteins and growth

1
2
3
4
5
6
7
8
&

factors, such as VEGF [64], which can lead to enhanced vascular permeability and retinal leukostasis and coincides with increased ICAM-1 expression [45]. In human DR, a PKC- β inhibitor was shown to moderately reduce visual loss, need for laser treatment, and macular edema progression in patients with diabetes [65]. In the rat retina, inhibition of PKC- β activation has been shown to ameliorate diabetes-induced leukostasis [14].

Leukocytes activated by the diabetic milieu in rodents and patients with diabetes adhere to the retinal vasculature and induce endothelial apoptosis [9, 43, 66] through Fas–Fas ligand interactions [66]. It has further been proposed that this chain of events possibly leads to vision loss via 2 separate pathways [66]. First, breakdown of the BRB can (at least in part) occur via induction of apoptosis in the endothelium. This endothelial cell death results in vascular leakage, which may contribute to the development of macular edema. Second, the accumulative effect of endothelial cell death because of the chronic nature of diabetes may lead to replicative senescence and avascular capillaries. That results in areas of retinal nonperfusion and hypoxia that induces increased VEGF expression, which ultimately leads to retinal neovascularization [66]. A schematic representation of those proposed pathways based on animal model studies is shown in Fig. 1. Despite the fact that the scheme is a simplified representation of the processes at hand, it provides an adequate overview of mechanisms of vascular pathology of DR in rats and mice, including leukostasis and inflammation.

Table 2. Factors known to decrease diabetes-induced retinal leukostasis

Factors decreasing leukostasis in DM	Fold decrease*
Aspirin	4.9 [52]
COX-2 inhibitor	5.6 [52]
Etanercept (anti-TNF- α)	5.1 [52]
Endothelin	2.1 [25]
Antioxidants	
α -lipoic acid	1.6 [14]
D- α -tocopherol	1.7 [14]
Corticosteroids	2.3 [53]
PKC- β inhibition	1.7 [14]
PPAR- γ signaling	1.6 [44]
5-Lipoxygenase deficiency	15 [54]
12/15-Lipoxygenase deficiency	6.5 [54]
AMA0428 (ρ -kinase inhibitor)	1.4 [7]
Vitamin B (Metanx)	1.7 [55]

*Fold decrease relative to diabetic controls with vehicle only.

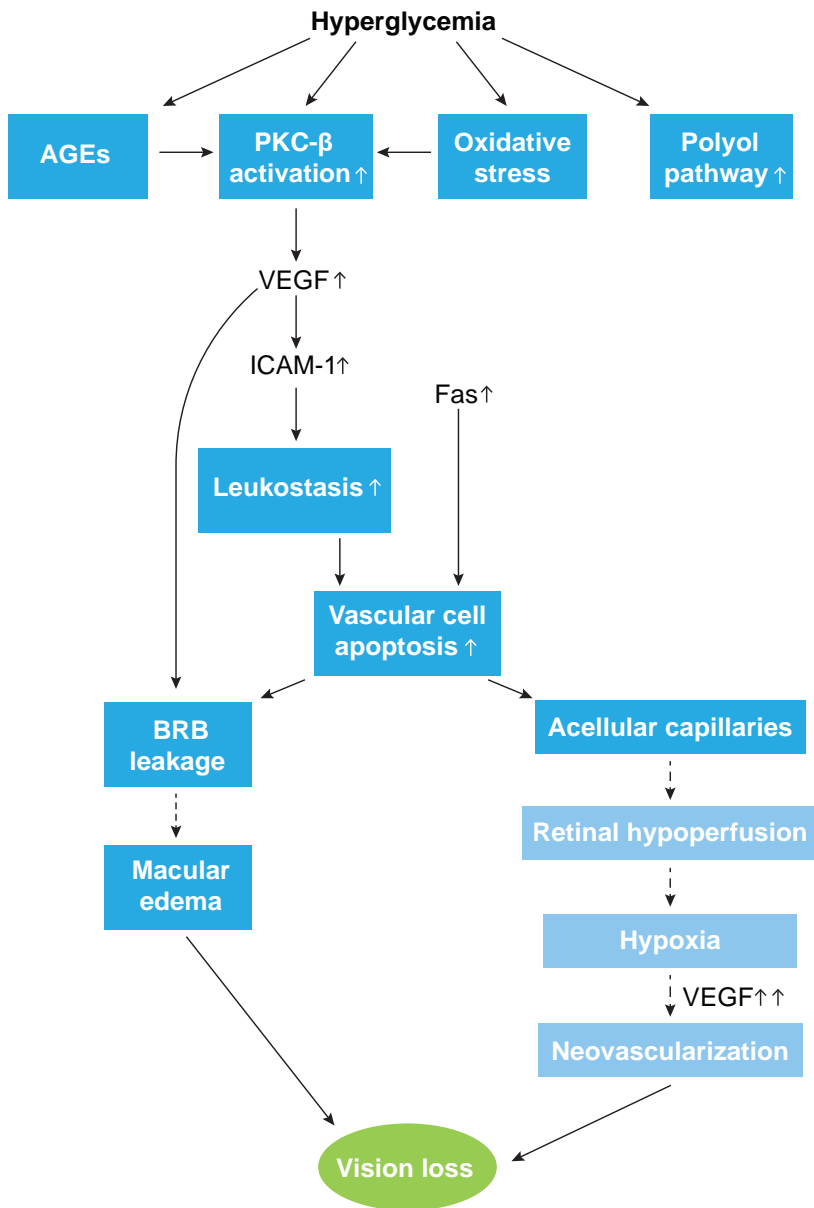


Figure 1. Schematic diagram of the role of leukostasis in the development of DR in animal models based on current literature. Pathways represented by dashed arrows are based on conjecture, whereas solid arrows represent pathways that have been shown to be involved.

Table 3. Comparison of retinal lesions found in various well-characterized animal models of DR, hypertension and hyperlipidemia as well as in human DR

	Pericyte loss	Acellular capillaries	Micro-aneurysms	LB thickening	Capillary narrowing	BRB leakage	Capillary toxicity/ capillary formation	Exudates	Haemorrhages	Capillary non-perfusion	Cotton wool spots	IRMA	Neovascularisation
Human diabetes (2)	+	+	+	+	+	+	+	+	+	+	+	+	+
Spontaneous diabetic rhesus monkeys (17, 86) (15 years)	-	+	+	+			+	+	+	+	+	+	-
Aloxan-induced diabetic dogs (87) (5 years)	+	+	+	+					+			+	-
Galactose-fed dog (88) (5 years)	+	+	+	+				+	+	+		+	+
Galactose-fed rats (89) (23 months)	+	+	-	+					-			+	-
Sucrose-fed diabetic Cohen rats (90) (26 weeks)	+	+	+										-
STZ-induced diabetic rats (91, 92) (12 months)	+	+	+	+		+				+			-
Diabetic BB rat (93) (4 months)	-	-	-	-		-							-
OLETF rats (21) (14 months)			+	+	+		+		-				-
Zucker diabetic fatty rat (94, 95) (5 months)	-	-	-	+	-		-		-				-
Spontaneous diabetic Torii rat (96, 97) (60 weeks)	-	-	-			-	+		+	+			+
Galactose-fed mice (5) (24 months)	+	+		+		+							
STZ-induced diabetic mice (98) (18 months)	+	+		-									-
db/db diabetic mice (18) (10 weeks)	+	+	-	+		-							-
RICO rats (99) (18 months)	+	+	-		+		+						
SHR rats (92, 100) (7 months)	+	+		+	+	+	+			+			+

EXPERIMENTAL EVIDENCE FOR THE ROLE OF LEUKOSTASIS IN THE DEVELOPMENT OF VASCULAR PATHOLOGY IN DR

1
2
3
4
5
6
7
8
&

The mounting evidence that leukostasis has a role in the development of sequelae characteristic for PCDR in diabetic animal models is the major basis of the assumption that human DR is a disease caused by low-grade, chronic inflammation [6]. This idea is not new (DR was initially termed “diabetic retinitis” [67]), but the data implicating increased retinal microvascular leukostasis as having a specific causal role in the development of PCDR has provided new support for the chronic inflammation hypothesis. The evidence seems substantial that this is the case in animal models, but a critical analysis of the current literature reveals conflicting evidence of this causal role.

TNF- α -dependent leukostasis was shown to be responsible for increased endothelial cell death and BRB leakage in rat retinas as early as 1 wk after induction of diabetes [52]. The TNF- α -dependent nature of VEGF-induced leukostasis was demonstrated in TNF- α knockout mice. However, BRB leakage was not significantly altered in that model, and the absence of TNF- α and leukostasis did not prevent or reduce retinal neovascularization when those mice were used in an oxygen-induced retinopathy assay [46]. Taken together, these data suggest that leukostasis may not be essential in animal models for the development of PCDR.

Leukostasis did not occur in ICAM-1^{-/-} and CD18^{-/-} mice with STZ-induced type 1 diabetes up to 11 mo. Retinas of those mice exhibited significantly fewer acellular capillaries and no altered numbers of pericytes and endothelial cells as compared with wild type diabetic mice [5]. STZ-induced diabetic, transgenic mice expressing neutrophil inhibitory factor, which is a selective antagonist for the integrin complex Mac-1 (CD11b/ CD18), do not develop retinal leukostasis, and in those mice degeneration of retinal capillaries and retinal superoxide production were inhibited [9]. In addition, recent studies demonstrated that inhibition of ROCK signaling [7], VEGFR1 blockade [68], retinal overexpression of ACE-2 [69], or inhibition of the VEGF coreceptor neuropilin-1 [70] attenuated leukostasis in the retina of mice with STZ-induced diabetes, and that was accompanied with decreased diabetes-induced retinal complications. These data suggest that leukostasis is causal for the development of sequelae characteristic for PCDR and non-proliferative DR.

In contrast, several recent studies provide evidence that this causal association is not always the case. Spontaneously diabetic db/db mice, known to develop acellular capillaries at 34 wk of age, showed no increase in leukostasis, suggesting that other factors than leukostasis lead to acellular capillaries in this model of type 2 diabetes [18]. Both STZ-induced diabetic mice deficient in either 5-lipoxygenase or 12/15-lipoxygenase, which are inducers of chronic inflammation and ROS production, demonstrated a similar reduction in leukostasis. However, pericyte loss and numbers of acellular capillaries were reduced only in the 5-lipoxygenase-deficient diabetic mice, whereas in the 12/15-lipoxygenase-deficient diabetic mice, those sequelae developed in spite of the reduction in leukostasis [54]. Moreover, when STZ-induced diabetic mice were treated with the medical food product

Metanx (containing the active forms of vitamins B₉, B₆, and B₁₂; Alfasigma, Covington, LA, USA), multiple inflammation-related molecular abnormalities, such as leukostasis, ICAM-1 expression, and activation of NF- κ B in the retina, were significantly inhibited, but no effects were observed on degeneration of retinal capillaries and formation of pericyte ghosts [55].

In our opinion, these studies provide evidence that dissociates the occurrence of leukostasis and low-grade inflammation from the development of the specific diabetic retinal sequelae. Reasons for these contradictory results can possibly be found in differences in methodologies and diabetic models that have been used (toxin-induced type 1 diabetes vs. genetically inbred strains of spontaneously induced, type 2 diabetes) or perhaps in the genetic differences among species. This is exemplified by the variation in retinal pathology observed in the various DR models; all of which fail to replicate the entire spectrum of retinal sequelae seen in human DR (Table 3).

RELEVANCE OF LEUKOSTASIS IN THE DEVELOPMENT OF DR IN HUMAN DIABETES

In this section, we set out to assess the relevance of leukostasis in the development of human DR. In addition to differences in sizes and functions of ocular tissues between species, differences in vascular patterns [86], cellular composition [87], cellular metabolism, and biochemistry [88] have been demonstrated.

Furthermore, a discrepancy in NF- κ B expression and activation exists between STZ-induced diabetes in rats and human patients with diabetes. NF- κ B is exclusively expressed in retinal vascular pericytes of human patients with diabetes [89], whereas in diabetic rats, its activity is increased in both retinal endothelial cells and pericytes [90]. This is a crucial difference because NF- κ B has an essential role in inflammatory processes, including leukostasis. Moreover, NF- κ B is also involved in retinal pathology in experimental rodent diabetes through induction of various molecules, such as ICAM-1 and Fas in retinal vascular endothelial cells [66, 52, 55, 91], whereas increased vascular expression of either ICAM-1 [39] or Fas [unpublished data] was not found in human diabetic retinas.

The ocular differences between man and rodent are further illustrated by the various interventions that effectively decrease leukostasis and its associated sequelae in rodents but fail to be effective in preventing or slowing down progression of DR in humans. Treatment of diabetic rats with antioxidants reduces retinal leukostasis as well as the formation of pericyte ghosts and acellular capillaries [14, 61, 92]. Although properly randomized clinical trials involving therapeutic doses of antioxidants have yet to be performed, dietary antioxidant intake in human subjects with diabetes is not associated with a decreased incidence of DR [93]. Aspirin therapy reduces the formation of diabetic retinal sequelae in dogs [94] and rats [95] but has not proven to be effective in slowing down the progress of DR in humans [96].

Inhibition of PKC- β has also led to significantly decreased diabetes-induced retinal vasculopathies, including leukostasis in animal models [14], but the preventive effect on the incidence or progression of DR in humans is very small. Finally, intravitreal corticosteroid

injections seem to have similar effects in animal models and human diabetes because leukostasis and vascular leakage are decreased in diabetic rats [16], and diabetic macular edema and visual acuity in humans are improved [96], which is in agreement with the hypothesis that DR is a disease of chronic inflammation. However, corticosteroids may also have a substantial direct effect on BRB endothelium, independent of their anti-inflammatory actions [97].

Thus far, the only therapies proven to decrease the incidence and progression of DR in humans is strict control of hypertension and glucose levels in the blood using insulin [98, 99] or sulphonylureas [98]. Surprisingly, s.c. or ocular administration of insulin in rats leads to increased retinal leukostasis [49] and vascular pathology [100], respectively. This, however, is likely due to the direct effects of insulin on its many receptors in the retina, whereas the beneficial effects of systemically administered insulin in humans with diabetes are derived from its ability to lower blood glucose levels. Studies on the effect of systemic insulin therapy on leukostasis in animal models of diabetes have not yet been performed.

Interpretation of animal DR data with respect to human DR is difficult for at least two reasons. First, the reported outcome measurements vary. In animal studies, those measurements usually consist of quantitative biochemical data or qualitative pathology, whereas in human DR studies, the outcomes are mainly based on vascular macropathology and vision loss, neither of which occurs in current animal models of DR. Second, quantification of leukostasis in the human retina in vivo remains problematic. Therefore, the exact role of leukostasis in human DR remains speculative.

CONCLUSION: IS LEUKOSTASIS A MAIN PLAYER IN DR DEVELOPMENT OR AN EPIPHENOMENON?

Leukostasis and associated signs of low-grade inflammation are increased in most rodent models of DR. The evidence that these phenomena have a specific causal role in the pathogenesis of DR in these models is conflicting. As shown in Table 1, various factors lead to increased leukostasis in the rodent retina. However, not all of those factors lead to the sequelae characteristic for PCDR or nonproliferative DR, such as pericyte loss and acellular capillaries. Retinal leukostasis is also observed in rodent models of hypertension [50], insulin resistance [14], hypercholesterolemia [51], and hyperinsulinemia [49]. Those disease states also lead to various forms of vasculopathy in both the rodent and human retina, but none of them result in macular edema and vascular proliferation, causal for vision loss associated with DR. Breakdown of the BRB and vascular hypoperfusion are considered to precede those events. Leukostasis likely contributes to retinal vascular leakage, but it is not necessary for it to occur [46]. Furthermore, increased leukostasis does not reduce overall retinal blood flow [14]. Locally decreased blood flow induced by leukocyte capillary plugging might cause the development of acellular capillaries and regional hypoperfusion, but then, it would be expected to happen in the retinas of rodents with hypertension, hypercholesterolemia, and hyperinsulinemia, as well, which is not the case. Leukostasis can induce apoptosis of microvascular endothelial cells [9, 43, 66] and

thus result in acellular capillaries and hypoperfusion. However, those sequelae are also observed in diabetic rodents without leukostasis [18]. Finally, when leukostasis is absent in diabetic retinas, the specific hallmark sequelae of PCDR or nonproliferative DR still occurs to the same degree [54, 55].

Taken together, it must be concluded that there is no compelling evidence for a significant role for leukostasis in the development of DR in humans. Increased leukostasis seems to be a result of aspecific endothelial cell dysfunction, rather than a crucial, specific step in the development of DR and is, therefore, likely an epiphenomenon of the retinal diabetic milieu. However, it cannot be ruled out (and is perhaps likely) that leukostasis enhances the pathogenic effects of the diabetic milieu on the retina. More research is needed to further elucidate the relevance of leukostasis and low-grade inflammation in the development of DR in the human retina. Improved animal models for DR, detailed pathologic studies in human DR, and the ability to quantify *in vivo* leukocyte dynamics in the human retina are critical to this endeavor.

ACKNOWLEDGMENTS

This study was made possible by the financial support of the Diabetes Fonds (Dutch Diabetes Fund, Grant 1998.131) and published with the help of Edmond en Marianne Blaauw Fonds voor Oogheelkunde (Edmond and Marianne Blaauw Fund for Ophthalmology). The authors thank Dr. H.P. Hammes from Heidelberg University for helpful suggestions and critical reading of the manuscript.

Disclosures: The authors declare no conflicts of interest.

AUTHORSHIP

J.M.H. designed the content of the review and prepared the figures. A.-E.v.d.W. and J.M.H. wrote the manuscript. I.K., C.J.F.V.N., and R.O.S. advised in the design of the content of the review and contributed to editing of the manuscript.

REFERENCES

1. Thylefors, B., Ne'grel, A. D., Pararajasegaram, R., Dadzie, K. Y. (1995) Global data on blindness. *Bull. World Health Organ.* 73, 115–121.
2. Garner, A. (1993) Histopathology of diabetic retinopathy in man. *Eye (Lond.)* 7, 250–253.
3. Arden, G. B., Sidman, R. L., Arap, W., Schlingemann, R. O. (2005) Spare the rod and spoil the eye. *Br. J. Ophthalmol.* 89, 764–769.
4. Schröder, S., Palinski, W., Schmid-Schönbein, G. W. (1991) Activated monocytes and granulocytes, capillary nonperfusion, and neovascularization in diabetic retinopathy. *Am. J. Pathol.* 139, 81–100.
5. Jousseaume, A. M., Poulaki, V., Le, M. L., Koizumi, K., Esser, C., Janicki, H., Schraermeyer, U., Kociok, N., Fauser, S., Kirchhof, B., Kern, T. S., Adamis, A. P. (2004) A central role for inflammation in the pathogenesis of diabetic retinopathy. *FASEB J.* 18, 1450–1452.
6. Adamis, A. P. (2002) Is diabetic retinopathy an inflammatory disease? *Br. J. Ophthalmol.* 86, 363–365.
7. Hollanders, K., Van Hove, I., Sergeys, J., Bergen, T. V., Lefevère, E., Kindt, N., Castermans, K., Vandewalle, E., van Pelt, J., Moons, L., Stalmans, I. (2017) AMA0428, a potent ROCK inhibitor, attenuates early and late experimental diabetic retinopathy. *Curr. Eye Res.* 42, 260–272.
8. Li, G., Veenstra, A. A., Talahalli, R. R., Wang, X., Gubitosi-Klug, R. A., Sheibani, N., Kern, T. S. (2012) Marrow-derived cells regulate the development of early diabetic retinopathy and tactile allodynia in mice. *Diabetes* 61, 3294–3303.
9. Veenstra, A. A., Tang, J., Kern, T. S. (2013) Antagonism of CD11b with neutrophil inhibitory factor (NIF) inhibits vascular lesions in diabetic retinopathy. *PLoS One* 8, e78405.
10. Hossain, A., Tauhid, L., Davenport, I., Huckaba, T., Graves, R., Mandal, T., Muniruzzaman, S., Ahmed, S. A., Bhattacharjee, P. S. (2017) LRP-1 pathway targeted inhibition of vascular abnormalities in the retina of diabetic mice. *Curr. Eye Res.* 42, 640–647.
11. Bullard, S. R., Hatchell, D. L., Cohen, H. J., Rao, K. M. (1994) Increased adhesion of neutrophils to retinal vascular endothelial cells exposed to hyperosmolarity. *Exp. Eye Res.* 58, 641–647.
12. Hirata, F., Yoshida, M., Ogura, Y. (2006) High glucose exacerbates neutrophil adhesion to human retinal endothelial cells. *Exp. Eye Res.* 82, 179–182.
13. Nishiwaki, H., Ogura, Y., Kimura, H., Kiryu, J., Honda, Y. (1995) Quantitative evaluation of leukocyte dynamics in retinal microcirculation. *Invest. Ophthalmol. Vis. Sci.* 36, 123–130.
14. Abiko, T., Abiko, A., Clermont, A. C., Shoelson, B., Horio, N., Takahashi, J., Adamis, A. P., King, G. L., Bursell, S. E. (2003) Characterization of retinal leukostasis and hemodynamics in insulin resistance and diabetes: role of oxidants and protein kinase-C activation. *Diabetes* 52, 829–837.
15. Miyamoto, K., Hiroshiba, N., Tsujikawa, A., Ogura, Y. (1998) In vivo demonstration of increased leukocyte entrapment in retinal microcirculation of diabetic rats. *Invest. Ophthalmol. Vis. Sci.* 39, 2190–2194.
16. Tamura, H., Miyamoto, K., Kiryu, J., Miyahara, S., Katsuta, H., Hirose, F., Musashi, K., Yoshimura, N. (2005) Intravitreal injection of corticosteroid attenuates leukostasis and vascular leakage in experimental diabetic retina. *Invest. Ophthalmol. Vis. Sci.* 46, 1440–1444.
17. Kim, S. Y., Johnson, M. A., McLeod, D. S., Alexander, T., Hansen, B. C., Lutty, G. A. (2005) Neutrophils are associated with capillary closure in spontaneously diabetic monkey retinas. *Diabetes* 54, 1534–1542.
18. Tadayoni, R., Paques, M., Gaudric, A., Vicaut, E. (2003) Erythrocyte and leukocyte dynamics in the retinal capillaries of diabetic mice. *Exp. Eye Res.* 77, 497–504.
19. Kur, J., Newman, E. A., Chan-Ling, T. (2012) Cellular and physiological mechanisms underlying blood flow regulation in the retina and choroid in health and disease. *Prog. Retin. Eye Res.* 31, 377–406.
20. Cheung, C. Y., Ikram, M. K., Klein, R., Wong, T. Y. (2015) The clinical implications of recent studies on the structure and function of the retinal microvasculature in diabetes. *Diabetologia* 58, 871–885.
21. Lu, Z. Y., Bhutto, I. A., Amemiya, T. (2003) Retinal changes in Otsuka Long-Evans Tokushima fatty rats (spontaneously diabetic rat)— possibility of a new experimental model for diabetic retinopathy. *Jpn. J. Ophthalmol.* 47, 28–35.
22. Hofman, P., van Blijswijk, B. C., Gaillard, P. J., Vrensen, G. F., Schlingemann, R. O. (2001) Endothelial cell hypertrophy induced by vascular endothelial growth factor in the retina: new insights into the pathogenesis of capillary nonperfusion. *Arch. Ophthalmol.* 119, 861–866.
23. Chakravarthy, U., Hayes, R. G., Stitt, A. W., Douglas, A. (1997) Endothelin expression in ocular tissues of diabetic and insulin-treated rats. *Invest. Ophthalmol. Vis. Sci.* 38, 2144–2151.
24. Evans, T., Xi Deng, D., Mukherjee, K., Downey, D., Chakrabarti, S. (2000) Endothelins, their receptors, and retinal vascular dysfunction in galactose-fed rats. *Diabetes Res. Clin. Pract.* 48, 75–85.
25. Masuzawa, K., Goto, K., Jesmin, S., Maeda, S., Miyauchi, T., Kaji, Y., Oshika, T., Hori, S. (2006) An endothelin type A receptor antagonist reverses upregulated VEGF and ICAM-1 levels in streptozotocin-induced diabetic rat retina. *Curr. Eye Res.* 31, 79–89.

26. Ashton, N., Graymore, C., Pedler, C. (1957) Studies on developing retinal vessels, V: mechanism of vaso-obliteration—a preliminary report. *Br. J. Ophthalmol.* 41, 449–460.
27. Kuiper, E. J., van Zijderveld, R., Roestenberg, P., Lyons, K. M., Goldschmeding, R., Klaassen, I., Van Noorden, C. J., Schlingemann, R. O. (2008) Connective tissue growth factor is necessary for retinal capillary basal lamina thickening in diabetic mice. *J. Histochem. Cytochem.* 56, 785–792.
28. Van Geest, R. J., Leeuwis, J. W., Dendooven, A., Pfister, F., Bosch, K., Hoeben, K. A., Vogels, I. M., Van der Giezen, D. M., Dietrich, N., Hammes, H. P., Goldschmeding, R., Klaassen, I., Van Noorden, C. J., Schlingemann, R. O. (2014) Connective tissue growth factor is involved in structural retinal vascular changes in long-term experimental diabetes. *J. Histochem. Cytochem.* 62, 109–118.
29. Bek, T., Ledet, T. (1996) Vascular occlusion in diabetic retinopathy: a qualitative and quantitative histopathological study. *Acta Ophthalmol. Scand.* 74, 36–40.
30. Tang, J., Mohr, S., Du, Y. D., Kern, T. S. (2003) Non-uniform distribution of lesions and biochemical abnormalities within the retina of diabetic humans. *Curr. Eye Res.* 27, 7–13.
31. Miyamoto, K., Ogura, Y., Kenmochi, S., Honda, Y. (1997) Role of leukocytes in diabetic microcirculatory disturbances. *Microvasc. Res.* 54, 43–48.
32. Noda, K., Nakao, S., Zandi, S., Sun, D., Hayes, K. C., Hafezi-Moghadam, A. (2014) Retinopathy in a novel model of metabolic syndrome and type 2 diabetes: new insight on the inflammatory paradigm. *FASEB J.* 28, 2038–2046.
33. Sasongko, M. B., Wong, T. Y., Nguyen, T. T., Cheung, C. Y., Shaw, J. E., Wang, J. J. (2011) Retinal vascular tortuosity in persons with diabetes and diabetic retinopathy. *Diabetologia* 54, 2409–2416.
34. Barouch, F. C., Miyamoto, K., Allport, J. R., Fujita, K., Bursell, S. E., Aiello, L. P., Luscinskas, F. W., Adamis, A. P. (2000) Integrin-mediated neutrophil adhesion and retinal leukostasis in diabetes. *Invest. Ophthalmol. Vis. Sci.* 41, 1153–1158.
35. Chibber, R., Ben-Mahmud, B. M., Coppini, D., Christ, E., Kohner, E. M. (2000) Activity of the glycosylating enzyme, core 2 GlcNAc (b1,6) transferase, is higher in polymorphonuclear leukocytes from diabetic patients compared with age-matched control subjects: relevance to capillary occlusion in diabetic retinopathy. *Diabetes* 49, 1724–1730.
36. Dosquet, C., Weill, D., Wautier, J. L. (1992) Molecular mechanism of blood monocyte adhesion to vascular endothelial cells. *Nouv. Rev. Fr. Hematol.* 34(Suppl), S55–S59.
37. Xu, H., Manivannan, A., Liversidge, J., Sharp, P. F., Forrester, J. V., Crane, I. J. (2003) Requirements for passage of T lymphocytes across non-inflamed retinal microvessels. *J. Neuroimmunol.* 142, 47–57.
38. Miyamoto, K., Khosrof, S., Bursell, S. E., Rohan, R., Murata, T., Clermont, A. C., Aiello, L. P., Ogura, Y., Adamis, A. P. (1999) Prevention of leukostasis and vascular leakage in streptozotocin-induced diabetic retinopathy via intercellular adhesion molecule-1 inhibition. *Proc. Natl. Acad. Sci. USA* 96, 10836–10841.
39. Hughes, J. M., Brink, A., Witmer, A. N., Hanraads-de Riemer, M., Klaassen, I., Schlingemann, R. O. (2004) Vascular leucocyte adhesion molecules unaltered in the human retina in diabetes. *Br. J. Ophthalmol.* 88, 566–572.
40. McLeod, D. S., Lefer, D. J., Merges, C., Luty, G. A. (1995) Enhanced expression of intracellular adhesion molecule-1 and P-selectin in the diabetic human retina and choroid. *Am. J. Pathol.* 147, 642–653.
41. Duguid, I. G., Boyd, A. W., Mandel, T. E. (1991) The expression of adhesion molecules in the human retina and choroid. *Aust. N. Z. J. Ophthalmol.* 19, 309–316.
42. Silverman, M. D., Babra, B., Pan, Y., Planck, S. R., Rosenbaum, J. T. (2005) Differential E-selectin expression by iris versus retina microvascular endothelial cells cultured from the same individuals. *Microvasc. Res.* 70, 32–42.
43. Tian, P., Ge, H., Liu, H., Kern, T. S., Du, L., Guan, L., Su, S., Liu, P. (2013) Leukocytes from diabetic patients kill retinal endothelial cells: effects of berberine. *Mol. Vis.* 19, 2092–2105.
44. Muranaka, K., Yanagi, Y., Tamaki, Y., Usui, T., Kubota, N., Iriyama, A., Terauchi, Y., Kadowaki, T., Araie, M. (2006) Effects of peroxisome proliferator-activated receptor gamma and its ligand on blood-retinal barrier in a streptozotocin-induced diabetic model. *Invest. Ophthalmol. Vis. Sci.* 47, 4547–4552.
45. Miyamoto, K., Khosrof, S., Bursell, S. E., Moromizato, Y., Aiello, L. P., Ogura, Y., Adamis, A. P. (2000) Vascular endothelial growth factor (VEGF)-induced retinal vascular permeability is mediated by intercellular adhesion molecule-1 (ICAM-1). *Am. J. Pathol.* 156, 1733–1739.
46. Viores, S. A., Xiao, W. H., Shen, J., Campochiaro, P. A. (2007) TNF- α is critical for ischemia-induced leukostasis, but not retinal neovascularization nor VEGF-induced leakage. *J. Neuroimmunol.* 182, 73–79.
47. Huang, H., Gandhi, J. K., Zhong, X., Wei, Y., Gong, J., Duh, E. J., Viores, S. A. (2011) TNF α is required for late BRB breakdown in diabetic retinopathy, and its inhibition prevents leukostasis and protects vessels and neurons from apoptosis. *Invest. Ophthalmol. Vis. Sci.* 52, 1336–1344.
48. Moore, T. C., Moore, J. E., Kaji, Y., Frizzell, N., Usui, T., Poulaki, V., Campbell, I. L., Stitt, A. W., Gardiner, T. A., Archer, D. B., Adamis, A. P. (2003) The role of advanced glycation end products in retinal microvascular leukostasis. *Invest. Ophthalmol. Vis. Sci.* 44, 4457–4464.
49. Hirata, F., Yoshida, M., Niwa, Y., Okouchi, M., Okayama, N., Takeuchi, Y., Itoh, M., Ogura, Y. (2005)

- Insulin enhances leukocyte-endothelial cell adhesion in the retinal microcirculation through surface expression of intercellular adhesion molecule-1. *Microvasc. Res.* 69, 135–141.
50. Miyahara, S., Kiryu, J., Miyamoto, K., Hirose, F., Tamura, H., Yoshimura, N. (2006) Alteration of leukocyte-endothelial cell interaction during aging in retinal microcirculation of hypertensive rats. *Jpn. J. Ophthalmol.* 50, 509–514.
 51. Tomida, K., Tamai, K., Matsuda, Y., Matsubara, A., Ogura, Y. (2001) Hypercholesterolemia induces leukocyte entrapment in the retinal microcirculation of rats. *Curr. Eye Res.* 23, 38–43.
 52. Jousseaume, A. M., Poulaki, V., Mitsiades, N., Kirchhof, B., Koizumi, K., Döhmen, S., Adamis, A. P. (2002) Nonsteroidal anti-inflammatory drugs prevent early diabetic retinopathy via TNF- α suppression. *FASEB J.* 16, 438–440.
 53. Wang, K., Wang, Y., Gao, L., Li, X., Li, M., Guo, J. (2008) Dexamethasone inhibits leukocyte accumulation and vascular permeability in retina of streptozotocin-induced diabetic rats via reducing vascular endothelial growth factor and intercellular adhesion molecule-1 expression. *Biol. Pharm. Bull.* 31, 1541–1546.
 54. Gubitosi-Klug, R. A., Talahalli, R., Du, Y., Nadler, J. L., Kern, T. S. (2008) 5-Lipoxygenase, but not 12/15-lipoxygenase, contributes to degeneration of retinal capillaries in a mouse model of diabetic retinopathy. *Diabetes* 57, 1387–1393.
 55. Liu, H., Tang, J., Lee, C. A., Kern, T. S. (2015) Metanx and early stages of diabetic retinopathy. *Invest. Ophthalmol. Vis. Sci.* 56, 647–653.
 56. Lorenzi M. (2007) The polyol pathway as a mechanism for diabetic retinopathy: attractive, elusive, and resilient. *Exp. Diabetes Res.* 2007, 61038.
 57. Hughes, J. M., Kuiper, E. J., Klaassen, I., Canning, P., Stitt, A. W., Van Bezu, J., Schalkwijk, C. G., Van Noorden, C. J., Schlingemann, R. O. (2007) Advanced glycation end products cause increased CCN family and extracellular matrix gene expression in the diabetic rodent retina. *Diabetologia* 50, 1089–1098.
 58. Chen, M., Curtis, T. M., Stitt, A. W. (2013) Advanced glycation end products and diabetic retinopathy. *Curr. Med. Chem.* 20, 3234–3240.
 59. Kowluru, R. A., Mishra, M. (2015) Oxidative stress, mitochondrial damage and diabetic retinopathy. *Biochim. Biophys. Acta* 1852, 2474–2483.
 60. Eshaq, R. S., Wright, W. S., Harris, N. R. (2014) Oxygen delivery, consumption, and conversion to reactive oxygen species in experimental models of diabetic retinopathy. *Redox Biol.* 2, 661–666.
 61. Tzeng, T. F., Liu, W. Y., Liou, S. S., Hong, T. Y., Liu, I. M. (2016) Antioxidant-rich extract from plantain seeds ameliorates diabetic retinal injury in a streptozotocin-induced diabetic rat model. *Nutrients* 8.
 62. Xia, P., Inoguchi, T., Kern, T. S., Engerman, R. L., Oates, P. J., King, G. L. (1994) Characterization of the mechanism for the chronic activation of diacylglycerol-protein kinase C pathway in diabetes and hypergalactosemia. *Diabetes* 43, 1122–1129.
 63. Mampuru, J. C., Renier, G. (2002) Advanced glycation end products increase, through a protein kinase C-dependent pathway, vascular endothelial growth factor expression in retinal endothelial cells. Inhibitory effect of glialactide. *J. Diabetes Complications* 16, 284–293.
 64. Clarke, M., Dodson, P. M. (2007) PKC inhibition and diabetic microvascular complications. *Best Pract. Res. Clin. Endocrinol. Metab.* 21, 573–586.
 65. Aiello, L. P., Davis, M. D., Girach, A., Kles, K. A., Milton, R. C., Sheetz, M. J., Vignati, L., Zhi, X. E.; PKC-DRS2 Group. (2006) Effect of ruboxistaurin on visual loss in patients with diabetic retinopathy. *Ophthalmology* 113, 2221–2230.
 66. Jousseaume, A. M., Poulaki, V., Mitsiades, N., Cai, W. Y., Suzuma, I., Pak, J., Ju, S. T., Rook, S. L., Esser, P., Mitsiades, C. S., Kirchhof, B., Adamis, A. P., Aiello, L. P. (2003) Suppression of Fas-FasL-induced endothelial cell apoptosis prevents diabetic blood-retinal barrier breakdown in a model of streptozotocin-induced diabetes. *FASEB J.* 17, 76–78.
 67. Rodriguez, R., Root, H. F. (1948) Capillary fragility and diabetic retinitis; with a note on the use of rutin. *N. Engl. J. Med.* 238, 391–397.
 68. He J, Wang H, Liu Y, Li W, Kim D, Huang H. (2015) Blockade of vascular endothelial growth factor receptor 1 prevents inflammation and vascular leakage in diabetic retinopathy. *J. Ophthalmol.* 2015, 605946.
 69. Dominguez II, J. M., Hu, P., Caballero, S., Moldovan, L., Verma, A., Oudit, G. Y., Li, Q., Grant, M. B. (2016) Adeno-associated virus overexpression of angiotensin-converting enzyme-2 reverses diabetic retinopathy in type 1 diabetes in mice. *Am. J. Pathol.* 186, 1688–1700.
 70. Wang, J., Wang, S., Li, M., Wu, D., Liu, F., Yang, R., Ji, S., Ji, A., Li, Y. (2015) The neuropilin-1 inhibitor, ATWLPFR peptide, prevents experimental diabetes-induced retinal injury by preserving vascular integrity and decreasing oxidative stress. *PLoS One* 10, e0142571.
 71. Kim, S. Y., Johnson, M. A., McLeod, D. S., Alexander, T., Otsuji, T., Steidl, S. M., Hansen, B. C., Luty, G. A. (2004) Retinopathy in monkeys with spontaneous type 2 diabetes. *Invest. Ophthalmol. Vis. Sci.* 45, 4543–4553.
 72. Engerman, R. L., Kern, T. S. (1987) Progression of incipient diabetic retinopathy during good glycemic control. *Diabetes* 36, 808–812.
 73. Takahashi, Y., Wyman, M., Ferris III, F., Kador, P. F. (1992) Diabeteslike preproliferative retinal changes in galactose-fed dogs. *Arch. Ophthalmol.* 110, 1295–1302.

74. Kern, T. S., Engerman, R. L. (1995) Galactose-induced retinal microangiopathy in rats. *Invest. Ophthalmol. Vis. Sci.* 36, 490–496.
75. Hammes, H. P., Klinzing, I., Wiegand, S., Bretzel, R. G., Cohen, A. M., Federlin, K. (1993) Islet transplantation inhibits diabetic retinopathy in the sucrose-fed diabetic Cohen rat. *Invest. Ophthalmol. Vis. Sci.* 34, 2092–2096.
76. Babel, J., Leuenerberger, P. (1974) A long term study on the ocular lesions in streptozotocin diabetic rats. *Albrecht Von Graefes Arch. Klin. Exp. Ophthalmol.* 189, 191–209.
77. Dosso, A. A., Leuenerberger, P. M., Rungger-Brändle, E. (1999) Remodeling of retinal capillaries in the diabetic hypertensive rat. *Invest. Ophthalmol. Vis. Sci.* 40, 2405–2410.
78. Blair, N. P., Tso, M. O., Dodge, J. T. (1984) Pathologic studies of the blood–retinal barrier in the spontaneously diabetic BB rat. *Invest. Ophthalmol. Vis. Sci.* 25, 302–311.
79. Danis, R. P., Yang, Y. (1993) Microvascular retinopathy in the Zucker diabetic fatty rat. *Invest. Ophthalmol. Vis. Sci.* 34, 2367–2371.
80. Yang, Y. S., Danis, R. P., Peterson, R. G., Dolan, P. L., Wu, Y. Q. (2000) Acarbose partially inhibits microvascular retinopathy in the Zucker Diabetic Fatty rat (ZDF/GMI-FA). *J. Ocul. Pharmacol. Ther.* 16, 471–479.
81. Kakehashi, A., Saito, Y., Mori, K., Sugi, N., Ono, R., Yamagami, H., Shinohara, M., Tamemoto, H., Ishikawa, S. E., Kawakami, M., Kanazawa, Y. (2006) Characteristics of diabetic retinopathy in SDT rats. *Diabetes Metab. Res. Rev.* 22, 455–461.
82. Yamada, H., Yamada, E., Higuchi, A., Matsumura, M. (2005) Retinal neovascularisation without ischaemia in the spontaneously diabetic Torii rat. *Diabetologia* 48, 1663–1668.
83. Feit-Leichman, R. A., Kinouchi, R., Takeda, M., Fan, Z., Mohr, S., Kern, T. S., Chen, D. F. (2005) Vascular damage in a mouse model of diabetic retinopathy: relation to neuronal and glial changes. *Invest. Ophthalmol. Vis. Sci.* 46, 4281–4287.
84. Yamakawa, K., Bhutto, I. A., Lu, Z., Watanabe, Y., Amemiya, T. (2001) Retinal vascular changes in rats with inherited hypercholesterolemia—corrosion cast demonstration. *Curr. Eye Res.* 22, 258–265.
85. Bhutto, I. A., Amemiya, T. (1997) Vascular changes in retinas of spontaneously hypertensive rats demonstrated by corrosion casts. *Ophthalmic Res.* 29, 12–23.
86. Kuwabara, T., Cogan, D. G. (1960) Studies of retinal vascular patterns, I: normal architecture. *Arch. Ophthalmol.* 64, 904–911.
87. Linberg, K., Cuenca, N., Ahnelt, P., Fisher, S., Kolb, H. (2001) Comparative anatomy of major retinal pathways in the eyes of nocturnal and diurnal mammals. *Prog. Brain Res.* 131, 27–52.
88. Obrosova, I. G., Drel, V. R., Kumagai, A. K., Szábo, C., Pacher, P., Stevens, M. J. (2006) Early diabetes-induced biochemical changes in the retina: comparison of rat and mouse models. *Diabetologia* 49, 2525–2533.
89. Romeo, G., Liu, W. H., Asnaghi, V., Kern, T. S., Lorenzi, M. (2002) Activation of nuclear factor-kappaB induced by diabetes and high glucose regulates a proapoptotic program in retinal pericytes. *Diabetes* 51, 2241–2248.
90. Zheng, L., Howell, S. J., Hatala, D. A., Huang, K., Kern, T. S. (2007) Salicylate-based anti-inflammatory drugs inhibit the early lesion of diabetic retinopathy. *Diabetes* 56, 337–345.
91. Kern, T. S. (2007) Contributions of inflammatory processes to the development of the early stages of diabetic retinopathy. *Exp. Diabetes Res.* 2007, 95103.
92. Kowluru, R. A., Tang, J., Kern, T. S. (2001) Abnormalities of retinal metabolism in diabetes and experimental galactosemia. VII. Effect of long-term administration of antioxidants on the development of retinopathy. *Diabetes* 50, 1938–1942.
93. Millen, A. E., Klein, R., Folsom, A. R., Stevens, J., Palta, M., Mares, J. A. (2004) Relation between intake of vitamins C and E and risk of diabetic retinopathy in the Atherosclerosis Risk in Communities study. *Am. J. Clin. Nutr.* 79, 865–873.
94. Kern, T. S., Engerman, R. L. (2001) Pharmacological inhibition of diabetic retinopathy: aminoguanidine and aspirin. *Diabetes* 50, 1636–1642.
95. Sun, W., Gerhardinger, C., Dagher, Z., Hoehn, T., Lorenzi, M. (2005) Aspirin at low-intermediate concentrations protects retinal vessels in experimental diabetic retinopathy through non-platelet-mediated effects. *Diabetes* 54, 3418–3426.
96. Mohamed, Q., Gillies, M. C., Wong, T. Y. (2007) Management of diabetic retinopathy: a systematic review. *JAMA* 298, 902–916.
97. Antonetti, D. A., Wolpert, E. B., DeMaio, L., Harhaj, N. S., Scaduto, Jr., R. C. (2002) Hydrocortisone decreases retinal endothelial cell water and solute flux coincident with increased content and decreased phosphorylation of occludin. *J. Neurochem.* 80, 667–677.
98. UK Prospective Diabetes Study (UKPDS) Group. (1998) Intensive blood-glucose control with sulphonylureas or insulin compared with conventional treatment and risk of complications in patients with type 2 diabetes (UKPDS 33). *Lancet* 352, 837–853.
99. Writing Team for the Diabetes Control and Complications Trial/ Epidemiology of Diabetes Interventions and Complications Research Group. (2002) Effect of intensive therapy on the microvascular complications of type 1 diabetes mellitus. *JAMA* 287, 2563–2569.
100. Koevary, S. B., Nussey, J., Kern, T. S. (2007) Long-term, topical insulin administration increases the severity of retinal vascular pathology in streptozotocin-induced diabetic rats. *Optomtry* 78, 574–581.





TNF α -induced disruption of the blood–retinal barrier in vitro is regulated by intracellular 3',5'-cyclic adenosine monophosphate levels

Anne-Eva van der Wijk,¹ Ilse M. C. Vogels,¹ Cornelis J. F. van Noorden,^{1,2} Ingeborg Klaassen,¹ and Reinier O. Schlingemann¹

¹Ocular Angiogenesis Group, Departments of Ophthalmology and Medical Biology, Academic Medical Center, University of Amsterdam, Amsterdam, The Netherlands

²Cellular Imaging Core Facility, Department of Medical Biology, Academic Medical Center, University of Amsterdam, Amsterdam, The Netherlands

Invest Ophthalmol Vis Sci. (2017) 58(9): 3496-3505

ABSTRACT

PURPOSE. Proinflammatory cytokines such as tumor necrosis factor (TNF α) may have a causative role in blood–retinal barrier (BRB) disruption, which is an essential step in the development of diabetic macular edema. The purpose of our study was to determine whether TNF α increases permeability in an in vitro model of the BRB and to explore the mechanisms involved.

METHODS. Primary bovine retinal endothelial cells (BRECs) were grown on Transwell inserts and cells were stimulated with TNF α or a combination of TNF α , IL1 β , and VEGF. Molecular barrier integrity of the BRB was determined by gene and protein expression of BRB-specific components, and barrier function was assessed using permeability assays.

RESULTS. TNF α reduced the expression of tight and adherens junctions in BRECs. Permeability for a 376 Da molecular tracer was increased after TNF α stimulation, but not for larger tracers. We found that 3',5'-cyclic adenosine monophosphate (cAMP) stabilized the barrier properties of BRECs, and that TNF α significantly decreased intracellular cAMP levels. When BRECs were preincubated with a membrane-permeable cAMP analog, the effects of TNF α on claudin-5 expression and permeability were mitigated. The effects of TNF α on barrier function in BRECs were largely independent of the small Rho guanosine triphosphate (GTP)ases RhoA and Rac1, which is in contrast to TNF α effects on the nonbarrier endothelium. The combination of TNF α , IL1 β , and VEGF increased permeability for a 70 kDa-FITC tracer, also mediated by cAMP.

CONCLUSIONS. TNF α alone, or in combination with IL1 β and VEGF, induces permeability of the BRB in vitro for differently sized molecular tracers mediated by cAMP, but independently of Rho/Rac signaling.

INTRODUCTION

More than one third of diabetic persons have some form of diabetic retinopathy (DR), and approximately 5% to 10% develop vision-threatening complications such as proliferative DR and macular edema¹; the latter is the leading cause of vision loss in DR.² Although disruption of the blood-retinal barrier (BRB) is an essential step in the development of diabetic macular edema, its mechanisms are poorly understood. This lack of understanding precludes the development of novel effective treatment strategies. Focal and diffuse BRB disruption is caused by retinal ischemia as a result of capillary nonperfusion³ and eventually leads to vascular leakage and the development of diabetic macular edema. Although it is widely accepted that vascular endothelial growth factor (VEGF) is one of the main drivers of BRB disruption, a subset of patients does not benefit from therapeutics targeting VEGF.⁴ Furthermore, these invasive treatments are burdensome for the patient, requiring monthly to bimonthly intravitreal injections⁵ for several years.

In addition to VEGF, it has been suggested that proinflammatory cytokines such as tumor necrosis factor (TNF α) have a causative role in BRB disruption.⁶⁻⁸ Indeed, there are studies that show elevated TNF α levels in the vitreous of patients with active DR,⁹⁻¹² but also studies that do not.¹³ Furthermore, (small) clinical trials using anti-TNF α antibodies or soluble TNF α receptors in patients with diabetic macular edema or other ocular diseases have had limited success to date.^{6,14-17} Therefore, whether and how proinflammatory cytokines contribute to the development of BRB disruption and subsequent macular edema is still controversial.

In nonbarrier type endothelium of peripheral origin, TNF α is known to induce vascular leakage via the second messenger molecule 3',5'-cyclic adenosine monophosphate (cAMP) and the Rho family of small GTPases, including Rac1 and RhoA. Upon receptor binding, TNF α can lower intracellular cAMP levels and inactivate Rac1^{18,19} or activate RhoA.²⁰⁻²² This leads to the disruption of adherens junctions and stress fiber formation and eventually increased permeability. Although these actions of TNF α have been shown to greatly affect peripheral (micro)vascular permeability, little is known about these mechanisms in the context of barrier-forming endothelia such as that of the BRB. The purpose of the present study was to address the following questions: In an *in vitro* model of the BRB, (a) does TNF α induce endothelial permeability and, if so, (b) is TNF α -induced endothelial barrier permeability mediated by cAMP and/or small Rho GTPases?

MATERIALS AND METHODS

Cell cultures

Bovine retinal endothelial cells (BRECs) were isolated from freshly enucleated cow eyes obtained from the slaughterhouse and cultured as described previously.²³ First passage BRECs were used in all experiments, and the cells were kept in complete Dulbecco's modified Eagle's medium containing 25 mM HEPES and 4.5 g/l glucose (Lonza, Breda, The Netherlands), supplemented with 10% fetal calf serum, 1x MEM nonessential amino

acids (Thermo Fisher Scientific, Landsmeer, The Netherlands), Fungizone® Antimycotic (Gibco, Landsmeer, The Netherlands), 1% penicillin-streptomycin-glutamine (PenStrep; Invitrogen, Landsmeer, The Netherlands), 2 mM L-glutamine (Thermo Fisher Scientific), and 10 µg/ml hydrocortisone (Sigma- Aldrich, Zwijndrecht, The Netherlands) in 10% CO₂ at 37°C.

Human umbilical vein endothelial cells (HUVECs; passage 3) were isolated as described previously.²⁴ HUVECs were cultured in 2% gelatin-coated plates and kept in M199 basal medium (Gibco) supplemented with 1% PenStrep, 10% fetal calf serum, and 10% human serum at 5% CO₂ at 37°C. The experiments were repeated with HUVECs of at least three donors.

In vitro BRB model

An in vitro model of the BRB was developed by us²³ and was used in this study with minor adaptations. When cells were confluent, they were transferred to 24-well Transwell inserts (0.33 cm², pore size 0.4 µm; Greiner Bio-One, Alphen a/d Rijn, The Netherlands) coated with collagen type IV (Sigma-Aldrich). The next day, fresh medium was given to the cells and in some experiments supplemented with 312.5 µM 8-(4-chlorophenylthio(CPT))-cAMP (Sigma-Aldrich) and 17.5 µM RO-20-1724 (a specific phosphodiesterase [PDE] inhibitor, to prevent cAMP breakdown²⁵; Calbiochem, Darmstadt, Germany). Based on a literature search, off-target effects of RO-20-1724 on endothelial cells are unlikely. After 3 or 4 days (depending on the duration of stimulation), rhTNFα (10 ng/ml; ProSpec, Ness Ziona, Israel) or a combination of rhTNFα (10 ng/ml), rhIL1β (10 ng/ml; ProSpec), and rhVEGF-165 (25 ng/ml; R&D Systems, Abingdon, UK) was added in 20 µl to the apical side of the insert.

Permeability analysis

Permeability assays were performed at 2, 6, and 24 hours after TNFα or triple cytokine (TNFα, IL1β, and VEGF) stimulation. Fluorescent tracers of different sizes (376 Da fluorescein sodium salt, 250 µg/ml [Invitrogen]; 766 Da Cy3, 50 µg/ml [GE Healthcare, Eindhoven, The Netherlands], 70 kDa FITC- dextran, 250 µg/ml [Invitrogen], or BSA-FITC, 250 µg/ml [Invitrogen]) were added to the apical side of the Transwell insert, and samples were collected from the upper and lower compartments after 4 hours. Concentrations of the tracer molecules were measured with a fluorescence plate reader (BMG POLARstar; MTX Lab Systems, Bradenton, FL, USA), and tracer passage to the lower compartment was calculated on the basis of the initial concentration in the upper compartment. The permeability of stimulated cells was calculated relative to that of unstimulated cells.

Immunofluorescence staining

BRECs were grown to confluence on collagen type IV- and fibronectin-coated plastic coverslips (Nunc, Thermo Fisher Scientific). Preincubation with 8-(4-CPT)-cAMP and RO-20- 1724 was performed during the night before stimulation with TNFα by changing

the medium to medium supplemented with 312.5 μM 8-(4-CPT)-cAMP and 17.5 μM RO-20-1724. The cells were fixed with ice-cold 75% ethanol for 15 minutes at -20°C (anti-claudin-5 antibody), or with 4% paraformaldehyde for 15 minutes at 4°C (other antibodies) and stained as described previously.²³ The following primary antibodies were used: rabbit anti-claudin-5 (cat. 34-1600, 1:100; Invitrogen), rabbit- anti-ZO1 (cat. 61-7300; 1:250, Invitrogen), rabbit-anti VE- cadherin (cat. ab33168; 1:400, Abcam, Cambridge, UK) or a phalloidin probe conjugated with Texas Red (cat. T7471; 1:200, Thermo Fisher Scientific). The secondary antibodies directed against the relevant species were conjugated with Alexa Fluor-488 (1:100; Thermo Fisher Scientific) or Cy3 (1:100; Jackson ImmunoResearch, Suffolk, UK). Cells were mounted on glass slides with Vectashield containing 4',6-diamidino-2-phenylindole (Vector Laboratories, Burlingame, CA, USA) for nuclear staining and embedding. Images were recorded using a confocal laser scanning microscope SP8 (Leica Microsystems, Wetzlar, Germany) at the van Leeuwenhoek Centre for Advanced Microscopy, AMC. Specificity of the staining reaction was checked by the absence of fluorescence signal in samples when the primary antibody was omitted.

F-actin staining of four independent experiments was quantified using Confocal Leica Application Suite X software (Leica Microsystems). In each experiment, six to eight regions of interest of approximately $725\ \mu\text{m}^2$ were selected per image, and the pixel intensity of these regions was averaged per condition. To correct for different pixel intensities between the experiments, factor correction was applied using Factor Correction software v2015.2.0.0.²⁶

RNA isolation and mRNA quantification

BRECs were grown to confluence in a 12-well plate and harvested in 500 μl TRIzol reagent (Invitrogen). Total RNA was isolated according to the manufacturer's protocol and dissolved in RNase-free water. RNA yield was measured spectrophotometrically using NanoDrop (Thermo Scientific, Wilmington, DE, USA), and 1 μg RNA was treated with DNase-I (Invitrogen) and reverse transcribed into first-strand cDNA with a Maxima First Strand cDNA Synthesis Kit (ThermoFisher). Real-time quantitative PCR was performed on 20x diluted cDNA samples using a CFX96 system (Bio-Rad, Hercules, CA, USA) as described previously.²⁷ Primer details are published in Klaassen et al.²⁷ Data were normalized to the geometric mean of the most stable reference genes as determined with NormFinder.²⁸

Measurement of intracellular cAMP levels

Intracellular levels of cAMP in BREC lysates were measured using the acetylated format of the Direct cyclic AMP ELISA kit (Enzo Life Sciences, Raamsdonkveer, The Netherlands), according to the manufacturer's protocol. Absorbance was measured at 405 nm using a microplate spectrophotometer (VERSAmax, Molecular Devices, Sunnyvale, CA, USA), and data were analyzed with SoftMax Pro software (v5.4.1, Molecular Devices). Protein concentration of the cell lysate was measured with Precision Red Advanced Protein Assay (Cytoskeleton, Inc., Denver, CO, USA). Concentrations of intracellular cAMP (pmol/ml) of unstimulated cells were set to one and compared to cAMP levels of treated cells.

RhoA and Rac1 activation assays

Activated RhoA and Rac1 in BREC lysates was measured with the absorbance-based RhoA or Rac1 Activation Assay G-LISA (Cytoskeleton, Inc.), according to the manufacturer's protocol. Absorbance was measured at 490 nm using a microplate spectrophotometer (VERSAmax, Molecular Devices).

Statistics

Data are depicted as mean \pm standard deviation. Experimental conditions were carried out in triplicate, and at least three independent experiments were performed. The differences between groups were determined using an unpaired Student's t-test or analysis of variance followed by Dunnett's test for multiple comparisons. Differences were considered statistically significant when $P < 0.05$. Statistical analyses and graphing were performed using GraphPad Prism 6 (GraphPad Software, Inc., La Jolla, CA, USA) software.

RESULTS

TNF α reduces mRNA and protein levels of tight and adherens junctions

Stimulation of BRECs with TNF α (10 ng/ml) for 24 hours significantly reduced mRNA expression of the tight junction components claudin-5 and zona occludens (ZO)-1, vascular endothelial (VE)-cadherin and β -catenin, the main constituents of adherens junctions (Fig. 1A). On the protein level, expression of claudin-5 appeared to be similar to that in control cells after 24 hours of stimulation with TNF α , except that claudin-5 was expressed in a more ruffled manner around cell membranes (Fig. 1B). Protein expression of ZO-1 and VE-cadherin was reduced after 24-hour TNF α stimulation compared to control cells (Fig. 1B). In contrast with what has been reported for peripheral endothelium (dermal, pulmonary, umbilical vein)^{18,20,29,30} and with what we observed in HUVECs (Supplementary Fig. S1), TNF α did not induce stress fiber formation in BRECs (Fig. 1C), and F-actin content was similar in control and TNF α -stimulated cells (Fig. 1D).

TNF α increases permeability only for small molecular tracers

To test the effect of TNF α -induced downregulation of endothelial junctions on barrier function, we performed permeability assays for molecular tracers of different sizes. TNF α increased the permeability of BREC monolayers for a small molecular tracer, sodium fluorescein (376 Da) after 6-hour and 24-hour stimulation (Fig. 2A) to 131% and 125%, respectively ($P < 0.05$). Permeability for two larger tracers (766 Da and 70 kDa) was not altered after TNF α treatment (Figs. 2B, 2C). These data suggest that TNF α has a selective effect on the paracellular transport pathway, likely as a consequence of disrupted tight junctions.

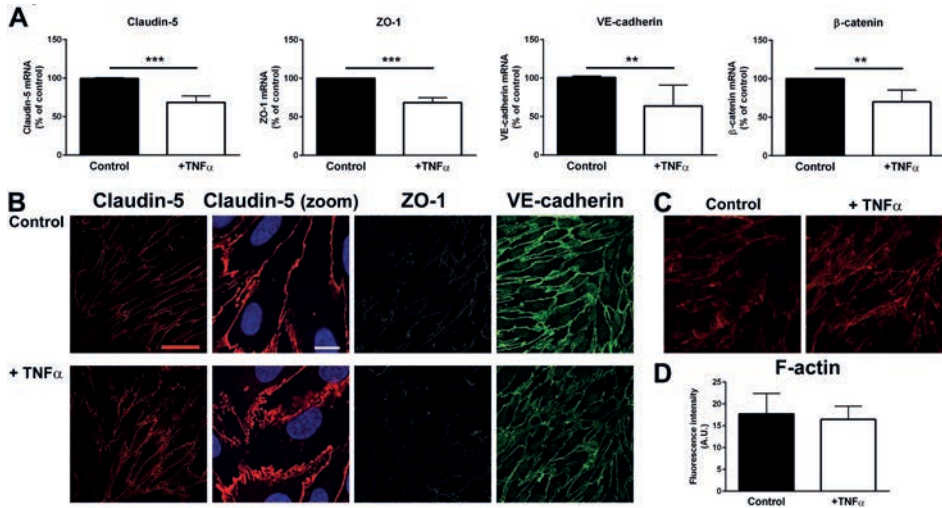


Figure 1. Effect of TNF α on endothelial junctions and the actin cytoskeleton in BRECs. (A) Stimulation of BRECs with TNF α (10 ng/ml) for 24 hours significantly decreased mRNA levels of the tight junction components claudin-5 and ZO-1, and the adherens junction components VE-cadherin and β -catenin. (B) Immunofluorescence staining of claudin-5 (red) shows a ruffled border around the cell membrane after 24 hours of stimulation with TNF α . Nuclear staining is shown in blue. ZO-1 (gray) and VE-cadherin (green) immunofluorescence staining is reduced after TNF α stimulation. (C) TNF α did not induce stress fiber formation in BRECs as shown by immunofluorescence staining with a phalloidin probe to label filamentous actin (F-actin; red). (D) Quantification of F-actin content showed similar results in control cells and TNF α -stimulated cells. ** $P < 0.01$, *** $P < 0.001$. Data are depicted as mean \pm standard deviation. Red scale bar is 50 μ m. White scale bar is 10 μ m.

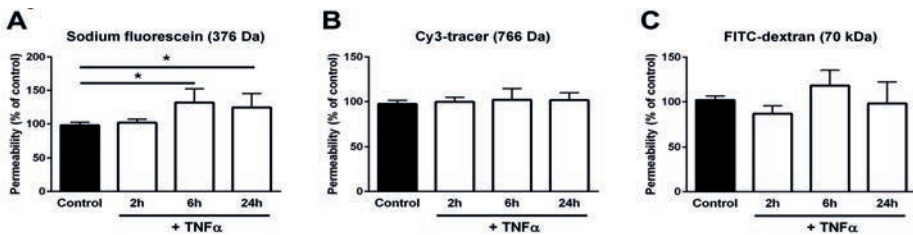


Figure 2. Effect of TNF α on permeability for differently-sized fluorescent tracers. (A) TNF α (10 ng/ml) significantly increased permeability for sodium fluorescein (376 Da) after 6 hours and 24 hours of stimulation. (B) Permeability for a 766 Da-Cy3 tracer and (C) 70 kDa-FITC tracer was not changed after TNF α stimulation. * $P < 0.05$. Data are depicted as mean \pm standard deviation.

cAMP has a stabilizing effect on barrier properties

Although cAMP signaling in barrier-forming endothelium in pathologic conditions has not been thoroughly investigated, the stabilizing effects of cAMP on barrier-endothelium properties *in vitro* are well known.^{23,31} To confirm that cAMP stabilizes the endothelial barrier in our BRB model, we used 8-(4-CPT)-cAMP (a membrane-permeable cAMP analog³²) and RO-20-1724 (a PDE IV inhibitor) to increase intracellular cAMP levels. We found a marked increase in barrier function, reflected by low permeability for both small (376 Da, 766 Da) and large (70 kDa) tracers with addition of the two compounds (Figs. 3A–C). A concentration-response experiment for RO-20-1724 revealed that 17.5 μ M RO-20-1724 (a concentration regularly used in BRB and BBB cell models)^{23,25,33,34} resulted in the lowest permeability (data not shown). The addition of 17.5 μ M RO-20-1724 alone significantly decreased permeability to sodium fluorescein and the 766 Da-Cy3 tracer, but this effect was reduced when simultaneously low levels (3.1 μ M or 31.2 μ M) of 8-(4-CPT)-cAMP were added to the cells. For all 3 tracers, permeability was lowest and significantly decreased when compared with control when 312.5 μ M 8-(4-CPT)-cAMP in combination with 17.5 μ M RO-20-1724 was added. Based on these findings, subsequent experiments were performed using 312.5 μ M 8-(4-CPT)-cAMP and 17.5 μ M RO-20-1724.

In addition, cAMP induced reorganization of the actin cytoskeleton (Figs. 3D, 3E). After preincubation of the cells with 8-(4-CPT)-cAMP and RO-20-1724, the F-actin content was significantly reduced and transverse actin stress fibers were decreased in numbers, whereas the amount of cortical F-actin bundles was increased. These actin rearrangements resulted in an altered morphology of the BRECs (i.e., less elongated; Fig. 3F) and may underlie in part the mechanisms of strengthening of the endothelial barrier by cAMP.

TNF α decreases intracellular cAMP levels

Similar to the peripheral endothelium,^{18,30,35} intracellular cAMP levels in BRECs were decreased after TNF α stimulation. Intracellular cAMP was significantly reduced up to at least 24 hours after the addition of TNF α (Fig. 4A), suggesting that TNF α -induced barrier disruption is mediated by reduced intracellular cAMP levels. Stimulating the cells with 8-(4-CPT)-cAMP and RO-20-1724 led to an approximately 10-fold increase in intracellular cAMP levels after 24 hours (Fig. 4B), and preincubation of the cells with 8-(4-CPT)-cAMP and RO-20-1724 prevented the TNF α -induced reduction in intracellular cAMP levels (Fig. 4C).

The effects of TNF α on barrier function are largely independent of the small Rho GTPases RhoA and Rac1

To test the activation state of Rac1 and RhoA, we measured GTP-bound (i.e., activated) RhoA and Rac1 in BREC lysates after TNF α stimulation. Because small Rho GTPases are generally activated very rapidly and transiently upon stimulation, we measured activation at 5, 30, and 120 minutes after TNF α stimulation. We observed a small increase in both RhoA and Rac1 activation as compared to unstimulated cells after TNF α stimulation. The effects

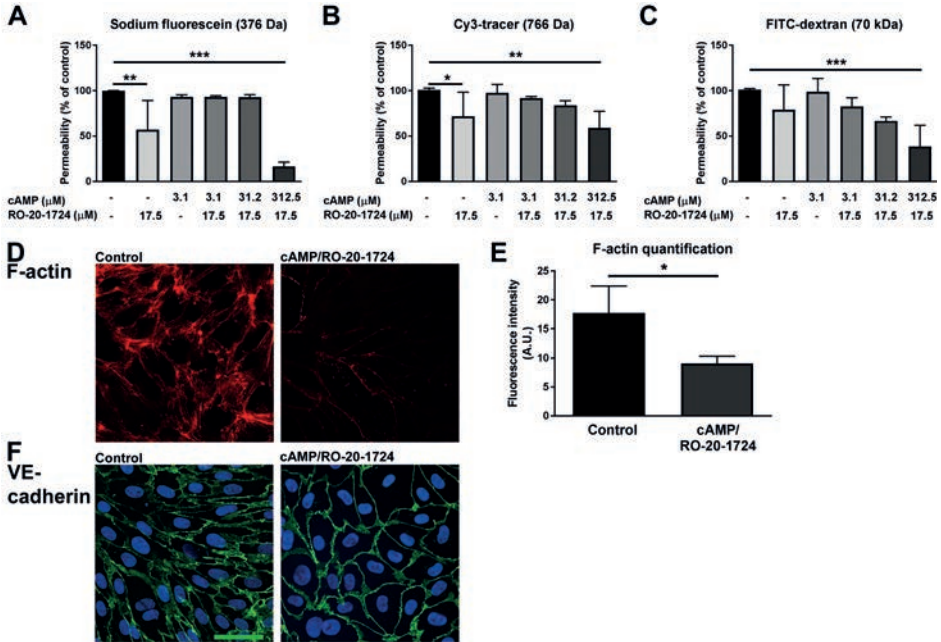


Figure 3. Effects of various concentrations of 8-(4-CPT)-cAMP (cAMP) and RO-20-1724 on BRECs. Permeability for sodium fluorescein (A), 766 Da- Cy3 tracer (B), and 70 kDa-FITC tracer (C) decreased with increasing concentrations of cAMP and was lowest when 17.5 μ M RO-20-1724 and 312.5 μ M cAMP were added simultaneously. (D) Preincubation of BRECs with 312.5 μ M cAMP and 17.5 μ M RO-20-1724 resulted in decreased transverse actin stress fibers and increased cortical F-actin bundles as shown by immunofluorescence using a phalloidin probe (red). (E) Quantification of F-actin content indicated a significantly decreased F-actin signal when compared with control cells. (F) Morphology of BRECs changed after addition of cAMP and RO-20-1724 as shown with VE-cadherin staining (green). Control cells are elongated, whereas addition of cAMP and RO-20-1724 to the BRECs resulted in a more cobblestone-like morphology. Nuclear staining is shown in blue. * $P < 0.05$, ** $P < 0.01$, *** $P < 0.001$. Data are depicted as mean \pm standard deviation. Green scale bar is 50 μ m.

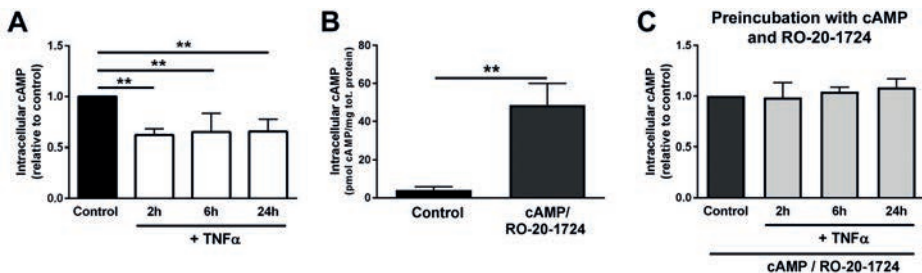


Figure 4. Intracellular cAMP levels after TNF α stimulation. (A) TNF α (10 ng/ml) significantly reduced intracellular cAMP levels when compared with control in BRECs up to at least 24 hours after stimulation. (B) Preincubation of BRECs for 24 hours with 312.5 μ M 8-(4-CPT)-cAMP (cAMP) and 17.5 μ M RO-20-1724 led to significantly increased intracellular cAMP levels. (C) TNF α had no effect on intracellular cAMP levels when cells were preincubated with cAMP and RO-20-1724. ** $P < 0.01$. Data are depicted as mean \pm standard deviation.

on RhoA activation were not statistically significant (Fig. 5A). Thirty minutes after TNF α addition, Rac1 activation showed a modest increase when compared with unstimulated cells (1.4-fold, $P < 0.05$, Fig. 5B). However, taking the small effects of TNF α on RhoA activation into consideration, the balance of Rac1/RhoA activation is not altered by TNF α . Therefore, the effects of TNF α on BRECs appear to be largely independent of RhoA and Rac1.

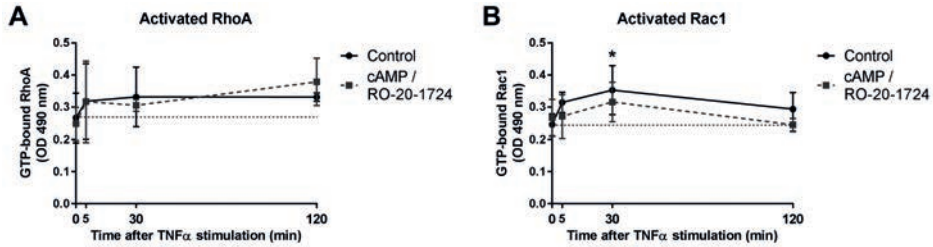


Figure 5. Effect of TNF α on activation of the small GTPases Rac1 and RhoA. (A) RhoA activation was slightly elevated after TNF α (10 ng/ml) stimulation (not significant), both in control cells in the presence of control medium (circles) and cells preincubated with 312.5 μ M 8-(4-CPT)-cAMP (cAMP) and 17.5 μ M RO-20-1724 (squares). (B) TNF α significantly increased Rac1 activation after 30 minutes when compared with unstimulated cells in the control medium (circles). TNF α -induced Rac1 activation did not occur when cells were preincubated with 312.5 μ M cAMP and 17.5 μ M RO-20-1724 (squares). * $P < 0.05$ versus unstimulated cells in the control medium. Data are depicted as mean \pm standard deviation.

Preincubation with 8-(4-CPT)-cAMP and RO-20-1724 prevents claudin-5 downregulation and TNF α -induced increase in permeability for sodium fluorescein

Finally, we determined whether the TNF α -induced decrease in intracellular cAMP levels was responsible for the disruption of tight junctions and increased permeability. We found that preincubation of the cells with 8-(4-CPT)-cAMP and RO-20-1724 effectively prevented the downregulation of claudin-5 mRNA levels (Fig. 6). Whereas TNF α stimulation reduced claudin-5 mRNA levels to 69% after 24 hours ($P < 0.001$), this effect was not observed when cells were preincubated with 8-(4-CPT)-cAMP and RO-20-1724 (Fig. 6A). On the protein level, we also found an unchanged and strong claudin-5 expression at the cell border in 8-(4-CPT)-cAMP- and RO-20-1724-treated cells, despite addition of TNF α (Fig. 6B). This effect was specific for claudin-5, as 8-(4-CPT)-cAMP and RO-20-1724 treatment did not prevent downregulation of ZO-1 and VE-cadherin (Supplementary Fig. S2). In addition, the TNF α -induced increased permeability for sodium fluorescein was prevented when cells were preincubated with 8-(4-CPT)-cAMP and RO-20-1724 (Fig. 6C), and also for the larger tracers there was no increased permeability after TNF α stimulation (Figs. 6D, 6E). These data indicate that TNF α is not able to exert its disruptive effects on the barrier of BRECs when intracellular cAMP levels are high. In addition, they show that reduced claudin-5 levels may be necessary for the functional BRB disruption induced by TNF α .

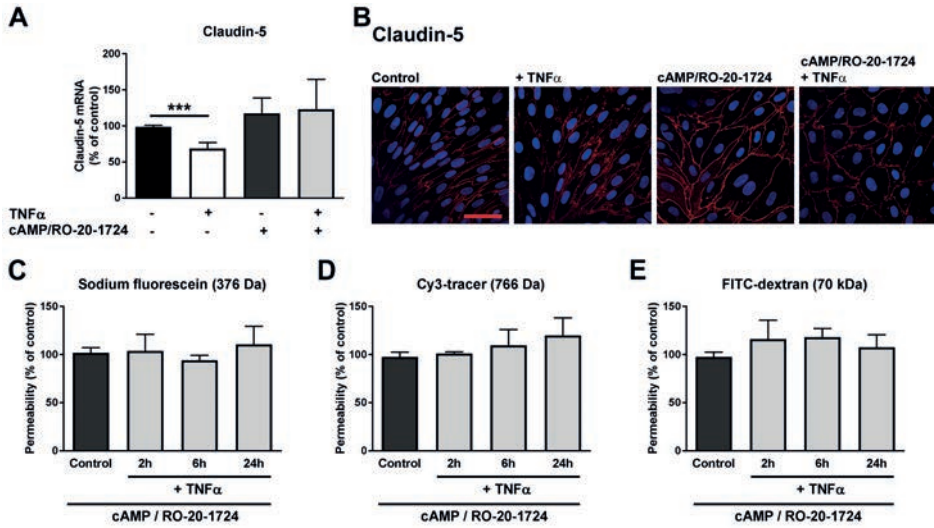


Figure 6. Preincubation of BRECs with 312.5 μ M 8-(4-CPT)-cAMP (cAMP) and 17.5 μ M RO-20-1724 prevented the TNF α -induced effects on claudin-5 expression and permeability. (A) TNF α (10 ng/ml) reduced mRNA expression of claudin-5, and this downregulation was prevented by preincubation of BRECs with cAMP and RO-20-1724. (B) On the protein level, claudin-5 expression as shown by immunofluorescence staining (red) was continuous around the cell membrane in TNF α -stimulated cells that were preincubated with cAMP and RO-20-1724. Nuclear staining is shown in blue. TNF α did not induce permeability for sodium fluorescein (C), 766 Da-Cy3 (D), and 70 kDa-FITC (E) when cells were preincubated with cAMP and RO-20-1724. *** $P < 0.001$. Data are depicted as mean \pm standard deviation. Red scale bar is 50 μ m.

Simultaneous stimulation with TNF α , IL1 β , and VEGF increases permeability for large molecular tracers, and this is reduced by preincubation with 8-(4-CPT)-cAMP and RO-20-1724

Because in (low grade) inflammatory states, such as DR, there is usually an interplay of multiple cytokines in the local microenvironment, we tested the effects of simultaneous stimulation with TNF α (10 ng/ml), IL1 β (10 ng/ml), and VEGF (25 ng/ml) on permeability status of BRECs. Stimulating the cells with this triple cytokine combination of 6 hours caused no change in permeability for sodium fluorescein, both without and with preincubation with 8-(4-CPT)-cAMP and RO-20-1724 (Fig. 7A). A nonsignificant trend for increased permeability for a 766 Da tracer (165% of control) was observed, which was less when cells were preincubated with 8-(4-CPT)-cAMP and RO-20-1724 (118% of control, Fig. 7B). However, permeability for a large 70 kDa molecular tracer was significantly increased to 400% when compared with unstimulated cells after triple cytokine stimulation ($P < 0.05$). This effect was largely prevented by preincubation of the cells with 8-(4-CPT)-cAMP and RO-20-1724 (136% of control, Fig. 7C). Because these results are indicative of selective transport for large tracers, we also tested permeability for FITC-conjugated BSA (66 kDa) because albumin is known to be predominantly translocated via the transcellular

route.³⁶ Permeability was increased significantly after 6-hour stimulation with the triple cytokine combination (121% of control, $P < 0.05$), and this was not the case when cells were preincubated with 8-(4-CPT)-cAMP and RO-20-1724 (Fig. 7D). These data suggest that cAMP may be a key signaling molecule in cytokine-induced permeability in BRECs and that modulation of intracellular cAMP levels may prevent cytokine-induced increases in permeability for large proteins, which is a prerequisite for the formation of macular edema.

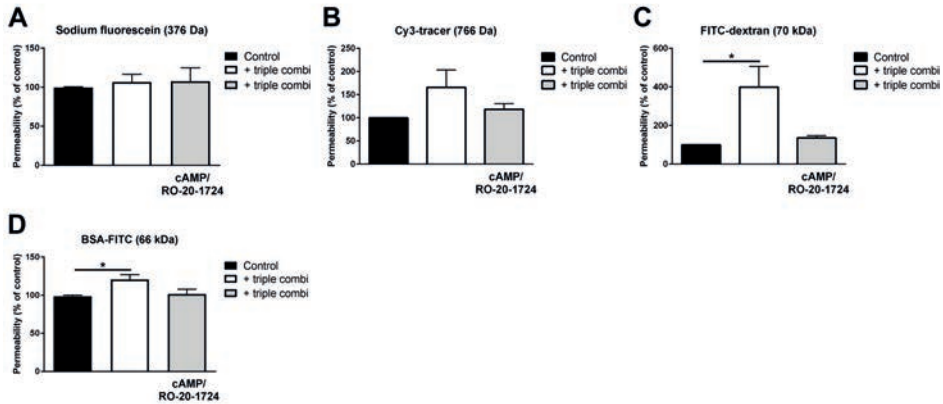


Figure 7. Effect of triple cytokine stimulation on permeability for differently sized fluorescent tracers with and without preincubation with 312.5 μ M 8-(4-CPT)-cAMP (cAMP) and 17.5 μ M RO-20-1724. (A) Simultaneous stimulation with TNF α (10 ng/ml), IL1 β (10 ng/ml), and VEGF (25 ng/ml; triple combi) for 6 hours did not change permeability for sodium fluorescein (376 Da), both without and with preincubation of cells with cAMP and RO-20-1724. (B) Permeability for a 766 Da-Cy3 tracer was slightly but nonsignificantly increased after triple cytokine stimulation and to a lesser extent when cells were preincubated with cAMP and RO-20-1724. (C) Permeability for a 70 kDa-FITC tracer was significantly increased to 400% of control after triple cytokine stimulation and this increase was largely reduced by preincubating the cells with cAMP and RO-20-1724. (D) Permeability for BSA-FITC was significantly increased after triple cytokine stimulation, and this was not the case when cells were preincubated with cAMP and RO-20-1724. * $P < 0.05$. Data are depicted as mean \pm standard deviation.

DISCUSSION

Our in vitro study shows that TNF α reduces the expression of tight and adherens junctions in BRECs and thereby increases permeability for small molecules in our BRB model. In contrast, a combination of TNF α with IL1 β and VEGF causes selectively increased permeability for large tracers. Furthermore, our data suggest that both TNF α - and TNF α /IL-1 β /VEGF-induced permeability in BRECs is mediated by cAMP and that barrier integrity can be rescued by increased intracellular cAMP levels.

The increased permeability of our cells after TNF α stimulation alone was small and specific for the small molecular tracer of 376 Da. These results do not match the findings of a previous study where an almost 4-fold increase in permeability was reported for a 70

kDa tracer by TNF α in BRECs.³⁷ However, in agreement with this study, we found that mRNA expression of pivotal tight and adherens junction molecules was decreased after TNF α treatment, and this was confirmed on the protein level. In addition, we did not observe any changes in the cytoskeletal arrangements and hence no gaps between cells after TNF α stimulation. Therefore, it seems unlikely that large molecular tracers with the size of small proteins such as albumin can pass through the cellular monolayer. We cannot readily explain the contradictory results of tracer permeability of our study and the report of Aveleira et al.³⁷ other than by differences in medium supplements and cell isolation method. On the basis of our results, however, we suggest that TNF α in the absence of IL1 β and VEGF selectively affects the paracellular pathway in retinal endothelial cells, resulting in increased permeability for small solutes and water.

We found that, similar to the situation in peripheral endothelial cells,^{18,30,35} TNF α caused a significant reduction in intracellular cAMP levels. In bovine aortic endothelial cells and HUVECs, it has been shown that hydrolysis of cAMP was consistently increased in the cytosol after TNF α treatment, most likely because of the activation of PDE II and IV.^{30,35} We did not investigate the mechanism underlying the TNF α -mediated reduction in intracellular cAMP levels in this study. However, it may well be at least partly attributable to PDE IV activation because the addition of RO-20-1724 and 8-(4-CPT)-cAMP to BRECs selectively prevented TNF α -induced changes. The mechanism of the TNF α -induced destabilization of barrier function appears to be different in retinal (barrier forming) endothelium than in endothelial cells of peripheral (nonbarrier forming) origin, as in our effort to identify the signaling pathways involved we found some interesting differences with endothelial cells of peripheral origin. Whereas multiple studies on nonbarrier endothelium have shown that TNF α induces permeability via RhoA or Rac1 GTPase activation or inhibition,^{18,20-22} respectively, we did not find evidence for such roles of these GTPases in our BRB endothelium. Rac1 activation was induced to a certain extent by TNF α , but the ratio of activated RhoA/Rac1 remained unchanged. In addition, the activation of Rap1 (another family member of the small Rho GTPases) was also unchanged after TNF α stimulation in BRECs (unpublished results). Therefore, it can be assumed that, although in these cells cAMP plays a central regulatory role in endothelial permeability, as is the case in the peripheral endothelium, the downstream pathway activated by cAMP is not the same. This may reflect differences between the barrier and nonbarrier endothelia, and may be in line with the need for the barrier endothelium to be more robust in preventing molecules entering the neural tissues from the bloodstream. However, endothelial cell responses to TNF α may be species dependent,^{35,38} and thus care should be taken in interpreting and extrapolating these data to the human situation.

We were able to prevent TNF α -induced permeability for sodium fluorescein by elevating the intracellular cAMP levels using exogenous cAMP and by preventing cAMP degradation. The protective effect of cAMP on TNF α -induced BRB disruption in BRECs was dependent on claudin-5, as we found that preincubation of the cells with 8-(4-CPT)-cAMP and RO-20-1724 did not rescue the expression of ZO-1 and VE-cadherin after TNF α stimulation. In contrast, the rescuing effect of cAMP on claudin-5 expression was sufficient to prevent the

TNF α - induced increased permeability for sodium fluorescein. This is in line with findings in claudin-5-knockout mice, which show only increased permeability of tracers <800 Da in the brain.³⁹ In fact, the intermediate-sized tracer of 766 Da that we have used may be just on the borderline of the molecules that can pass or not pass through the disrupted junctions.

In addition to direct barrier-promoting effects of increased levels of cAMP, as shown in the present study, 8-(4-CPT)-cAMP and RO-20-1724 may have additional effects that may be beneficial for the diabetic retina. We observed a downregulation of vascular adhesion molecule-1, intracellular adhesion molecule-1, and E-selectin after addition of 17.5 μ M RO-20-1724 alone, whereas intracellular cAMP levels were similar as in unstimulated cells after 24 hours (data not shown). This suggests that RO-20-1724 may have anti-inflammatory effects as well as barrier-promoting effects, as was also shown in other cell types⁴⁰ and animal models.⁴¹ Furthermore, 8-(4-CPT)-cAMP is a highly lipophilic analog with good membrane permeability, and once in the cell, can activate downstream targets with anti-inflammatory potential, such as protein kinase A.³²

With the effects observed in this study, it seems unlikely that TNF α alone can cause an influx of proteins and lipids into the neural retina and thereby disrupt Starling's forces with consequent macular edema.⁴² However, it may be possible that TNF α makes the retinal endothelial cells more prone to the effects of VEGF and other cytokines. Indeed, we found that simultaneous stimulation of the cells with TNF α , IL1 β , and VEGF, three cytokines that are known to be increased in the vitreous of DR patients,^{9,11,12} caused a significant increase in permeability for a 70 kDa-FITC tracer and a BSA-FITC tracer, but not for the two smaller tracers. Increased transport of macromolecules such as albumin induced by this combination of cytokines can lead to an increased tissue oncotic pressure and subsequent edema in vivo. This possibility is further supported by a study in which BRB function was assessed at different time points in a streptozotocin-induced diabetic mouse model and a mutant (Ins2^{Alkita}) diabetic mouse model, both lacking TNF α . It was concluded that neither TNF α nor inflammation were necessary for early BRB breakdown, but were essential for BRB breakdown at later time points as the disease progressed.⁴³ We suggest that the interplay between different cytokines, rather than one cytokine alone, leads to the development of vision-threatening edema, prompting the need for multitargeted therapy.

The prominent difference in permeability after triple cytokine stimulation of BSA-FITC (121% of control) and the 70 kDa-FITC tracer (400% of control) may be a result of different modes of transportation. Both molecules are hydrophilic, have a comparable molecular weight and have a diameter that does not allow them to pass via paracellular junctions² (BSA-FITC approximately 7.2 nm,⁴⁴ 70 kDa-FITC approximately 12 nm⁴⁵). Indeed, albumin was observed to translocate predominantly through receptor-mediated transcytosis.^{36,46} Therefore, the uptake of BSA-FITC by the cells requires free binding sites, which can be a rate-limiting factor. In contrast, dextrans do not adsorb to the cell surface and are internalized via nonspecific fluid-phase endocytosis.⁴⁷ More pronounced effects of cytokines on fluid-phase permeability, which has been shown to occur in the BBB,⁴⁸ than on receptor-mediated transcytosis can explain the difference in transcellular transport for these two similarly sized fluorescent tracers. Alternatively, it is possible that a larger portion

of albumin is targeted for degradation or recycling in the cell instead of being transported to the extracellular compartment. Although it was rather surprising that the triple cytokine stimulation did not induce increased permeability for sodium fluorescein after 6 hours, this is not uncommon in patients with diabetic macular edema. Several studies reported that patients presenting with cystoid abnormalities on optical coherence tomography had no signs of leakage on fluorescein angiography or vice versa.^{49,50} Hence, leakage of small solutes and larger proteins do not always occur in concert in the retina. Regardless, our findings are limited to an in vitro model of the BRB and a monoculture of endothelial cells, and it is of high interest to validate our findings on the BRB in an in vivo retinal environment.

We conclude that TNF α alone induces small-molecule permeability of the BRB in vitro, whereas the combination of TNF α , IL1 β , and VEGF induces permeability to large molecules and provide evidence that this permeability is mediated via cAMP. This suggests that TNF α can contribute to the development of retinal vascular leakage and consequently diabetic macular edema, although likely as part of a multifaceted pathogenesis.

ACKNOWLEDGMENTS

Supported by Landelijke Stichting voor Blinden en Slechtienden and Stichting Oogfonds Nederland that contributed through UitZicht (Grant UitZicht 2012-16), Nederlandse Vereniging ter Verbetering van het Lot der Blinden, Rotterdamse Stichting Blindenbelangen (Grant B20120030), Stichting Winkel Sweep, and Stichting Nederlands Oogheelkundig Onderzoek (Grant 2012-05). This study was published with the help of Edmond en Marianne Blaauw Fonds voor Oogheelkunde (Edmond and Marianne Blaauw Fund for Ophthalmology).

Disclosure: A.-E. van der Wijk, None; I.M.C. Vogels, None; C.J.F. van Noorden, None; I. Klaassen, None; R.O. Schlingemann, None

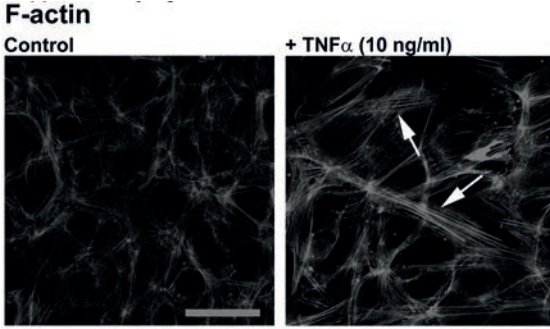
REFERENCES

1. Yau JW, Rogers SL, Kawasaki R, et al. Global prevalence and major risk factors of diabetic retinopathy. *Diabetes Care*. 2012;35:556–564.
2. Klaassen I, Van Noorden CJ, Schlingemann RO. Molecular basis of the inner blood-retinal barrier and its breakdown in diabetic macular edema and other pathological conditions. *Prog Retin Eye Res*. 2013;34:19–48.
3. Mathews MK, Merges C, McLeod DS, Luty GA. Vascular endothelial growth factor and vascular permeability changes in human diabetic retinopathy. *Invest Ophthalmol Vis Sci*. 1997;38:2729–2741.
4. Ford JA, Lois N, Royle P, Clar C, Shyangdan D, Waugh N. Current treatments in diabetic macular oedema: systematic review and meta-analysis. *BMJ Open*. 2013;3.
5. Nguyen QD, Brown DM, Marcus DM, et al. Ranibizumab for diabetic macular edema: results from 2 phase III randomized trials: RISE and RIDE. *Ophthalmology*. 2012;119:789–801.
6. Arias L, Caminal JM, Badia MB, Rubio MJ, Catala J, Pujol O. Intravitreal infliximab in patients with macular degeneration who are nonresponders to anti-vascular endothelial growth factor therapy. *Retina*. 2010;30:1601–1608.
7. Arita R, Nakao S, Kita T, et al. A key role for ROCK in TNF-alpha-mediated diabetic microvascular damage. *Invest Ophthalmol Vis Sci*. 2013;54:2373–2383.
8. Jousen AM, Poulaki V, Mitsiades N, et al. Nonsteroidal anti-inflammatory drugs prevent early diabetic retinopathy via TNF-alpha suppression. *FASEB J*. 2002;16:438–440.
9. Demircan N, Safran BG, Soyulu M, Ozcan AA, Sizmaz S. Determination of vitreous interleukin-1 (IL-1) and tumour necrosis factor (TNF) levels in proliferative diabetic retinopathy. *Eye (Lond)*. 2006;20:1366–1369.
10. Malik AN, Parsade CK, Ajaz S, et al. Altered circulating mitochondrial DNA and increased inflammation in patients with diabetic retinopathy. *Diabetes Res Clin Pract*. 2015;110: 257–265.
11. Schoenberger SD, Kim SJ, Sheng J, Rezaei KA, Lalezary M, Cherney E. Increased prostaglandin E2 (PGE2) levels in proliferative diabetic retinopathy, and correlation with VEGF and inflammatory cytokines. *Invest Ophthalmol Vis Sci*. 2012;53:5906–5911.
12. Zhou J, Wang S, Xia X. Role of intravitreal inflammatory cytokines and angiogenic factors in proliferative diabetic retinopathy. *Curr Eye Res*. 2012;37:416–420.
13. Koskela UE, Kuusisto SM, Nissinen AE, Savolainen MJ, Liinamaa MJ. High vitreous concentration of IL-6 and IL-8, but not of adhesion molecules in relation to plasma concentrations in proliferative diabetic retinopathy. *Ophthalmic Res*. 2013;49:108–114.
14. Sfikakis PP, Grigoropoulos V, Emfietzoglou I, et al. Infliximab for diabetic macular edema refractory to laser photocoagulation: a randomized, double-blind, placebo-controlled, cross-over, 32-week study. *Diabetes Care*. 2010;33:1523–1528.
15. Sfikakis PP, Markomichelakis N, Theodosiadis GP, Grigoropoulos V, Katsilambros N, Theodosiadis PG. Regression of sight-threatening macular edema in type 2 diabetes following treatment with the anti-tumor necrosis factor monoclonal antibody infliximab. *Diabetes Care*. 2005;28:445–447.
16. Tsilimbaris MK, Panagiotoglou TD, Charisis SK, Anastasakis A, Krikonis TS, Christodoulakis E. The use of intravitreal etanercept in diabetic macular oedema. *Semin Ophthalmol*. 2007;22:75–79.
17. Wu L, Hernandez-Bogantes E, Roca JA, Arevalo JF, Barraza K, Lasave AE. Intravitreal tumor necrosis factor inhibitors in the treatment of refractory diabetic macular edema: a pilot study from the Pan-American Collaborative Retina Study Group. *Retina*. 2011;31:298–303.
18. Schlegel N, Waschke J. Impaired cAMP and Rac 1 signaling contribute to TNF-alpha-induced endothelial barrier breakdown in microvascular endothelium. *Microcirculation*. 2009; 16:521–533.
19. Shao M, Yue Y, Sun GY, You QH, Wang N, Zhang D. Caveolin-1 regulates Rac1 activation and rat pulmonary microvascular endothelial hyperpermeability induced by TNF-alpha. *PLoS One*. 2013;8:e55213.
20. McKenzie JA, Ridley AJ. Roles of Rho/ROCK and MLCK in TNF-alpha-induced changes in endothelial morphology and permeability. *J Cell Physiol*. 2007;213:221–228.
21. Peng J, He F, Zhang C, Deng X, Yin F. Protein kinase C-alpha signals P115RhoGEF phosphorylation and RhoA activation in TNF-alpha-induced mouse brain microvascular endothelial cell barrier dysfunction. *J Neuroinflammation*. 2011;8:28.
22. Wojciak-Stothard B, Entwistle A, Garg R, Ridley AJ. Regulation of TNF-alpha-induced reorganization of the actin cytoskeleton and cell-cell junctions by Rho, Rac, and Cdc42 in human endothelial cells. *J Cell Physiol*. 1998;176:150–165.
23. Wisniewska-Kruk J, Hoeben KA, Vogels IM, et al. A novel co-culture model of the blood-retinal barrier based on primary retinal endothelial cells, pericytes and astrocytes. *Exp Eye Res*. 2012;96:181–190.
24. Siemerink MJ, Klaassen I, Vogels IM, Griffioen AW, Van Noorden CJ, Schlingemann RO. CD34 marks angiogenic tip cells in human vascular endothelial cell cultures. *Angiogenesis*. 2012;15:151–163.
25. Rubin LL, Hall DE, Porter S, et al. A cell culture model of the blood-brain barrier. *J Cell Biol*. 1991;115:1725–1735.

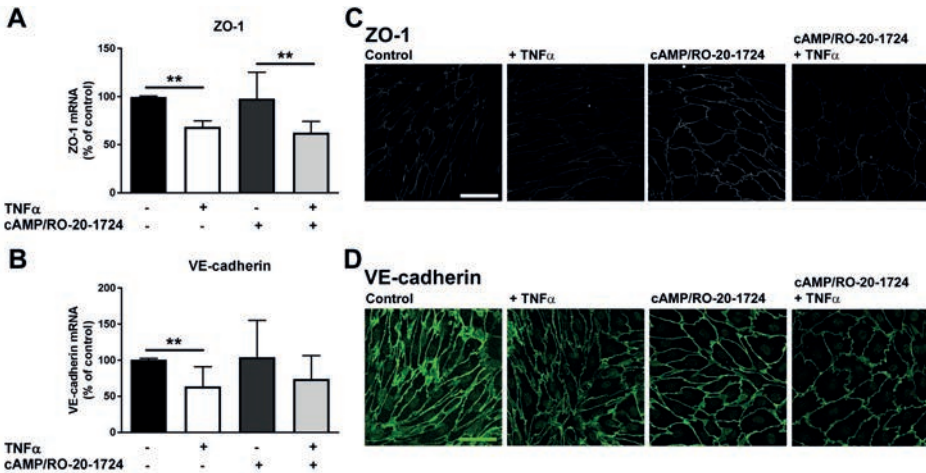
26. Ruijter JM, Thygesen HH, Schoneveld OJ, Das AT, Berkhout B, Lamers WH. Factor correction as a tool to eliminate between-session variation in replicate experiments: application to molecular biology and retrovirology. *Retrovirology*. 2006;3:2.
27. Klaassen I, Hughes JM, Vogels IM, Schalkwijk CG, Van Noorden CJ, Schlingemann RO. Altered expression of genes related to blood-retina barrier disruption in streptozotocin-induced diabetes. *Exp Eye Res*. 2009;89:4–15.
28. Andersen CL, Jensen JL, Orntoft TF. Normalization of real-time quantitative reverse transcription-PCR data: a model-based variance estimation approach to identify genes suited for normalization, applied to bladder and colon cancer data sets. *Cancer Res*. 2004;64:5245–5250.
29. Petrache I, Birukova A, Ramirez SI, Garcia JG, Verin AD. The role of the microtubules in tumor necrosis factor- α -induced endothelial cell permeability. *Am J Respir Cell Mol Biol*. 2003;28:574–581.
30. Seybold J, Thomas D, Witzernath M, et al. Tumor necrosis factor- α -dependent expression of phosphodiesterase 2: role in endothelial hyperpermeability. *Blood*. 2005;105:3569–3576.
31. Deli MA, Dehouck MP, Abraham CS, Cecchelli R, Joo F. Penetration of small molecular weight substances through cultured bovine brain capillary endothelial cell monolayers: the early effects of cyclic adenosine 3',5'-monophosphate. *Exp Physiol*. 1995;80:675–678.
32. Schwede F, Maronde E, Genieser H, Jastorff B. Cyclic nucleotide analogs as biochemical tools and prospective drugs. *Pharmacol Ther*. 2000;87:199–226.
33. Gaillard PJ, Voorwinden LH, Nielsen JL, et al. Establishment and functional characterization of an in vitro model of the blood-brain barrier, comprising a co-culture of brain capillary endothelial cells and astrocytes. *Eur J Pharm Sci*. 2001;12: 215–222.
34. Perriere N, Demeuse P, Garcia E, et al. Puromycin-based purification of rat brain capillary endothelial cell cultures. Effect on the expression of blood-brain barrier-specific properties. *J Neurochem*. 2005;93:279–289.
35. Koga S, Morris S, Ogawa S, et al. TNF modulates endothelial properties by decreasing cAMP. *Am J Physiol*. 1995;268: C1104–C1113.
36. Schubert W, Frank PG, Razani B, Park DS, Chow CW, Lisanti MP. Caveolae-deficient endothelial cells show defects in the uptake and transport of albumin in vivo. *J Biol Chem*. 2001; 276:48619–48622.
37. Aveleira CA, Lin CM, Abcouwer SF, Ambrosio AF, Antonetti DA. TNF- α signals through PKC ζ /NF- κ B to alter the tight junction complex and increase retinal endothelial cell permeability. *Diabetes*. 2010;59:2872–2882.
38. Langeler EG, Fiers W, van Hinsbergh VW. Effects of tumor necrosis factor on prostacyclin production and the barrier function of human endothelial cell monolayers. *Arterioscler Thromb*. 1991;11:872–881.
39. Nitta T, Hata M, Gotoh S, et al. Size-selective loosening of the blood-brain barrier in claudin-5-deficient mice. *J Cell Biol*. 2003;161:653–660.
40. Derian CK, Santulli RJ, Rao PE, Solomon HF, Barrett JA. Inhibition of chemotactic peptide-induced neutrophil adhesion to vascular endothelium by cAMP modulators. *J Immunol*. 1995;154:308–317.
41. Clayton RA, Dick CA, Mackenzie A, et al. The effect of selective phosphodiesterase inhibitors, alone and in combination, on a murine model of allergic asthma. *Respir Res*. 2004;5:4.
42. Cunha-Vaz JG, Travassos A. Breakdown of the blood-retinal barriers and cystoid macular edema. *Surv Ophthalmol*. 1984;28(suppl):485–492.
43. Huang H, Gandhi JK, Zhong X, et al. TNF α is required for late BRB breakdown in diabetic retinopathy, and its inhibition prevents leukostasis and protects vessels and neurons from apoptosis. *Invest Ophthalmol Vis Sci*. 2011;52:1336–1344.
44. Tao L, Nicholson C. Diffusion of albumins in rat cortical slices and relevance to volume transmission. *Neuroscience*. 1996; 75:839–847.
45. Forster C, Burek M, Romero IA, Weksler B, Couraud PO, Drenckhahn D. Differential effects of hydrocortisone and TNF α on tight junction proteins in an in vitro model of the human blood-brain barrier. *J Physiol*. 2008;586:1937–1949.
46. Ghitescu L, Fixman A, Simionescu M, Simionescu N. Specific binding sites for albumin restricted to plasmalemmal vesicles of continuous capillary endothelium: receptor-mediated transcytosis. *J Cell Biol*. 1986;102:1304–1311.
47. Huotari J, Helenius A. Endosome maturation. *EMBO J*. 2011; 30:3481–3500.
48. Duchini A, Govindarajan S, Santucci M, Zampi G, Hofman FM. Effects of tumor necrosis factor- α and interleukin-6 on fluid-phase permeability and ammonia diffusion in CNS-derived endothelial cells. *J Investig Med*. 1996;44:474–482.
49. Danis RP, Scott IU, Qin H, et al. Association of fluorescein angiographic features with visual acuity and with optical coherence tomographic and stereoscopic color fundus photographic features of diabetic macular edema in a randomized clinical trial. *Retina*. 2010;30:1627–1637.
50. Ozdek SC, Erdinc MA, Gurelik G, Aydin B, Bahceci U, Hasanreisoglu B. Optical coherence tomographic assessment of diabetic macular edema: comparison with fluorescein angiographic and clinical findings. *Ophthalmologica*. 2005; 219:86–92.

1
2
3
4
5
6
7
8
&

SUPPLEMENTARY FIGURES



Supplementary Figure 1. TNF α (10 ng/ml) induced stress fiber formation in HUVECs. Immunofluorescence staining with a phalloidin probe against F-actin (grey) showed thick filamentous actin bundles traversing through the endothelial cells (white arrows), indicating stress fiber formation. Grey scale bar is 50 μ m.



Supplementary Figure 2. Preincubation with 312.5 μ M 8(4-CPT) cAMP (cAMP) and 17.5 μ M RO-20-1724 did not prevent the TNF α -induced effects on ZO-1 and VE-cadherin. TNF α (10 ng/ml) significantly decreased mRNA expression of ZO-1 (A) and VE-cadherin (B) after 24h and this could not be prevented by preincubation of BRECs by cAMP and RO-20-1724. (C) Immunofluorescence staining of ZO-1 (grey) shows a decrease after stimulation with TNF α both in cells grown in normal medium and in medium with cAMP and RO-20-1724. (D) Immunofluorescence staining of VE-cadherin (green) shows a slight decrease after stimulation with TNF α , which was also the case when cells were preincubated with cAMP and RO-20-1724. **P<0.01. Data are depicted as mean \pm s.d. White scale bar is 50 μ m.





Glucocorticoids exert differential effects on the endothelium in an in vitro model of the blood-retinal barrier

Anne-Eva van der Wijk,^{1,2} Paul Canning,³ Rutger P. van Heijningen,^{1,2} Ilse M.C. Vogels,^{1,2} Cornelis J.F. van Noorden,² Ingeborg Klaassen,^{1,2*} Reinier O. Schlingemann^{1,4}

¹ Ocular Angiogenesis Group, Departments of Ophthalmology and ²Medical Biology, Academic Medical Center, University of Amsterdam, Amsterdam, The Netherlands

³ The Wellcome-Wolfson Institute for Experimental Medicine, School of Medicine, Dentistry and Biomedical Sciences, Queen's University Belfast, Belfast, UK

⁴Department of Ophthalmology, University of Lausanne, Jules Gonin Eye Hospital, Lausanne, Switzerland

Accepted for publication in Acta Ophthalmol. (2018)

ABSTRACT

Purpose: Glucocorticoids (GCs) are used as treatment in diabetic macular edema, a condition caused by blood-retinal barrier (BRB) disruption. The proposed mechanisms by which GCs reduce macular edema are indirect anti-inflammatory effects and inhibition of VEGF production, but direct effects on the BRB endothelium may be equally important. Here, we investigated direct effects of GCs on the endothelium to understand the specific pathways of GC action, to enable development of novel therapeutics lacking the adverse side effects of the presently used GCs.

Methods: Primary bovine retinal endothelial cells (BRECs) were grown on Transwell inserts and treated with hydrocortisone (HC), dexamethasone (Dex) or triamcinolone acetonide (TA). Molecular barrier integrity of the BRB was determined by mRNA and protein expression, and barrier function was assessed using permeability assays. In addition, we investigated whether TA was able to prevent barrier disruption after stimulation with VEGF or cytokines.

Results: Treatment of BRECs with GCs resulted in upregulation of tight junction mRNA (claudin-5, occludin, ZO-1) and protein (claudin-5 and ZO-1). In functional assays, only TA strengthened the barrier function by reducing endothelial permeability. Moreover, TA was able to prevent cytokine-induced permeability in human retinal endothelial cells and VEGF-induced expression of plasmalemma vesicle-associated protein (PLVAP), a key player in VEGF-induced retinal vascular leakage, in BRECs.

Conclusion: GCs have differential effects in an experimental *in vitro* BRB model. TA is the most potent in improving barrier function, both at the molecular and functional level, and TA prevents VEGF-induced expression of PLVAP.

INTRODUCTION

Glucocorticoids (GCs) are a subclass of adrenal cortex-derived steroids involved in numerous physiological functions throughout the human body, such as regulation of stress responses, maintenance of circadian rhythms and suppression of immune reactions (Clark & Belvisi 2012). GCs suppress immune reactions by inhibiting the early phases of inflammatory responses, *e.g.*, by mediating vascular adhesion and permeability (Salvador et al. 2014) and are used as drugs because of these actions. In addition, GCs are used as therapeutic agents to reduce vasogenic edema in the central nervous system (Murayi & Chittiboina 2016; Pitter et al. 2016), including cerebral edema secondary to brain tumors, and diabetic macular edema (DME) in the eye.

DME is the leading cause of vision loss in the working-age population (Yau et al. 2012), and is a result of vascular leakage caused by disruption of the blood-retinal barrier (BRB). In DME, BRB disruption is mediated by vascular endothelial growth factor-A (VEGF), inflammation and other yet unknown mechanisms. GCs are used to treat DME, as they often have a rapid beneficial effect on retinal swelling (Kiernan & Mieler 2009; Dugel et al. 2015). However, GCs are associated with severe adverse side effects in the eye, such as increased intraocular pressure leading to glaucoma (Kocabora et al. 2008), and cataract formation (Chu et al. 2008). The proposed mechanisms by which steroids reduce macular edema are mostly indirect, *e.g.* by anti-inflammatory effects and by inhibition of VEGF production in non-endothelial cells, but direct effects on BRB endothelium may be important as well (Klaassen et al. 2013). A better understanding of the mechanisms by which GCs restore the BRB, in particular of their direct effects on BRB endothelial cells, may help to identify novel pathways or targets that may allow DME treatment strategies that circumvent adverse effects of GC therapy.

GCs are relatively small, lipophilic hormones, which allows them to enter target cells by passive diffusion. Once in the cytoplasm, GCs bind to the intracellular glucocorticoid receptor (GR) complex which causes a conformational change that leads to the shedding of heat-shock protein 90 (Hsp90). A nuclear localization signal becomes exposed upon Hsp90 release and the ligated GR complex is translocated to the nucleus (Felinski & Antonetti 2005). Here, it can physically interact with (pro-inflammatory) transcription factors, such as NF- κ B or AP-1, which represses gene transcription (Newton 2014). Alternatively, the GR complex can directly bind to glucocorticoid response elements within the promoter region of target genes, causing transactivation (Beato 1989). In addition to these relatively slow genomic effects of transrepression and transactivation, GCs can exert rapid non-genomic effects through direct actions on signaling cascades in the cytoplasm (Tasker et al. 2006), but these effects are not well understood as yet.

Besides the extensively studied anti-inflammatory effects (usually transrepression activity through NF- κ B or AP-1), GCs have been reported to have direct barrier-enhancing effects on brain and retinal endothelial cells. In immortalized human and murine brain endothelial cell lines (hCMEC/D3 and cEND, respectively), dexamethasone (Dex) and hydrocortisone (HC) upregulate expression of the junctional proteins claudin-5, occludin and VE-cadherin (Forster et al. 2005; Forster et al. 2006; Forster et al. 2008). In addition,

downregulation of the matrix metalloproteinase MMP-9 was observed in Dex-treated cEND cells (Blecharz et al. 2010), which may reduce MMP-mediated degradation of tight junctions. In bovine retinal endothelial cells (BRECs), GC treatment increased expression of tight and adherens junction proteins and altered localization and phosphorylation status of junctional components (Antonetti et al. 2002; Felinski et al. 2008). These molecular changes resulted in enhanced barrier properties of blood-brain barrier and BRB endothelial cells, as demonstrated by increased trans-endothelial electrical resistance (TEER) and decreased permeability to molecular tracers (Antonetti et al. 2002; Forster et al. 2006; Felinski et al. 2008). Thus, besides the anti-inflammatory actions, which may mainly work via non-endothelial cells, GCs have direct effects on the BRB endothelial cells, but these effects are poorly understood.

In the present study, we investigated the effects of 2 synthetic GCs that are used in the ocular clinic, Dexamethasone (Dex) and triamcinolone acetonide (TA), and the naturally occurring GC, hydrocortisone (HC), in an *in vitro* model of the BRB (Wisniewska-Kruk et al. 2012). As we identified TA as the most potent GC in restoring the BRB in BRECs, when compared to HC and Dex, we further studied the mechanisms of the effects of TA on BRECs.

MATERIAL AND METHODS

Cell culture

BRECs were isolated from freshly-enucleated cow eyes obtained from the abattoir and cultured as described previously (van der Wijk et al. 2017), in the absence of HC. First passage BRECs were used in all experiments.

RNA isolation and mRNA quantification

BRECs were grown in 12-well plates coated with collagen type IV (Sigma, Beverwijk, The Netherlands) and fibronectin (Merck Millipore, Amsterdam, The Netherlands), treated with the GCs Dex, HC and TA for 24 h, and harvested in 500 μ l TRIzol reagent (Invitrogen; Landsmeer, The Netherlands). We tested various concentrations of the 3 GCs in qPCR experiments to determine their optimum concentrations for maximum effects, on the basis of literature and drug potency (Nehme & Edelman 2008; Edelman 2010; Schwartz et al. 2016) (data not shown). On the basis of these results, we performed all further experiments with 10 μ g/ml HC (Sigma), 1 μ M Dex (~400 ng/ml; Sigma) and 10 μ g/ml TA (Vistrec®, Alcon Nederland BV, Breda, The Netherlands). Preincubation with the GC receptor antagonist RU-486 (10 μ M (Felinski et al. 2008), Sigma) was performed 1 h before GC stimulation. Total RNA was isolated according to the manufacturer's protocol and dissolved in RNase-free water. RNA yield was measured using a NanoDrop spectrophotometer (Thermo Scientific, Wilmington, DE) and 1 μ g RNA was treated with DNase-I (Invitrogen) and reverse transcribed into first strand cDNA with Maxima First Strand cDNA Synthesis Kit (ThermoFisher). Real-time quantitative PCR was performed on 20x diluted cDNA samples

using a CFX96 system (Bio-Rad, Hercules, CA) as described previously (Klaassen et al. 2009). Primer details are published in Klaassen *et al.* (2009). Data was normalized to the geometric mean of 4 reference genes (*Hmbs*, *Gapdh*, *Yhwaz* and *Actb*), and is presented as mean values relative to control, which was set at 100%.

Immunofluorescence staining

BRECs were grown on plastic coverslips coated with collagen type IV and fibronectin. Immunofluorescence staining was performed as described previously (van der Wijk et al. 2017), using the following primary antibodies: rabbit anti-claudin-5 (cat. 34-1600, 1:100; Invitrogen), rabbit-anti-ZO1 (cat. 61-7300; 1:250, Invitrogen), rabbit-anti VE-cadherin (cat. ab33168; 1:400, Abcam, Cambridge, UK). Secondary antibodies directed against the relevant species were conjugated with Alexa Fluor-488 (1:100; Thermo Scientific). Images were recorded using a confocal laser scanning microscope SP8 (Leica Microsystems, Wetzlar, Germany) at the Cellular Imaging core facility of the AMC, and exposure time and gain were kept constant between treatments. Specificity of the staining reaction was checked on the basis of absence of fluorescence signal in samples that were incubated in the absence of primary antibody.

In vitro BRB model

An *in vitro* model of the BRB was used as previously described (van der Wijk et al. 2017) with the following adjustments. The day after seeding the cells on Transwell inserts (0.33 cm², pore size 0.4 μm; Greiner Bio-One, Alphen a/d Rijn, The Netherlands), medium of the upper compartment was refreshed. After 3 days, part of the medium of the lower compartment was refreshed, and medium of the upper compartment was changed completely. Pre-buffered medium was used at all times to ensure the correct pH of the medium.

Permeability analysis

Permeability assays were performed in the *in vitro* BRB model using BRECs at 24 or 48 h after GC stimulation. GCs were added in a volume of 10 μl medium to the upper and lower compartments of the Transwell inserts, once for the 24 h condition, and a second time after 24 h for the 48 h condition. Fluorescent tracers of different sizes (766 Da Cy3, 50 μg/ml (GE Healthcare, Eindhoven, The Netherlands), 70 kDa FITC-dextran, 250 μg/ml (Invitrogen) or 66 kDa BSA-FITC, 250 μg/ml (Invitrogen)) were added in a volume of 15 μl to the upper compartment of the Transwell insert on the day of the experiment. After 2 h, 50 μl (upper compartment) and 200 μl (lower compartment) samples were collected. Concentrations of the tracer molecules were measured with a fluorescence plate reader (CLARIOstar, BMG Labtech, De Meern, The Netherlands) and tracer passage to the lower compartment was calculated on the basis of the initial concentration in the upper compartment. To correct for inter-experiment variation, factor correction was applied using Factor Correction software v2015.2.0.0 (Ruijter et al. 2006).

Impedance measurements of HRECs

Human retinal endothelial cells (HRECs; Innoprot, Derio-Bizkaia, Spain) at passage 8 were grown to 80% confluence in EGM2 medium (Lonza, Basel, Switzerland) in the absence of hydrocortisone and transferred to xCELLigence plates (E-Plate VIEW 16 PET, ACEA Biosciences, San Diego, CA) at 20.000 cells per well in 200 μ l medium. Impedance was measured in real time (expressed as unit-less cell index) and stabilized cell index reflected barrier stabilization. At the indicated time points, rhTNF α (10 ng/ml; ProSpec, Ness Ziona, Israel), rhIL1 β (10 ng/ml; ProSpec) and rhVEGF-165 (25 ng/ml; R&D Systems, Abingdon, UK), and/or TA (10 μ g/ml) were added to the cells in 200 μ l EGM2 media. Impedance measurements were stopped after 40 h. Data are presented as normalized cell index, normalized to the time point just prior to addition of cytokines and/or TA. Two independent experiments were completed with a total of n=11 wells per condition. Bar graphs show pooled data of all the wells from the 2 experiments.

Statistics

Data are depicted as mean \pm standard deviation (s.d.). Experimental conditions were performed in triplicate and averaged and at least 3 independent experiments were performed, unless otherwise indicated. Differences between groups were determined using analysis of variance (ANOVA) followed by Dunnett's test for multiple comparisons. Differences were considered statistically significant when $P \leq 0.05$. Statistical analyses and graphing were performed using GraphPad Prism 6 software (GraphPad Software, La Jolla, CA).

RESULTS

TA decreases permeability for molecular tracers

To assess the effects of GCs on BRB function, we performed permeability assays for molecular tracers of different sizes in our *in vitro* BRB model. We used a small 766 Da Cy3-tracer, which is small enough to be transported through endothelial junctions (paracellular transport), whereas the larger FITC-conjugated dextran (70 kDa) and the FITC-conjugated BSA (66 kDa) cannot pass endothelial junctions in barrier endothelium, and are therefore most likely transported via transcytosis (Klaassen et al. 2013; van der Wijk et al. 2017). After 24 h of stimulation with HC (10 μ g/ml), Dex (1 μ M) or TA (10 μ g/ml), effects on permeability were not observed (data not shown). After 48 h, permeability for all 3 molecular tracers was significantly decreased in TA-treated cells, but not in HC-treated and Dex-treated cells (Fig. 1A-C), suggesting that TA, but not HC and Dex, reduces both paracellular and transcellular permeability.

Effects on the paracellular pathway: GCs enhance the expression of tight and adherens junctions

To investigate the effects of GCs on paracellular permeability, we tested their effects on

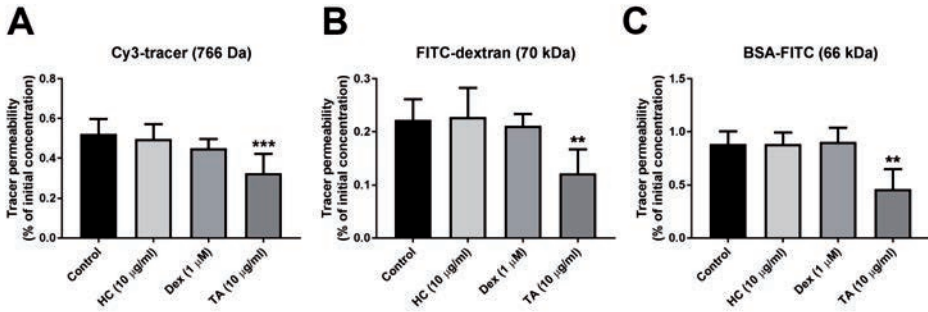


Figure 1. Effects of GCs on permeability of BREC cells for differently-sized fluorescent tracers. Treatment with TA (10 µg/ml), but not HC (10 µg/ml) and Dex (1 µM) significantly decreased permeability for a 766 Da-Cy3 tracer (A), 70 kDa-FITC tracer (B) and 66 kDa BSA-FITC tracer (C) after 48 h. ** $P < 0.01$, *** $P < 0.001$ vs. unstimulated cells. Data are depicted as mean \pm s.d.

molecular components of the main regulators of the paracellular pathway, the tight and adherens junctions. Stimulation of the cells with TA for 24 h enhanced occludin mRNA expression (Fig. 2A). Claudin-5 mRNA expression was increased after treatment with all 3 GCs for 24 h (Fig. 2A). Expression of ZO-1 was not affected by GC stimulation at the mRNA level, whereas VE-cadherin mRNA levels were upregulated after stimulation with Dex only (Fig. 2A).

Immunohistochemical staining showed that claudin-5 protein was aligned at the cell borders of adjacent endothelial cells, and its alignment was enhanced by all 3 GCs (Fig. 2B, C). Although ZO-1 mRNA levels were not altered, ZO-1 protein expression was increased after GC treatment, particularly after HC and Dex stimulation (Fig. 2B, D). VE-cadherin protein levels were not changed after treatment with HC or TA, in line with the mRNA findings. In contrast, VE-cadherin expression in Dex-treated cells was increased (Fig. 2B), especially at the tricellular junctions (Fig. 2E). Taken together, these results indicate that all 3 GCs induce the expression of tight and adherens junction proteins.

Effects on the transcellular pathway: GCs induce caveolin-1 expression and reduce MFSD2A expression

In barrier-forming endothelia of the blood-brain barrier and BRB, the rate of transcytosis is low, which is reflected by a paucity of caveolae in brain and retinal endothelial cells (Hofman et al. 2000). Here, we found that all 3 GCs induced increased mRNA expression of caveolin-1, the primary structural protein of caveolae (Stan 2005), after 24 h treatment (Fig. 3A). mRNA expression of *PLVAP*, a marker protein of leaky vessels in mature barrier-forming endothelium (Schlingemann et al. 1999; Wisniewska-Kruk et al. 2016) involved in vesicle-mediated transcytosis (Herrnberger et al. 2012; Stan et al. 2012), was slightly upregulated after stimulation with TA (~1.5-fold, Fig. 3B). On the other hand, mRNA expression of *MFSD2A*, a suppressor of transcytosis (Chow & Gu 2017), was downregulated after treatment with all 3 GCs (Fig. 3C).

1
2
3
4
5
6
7
8
&

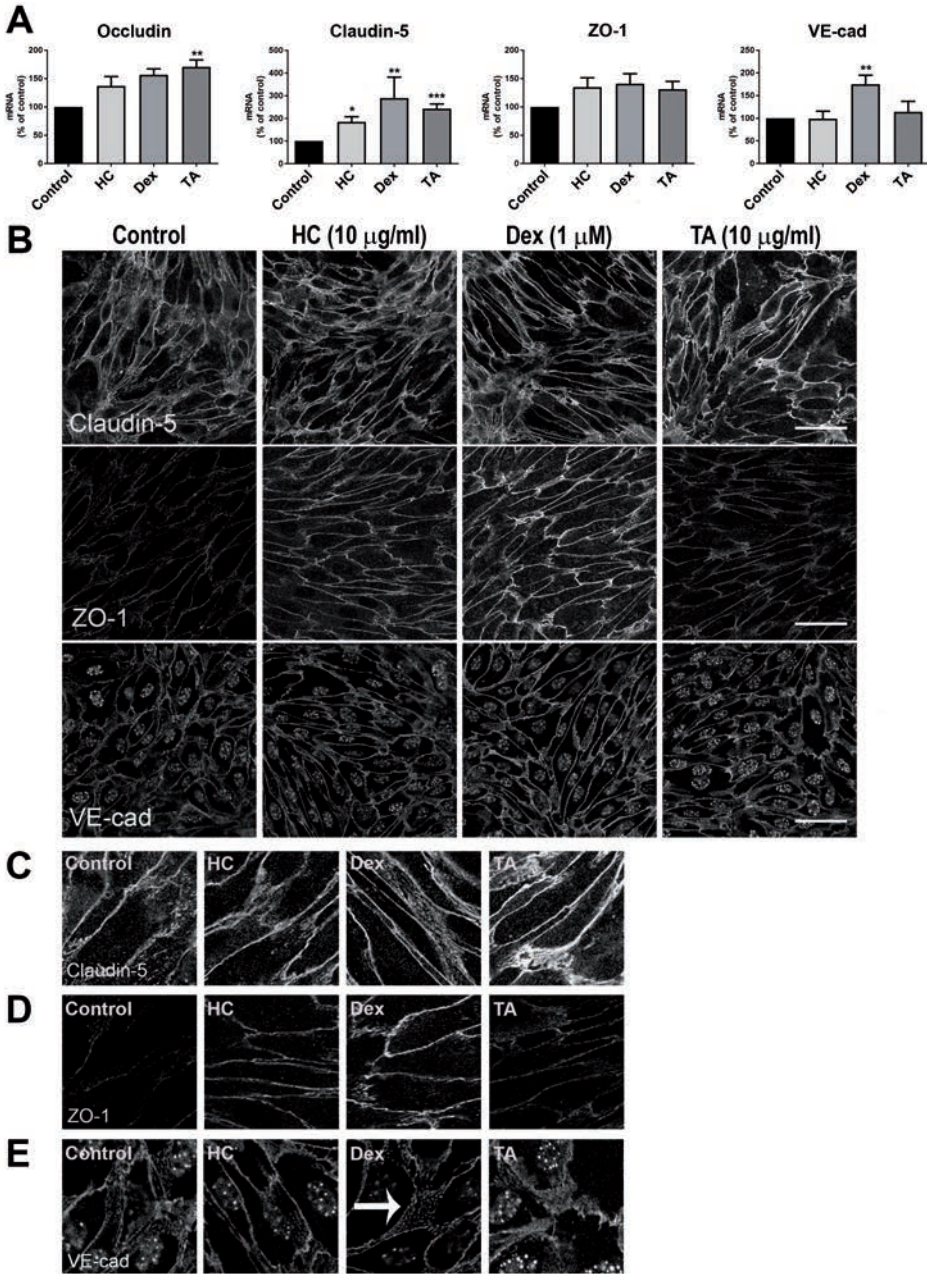


Figure 2. Effect of GCs on tight and adherens junctions of BRECs. (A) mRNA levels of the tight junction components occludin, claudin-5 and ZO-1, and the adherens junction component VE-cadherin after 24 h treatment with HC (10 μ g/ml), Dex (1 μ M) and TA (10 μ g/ml). * $P < 0.05$, ** $P < 0.01$, *** $P < 0.001$ vs. unstimulated cells. Data are depicted as mean \pm s.d. (B) Immunofluorescence staining of claudin-5, ZO-1 and VE-cadherin proteins after 24 h stimulation with HC, Dex and TA. Scale bar is 50 μ m. (C-D) Enlarged areas (2.5 x) of images shown in (B). (C) GCs enhanced the alignment of claudin-5

(continued) along the contours of cells. (D) ZO-1 expression was increased after GC treatment, particularly in HC-treated and Dex-treated cells. (E) VE-cadherin expression was increased after Dex treatment, particularly at the tricellular junctions (white arrow).

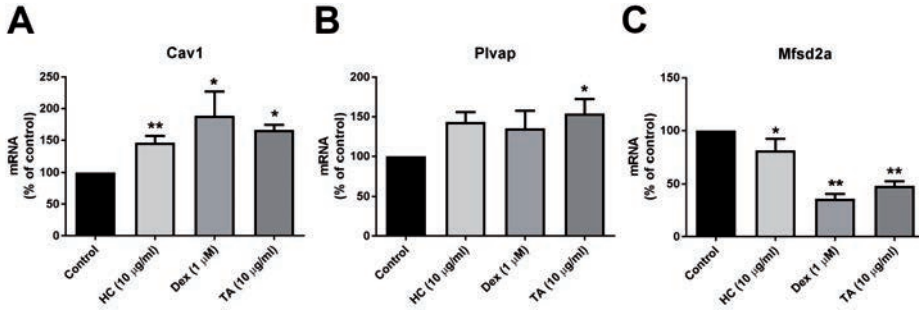


Figure 3. Effect of GCs on the expression of genes involved in transcytosis of BREC. mRNA levels of (A) caveolin-1, (B) PLVAP and (C) MFSD2A after 24 h stimulation with HC (10 µg/ml), Dex (1 µM) and TA (10 µg/ml). * $P < 0.05$, ** $P < 0.01$, *** $P < 0.001$ vs. unstimulated cells. Data are depicted as mean \pm s.d.

Effects of TA and HC on claudin-5 and occludin expression are mediated via the GR

To assess whether the effects of GCs on tight and adherens junction expression are GR mediated, we pretreated the cells with RU-486, a GR antagonist that prevents translocation of the ligated GR-complex into the nucleus (Agarwal 1996), thus inhibiting GR-mediated transactivation or transrepression. Addition of 10 µM RU-486 (Felinski et al. 2008) alone had no effect on expression of tight and adherens junction mRNA (Fig. 4A, white bars), ruling out direct effects of this antagonist on gene expression, but preincubation of the cells with RU-486 1 h before stimulation with TA (largely) prevented TA-induced increased mRNA expression of occludin, claudin-5 and ZO-1 (Fig. 4A, dark grey bars). VE-cadherin mRNA levels were unchanged after stimulation with either TA alone, RU-486 alone or TA and RU-486 (Fig. 4A). Similar results of the expression of all genes were obtained with HC stimulation (data not shown).

Immunohistochemical staining showed that claudin-5 protein staining was stronger in TA-stimulated cells and addition of RU-486 had no direct effect on claudin-5, yet when cells were preincubated with RU-486, TA was not able to induce claudin-5 expression (Fig. 4B). ZO-1 protein expression was increased in TA-stimulated cells, but a slight increase was also observed in cells treated with RU-486 alone. In addition, ZO-1 expression was higher when RU-486 and TA were added together (yet there was also more cytoplasmic ZO-1 staining; Fig. 4B). Protein expression of VE-cadherin was similar in all conditions (Fig. 4B). These data suggest that the effects of TA on the tight junction components occludin and claudin-5 are, at least partly, GR-mediated, but that the effect of TA on ZO-1 expression may occur independent of GR translocation.

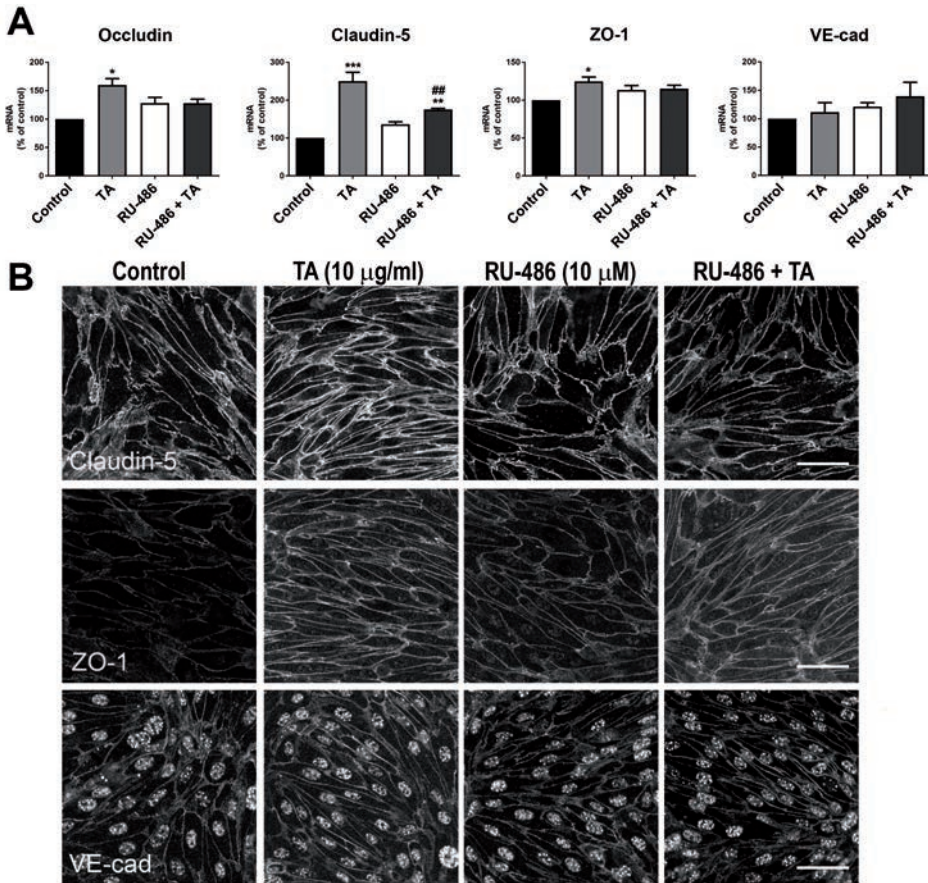


Figure 4. Effects of TA on tight and adherens junctions of BRECs in the presence or absence of RU-486. (A) mRNA levels of occludin, claudin-5, ZO-1 and VE-cadherin after 24 h stimulation with TA (10 µg/ml), RU-486 (10 µM) or preincubation for 1 h with RU-486 followed by 24 h stimulation with TA. * $P < 0.05$, ** $P < 0.01$, *** $P < 0.001$ vs. unstimulated cells. ## $P < 0.01$ vs. TA-stimulated cells. Data are depicted as mean \pm s.d. (B) Immunofluorescence staining of claudin-5, ZO-1 and VE-cadherin proteins after 24 h stimulation with TA in the absence or presence of RU-486 preincubation. Claudin-5 protein expression was increased in TA-stimulated cells, and this effect was diminished when cells were preincubated with RU-486 and then stimulated with TA. Protein expression of ZO-1 was increased after TA stimulation, but also in RU-486 treated cells. Protein expression of VE-cadherin was similar in all conditions. Scale bar is 50 µm.

Effects of TA on caveolin-1 and MFSD2A expression are not GR mediated

Next, we checked whether the effects of GCs on the expression of genes involved in transcytosis and transcellular transport were mediated via the GR. Cells treated with TA showed increased caveolin-1 mRNA expression and decreased *MFSD2A* mRNA expression, an effect not affected by preincubation with RU-486 (Fig. 5A, C), suggesting that regulation

of the expression of these genes by TA is not mediated by GR translocation. On the other hand, HC-induced upregulation of caveolin-1 and downregulation of *MFSD2A* was diminished in the presence of RU-486 (data not shown), suggesting that TA and HC regulate expression of these genes via different mechanisms. *PLVAP* mRNA expression was not significantly affected by TA or RU-486 treatment, although simultaneous treatment with TA and RU-486 decreased *PLVAP* mRNA when compared to cells treated with TA (Fig. 5B).

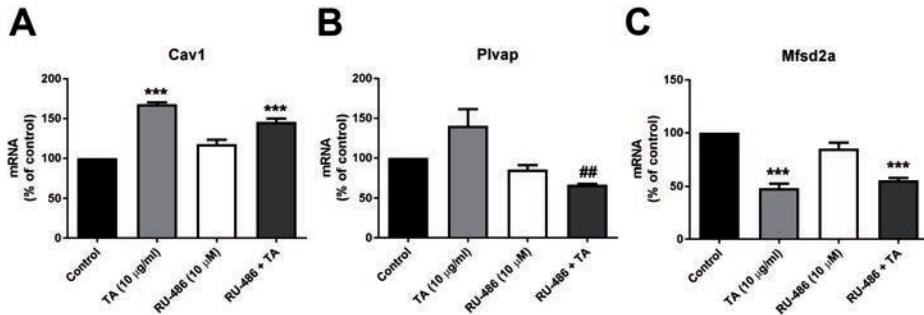


Figure 5. Effects of TA on the expression of genes involved in transcytosis in BRECs in the presence or absence of RU-486. mRNA levels of (A) caveolin-1, (B) *PLVAP* and (C) *MFSD2A* after 24 h stimulation with TA (10 µg/ml), RU-486 (10 µM) or preincubation for 1 h with RU-486 followed by 24 h stimulation with TA. * $P < 0.05$, ** $P < 0.01$, *** $P < 0.001$. ## $P < 0.01$ vs. TA-stimulated cells. Data are depicted as mean \pm s.d.

TA attenuates VEGF-induced upregulation of *PLVAP* expression

VEGF is a key contributor in BRB disruption (Antonetti et al. 2012) in DME and other conditions, and GCs have been suggested to restore barrier function by counteracting effects of VEGF and by reducing VEGF production (Heiss et al. 1996; Kim et al. 2008; Igarashi et al. 2013). We stimulated BRECs with VEGF (25 ng/ml) for either 24 h or 48 h, and assessed the effects on mRNA expression of caveolin-1, *PLVAP* and *MFSD2A*. Moreover, we investigated the effect of TA on VEGF-induced changes, either by simultaneously adding VEGF and TA (for 24 h) or by adding TA at 24 h after VEGF stimulation (48 h VEGF stimulation in total). Whereas caveolin-1 mRNA expression was increased after TA alone and after combined TA and VEGF stimulation, VEGF alone had no direct effect on caveolin-1 mRNA expression (Fig. 6A). VEGF is a well-known inducer of *PLVAP* expression (Hofman et al. 2000) and indeed caused a ~4-fold and ~6.5-fold upregulation of *PLVAP* mRNA after 24 h and 48 h, respectively (Fig. 6B). Crucially, simultaneous stimulation of VEGF and TA for 24 h prevented VEGF-induced upregulation of *PLVAP* expression, and TA also reduced VEGF-induced upregulation of *PLVAP* when added at 24 h after VEGF stimulation (Fig. 6B). *MFSD2A* expression was reduced after TA treatment alone and after combined TA and VEGF treatment, whereas VEGF induced increased *MFSD2A* levels after 24 h (Fig. 6C).

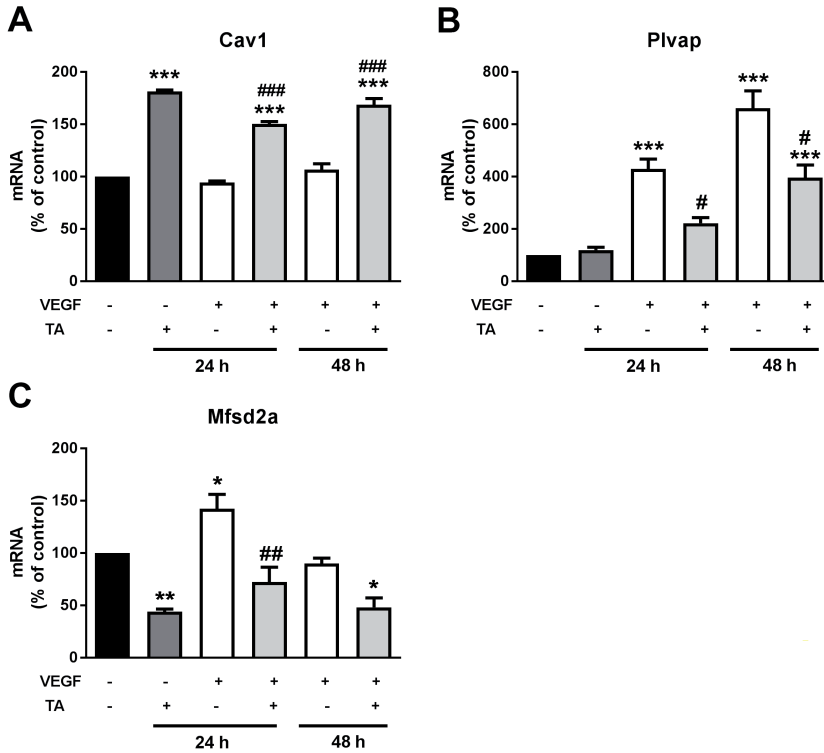


Figure 6. Effects of VEGF and TA on the expression of genes involved in transcytosis in BRECs. (A) mRNA levels of caveolin-1 were increased after TA treatment, whereas VEGF had no direct effect on caveolin-1 expression. (B) Stimulation with VEGF (25 ng/ml) for 24 h and 48 h significantly increased mRNA expression of PLVAP. Addition of TA in combination with VEGF (24 h) or at 24 h after VEGF stimulation (48 h) prevented the VEGF-induced upregulation of PLVAP. (C) TA decreased MFSD2A expression when added alone or in combination with VEGF. * $P < 0.05$, ** $P < 0.01$, *** $P < 0.001$ vs. unstimulated cells. # $P < 0.05$, ## $P < 0.01$, ### $P < 0.001$ vs. VEGF-stimulated cells. Data are depicted as mean \pm s.d.

TA attenuates effects of TNF α , IL1 β and VEGF on endothelial barrier function

Previously, we have shown that simultaneous stimulation of BRECs with TNF α , IL1 β and VEGF for 6 h resulted in increased permeability for the 70 kDa-FITC and 66 kDa BSA-FITC tracers, but not in changes in permeability for smaller molecular tracers (van der Wijk et al. 2017). These results indicated that paracellular permeability was not affected in BRECs under these circumstances. In the present study, claudin-5 protein staining was decreased after 24 h stimulation with TNF α (10 ng/ml), IL1 β (10 ng/ml) and VEGF (25 ng/ml; Fig. 7A). As described before, TA prevented the triple cytokine-induced downregulation of claudin-5 expression (Fig. 7A), and also had a beneficial effect on claudin-5 alignment on cell-cell borders.

1
2
3
4
5
6
7
8
&

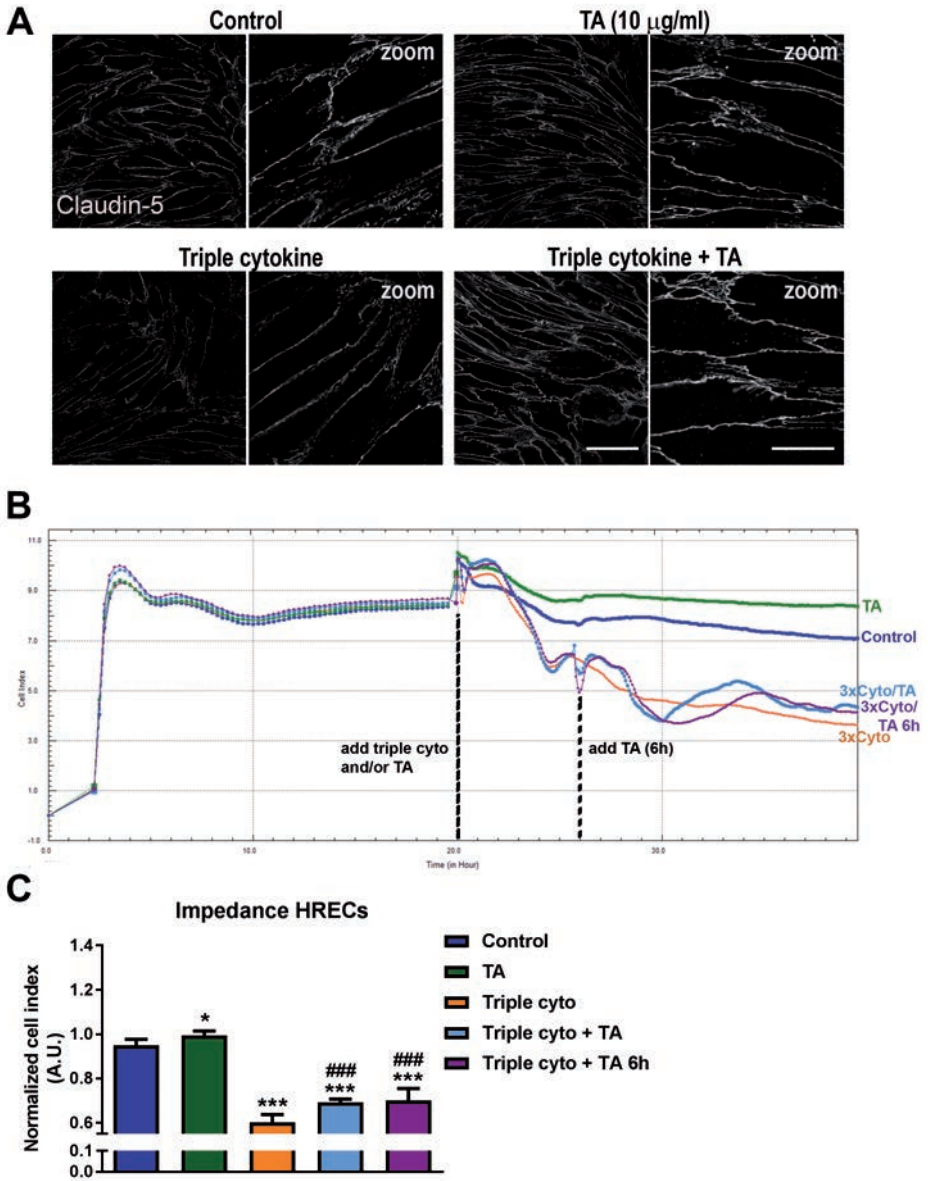


Figure 7. Effects of $\text{TNF}\alpha$, $\text{IL1}\beta$ and VEGF (triple cytokine) stimulation in the absence or presence of TA on BRECs and HRECs. (A) Claudin-5 expression was diminished after triple cytokine stimulation in BRECs, and this effect was prevented in the presence of TA. Scale bar is 50 μm in the left-hand images, and 20 μm in the right-hand images. (B) Representative impedance trace of an xCELLigence barrier experiment using HRECs. Impedance measurements stabilize within 20 h indicating that a stable barrier has formed. Upon addition of compounds to the cells, impedance increases shortly resulting from temperature and pH changes, also in (PBS) control cells (dark blue line). TA treatment (green line) increased impedance levels, whereas triple cytokine stimulation (orange line) decreased impedance levels. Simultaneous addition of TA and triple cytokine (light blue line) or addition of TA 6 h after triple cytokine stimulation (purple line) partly prevented or restored the cytokine-induced decrease in

(continued) impedance. (C) Pooled data from all the wells of 2 independent xCELLigence experiments presented as normalized cell index at 40 h post-seeding (i.e. the end of the experiment). * $P < 0.05$, *** $P < 0.001$ vs. unstimulated cells. ### $P < 0.001$ vs. cytokine-stimulated cells. Data are depicted as mean \pm s.d.

In order to confirm our tracer permeability data in BRECs (van der Wijk et al. 2017), we repeated this experiment in HRECs and measured impedance of HREC monolayers (expressed as cell index) using the xCELLigence system. Figure 7B shows the raw data of a representative impedance trace with the initial steep increase in cell index reflecting cell adherence and barrier stabilization within 20 h after cell seeding. Triple cytokine stimulation resulted in decreased impedance as compared to control cells, and this effect was maintained until the end of the experiment. In contrast, addition of TA to the cells induced increased impedance levels, indicating an enhanced barrier function, although the effect was small. When HRECs were stimulated with triple cytokines in combination with TA treatment, impedance decreased as compared to control cells, but to a slightly lesser extent than cells stimulated with triple cytokines only. Moreover, addition of TA at 6 h after triple cytokine stimulation led to an initial drop in impedance, but over time impedance restored to levels similar to simultaneous stimulation with triple cytokines and TA. These experiments suggest that TA can partly restore endothelial barrier loss induced by a mix of cytokines. Pooled data from the end point (i.e. 40 h post seeding) of 2 independent experiments are presented in Figure 7C.

DISCUSSION

In this study, we assessed the effects of 3 different glucocorticosteroids on the retinal endothelium in an *in vitro* model of the BRB. Whereas all 3 GCs increased expression of tight and/or adherens junction components, only TA decreased basal and cytokine-induced leakage in the functional assays. In our attempt to elucidate the underlying mechanisms of barrier enhancement by TA, we found that at least the effects on claudin-5 are mediated via the GR, but that this is not the case for caveolin-1 and *MFSD2A*.

Several mechanisms have been postulated by which GCs may improve DME or cerebral edema, mostly involving anti-inflammatory effects. This is logical, as GCs can repress transcription of pro-inflammatory cytokines in multiple perivascular cell types, such as astrocytes, Müller cells and pericytes (Kim et al. 2008; Nehme & Edelman 2008). Moreover, GCs have been shown to regulate VEGF expression in human brain astrocytes and pericytes (Kim et al. 2008), and thus may diminish VEGF-induced permeability and angiogenesis. In addition, GC treatment of endothelium *in vitro* reduces expression of adhesion molecules such as VCAM-1 and ICAM-1 (Sloka & Stefanelli 2005; Mizuno et al. 2007), thereby limiting the adherence of leukocytes and their consequent effects on barrier function (although the relevance of leukostasis in human DR was challenged in a recent review (van der Wijk et al. 2017)). However, the effects of GCs must comprise more than (indirect) anti-inflammatory effects, since in the eye, the observed reduction of macular edema can

be very rapid. That this may be due to direct effects on the retinal endothelium is supported by our present observations that TA was able to enhance the endothelial barrier function under basal conditions, shown by a significant reduction in permeability for small (766 Da) and large (66 kDa and 70 kDa) molecular tracers. These experiments were performed in monocultures of BRECs, and as the endothelium has only a limited contribution to the production of pro-inflammatory cytokines (Kim et al. 2008; Wang et al. 2010), it is not likely that GCs act by anti-inflammatory mechanisms in these experiments. Secondly, TA enhanced the barrier function of unstimulated cells, *i.e.*, there were no inflammatory conditions at hand. Therefore, we conclude that GCs induce barrier properties and restore BRB function at least partly via direct effects on the endothelium.

The effects of GCs on tight and adherens junction component expression, their assembly and phosphorylation have been described previously. In BRECs and HRECs, HC and Dex were shown to increase occludin content and phosphorylation status after 24 h (Felinski et al. 2008) and 48 h (Antonetti et al. 2002). In addition, claudin-5 protein expression was significantly increased in BRECs after 24 h HC treatment, whereas no effects were seen on ZO-1 protein content (Felinski et al. 2008). Förster et al. reported in cEND cells (Forster et al. 2005) and hCMEC/D3 cells (Forster et al. 2008) that occludin and claudin-5 were upregulated by HC treatment, whereas claudin-5 was not responsive to Dex stimulation (Forster et al. 2006). These data indicate that different endothelial barrier cell lines do not respond uniformly to GCs, and that the tested GCs have differential effects on endothelial cells. Differential effects of GCs have also been shown in trabecular meshwork cells, where TA affected proteins involved in cell morphology or cell adhesion, and Dex affected RNA posttranscriptional modification and histone methylation (Schwartz et al. 2016). Here, we observed increased occludin, claudin-5 and ZO-1 expression upon 24 h GC stimulation, albeit to different levels depending on the specific GC. VE-cadherin was upregulated at the mRNA and protein level only by Dex, as has also been shown in cEND cells (Blecharz et al. 2008). The decrease in paracellular leakage after treatment with GCs may very well be caused by an increase in tight junction assembly, although we could demonstrate this effect in BRECs only for TA, and only after 48 h. It is possible that the unique pharmacokinetics of GCs underlie different modes of actions and/or the duration of the effect in cell systems, since, *e.g.*, Dex has an elimination half-life of hours and TA of several days (Edelman 2010). Moreover, this time frame suggests that functional effects on the endothelium require more time than molecular effects, which favors transcriptional transactivation or transrepression actions of GCs, rather than non-genomic effects that have been reported to take place very rapidly in the cytoplasm (Tasker et al. 2006).

Indeed, we found that TA and HC actions on occludin and claudin-5 expression are, at least in part, mediated via the GR, with the use of the GR antagonist RU-486. In contrast, it appears that the effects of TA on ZO-1 were independent of the GR. Previously, an occludin enhancer element (OEE) was identified to be a GC-responsive sequence in the human occludin promoter region, but this OEE was not bound directly by the GR (Felinski et al. 2008). Later, it was discovered that the OEE binds to the transcription factor p54/NONO upon GC stimulation, and that this transcription factor is not only necessary for induction

of occludin expression, but also for that of claudin-5 (Keil et al. 2013). Thus, GR-mediated transactivation of occludin and claudin-5, through binding of the OEE sequence in these genes, may be induced upon stimulation with TA and HC, while other mechanisms may be responsible for ZO-1 upregulation.

Given the size of plasma proteins like albumin (Tao & Nicholson 1996), they are unlikely to pass through paracellular junctions of the BRB (Klaassen et al. 2013), even when these junctions are disrupted in conditions such as DME. Because extravasation of plasma proteins is probably the main determinant in oncotic pressure changes driving the development of DME (Cunha-Vaz & Travassos 1984), this suggests that increased transcytosis would be the most important mechanism underlying the development of DME. Hence, ameliorating effects of GCs on transcytosis may be more important for the successful resolution of vasogenic edema than barrier-enhancing effects in terms of decreased paracellular leakage. Here, we found that GCs increased mRNA expression of the key scaffolding protein of caveolae, caveolin-1, in BRECs. This is in line with an earlier study, where caveolin-1 expression was increased in vascular endothelium *in vitro* (human umbilical vein endothelial cells) and *in vivo* (rat aorta and lung arterial cells) treated with Dex (Igarashi et al. 2013). Moreover, mRNA levels of *MFSD2A* were downregulated after GC treatment, suggesting that GCs may impair the suppression of transcytosis. However, since we observed unchanged (HC and Dex) or decreased (TA) permeability in BRECs for large molecular tracers of 66-70 kDa upon GC treatment, it seems improbable that the upregulation of caveolin-1 and/or downregulation of *MFSD2A*, would lead to increased transcytosis rates. In addition to its involvement in vesicle-mediated transcytosis, caveolin-1 also plays a role in signal transduction pathways, *e.g.* in VEGF signaling (Labrecque et al. 2003). Based on this, Igarashi *et al.* suggested that GC-induced increased caveolin-1 expression in vascular endothelium led to attenuated VEGF signaling, as they also observed that pretreatment of endothelial cells with Dex reduced VEGF-induced protein phosphorylation, migration and tube formation (Igarashi et al. 2013). We found here that VEGF-induced upregulation of *PLVAP* mRNA was prevented by TA treatment. PLVAP is a protein specifically involved in trans-endothelial transcytosis, which is normally absent in barrier-forming endothelia (Schlingemann et al. 1997; Stan et al. 1999), but is upregulated in leaky vessels in diabetic retinopathy (Schlingemann et al. 1999). We have previously demonstrated that PLVAP is an essential factor in VEGF-induced vascular permeability in the retina (Wisniewska-Kruk et al. 2016). Thus, by preventing VEGF-mediated upregulation of PLVAP, TA may be able to reduce VEGF-induced transcytosis in the retina. Although at this point rather speculative, our results may suggest that TA-induced upregulation of caveolin-1 is responsible for this process by attenuating VEGF signaling in the retina.

Finally, confirming and extending data from a previous study (van der Wijk et al., 2017), we observed that triple cytokine stimulation reduced the impedance of HRECs. Crucially, addition of TA to cytokine-stimulated HRECs was beneficial to endothelial cell barrier function, since simultaneous addition diminished the cytokine-induced reduction in impedance. Furthermore, adding TA at 6 h after triple cytokine stimulation also partly restored barrier function, underlining the therapeutic potential of TA.

In conclusion, we identified TA as the most potent GC in improving barrier function in our *in vitro* model of the BRB. These effects of TA are not exclusively GR-mediated. In addition, the different GCs have differential effects on BRECs, which should be kept in mind when investigating GC actions. We demonstrated that TA has barrier-inducing effects at the molecular and functional level on a primary source of retinal endothelium and, in addition to decreasing the permeability under basal conditions, TA diminished cytokine-induced barrier disruption and VEGF-induced expression of PLVAP, a key player in VEGF-induced retinal vascular leakage.

ACKNOWLEDGMENTS

The study was supported by Landelijke Stichting voor Blinden en Slechtzienenden (LSBS) and Stichting Oogfonds Nederland that contributed through UitZicht (Grant UitZicht 2012-16), Nederlandse Vereniging ter Verbetering van het Lot der Blinden, Rotterdamse Stichting Blindenbelangen (Grant B20120030), Stichting Winkel Sweep and Stichting Nederlands Oogheekundig Onderzoek (Grant 2012-05). This study was published with the help of Edmond en Marianne Blaauw Fonds voor Oogheelkunde.

Disclosures: None of the authors disclosed any relevant financial relationships.

REFERENCES

- Agarwal MK (1996): The antiglucocorticoid action of mifepristone. *Pharmacol Therapeut* **70**: 183-213.
- Antonetti DA, R Klein & TW Gardner (2012): Diabetic retinopathy. *N Engl J Med* **366**: 1227-1239.
- Antonetti DA, EB Wolpert, L DeMaio, NS Harhaj & RC Scaduto, Jr. (2002): Hydrocortisone decreases retinal endothelial cell water and solute flux coincident with increased content and decreased phosphorylation of occludin. *J Neurochem* **80**: 667-677.
- Beato M (1989): Gene regulation by steroid hormones. *Cell* **56**: 335-344.
- Blecharz KG, D Drenckhahn & CY Forster (2008): Glucocorticoids increase VE-cadherin expression and cause cytoskeletal rearrangements in murine brain endothelial cEND cells. *J Cereb Blood Flow Metab* **28**: 1139-1149.
- Blecharz KG, A Haghikia, M Stasiolek, N Kruse, D Drenckhahn, R Gold, N Roewer, A Chan & CY Forster (2010): Glucocorticoid effects on endothelial barrier function in the murine brain endothelial cell line cEND incubated with sera from patients with multiple sclerosis. *Mult Scler* **16**: 293-302.
- Chow BW & CH Gu (2017): Gradual Suppression of Transcytosis Governs Functional Blood-Retinal Barrier Formation. *Neuron* **93**: 1325-+.
- Chu YK, EJ Chung, OW Kwon, JH Lee & HJ Koh (2008): Objective evaluation of cataract progression associated with a high dose intravitreal triamcinolone injection. *Eye (Lond)* **22**: 895-899.
- Clark AR & MG Belvisi (2012): Maps and legends: the quest for dissociated ligands of the glucocorticoid receptor. *Pharmacol Ther* **134**: 54-67.
- Cunha-Vaz JG & A Travassos (1984): Breakdown of the blood-retinal barriers and cystoid macular edema. *Surv Ophthalmol* **28 Suppl**: 485-492.
- Dugel PU, F Bandello & A Loewenstein (2015): Dexamethasone intravitreal implant in the treatment of diabetic macular edema. *Clin Ophthalmol* **9**: 1321-1335.
- Edelman JL (2010): Differentiating intraocular glucocorticoids. *Ophthalmologica* **224 Suppl 1**: 25-30.
- Felinski EA & DA Antonetti (2005): Glucocorticoid regulation of endothelial cell tight junction gene expression: novel treatments for diabetic retinopathy. *Curr Eye Res* **30**: 949-957.
- Felinski EA, AE Cox, BE Phillips & DA Antonetti (2008): Glucocorticoids induce transactivation of tight junction genes occludin and claudin-5 in retinal endothelial cells via a novel cis-element. *Exp Eye Res* **86**: 867-878.
- Forster C, M Burek, IA Romero, B Weksler, PO Couraud & D Drenckhahn (2008): Differential effects of hydrocortisone and TNFalpha on tight junction proteins in an in vitro model of the human blood-brain barrier. *J Physiol* **586**: 1937-1949.
- Forster C, C Silwedel, N Golenhofen, M Burek, S Kietz, J Mankertz & D Drenckhahn (2005): Occludin as direct target for glucocorticoid-induced improvement of blood-brain barrier properties in a murine in vitro system. *J Physiol* **565**: 475-486.
- Forster C, J Waschke, M Burek, J Leers & D Drenckhahn (2006): Glucocorticoid effects on mouse microvascular endothelial barrier permeability are brain specific. *J Physiol* **573**: 413-425.
- Heiss JD, E Papavassiliou, MJ Merrill, L Nieman, JJ Knightly, S Walbridge, NA Edwards & EH Oldfield (1996): Mechanism of dexamethasone suppression of brain tumor-associated vascular permeability in rats. Involvement of the glucocorticoid receptor and vascular permeability factor. *J Clin Invest* **98**: 1400-1408.
- Herrnberger L, R Seitz, S Kuespert, MR Bosl, R Fuchshofer & ER Tamm (2012): Lack of endothelial diaphragms in fenestrae and caveolae of mutant Plvap-deficient mice. *Histochem Cell Biol* **138**: 709-724.
- Hofman P, HG Blaauwgeers, MJ Tolentino, AP Adamis, BJ Nunes Cardozo, GF Vrensen & RO Schlingemann (2000): VEGF-A induced hyperpermeability of blood-retinal barrier endothelium in vivo is predominantly associated with pinocytotic vesicular transport and not with formation of fenestrations. Vascular endothelial growth factor-A. *Curr Eye Res* **21**: 637-645.
- Igarashi J, T Hashimoto, K Shoji, K Yoneda, I Tsukamoto, T Moriue, Y Kubota & H Kosaka (2013): Dexamethasone induces caveolin-1 in vascular endothelial cells: implications for attenuated responses to VEGF. *Am J Physiol Cell Physiol* **304**: C790-800.
- Keil JM, X Liu & DA Antonetti (2013): Glucocorticoid induction of occludin expression and endothelial barrier requires transcription factor p54 NONO. *Invest Ophthalmol Vis Sci* **54**: 4007-4015.
- Kiernan DF & WF Mieler (2009): The use of intraocular corticosteroids. *Expert Opin Pharmacother* **10**: 2511-2525.
- Kim H, JM Lee, JS Park, SA Jo, YO Kim, CW Kim & I Jo (2008): Dexamethasone coordinately regulates angiopoietin-1 and VEGF: a mechanism of glucocorticoid-induced stabilization of blood-brain barrier. *Biochem Biophys Res Commun* **372**: 243-248.
- Klaassen I, JM Hughes, IM Vogels, CG Schalkwijk, CJ Van Noorden & RO Schlingemann (2009): Altered expression of genes related to blood-retina barrier disruption in streptozotocin-induced diabetes. *Exp Eye Res* **89**: 4-15.
- Klaassen I, CJ Van Noorden & RO Schlingemann (2013): Molecular basis of the inner blood-retinal barrier and its breakdown in diabetic macular edema and other pathological conditions. *Prog Retin Eye Res* **34**: 19-48.

- Kocabora MS, C Yilmazli, M Taskapili, G Gulkilik & S Durmaz (2008): Development of ocular hypertension and persistent glaucoma after intravitreal injection of triamcinolone. *Clin Ophthalmol* **2**: 167-171.
- Labrecque L, I Royal, DS Surprenant, C Patterson, D Gingras & R Beliveau (2003): Regulation of vascular endothelial growth factor receptor-2 activity by caveolin-1 and plasma membrane cholesterol. *Mol Biol Cell* **14**: 334-347.
- Mizuno S, A Nishiwaki, H Morita, T Miyake & Y Ogura (2007): Effects of periocular administration of triamcinolone acetonide on leukocyte-endothelium interactions in the ischemic retina. *Invest Ophthalmol Vis Sci* **48**: 2831-2836.
- Muray R & P Chittiboina (2016): Glucocorticoids in the management of peritumoral brain edema: a review of molecular mechanisms. *Childs Nerv Syst* **32**: 2293-2302.
- Nehme A & J Edelman (2008): Dexamethasone inhibits high glucose-, TNF-alpha-, and IL-1beta-induced secretion of inflammatory and angiogenic mediators from retinal microvascular pericytes. *Invest Ophthalmol Vis Sci* **49**: 2030-2038.
- Newton R (2014): Anti-inflammatory glucocorticoids: changing concepts. *Eur J Pharmacol* **724**: 231-236.
- Pitter KL, I Tamagno, K Alikhanyan, A Hosni-Ahmed, SS Pattwell, S Donnola, C Dai, T Ozawa, M Chang, TA Chan, K Beal, AJ Bishop, CA Barker, TS Jones, B Hentschel, T Gorlia, U Schlegel, R Stupp, M Weller, EC Holland & D Hambarzumyan (2016): Corticosteroids compromise survival in glioblastoma. *Brain* **139**: 1458-1471.
- Ruijter JM, HH Thygesen, OJ Schoneveld, AT Das, B Berkhout & WH Lamers (2006): Factor correction as a tool to eliminate between-session variation in replicate experiments: application to molecular biology and retrovirology. *Retrovirology* **3**: 2.
- Salvador E, S Shityakov & C Forster (2014): Glucocorticoids and endothelial cell barrier function. *Cell Tissue Res* **355**: 597-605.
- Schlingemann RO, P Hofman, L Andersson, D Troost & R vanderGaag (1997): Vascular expression of endothelial antigen PAL-E indicates absence of blood-ocular barriers in the normal eye. *Ophthalmic Res* **29**: 130-138.
- Schlingemann RO, P Hofman, GF Vrensen & HG Blaauwgeers (1999): Increased expression of endothelial antigen PAL-E in human diabetic retinopathy correlates with microvascular leakage. *Diabetologia* **42**: 596-602.
- Schwartz SG, IU Scott, MW Stewart & HW Flynn, Jr. (2016): Update on corticosteroids for diabetic macular edema. *Clin Ophthalmol* **10**: 1723-1730.
- Sloka JS & M Stefanelli (2005): The mechanism of action of methylprednisolone in the treatment of multiple sclerosis. *Mult Scler* **11**: 425-432.
- Stan RV (2005): Structure of caveolae. *Biochim Biophys Acta* **1746**: 334-348.
- Stan RV, L Ghitescu, BS Jacobson & GE Palade (1999): Isolation, cloning, and localization of rat PV-1, a novel endothelial caveolar protein. *J Cell Biol* **145**: 1189-1198.
- Stan RV, D Tse, SJ Deharvengt, NC Smits, Y Xu, MR Luciano, CL McGarry, M Buitendijk, KV Nemani, R Elgueta, T Kobayashi, SL Shipman, KL Moodie, CP Daghljan, PA Ernst, HK Lee, AA Suriawinata, AR Schned, DS Longnecker, SN Fiering, RJ Noelle, B Gimi, NW Shworak & C Carriere (2012): The diaphragms of fenestrated endothelia: gatekeepers of vascular permeability and blood composition. *Dev Cell* **23**: 1203-1218.
- Tao L & C Nicholson (1996): Diffusion of albumins in rat cortical slices and relevance to volume transmission. *Neuroscience* **75**: 839-847.
- Tasker JG, S Di & R Malcher-Lopes (2006): Minireview: rapid glucocorticoid signaling via membrane-associated receptors. *Endocrinology* **147**: 5549-5556.
- van der Wijk AE, JM Hughes, I Klaassen, CJF Van Noorden & RO Schlingemann (2017): Is leukostasis a crucial step or epiphenomenon in the pathogenesis of diabetic retinopathy? *J Leukoc Biol* **102**: 993-1001.
- van der Wijk AE, IMC Vogels, CJF van Noorden, I Klaassen & RO Schlingemann (2017): TNFalpha-Induced Disruption of the Blood-Retinal Barrier In Vitro Is Regulated by Intracellular 3',5'-Cyclic Adenosine Monophosphate Levels. *Invest Ophthalmol Vis Sci* **58**: 3496-3505.
- Wang J, X Xu, MH Elliott, M Zhu & YZ Le (2010): Muller cell-derived VEGF is essential for diabetes-induced retinal inflammation and vascular leakage. *Diabetes* **59**: 2297-2305.
- Wisniewska-Kruk J, KA Hoeben, IM Vogels, PJ Gaillard, CJ Van Noorden, RO Schlingemann & I Klaassen (2012): A novel co-culture model of the blood-retinal barrier based on primary retinal endothelial cells, pericytes and astrocytes. *Exp Eye Res* **96**: 181-190.
- Wisniewska-Kruk J, AE van der Wijk, HA van Veen, TG Gorgels, IM Vogels, D Versteeg, CJ Van Noorden, RO Schlingemann & I Klaassen (2016): Plasmalemma Vesicle-Associated Protein Has a Key Role in Blood-Retinal Barrier Loss. *Am J Pathol* **186**: 1044-1054.
- Yau JW, SL Rogers, R Kawasaki, EL Lamoureux, JW Kowalski, T Bek, SJ Chen, JM Dekker, A Fletcher, J Grauslund, S Haffner, RF Hamman, MK Ikram, T Kayama, BE Klein, R Klein, S Krishnaiah, K Mayurasakorn, JP O'Hare, TJ Orchard, M Porta, M Rema, MS Roy, T Sharma, J Shaw, H Taylor, JM Tielsch, R Varma, JJ Wang, N Wang, S West, L Xu, M Yasuda, X Zhang, P Mitchell, TY Wong & G Meta-Analysis for Eye Disease Study (2012): Global prevalence and major risk factors of diabetic retinopathy. *Diabetes Care* **35**: 556-564.



8

GENERAL DISCUSSION AND CONCLUSIONS

GENERAL DISCUSSION AND SUMMARY

The blood-retinal barrier (BRB) is formed by the retinal vascular endothelium and is regulated by the neurovascular unit, which is a cellular complex of endothelial cells, glial cells and pericytes. It protects the neural retina against disturbances of homeostasis, and from potentially harmful substances in the circulation. Disruption of the BRB results in vascular leakage and as a consequence edema formation and retinal damage. In this thesis, molecular and cellular mechanisms of BRB disruption are investigated in the context of DME and DR.

The first part of this thesis is focused on the development of the BRB and the role of PLVAP in BRB development and disruption. After a general introduction in **chapter 1**, the temporal and spatial recruitment of the neurovascular unit in the neonatal mouse retina is described in detail in **chapter 2**. It was observed that astrocytes preceded the vascular sprouting front, and that pericytes and tip cells invaded the retina together as vascular sprouting front, suggesting that in the retina, recruitment of perivascular cell types is a prerequisite for retinal vascularization and BRB formation.

Chapter 3 is a comprehensive study of the formation of the BRB in neonatal mice, showing that expression of tight and adherens junctions in the retina is temporally regulated, and that immature (and still leaky) vessels already have tight junctions. In addition, PLVAP expression decreased during BRB development, and the absence of PLVAP is a prerequisite for a functional BRB. With the use of heterozygous *Plvap* mice, it was shown that reduced PLVAP levels affect expression of proteins involved in both paracellular and transcellular transport, but without functional consequences for the BRB. Moreover, VEGF signaling was disturbed and these mice had a delay in retinal vascularization during early development, indicating a role for PLVAP in early developmental angiogenesis.

Chapter 4 describes the role of PLVAP in BRB permeability, both *in vitro* and *in vivo*. In an *in vitro* BRB model, knockdown of PLVAP resulted in significantly diminished VEGF-induced permeability for a 70 kDa molecular tracer, in both monocultures of BRECs and triple co-cultures of BRECs, pericytes and astrocytes. In human retinal explants, PLVAP inhibition prevented caveolae formation induced by VEGF stimulation, a phenomenon which may be involved in the reduction of endothelial permeability by PLVAP inhibition. Knockdown of PLVAP reduced hypoxia-induced retinal permeability in the mouse oxygen-induced retinopathy model, showing that PLVAP is involved in both VEGF-mediated and hypoxia-mediated BRB disruption.

The second part of this thesis consists of a literature review and *in vitro* studies of the BRB to establish the role of inflammation in the pathogenesis of DR or DME (**chapter 5 and 6**), and the effects of glucocorticoids on the BRB (**chapter 7**). In **chapter 5**, the prevailing paradigm that leukostasis and subsequent low-grade inflammation are central causes of early DR is questioned because of conflicting evidence in the literature on the causal role of leukostasis in DR.

In **chapter 6**, the controversy on the role of pro-inflammatory cytokines in BRB disruption in the context of DME was studied *in vitro*. TNF α induced permeability for small molecular sodium fluorescein, but not for larger tracers, whereas TNF α in combination

with IL1 β and VEGF induced permeability for the larger molecules 70 kDa FITC-dextran and 66 kDa albumin-FITC. Both permeability effects were mediated by a second messenger molecule, cyclic AMP. However, the downstream pathway activated by cyclic AMP appeared to be different in barrier endothelium in comparison to non-barrier endothelium. This study shows the relevance of TNF α in BRB disruption and DME as part of its complex pathogenesis.

The effects of glucocorticoids on retinal endothelial cells are described in **chapter 7**. Glucocorticoids directly affected barrier properties of BRECs. Hydrocortisone, dexamethasone and triamcinolone acetonide induced improved tight junction expression and/or localization. Triamcinolone acetonide, but not hydrocortisone and dexamethasone reduced endothelial permeability for small (766 Da) and larger (70 kDa-FITC and 66 kDa albumin-FITC) molecular tracers. The 3 glucocorticoids also increased expression of caveolin-1, and triamcinolone acetonide prevented VEGF-induced upregulation of *Plvap* expression. We identified triamcinolone acetonide as the most potent glucocorticoid in retinal endothelium, and show that most, but not all, effects of triamcinolone acetonide are mediated via the glucocorticoid receptor in BRECs.

CONCLUDING REMARKS

The studies described in this thesis unraveled cellular and molecular mechanisms of BRB formation and BRB disruption. We have shed light on the function of PLVAP in barrier endothelium and thereby raised new hypotheses for the unique role of PLVAP in the central nervous system (CNS), *i.e.*, that the absence of PLVAP is imperative for a functional BRB and BBB, and that acquisition of PLVAP is necessary for loss of the CNS barriers. Therefore, lack of PLVAP may provide continuous endothelium with a more barrier-like endothelium status, whereas outside the CNS loss of PLVAP in fenestrated endothelium causes excessive extravasation of serum proteins from the circulation.

In the light of a possible contribution of inflammation in the development of DME and DR, it is concluded here that 1) retinal leukostasis is more likely an epiphenomenon of the diabetic retinal milieu than a crucial and specific step in human DR development, 2) the interplay of 3 cytokines (VEGF, TNF α and IL1 β) induces increased BRB permeability for larger tracers but, *e.g.*, TNF α alone is not potent enough to induce such changes, and 3) the mechanism of action of glucocorticoids on BRB function encompasses more than anti-inflammatory effects. On the basis of these conclusions, it can be stated that DR is primarily not an inflammatory disease, although para-inflammation may enhance the progression and severity of DR and DME. Ultimately, all roads seem to lead to VEGF, as hypoxia-induced VEGF is the main driver of PLVAP expression – which is key in BRB permeability as observed in DR, and VEGF is needed *in vitro* to induce permeability changes for large tracers. Finally, the glucocorticoid triamcinolone acetonide directly enhances barrier properties of BRECs but may also prevent VEGF-induced upregulation of *Plvap* expression, which is highly likely to be important in the successful resolution of DME.





Nederlandse samenvatting en conclusies

List of publications

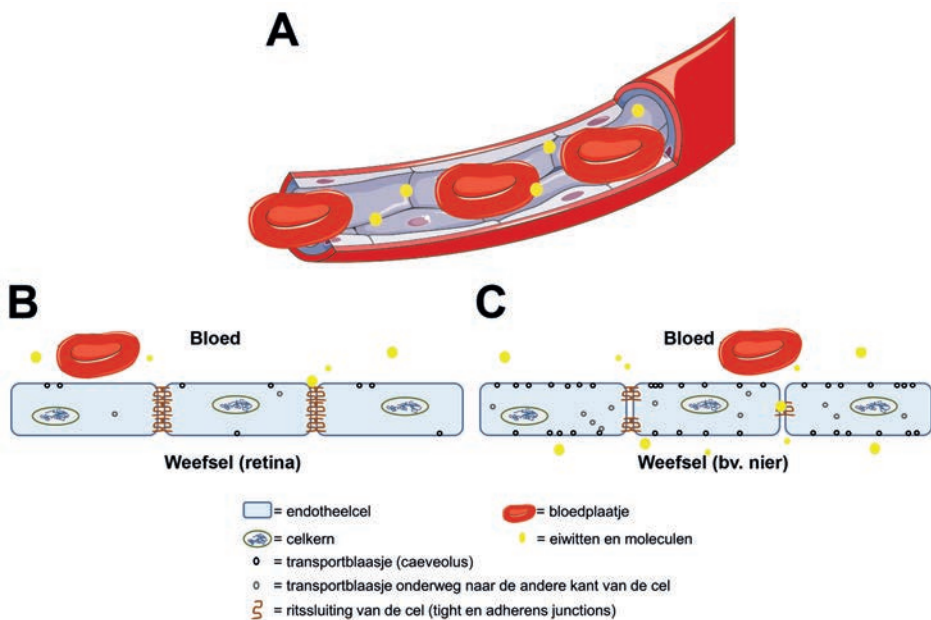
Curriculum vitae

Portfolio

Dankwoord

INTRODUCTIE VOOR DE LEEK

Ons lichaam bestaat uit miljarden cellen die samen weefsels vormen, en verschillende weefsels vormen samen weer organen. Alle verschillende celtypen hebben hun eigen functie. De wanden van onze bloedvaten zijn volledig bekleed met de zogeheten **endotheelcellen** (Fig. 1A). Deze endotheelcellen komen ook weer in vele soorten en smaken, afhankelijk van in welke organen ze de bloedvatwand bekleden (Fig. 1B, C). Nieren bijvoorbeeld hebben als functie om het bloed te filteren en urine te produceren. Voor nieren komt het dus goed uit als het endotheel doorlaatbaar is voor water en eiwitten of andere stoffen uit het bloed zodat er snel gefiltreerd kan worden. In het netvlies (de retina) daarentegen, alsook in de hersenen, is het heel belangrijk dat er geen ongewenste stoffen uit het bloedvat treden die het omliggende neurale weefsel kunnen beschadigen.



Figuur 1. Endotheelcellen hebben eigenschappen passend bij de verschillende benodigdheden van de organen. (A) De wanden van onze bloedvaten zijn volledig bekleed met endotheelcellen. (B) Endotheelcellen in de retina vormen een barrière tussen het bloed en het weefsel zodat er minimaal transport van stoffen plaatsvindt. Retinale endotheelcellen hebben daarom veel tight en adherens junctions en weinig transportblaasjes. (C) In de nieren is het endotheel doorlaatbaar voor water en eiwitten zodat er snelle filtratie plaats kan vinden van het bloed. Endotheelcellen in de nier hebben weinig tight en adherens junctions en veel transportblaasjes.

Daarom hebben de retina en de hersenen een barrière tussen het bloed en het omliggende weefsel, respectievelijk de **bloed-retina en bloed-hersen barrière**. De bloed-retina barrière wordt in de eerste plaats gevormd door de endotheelcellen (hoewel ook andere celtypen een belangrijke rol spelen in het in stand houden van de bloed-retina barrière). Deze specifieke barrière-endotheelcellen zitten aan elkaar vast door eiwitten die **tight en adherens junctions** vormen, een soort ritssluiting tussen de cellen. Daarnaast hebben de barrière-endotheelcellen zeer weinig transportblaasjes (*caveolae*) die stoffen vanuit het bloed naar het weefsel vervoeren. Deze eigenschappen zorgen ervoor dat er onder normale omstandigheden bijna geen uittreding van eiwitten of andere stoffen uit de bloedvaten van de retina plaatsvindt.

Er zijn echter omstandigheden waarbij er schade optreedt aan de endotheelcellen (of andere celtypen) in de retina, waardoor de bloed-retina barrière verbroken wordt. Wanneer dit gebeurt treden eiwitten uit de bloedvaten, gevolgd door water (het principe van osmose, een mechanisme dat het evenwicht tussen eiwitten in bloed en weefsel bewaart), met vochtophoping in de neurale weefsels tot gevolg (oedeem). Dit is een proces dat bij patiënten met suikerziekte optreedt. Jarenlang hoge suikers in het bloed heeft allerlei effecten op het lichaam, en een groot deel van deze patiënten ontwikkelt uiteindelijk **diabetische retinopathie**. **Diabetisch macula oedeem**, dus vochtophoping in de retina als gevolg van een verbroken bloed-retina barrière door diabetes, is een ernstige klinische vorm van diabetische retinopathie. In veel gevallen leidt diabetisch macula oedeem tot vermindering van het zicht of zelfs blindheid.

Al decennialang wordt onderzoek gedaan naar hoe de bloed-retina barrière precies wordt verstoord bij patiënten met diabetisch macula oedeem, en dit heeft veel opgeleverd. Zo is bekend dat het stofje *vascular endothelial growth factor (VEGF)* verhoogd wordt aangemaakt in de retina van deze patiënten. De verhoogde VEGF productie leidt er toe dat de ritssluitingen tussen endotheelcellen verbroken worden, maar ook dat er meer transportblaasjes in de endotheelcellen worden aangemaakt; het endotheel wordt dus meer doorlaatbaar (permeabel). Een belangrijke speler in dit proces lijkt het eiwit *plasmalemma-vesicle associated protein (PLVAP)*. De aanmaak van dit eiwit wordt sterk beïnvloed door VEGF, en het is betrokken bij de hogere doorlaatbaarheid van het endotheel in de retina. De bevinding dat VEGF een grote rol speelt in de ontwikkeling van diabetisch macula oedeem heeft succesvolle medicijnen opgeleverd die de beschikbaarheid van VEGF in de retina verminderen. Er is echter ook een groep patiënten die onvoldoende baat heeft bij deze medicijnen. Een andere optie is het gebruik van **corticosteroiden**, die bij een grote groep patiënten een snel positief effect hebben op het macula oedeem. Steroiden hebben echter ook nadelen: zo is het effect vaak niet blijvend, en ondervinden patiënten bij deze medicijnen in veel gevallen negatieve bijwerkingen.

Alles in beschouwing genomen is er dus nog veel ruimte voor verbetering in de behandeling van patiënten met diabetisch macula oedeem. Hiervoor is nog meer kennis en gedetailleerder begrip nodig van de processen die leiden tot beschadiging van de bloed-retina barrière. In dit proefschrift heb ik geprobeerd meer inzichten te verkrijgen in deze processen. Ik heb met behulp van muismodellen in kaart gebracht hoe de bloed-

retina barrière bij pasgeboren muizen precies wordt gevormd, omdat dit wellicht als een omgekeerd model kan dienen voor pathologische situaties waarbij de barrière verloren gaat. Daarnaast hebben we met genetisch gemodificeerde muizen die minder PLVAP aanmaken onderzocht wat de rol van PLVAP is in de vorming en het behoud van de bloed-retina barrière. Ook hebben we de bloed-retina barrière nagebootst in het lab door endotheelcellen uit het netvlies van koeien te isoleren en te kweken. Aan deze cellen in kweek kunnen vervolgens allerlei stoffen toegevoegd worden om bepaalde omstandigheden te simuleren, zoals VEGF of steröiden. Op deze manier kan direct onderzocht worden wat de effecten van deze stoffen op de endotheelcellen zijn, en dus op welke manier de bloed-retina barrière beïnvloed wordt. In de volgende sectie zijn de resultaten van mijn onderzoeken samengevat en algemene conclusies getrokken.

SAMENVATTING

De bloed-retina barrière (BRB) wordt gevormd door het vasculaire endotheel van de retina en gereguleerd door de neurovasculaire eenheid, een complex van endotheelcellen, gliacellen, pericyten en een basale lamina. De BRB is betrokken bij handhaving van de homeostase van de neurale retina en beschermt deze tegen potentieel gevaarlijke stoffen in de bloedsomloop. Als de BRB niet meer intact is, dan leidt dit tot vaatlekkage met als gevolg vochtophoping (oedeem) en schade aan de retina. In dit proefschrift zijn de cellulaire en moleculaire mechanismen van BRB beschadiging onderzocht in de context van diabetisch macula oedeem (DMO) en diabetische retinopathie (DR).

In het eerste deel van dit proefschrift ligt de focus op de ontwikkeling van de BRB en de rol van plasmalemma vesicle-associated protein (PLVAP) in BRB ontwikkeling en beschadiging. Na de inleiding in **hoofdstuk 1**, wordt in **hoofdstuk 2** in detail beschreven hoe en in welk stadium de verschillende cellulaire componenten van de neurovasculaire eenheid in de retina van neonatale muizenpups verschijnen. Vastgesteld is dat astrocyten voor de neovasculaire spruiten in de neurale retina uit migreren, en pericyten samen met de neovasculaire spruiten in de retina verschijnen, hetgeen suggereert dat de perivasculaire celtypen nodig zijn voor retinale bloedvatvorming en ontwikkeling van de BRB.

Hoofdstuk 3 is een uitgebreide studie van de ontwikkeling van de BRB in pasgeboren muizenpups. Hier werd de expressie van endotheliale intercellulaire eiwitverbindingen in de retina gedurende de eerste 25 dagen na geboorte gevolgd en gedemonstreerd dat onrijpe nog lekkende vaten toch *tight junctions* hebben. Daarnaast bleek dat de expressie van PLVAP afneemt tijdens de ontwikkeling en afwezigheid van PLVAP expressie bleek een voorwaarde te zijn voor een functionele BRB. In heterozygote *Plvap*^{+/-} muizen werd aangetoond dat verminderde PLVAP expressie invloed heeft op de expressie van genen die betrokken zijn bij zowel paracellulair als transcellulair transport, zonder dat dit invloed heeft op het functioneren van de BRB. In de *Plvap*^{+/-} muizen bleek vascular endothelial growth factor (VEGF) signalering verstoord te zijn en de retinale bloedvatvorming vertraagd, hetgeen duidt op een rol voor PLVAP in bloedvatvorming in de vroege ontwikkelingsfase.

In **hoofdstuk 4** wordt de rol van PLVAP in BRB permeabiliteit *in vitro* en *in vivo*

beschreven. In een *in vitro* celmodel resulteerde het remmen van PLVAP in significant verminderde vascular endothelial growth factor (VEGF)-geïnduceerde permeabiliteit voor moleculaire tracers van 70 kDa, zowel in mono-cultures van *bovine retinal endothelial cells* (BRECs), als in co-cultures van BRECs, pericyten en astrocyten. In humane retinale explants bleek remming van PLVAP het vormen van endotheliale caveolae na stimulatie met VEGF te verhinderen, hetgeen een verklaring kan zijn voor de verminderde permeabiliteit na remming van PLVAP. PLVAP remming verminderde ook hypoxia-geïnduceerde vaatlekkage in de retina in het hypoxie-geïnduceerde retinopathie muizenmodel, hetgeen aantoont dat PLVAP betrokken is bij VEGF- en hypoxia-gemedieerde lekkage van de BRB.

Het tweede deel van dit proefschrift bestaat uit een literatuurreview en *in vitro* studies betreffende de rol van ontsteking in de pathogenese van DMO en DR (**hoofdstuk 5 en 6**) en de effecten van glucocorticoiden op de BRB (**hoofdstuk 7**). In **hoofdstuk 5** wordt het heersende paradigma dat leukostase en daaropvolgende chronische ontsteking belangrijke oorzaken zijn van vroege DR ter discussie gesteld vanwege tegenstrijdig bewijs in de literatuur betreffende de causale rol van leukostase in DR. Het paradigma bleek voornamelijk gebaseerd te zijn op dierproefstudies en er zijn bij de mens vrijwel geen indicaties gevonden dat leukostase en/of chronische ontsteking een rol van betekenis spelen in de ontwikkeling van vroege DR.

In **hoofdstuk 6** wordt de rol van pro-inflammatoire cytokines in BRB schade in de context van DMO bestudeerd *in vitro*. Tumor necrosis factor (TNF α) bleek permeabiliteit voor laag-moleculaire tracers zoals fluoresceïne (376 Da), maar niet voor hoog-moleculaire tracers zoals 70 kDa FITC-dextran te induceren, terwijl TNF α in combinatie met IL1 β en VEGF daarentegen permeabiliteit voor de hoog-moleculaire tracers 66 kDa albumin-FITC en 70 kDa FITC-dextran induceerde. Beide effecten werden gemedieerd door de *second messenger* cyclisch AMP. De signaaltransductie route die geactiveerd werd door cyclisch AMP is een andere in barrière endotheel dan in niet-barrière endotheel. RhoA en Rac1 worden in niet-barrière endotheel geactiveerd, respectievelijk geremd via cyclisch AMP na TNF α stimulatie, maar de effecten van TNF α op BRECs waren onafhankelijk van deze kleine Rho GTPase eiwitten. Deze bevindingen duiden op een rol van TNF α in BRB lekkage en DMO als onderdeel van een complexe pathogenese en benadrukken de specifieke regulatie van doorlaatbaarheid in barrière endotheel.

De effecten van glucocorticoiden op retinale endotheelcellen worden beschreven in **hoofdstuk 7**. Glucocorticoiden hebben een direct effect op de barrière eigenschappen van BRECs. Hydrocortison, dexamethason en triamcinolon acetonide verhoogden tight junction expressie en de lokalisatie van deze eiwitten op de celmembranen. Voorts reduceerde triamcinolon acetonide, maar niet hydrocortison en dexamethason, de endotheliale permeabiliteit voor laag- (766 Da) en hoog- (66 en 70 kDa) moleculaire tracers. Alle 3 glucocorticoiden verhoogden expressie van caveoline-1, en triamcinolon acetonide reduceerde VEGF-geïnduceerde verhoging van Plvap expressie. Op basis van deze bevindingen is door ons geconcludeerd dat triamcinolon acetonide de meest potente glucocorticoid is voor retinaal barrière endotheel en dat de meeste, maar niet alle, effecten van triamcinolon acetonide gemedieerd worden via de glucocorticoid receptor in BRECs.

CONCLUSIES

De studies beschreven in dit proefschrift hebben een aantal cellulaire en moleculaire mechanismen van BRB vorming en BRB schade aan het licht gebracht. De functie van PLVAP in barrière endotheel is deels opgehelderd en op basis daarvan zijn nieuwe hypothesen geformuleerd met betrekking tot de unieke rol van PLVAP in het centrale zenuwstelsel. Afwezigheid van PLVAP is essentieel voor een functionele BRB en bloed-hersen barrière, en het verwerven van PLVAP expressie leidt tot verlies van barrièrefuncties in het centrale zenuwstelsel. Daarnaast kan remming van PLVAP expressie continu (niet-barrière) endotheel wellicht voorzien van een barrière-achtige status, terwijl verlies van PLVAP expressie in perifere gefenestreerd (lekkend) endotheel paradoxaal leidt tot een toename van uittreding van plasma eiwitten uit de circulatie.

Betreffende de rol van chronische ontsteking in de ontwikkeling van DMO en DR wordt in dit proefschrift geconcludeerd dat 1) het waarschijnlijk is dat retinale leukostase een bijverschijnsel van het diabetische milieu is en geen cruciale stap in de ontwikkeling van DR bij de mens, 2) het samenspel van 3 cytokines (TNF α , IL1 β en VEGF) BRB permeabiliteit induceert voor hoog-moleculaire tracers, maar bijvoorbeeld TNF α op zichzelf deze veranderingen niet teweeg brengt, en 3) effecten van glucocorticoiden op de BRB meer inhouden dan louter anti-inflammatoire effecten. Op basis van deze conclusies kan gesteld worden dat DR geen chronische ontstekingsziekte is, ook al kan para-inflammatie het verloop en de ernst van DR en DMO versnellen en/of verergeren. Uiteindelijk lijkt expressie van VEGF de grote boosdoener bij DR en DMO, aangezien hypoxie-geïnduceerde expressie van VEGF PLVAP expressie induceert, hetgeen BRB permeabiliteit verhoogt zoals voorkomt bij DR. Bovendien is VEGF *in vitro* nodig om veranderingen in permeabiliteit te induceren voor hoog-moleculaire tracers. Verder is geconcludeerd dat de glucocorticoid triamcinolon acetonide de barrière functie van BRECs verbetert via directe effecten op de barrière endotheelcellen en deze glucocorticoid VEGF-geïnduceerde verhoging van PLVAP expressie kan voorkomen, wat waarschijnlijk minstens zo belangrijk is voor het succesvol behandelen van DMO en DR.

LIST OF PUBLICATIONS

van der Wijk AE, Wisniewska-Kruk J, Vogels IM, van Veen HA, Ip WF, van der Wel NN, van Noorden CJ, Schlingemann RO, Klaassen I. Formation of the retinal vasculature and blood-retinal barrier during early development and the role of Plasmalemma Vesicle-Associated Protein (PLVAP). Submitted.

van der Wijk AE, Canning P, van Heijningen RP, Vogels IM, van Noorden CJ, Klaassen I, Schlingemann RO. Glucocorticoids exert differential effects on the endothelium in an in vitro model of the blood-retinal barrier. *Acta Ophthalmologica* 2018; doi: 10.1111/aos.13909.

van der Wijk AE, Vogels IM, van Veen HA, van Noorden CJ, Schlingemann RO, Klaassen I. Spatial and temporal recruitment of the neurovascular unit during development of the mouse blood-retinal barrier. *Tissue and Cell* 2018; 52:42-50.

van der Wijk AE*, Hughes JM*, Klaassen I, van Noorden CJ, Schlingemann RO. Is leukostasis a crucial step or epiphenomenon in the pathogenesis of diabetic retinopathy? *J Leukoc Biol* 2017; 102:993-1001. *Equal contribution.

van der Wijk AE, Vogels IMC, van Noorden CJF, Klaassen I, Schlingemann RO. TNF α -induced disruption of the blood-retinal barrier in vitro is regulated by intracellular cyclic AMP levels. *IOVS* 2017; 58:3496-3505.

van Dijk IA, Ferrando ML, **van der Wijk AE**, Hoebe RA, Nazmi K, de Jonge WJ, Krawczyk PM, Bolscher JG, Veerman EC, Stap J. Human salivary peptide histatin-1 stimulates epithelial and endothelial cell adhesion and barrier function. *FASEB J* 2017; 31:3922-3933.

Wisniewska-Kruk J, **van der Wijk AE**, van Veen HA, Gorgels TG, Vogels IM, Versteeg D, van Noorden CJ, Schlingemann RO, Klaassen I. Plasmalemma vesicle-associated protein has a key role in blood-retinal barrier loss. *Am J Pathol* 2016; 186:1044-1054.

Groen B, **van der Wijk AE**, van den Berg PP, Lefrandt JD, van den Berg G, Sollie KM, de Vos P, Links TP, Faas MM. Immunological adaptations to pregnancy in women with type 1 diabetes. *Sci Rep* 2015; 5:13618.

van der Wijk AE, Schreurs MP, Cipolla MJ. Pregnancy causes diminished myogenic tone and outward hypotrophic remodeling of the cerebral vein of Galen. *J Cereb Blood Flow Metab* 2013; 33:542-549.

CURRICULUM VITAE

Anne-Eva van der Wijk werd op 24 april 1989 geboren in Groningen. In 2001 ging zij naar middelbare scholengemeenschap Vincent van Gogh te Assen, waar ze in 2007 haar VWO diploma in de richting Natuur & Gezond haalde. Na het behalen van haar diploma besloot zij Biomedische Wetenschappen te gaan studeren aan de Rijksuniversiteit Groningen, waar ze in september 2010 haar bachelor haalde. Voor zij aan haar master begon is zij voor een extra curriculaire stage van 6 weken naar Berlijn geweest, welke werd georganiseerd door ISCOMS. Terug in Groningen begon zij aan haar researchmaster Biomedical Sciences. In het kader van deze master heeft zij 2 stages afgerond, de eerste bij het Universitair Medisch Centrum Groningen in de groep van Dr. Marijke Faas, waar zij onderzoek deed naar de perifere immuunrespons van patiënten met diabetes type I en II. Haar tweede stage heeft zij gedaan in Burlington, VT, aan de University of Vermont in de groep van prof. Marilyn Cipolla. In dit project keek zij naar de aanpassing van bloedvaten in de hersenen aan zwangerschap in een ratmodel. In september 2012 heeft zij haar master behaald met het predicaat *cum laude*. Vanaf december 2012 is zij begonnen met haar promotie in de Oculaire Angiogenese Group bij het Academisch Medisch Centrum in Amsterdam, wat resulteerde in dit proefschrift. Na haar promotie is zij gestart als post-doc bij een alliantieproject tussen het AMC en het VUmc bij prof. Ed van Bavel en prof. Peter Hordijk.

1

2

3

4

5

6

7

8

&

PORTFOLIO

PhD student: Anne-Eva van der Wijk
PhD period: December 2012 – December 2017
Promotores: Prof.dr. R.O. Schlingemann
Prof.dr. C.J.F. van Noorden
Co-promotor: Dr. I. Klaassen

PhD training

Year ECTS

Courses

Basic laboratory safety	2012	0.40
Proefdierkunde (art. 9)	2013	3.90
Basic microscopy course	2013	1.60
AMC World of Science	2013	0.70
Macroscopic, microscopic and pathology anatomy of the house mouse	2013	1.10
Practical Biostatistics	2013	1.10
Vascular Biology (Nederlandse Hartstichting)	2014	1.50
EndNote	2015	0.10
Advanced qPCR	2015	0.70
Career development	2015	0.80
Scientific writing in English	2016	1.50

Seminars, lectures, workshops

Immunohistochemistry staining (BIOKE)	2014	0.10
qPCR and housekeeping genes (ThermoFisher)	2014	0.10
Pimp my poster (APROVE-AMC)	2015	0.10
Theater skills (ICaR)	2016	0.10
Weekly department seminars	2012-17	4.00

Conferences and meetings

EASD eye complications (EASDec, 23 rd meeting), Barcelona, ES	2013	2.25
Oral presentation		
Minisymposium on Angiogenesis organized by AAA, Amsterdam, NL	2013	0.25
DOPsvision Ophthalmology, Nijmegen, NL	2014	0.25
Oral presentation		
ARVO, The Association for Research in Vision and Ophthalmology, annual meeting, Orlando, FL, USA	2014	2.75

EASDec (25 th meeting), Turin, IT	2015	2.25	1
Oral presentation			
BBB Signaling satellite meeting, Paris, FR	2015	0.25	2
Oral presentation			
Cerebral Vascular Biology meeting, Paris, FR	2015	2.75	3
			4
AMC-VUmc Cardiovascular Research Institute meeting, Amsterdam, NL	2015	0.25	5
Poster presentation			
6 th Rembrandt symposium, Noordwijkerhout, NL	2015	0.25	6
Poster presentation			
BBBNetwork meeting, Leiden, NL	2016	0.25	7
Oral presentation			
EASDec (26 th meeting), Manchester, UK	2016	2.25	8
Poster presentation			
Vasculata, Uppsala, SE	2016	1.00	&
DEBS/Netherlands Vascular Biology meeting, Biezenmortel, NL	2016	0.50	
Poster presentation			
BBBNetwork meeting, Leiden, NL	2017	0.25	
EASDec (27 th meeting), Budapest, HU	2017	2.25	
Oral presentation			
Amsterdam Neuroscience annual meeting, Amsterdam, NL	2017	0.25	
Poster presentation			
DEBS/Netherlands Vascular Biology meeting, Biezenmortel, NL	2017	0.50	
Poster presentation			
Other			
Visiting researcher, Lions Eye Institute, The University of Western Australia, Perth, WA, AU	2015 (March)		
Teaching			
Medicine student, voluntarily	2015	0.50	
Bachelor student (Laboratory Science, Hogeschool Leiden)	2015-16	3.00	
Bachelor student (Biomedical Sciences, UvA)	2016-17	2.00	
Medicine student, voluntarily	2017	0.10	

DANKWOORD

Voor iemand die op de middelbare school helemaal niet van practica hield was de studie biomedische wetenschappen misschien niet de meest logische keuze. Tien jaar later echter, heb ik een proefschrift afgerond gebaseerd op hardcore labwerk – al ging dit zeker niet zonder slag of stoot. Hoewel de titel van mijn proefschrift niet één-op-één te vertalen is naar het hele proces van promoveren (zo heftig was het nou ook weer niet), komt het natuurlijk niet helemaal uit de lucht vallen. Waar ik halverwege mijn tijd nog met mijn handen in het haar zat over hoe ik alle projecten in een proefschrift moest gaan verwerken, viel later alles steeds beter op zijn plaats, en nu denk ik dat deze titel de inhoud van de studies eigenlijk heel mooi dekt. Daarnaast gaat het promoveren absoluut gepaard met pieken en dalen, ik denk dat ik niet alleen sta met deze mening. Gelukkig hoeven we het niet alleen te doen. Daarom neem ik hier graag de gelegenheid om iedereen die aan dit proefschrift heeft bijgedragen te bedanken.

Allereerst mijn (co-)promotores. Reinier, bedankt voor het vertrouwen en de grote vrijheid die ik kreeg om mijn onderzoek te doen. Hoewel ik in het begin moest wennen aan de manier van werken in de OAG ben ik meer en meer je input vanaf de zijlijn gaan waarderen. Waar ik soms beren op de weg zag bleken jouw ideeën en voorstellen de meerderheid van de tijd toch van grote waarde te zijn en ik blijf onder de indruk van jouw snelle manier van denken. Gelukkig hebben we op de valreep ook nog het steroïdenproject kunnen publiceren waarvoor ik in eerste instantie was aangenomen.

Ron, mede door jou zijn alle puntjes op de goede i's terecht gekomen. Als er even spijkers met koppen geslagen moesten worden of een manuscript nog binnen een weekend gecontroleerd, dan was dat voor jou geen probleem. Dit heb ik erg gewaardeerd.

Ingeborg, waar de promotores meer op de achtergrond fungeerden, stond jij altijd midden in het onderzoek. Ondanks dat je op het hoogtepunt vier promovendi tegelijkertijd moest begeleiden en daarnaast ook nog bezig was met beurzen aanvragen en eigen projecten, maakte je altijd tijd vrij om te overleggen of brainstormen als dat nodig was. Ik heb altijd het gevoel gehad dat ik wanneer nodig ruggensteun van je had, bedankt daarvoor.

Ik wil de leden van de leescommissie hartelijk danken voor het lezen en beoordelen van mijn proefschrift.

Zoals ik al aanstipte hield ik vroeger niet eens van experimenten, het is daarom voor mij niet vanzelfsprekend dat ik een carrière in het onderzoek ben gestart. Mijn interesse voor wetenschappelijk onderzoek is goed aangewakkerd tijdens mijn studie en daarvoor wil ik hier nog even kort Marijke Faas en Marilyn Cipolla noemen en bedanken, die beiden instrumenteel waren voor de kickstart van mijn wetenschappelijke carrière.

Een onderzoek bestaat niet zonder onderzoeksgroep, waarvan het fundament natuurlijk bestaat uit de analist. Ilse, wat vind ik het jammer dat je niet bij mijn verdediging kan zijn, maar ik kon echt niet langer wachten. Bedankt voor alle oogjes die je hebt gesneden, BRECs die we samen hebben geïsoleerd (net na het ontbijt tot aan mijn ellebogen in de koeienogen is iets wat ik niet mis), de mRNA isolaties, eeuwige PCRs en ga zo maar door. Bahar, wat gezellig dat we zo lang hebben samen gewerkt, samen hebben kunnen afreageren, koffie halen, enzovoort. Heel veel succes met de laatste stappen. Esmeralda, leuk dat ik jou op de

valreep nog heb leren kennen. Ik hoop dat PLVAP eindelijk mee gaat werken, als iemand het kan dan ben jij het denk ik! Marchien, het lijkt alweer zo lang geleden dat we samen in het lab stonden. Volgens mij zit je weer lekker als een visje in de artsenvijver, succes met het afronden van de splendende promotiekwesties, er komt een keer een einde aan weet ik nu uit ervaring. Verder dank aan de studenten die hebben mee gewerkt in onze groep en aan mijn projecten. Richelle, succes met de studies! Louise, jij was mijn eerste “student”, bedankt dat ik op je mocht oefenen! Wing, dank voor alle 100.000 PCRs en kleuringen die je hebt gedaan, het paper zit er eindelijk aan te komen. Rutger, al ben je een beetje af geschrokken door de langzame onderzoekswereld, we hebben de steroidendata toch mooi gepubliceerd, een leuk souvenirkje!

Joanna, I never thought that I would visit your hometown somewhere in Poland, and I least expected it to be for this terrible reason. You are a big part of this thesis and I wish I could have also shared the moments that things started to work out for my project with you, like my first paper and the defense. You made me feel very welcome when I first came to the AMC and I'm very glad that we got to work together for two years.

Gelukkig kon ik ook hier en daar wat experimenten en andere dingen uit handen geven. Henk, bedankt voor alle oogjes die je voor me hebt opgewerkt en gescand en Nicole, voor EM advies. Ron Hoebe en Ard, dank voor jullie hulp met de image analyse. John Hughes, wat fijn dat ik aan de slag mocht met jouw leukostase stuk. Paul Canning, thank you for the collaboration on the steroid manuscript! Prof. Rakoczy, May and Aaron, thank you for having me in your lab for 2 weeks. Unfortunately we didn't get to publish a paper, but I really enjoyed my time in Perth. Een dankjewel voor mijn steroiden-dealers van de Oogheekunde en de dierverzorgers van (NKI) ARIA voor het muizenonderhoud.

Dan zijn we aangekomen bij de afdeling waar ik me zo thuis heb gevoeld de afgelopen vijf jaar, de lieve mensen van de Medische Biologie. De Reits-meiden: Alicia, Sabine, Jolien, Karen en Anne, niet alleen hebben we veel lunches gedeeld, op een goed moment werden zelfs bijna dagelijks de matjes uit de kast getrokken voor de 7 min work out (die toch vaak zo rond de 15 min in beslag nam). Ik ben nog nooit zo fit geweest. Eric, bedankt voor je advies omtrent zaken rondom het promoveren. The Krawczyk group: Przemek, Kuba, Emilie, thank you for blurring my memory with nothing less than gürken juice-wodka shots on after-wine tastings and other occasions. Przemek, thanks for your help with the lay out, it makes me even more proud of the whole book. Alle mensen die verder bij de afdeling horen, de L3/M3 gang (dermatologen, microscopisten, KNO-ers, ga zo maar door), bedankt voor de algehele sfeer. Gelukkig zit ik de komende tijd nog lekker in de buurt op L0!

Vanzelfsprekend een speciale alinea voor Ivo en Lianne, mijn borrelmaatjes. Ik ben erg blij dat jullie me destijds hebben gevraagd medezitting te nemen in de borrelcommissie voor onze CBH-activiteiten. Eén dag per jaar Labuitje is natuurlijk nooit voldoende voor de sociale cohesie binnen een afdeling met allerlei losstaande onderzoeksgroepen, gelukkig waren veel mensen dat met ons eens (hoewel borrels met 3 tot 5 man, inclusief wij zelf, ook geen uitzondering waren). Naast hoogtepunten als de kerstborrels met 50 man heb ik ook erg genoten van onze kroegentochten, waar belangrijk werk (met een goede locatie ben je al half binnen) werd gecombineerd met heel veel, tja, borrelen.

1

2

3

4

5

6

7

8

&

Alhoewel ik naast werk niet bepaald heb opgetreden als de persvoorlichter van mijn onderzoek zijn op privégebied een aantal mensen onontbeerlijk geweest voor mijn algehele welbevinden, en daarom voor dit uiteindelijke resultaat. Zita, met jou heb ik mijn eerste tanden gewisseld en mijn eerste grijze haar gevonden, ik hoop dat we later samen onze eerste advocaatjes gaan drinken. Hilde en Martine, jullie maken het leven hier in het westen zo veel gezelliger. Bedankt dat jullie er altijd voor me zijn! Amra en Karin, hoewel de katers nu erger zijn dan vroeger heb ik dat graag over voor onze avonden. Malou, terug in het mooie Nederland zie ik door jou gelukkig nog wat van het warme zuiden, bedankt voor alle gezellige avondjes! Verder moet ik natuurlijk voor ontspanning even de lieve meiden van de boekenclub bedanken (waar we met gepaste trots over praten), bij deze is BC Het Boekenleggertje ook vereeuwigd in print.

Dan eindig ik bij de familie. Charlotte en Judith, toen ik in de afgelopen jaren zo nu en dan ging nadenken over mijn verdediging dacht ik er vrijwel meteen over om jullie als paranimfen (een soort gevederde getuigen) te vragen, en gelukkig zeiden jullie ja. Bedankt dat jullie me gaan flankeren in misschien wel het engste uurtje van mijn leven. Nog meer dank voor altijd een welkom gevoel, dat geldt natuurlijk ook voor de rest van de familie, Gerard en Ernst en alle kinderen. Papa en mama, ik hoop dat het ook zonder te zeggen duidelijk is dat ik jullie heel erg nodig heb, misschien niet voor de praktische uitvoering van mijn werk maar in het algemeen.

Dat was het dan, het woord 'dank' is 21 keer genoemd dus ik denk dat dit met recht een Dankwoord mag heten. Op naar de volgende uitdaging!

1

2

3

4

5

6

7

8

&

